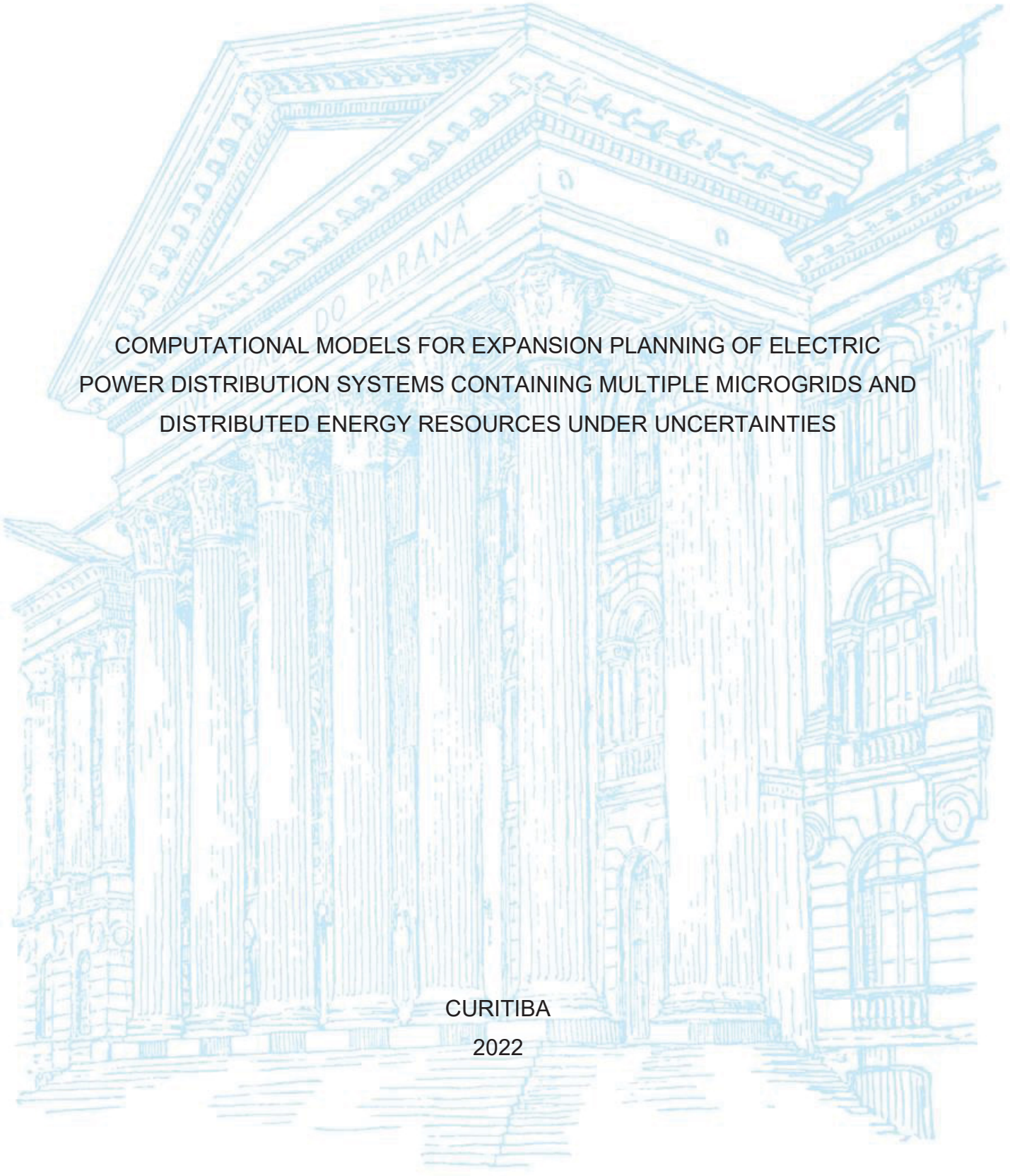
UNIVERSIDADE FEDERAL DO PARANÁ

RAFAEL SILVA PINTO



COMPUTATIONAL MODELS FOR EXPANSION PLANNING OF ELECTRIC POWER DISTRIBUTION SYSTEMS CONTAINING MULTIPLE MICROGRIDS AND DISTRIBUTED ENERGY RESOURCES UNDER UNCERTAINTIES

CURITIBA

2022

RAFAEL SILVA PINTO

COMPUTATIONAL MODELS FOR EXPANSION PLANNING OF ELECTRIC POWER DISTRIBUTION SYSTEMS CONTAINING MULTIPLE MICROGRIDS AND DISTRIBUTED ENERGY RESOURCES UNDER UNCERTAINTIES

Documento apresentado ao Programa de Pós-Graduação em Engenharia Elétrica, Setor de Tecnologia, Universidade Federal do Paraná, para obtenção do título de doutor em Engenharia Elétrica.

Orientador: Prof. Dr. Clodomiro Unsihuay Vila

CURITIBA

2022

Catalogação na Fonte: Sistema de Bibliotecas, UFPR
Biblioteca de Ciência e Tecnologia

P659c Pinto, Rafael Silva

Computational models for expansion planning of electric power distribution systems containing multiple microgrids and distributed energy resources under uncertainties [recurso eletrônico] / Rafael Silva – Curitiba, 2022.

Tese - Universidade Federal do Paraná, Programa de Pós-Graduação Engenharia Elétrica, Setor de Tecnologia, para obtenção do título de doutor em Engenharia Elétrica.

Orientador: Prof. Dr. Clodomiro Unsihuay Vila

1. Sistemas de energia eletrica. 2. Engenharia elétrica. I. Vila, Clodomiro Unsihuay. II. Universidade Federal do Paraná. III. Título.

CDD 621.319

Bibliotecária: Vilma Machado CRB-9/1563

MINISTÉRIO DA EDUCAÇÃO
SETOR DE TECNOLOGIA
UNIVERSIDADE FEDERAL DO PARANÁ
PRÓ-REITORIA DE PESQUISA E PÓS-GRADUAÇÃO
PROGRAMA DE PÓS-GRADUAÇÃO ENGENHARIA ELÉTRICA - 40001016043P4

TERMO DE APROVAÇÃO

Os membros da Banca Examinadora designada pelo Colegiado do Programa de Pós-Graduação ENGENHARIA ELÉTRICA da Universidade Federal do Paraná foram convocados para realizar a arguição da tese de Doutorado de **RAFAEL SILVA PINTO** intitulada: **Computational Models for the Expansion Planning of Electric Power Distribution Systems Containing Multiple Microgrids and Distributed Energy Resources Under Uncertainties**, sob orientação do Prof. Dr. CLODOMIRO UNSIHUAY-VILA, que após terem inquirido o aluno e realizada a avaliação do trabalho, são de parecer pela sua APROVAÇÃO no rito de defesa.
A outorga do título de doutor está sujeita à homologação pelo colegiado, ao atendimento de todas as indicações e correções solicitadas pela banca e ao pleno atendimento das demandas regimentais do Programa de Pós-Graduação.

CURITIBA, 05 de Dezembro de 2022.

Assinatura Eletrônica
06/12/2022 12:13:56.0
CLODOMIRO UNSIHUAY-VILA
Presidente da Banca Examinadora

Assinatura Eletrônica
06/12/2022 18:27:54.0
DJALMA MOSQUEIRA FALCÃO
Avaliador Externo (UNIVERSIDADE FEDERAL DO RIO DE JANEIRO)

Assinatura Eletrônica
06/12/2022 13:46:11.0
EDUARDO NOBUHIRO ASADA
Avaliador Externo (ESCOLA DE ENGENHARIA DE SÃO CARLOS - EESC-USP)

Assinatura Eletrônica
06/12/2022 16:03:00.0
ELIZETE MARIA LOURENÇO
Avaliador Interno (UNIVERSIDADE FEDERAL DO PARANÁ)

Assinatura Eletrônica
06/12/2022 14:36:09.0
MARIANA RESENER
Avaliador Externo (SIMON FRASER UNIVERSITY (CANADA))

ACKNOWLEDGMENT

I want to thank God for the opportunity to complete this important stage in my life, for the motivation, energy, and effort it took to get here.

Many thanks to my supervisor Dr. Clodomiro Unsihuay Vila, for his enthusiasm for the project, support, encouragement, and patience. His guidance was critical to complete this project.

Thanks to my wife Élida and stepdaughters Ana Clara and Rafaela for the support, patience, love, and leisure time. Thanks to my father, mother, and siblings for their support and attention during the last years. They helped me through the hard times.

Thanks to all professors at UFPR that were part of this moment in my life, helping with knowledge and support. Thanks to my colleagues and research group, that provided important discussions.

This research was funded by the Companhia Paranaense de Energia - COPEL research and technological development (RTD) program, through the PD-02866-0511/2019 project, regulated by ANEEL.

The author also thanks the support of CAPES–Brazilian Federal Agency for Support and Evaluation of Graduate Education within the Ministry of Education of Brazil. Thanks to CAPES-PRINT-UFPR Project – Finance Code 001.

RESUMO

Sistemas de distribuição incorporaram diversas tecnologias nos últimos anos, e a introdução de recursos energéticos distribuídos (DERs) proporcionam desafios para o planejamento da sua expansão e operação, como a inserção de geração distribuída (DG), sistemas de armazenamento de energia (ESSs), resposta da demanda (DR) e incertezas associadas com fontes de energia renováveis. Além disso, sistemas de distribuição modernos com múltiplas microrredes (MMG) e tecnologias para automação e monitoramento possibilitam a criação de um mercado local para comercialização de energia entre as microrredes. Devido às incertezas e ambientes competitivos gerados por microrredes que podem tomar suas próprias decisões e comercializar energia, a decisão para expansão do sistema é uma tarefa complexa feita pelo operador do sistema de distribuição (DSO). Dessa forma, essa tese propõe quatro modelos computacionais para o planejamento da expansão de sistemas elétricos de distribuição contendo MMGs e DERs sob incertezas. Cada modelo é projetado para um cenário específico: o primeiro soluciona o planejamento robusto para casos sem MMGs, não usa dados históricos e inclui confiabilidade; o segundo insere MMGs e contingências; o terceiro considera cenários com dados históricos disponíveis; e o quarto inclui o mercado de comercialização de energia para MMG em ambientes competitivos. Todos os modelos buscam minimizar os custos com investimento e operação na perspectiva do DSO, alocando novos componentes (DG, ESSs, capacitores e linhas) sob incertezas, considerando a coordenação das DERs, DR e confiabilidade/contingências. Eles são formulados como problemas multiníveis e solucionados através de decomposições multiestágio usando abordagens como *adaptative robust optimization*, *distributionally robust optimization* e *column-and-constraint generation*. Os métodos propostos são ilustrados usando uma versão modificada do sistema teste IEEE 123-bus. Os resultados mostram que os aspectos apresentados neste trabalho são importantes no planejamento da expansão de redes de distribuição pois reduzem o custo total ao mesmo tempo que melhor representam redes modernas. Incluir contingências melhora significativamente os índices de confiabilidade, reduzindo em 70% do índice EENS no caso de estudo. Cenários considerando mercado de energia tendem a aumentar o custo total do plano em ambientes de competição, 14% no caso de estudo. Ao mesmo tempo, esse caso tem a vantagem do compartilhamento de riscos entre o DSO e investidores. Ademais, os métodos propostos que usam dados históricos se comportam similarmente a métodos robustos ou estocásticos, dependendo do volume de dados disponível.

Palavras-chave: Múltiplas Microrredes; Rede de Distribuição Ativa; Recursos Energéticos Distribuídos; Resposta da Demanda; Confiabilidade; Contingência; Incertezas; Mercado de energia; Teoria dos Jogos.

ABSTRACT

Power distribution systems have incorporated many new technologies in recent years, and the introduction of distributed energy resources (DERs) provides challenges for their operation and expansion planning, such as the inclusion of distributed generation (DG), energy storage systems (ESSs), demand response (DR), and uncertainties associated with renewable power sources. Moreover, modern distribution networks with multiple microgrids (MMG) and automation/monitoring technologies enable the creation of a market framework for local energy trading among the microgrids. Due to uncertainties and the competitive environment where microgrids can make their own decisions and trade energy, the expansion decision is a complex task performed by the distribution system operator (DSO). Thus, this dissertation proposes four computational models for the expansion planning of electric power distribution systems containing multiple microgrids and DERs under uncertainties. Each model is designed for specific scenarios: the first one solves a robust plan for cases without MMGs, has no historical data, and includes reliability; the second model inserts MMGs and contingencies; the third one considers cases having historical data; and the last model formulates the energy trading market for MMGs in competitive environments. All models aim to minimize the investment and operational costs from the DSO's perspective, placing new components (DG, ESSs, capacitors, and lines) under uncertainties, considering the DERs' optimal daily operation, DR, and reliability/contingency. They are formulated as multi-level problems and solved through multi-stage decompositions using robust adaptative optimization, distributionally robust optimization, and column-and-constraint approaches. The proposed methods are illustrated using a modified version of the IEEE 123-bus test system. The results show that the aspects presented in this work are important for the expansion planning of distribution networks since they reduce the total cost and better represent modern new tasks. Including contingencies significantly improves reliability indexes, reducing by 70% the EENS (Expected Energy Not Served) index in the study case. Scenarios considering energy trade markets tend to increase the total cost of the plan in competitive environments, 14% in the case study; at the same time, they have the benefit of sharing the investment risks among investors and the DSO. Furthermore, the proposed methods that use historical data behaved similarly to robust or stochastic approaches, depending on the amount of data available.

Keywords: Multiple Microgrids; Active Distribution Networks; Distributed Energy Resources; Demand Response; Reliability; Contingency; Uncertainties; Competitive Electricity Markets; Game Theory.

LIST OF FIGURES

FIGURE 1 – HISTORICAL ELECTRICITY CONSUMPTION IN BRAZIL.....23
FIGURE 2 – PROJECTION FOR INSTALLED CAPACITY OF DGs IN BRASIL (2015-2031).....25
FIGURE 3 – CLASSIFICATION FOR POWER SYSTEM STUDIES 44
FIGURE 4 – EXAMPLE OF 24-HOUR REPRESENTATION OF GENERATION CAPACITY, LOAD PROFILE, AND GRID POWER COST 45
FIGURE 5 – RADIAL ARCHITECTURE OF MMG 53
FIGURE 6 – DAISY-CHAIN ARCHITECTURE 53
FIGURE 7 – MESH ARCHITECTURE OF MMG 53
FIGURE 8 – DISTRIBUTED ENERGY TRADING AMONG MULTIPLE INTERCONNECTED MICROGRIDS 55
FIGURE 9 – EXAMPLE OF UNCERTAINTY IN POWER GENERATION 57
FIGURE 10 – EXAMPLE OF UNCERTAINTY IN LOAD DEMAND 57
FIGURE 11 – GENERIC UNCERTAINTY ROBUST SETS 61
FIGURE 12 – ADAPTIVE ROBUST OPTIMIZATION APPROACH: INTERACTIONS BETWEEN MASTER PROBLEM AND SUBPROBLEM.....63
FIGURE 13 – UNCERTAINTY ROBUST SETS WITH HISTORICAL DATA 68
FIGURE 14 – DATA-DRIVEN ROBUST SET (IN BLUE).....69
FIGURE 15 – EFFECTS OF THE SIZE OF HISTORICAL DATA ON TOTAL COST. 70
FIGURE 16 – HISTORICAL DATA FOR WIND SPEED FOR SAO PAULO, BRAZIL (2017-2021).....72
FIGURE 17 – DATA BINS FOR THE HISTORICAL DATA FOR WIND SPEED FOR SAO PAULO, BRAZIL (2017-2021) 72
FIGURE 18 – TRI-STAGE DECOMPOSITION MODELING.....83
FIGURE 19 – ALGORITHM TO BUILD THE SENSITIVITY MATRIX.....84
FIGURE 20 – IEEE 123-BUS TEST SYSTEM Kersting (1991).....94
FIGURE 21 – NUMBER OF COMPONENTS PLACED IN THE IEEE 123-BUS TEST SYSTEM VARYING UNCERTAINTY BUDGETS.....95
FIGURE 22 – INVESTMENT, OPERATIONAL, AND TOTAL COST IN THE IEEE 123-BUS TEST SYSTEM VARYING UNCERTAINTY BUDGETS 97

FIGURE 23 – EXPANSION PLANNING DECISION AT THE LAST YEAR OF THE EXPANSION PLANNING DECISION CONSIDERING UNCERTAINTY BUDGET OF 25% 98
FIGURE 24 – NUMBER OF ITERATIONS (K AND W) AND PROCESSING TIME FOR THE TEST SYSTEM VARYING THE UNCERTAINTY BUDGETS 99
FIGURE 25 - PROCESSING TIME, TOTAL COST, AND NUMBER OF ITERATIONS FOR CASES A TO E 101
FIGURE 26 – COMPARISON OF THE TOTAL COST OF THE COMPLETE CASE STUDY WITH CASES NOT INCLUDING (N.I.) SOME COMPONENTS 102
FIGURE 27 – SCOPE AND OBJECTIVE OF THE MODEL IN THIS CHAPTER USING A GENERIC STRUCTURE OF MMG SYSTEMS 107
FIGURE 28 – TWO-STAGE DECOMPOSITION TO SOLVE THE TRI-LEVEL FORMULATION 114
FIGURE 29 – MODIFIED VERSION OF THE IEEE 123-BUS TEST SYSTEM WITH THREE MICROGRIDS 119
FIGURE 30 – DAILY POWER GENERATION CAPACITY OF DGS, LOAD PROFILE, AND MAIN GRID POWER PRODUCTION COST (GEN.: GENERATION) 120
FIGURE 31 – NUMBER OF COMPONENTS PLACED IN THE IEEE-123 BUS TEST SYSTEM 121
FIGURE 32 – EXPANSION PLANNING DECISIONS FOR THE TEST SYSTEM UNDER UNCERTAINTY BUDGET OF 0.25 IN THE LAST PERIOD 122
FIGURE 33 – DERS COORDINATION FOR THE 24-HOUR OPERATION AT THE LAST PERIOD AND UNCERTAINTY BUDGET OF 0 123
FIGURE 34 – DERS COORDINATION FOR THE 24-HOUR OPERATION AT THE LAST PERIOD AND UNCERTAINTY BUDGET OF 0.25 123
FIGURE 35 – NET POWER FLOW IN LINES CONNECTING THE ADN AND THE MGS AT THE LAST PERIOD OF THE EXPANSION PLANNING CONSIDERING AN UNCERTAINTY BUDGET OF 0.25 125
FIGURE 36 – MINIMUM AND MAXIMUM VALUES FOR VOLTAGE IN THE BUSES DURING THE DAILY OPERATION FOR THE LAST YEAR OF THE EXPANSION PLANNING HORIZON 126

FIGURE 37 – POWER FLOW IN THE LINES CONNECTING THE ADN AND THE MGs AT THE LAST PERIOD OF THE EXPANSION PLANNING HORIZON.....127
FIGURE 38 – POWER AVAILABLE AND LOAD FOR THE N-1 GENERATION CONTINGENCY CASES FOR ALL MGS OPERATING ISOLATED FROM THE GRID AT THE LAST PERIOD AND UNCERTAINTY BUDGET OF 0.25 128
FIGURE 39 – ISOLATED OPERATION FOR ALL MGS UNDER CONTINGENCIES "*GCONT*" AT THE LAST PERIOD AND UNCERTAINTY BUDGET OF 0.25 128
FIGURE 40 – TOTAL EXPANSION AND OPERATIONAL COSTS FOR DIFFERENT CASES USING AN UNCERTAINTY BUDGET OF 0.25 130
FIGURE 41 – HISTORICAL DATA FOR SOLAR IRRADIANCE, WIND SPEED, AND LOAD DEMAND FOR SAO PAULO, BRAZIL (2017-2021).....135
FIGURE 42 – HISTORICAL DATA IN 24 HOUR HORIZON FOR SOLAR IRRADIANCE, WIND SPEED, AND LOAD DEMAND FOR SAO PAULO, BRAZIL (2017-2021).....135
FIGURE 43 – CLUSTER OF 6 SCENARIOS USING K-MEANS.....136
FIGURE 44 – TWO-STAGE DECOMPOSITION TO SOLVE THE TRI-LEVEL FORMULATION.....141
FIGURE 45 – EXPANSION PLANNING DECISIONS FOR THE TEST SYSTEM AT THE LAST PERIOD (YEAR 3).....145
FIGURE 46 – DERS' COORDINATION FOR THE 24-HOUR OPERATION AT THE LAST PERIOD (YEAR 3).....146
FIGURE 47 – EVOLUTION OF THE DATA BIN PROBABILITIES FOR EACH ITERATION (K).....147
FIGURE 48 – STRUCTURE OF A MULTIPLE MICROGRIDS SYSTEM 152
FIGURE 49 – REPRESENTATION OF THE SCOPE OF THIS WORK USING A GENERIC STRUCTURE OF MMG SYSTEMS. 154
FIGURE 50 – FOUR-STAGE DECOMPOSITION TO SOLVE THE TRI-LEVEL FORMULATION.....160
FIGURE 51 – NUMBER OF COMPONENTS PLACED IN THE MGS AND IN THE AND PER YEAR 166

FIGURE 52 – COMPARISON OF COSTS FOR CASES CONSIDERING OR NOT ENERGY TRADE AMONG THE MGS 167
FIGURE 53 – POWER BALANCE FOR THE ENTIRE SYSTEM IN THE LAST YEAR OF THE EXPANSION PLANNING 169
FIGURE 54 – PRICE STRATEGY FOR EACH MG PER HOUR IN THE LAST YEAR OF THE EXPANSION PLANNING 170
FIGURE 55 – AVERAGE PRICE STRATEGY 171

LIST OF TABLES

TABLE I – GROUPS OF KEYWORDS 33

TABLE II – COMPARISON OF THE LITERATURE REVIEW WITH THE PROPOSED MODEL 40

TABLE III – RESULTS FOR DIFFERENT CASES USING AN UNCERTAINTY BUDGET OF 0.25 130

TABLE IV – COMPARISON AMONG MODELS FROM CHAPTERS 4 AND 5 132

TABLE V – TOTAL COST OF DDDRO MODEL IN RELATION OF THE TOTAL COST FROM ARO MODEL 148

TABLE VI – COMPARISON AMONG MODELS FROM CHAPTERS 4, 5, AND 6 149

TABLE VII – DETAILS ON WHERE COMPONENTS HAVE BEEN PLACED IN THE EXPANSION PLANNING DECISION 166

TABLE VIII – COMPARISON AMONG MODELS FROM CHAPTERS 4, 5, 6, AND 7 171

LIST OF ABBREVIATIONS

24H-OP	24-hour Operation
AC	Alternating current
ADN	Active Distribution Network
ARO	Adaptative Robust Optimization
C&CG	Column-and-Constraint Generation
DER	Distributed Energy Resource
DDRO	Data-Driven Robust Optimization
DDDRO	Data-Driven Distributionally Robust Optimization
DC	Direct Current
DG	Distributed Generation
DR	Demand Response
DSO	Distribution System Operator
E-PDF	Estimated Probability Distribution Function
ESS	Energy Storage System
EV	Electric Vehicle
GA	Genetic Algorithm
IGDT	Info-Gap Decision Theory
LB	Lower Bound
LP	Linear Programing
MG	Microgrid
MILP	Mixed Integer Linear Programing
MMG	Multiple Microgrids
NWAs	Non-Wired Alternatives
OPF	Optimal Power Flow
SP	Stochastic Programming
T-PDF	True Probability Distribution Function
UB	Upper Bound

LIST OF SYMBOLS

Indices

c	Identifier of expansion planning candidates
cp	Index of capacitors
ctl	Index for controllable portion of loads
d	Index of loads
df	Index for deferrable portion of loads
e	Index of ESS unit
i	Index for MG buyers of electricity in the MMG environment
j	Index for MG sellers of electricity in the MMG environment
g	Index of generators
k, w	Index of iterations among the stages of the C&CG algorithm
l	Index of lines
m	Index of microgrids
n	Index of buses / nodes
nc	Index for non-controllable portion of loads
n_s, n_r	Index of sending end bus / receiving end bus
$\mathcal{s}$	Index for scenarios inside the data bins for the DDDRO model
s, r	Index of sending and receiving nodes for a line
t_h	Index for the hours of the day
t_y	Index for the year in the expansion planning horizon

Sets

t	Set $\{t_h, t_y\}$ in order to simplify notation
Ω^C	Set of components (existing and new components)
Ω_m^C	Set of components located in microgrid m
$\Omega_{m,adn}^L$	Set of lines connecting the microgrid m with the ADN
Δ	All varriables
$\Delta Smax$	Set of variables for the max problem inside the minmaxmin formulation

$\Delta Smin$	Set of variables for the min subproblem inside the minmaxmin formulation
$\Psi^{(NAME)}$	Set of constraints

Parameters

C_g^G	Production cost of generating unit *g*
C_d^{LS}	Load-shedding cost of demand *d*
$EENS^{TG}$	Target for the EENS reliability index inside the expansion planning problem
I_c^C	Annualized investment cost of component *c*
I^{max}	Investment budget
G_l, B_l	Real/imaginary part of the admittance of line *l*
M	Large enough positive constant (BigM)
$\bar{P}_g^{G^{max}}$	Upper bound (UB) of the production capacity of generating unit *g*
$P_g^{G^{min}}$	Minimum production capacity of generating unit *g*
$\bar{P}_d^{D_{nc,ctl,df}}$	UB for the load portion (*nc, ctl, df*) of demand *d* at period *t* and time t_d
$\underline{P}_d^{D_{nc,ctl,df}}$	Lower bound (LB) of the load portion (*nc, ctl, df*) of demand *d* at period *t* and time t_d
$P_d^{D_{ctl}^{total}}$	Total amount of the daily controllable load *d*
$\bar{P}_d^D$	UB for the load demand under uncertainty
$\underline{P}_d^D$	LB for the load demand under uncertainty
P_l^{Lmax}	Active power capacity in line l
$P_{e/n}^{Emax}$	Maximum active power output from the ESS e / located at bus n
$P_{e/n}^{Emin}$	Minimum active power output from the ESS e / located at bus n
$Q_{cp/n}^{SH}$	Reactive power capacity for capacitor cp / located at bus n
R	Rate of return
SOC_e^{min}	Minimum state of charge for ESS e
SOC_e^{max}	Maximum state of charge for ESS e
V_n^{max}	Maximum voltage at bus n
V_n^{min}	Minimum voltage at bus n

σ	Number of days in the year (365)
Γ^G	Uncertainty budget for production capacity
Γ^D	Uncertainty budget for load demand
$\Gamma^{D_{nc,df}}$	Uncertainty budget for load demand (non-controllable and deferrable)
$Lfac_d$	Minimum load factor of demand *d*
δ_1, δ_∞	Tolerance coefficients associated with given confidence level and historical data used in the DDDRO model

Binary Variables

α^C_{c,t_y}	Binary variable to represent the period when the new component *c* is installed in the system
x^C_{c,t_y}	Binary variable to indicate if component *c* is in service (1) or not (0) at year t_y
$bsw_l^{con(m)}$	Binary variable to represent switching for the isolated operation of the microgrid *m*: 1 if line l connecting the MG m to the ADN is in service; otherwise, 0
μ	Auxiliary variable used to activate or not complementary constraints in the KKTs conditions
z_l	Auxiliary variable used to linearize the multiplication of $x^L_{l,t_y} bsw_l^{con(m)}$

Matrices

$\xi[c,d]$	Sensitivity matrix to insert the reliability index inside the robust model. The rows are the candidates for the expansion planning, the columns are the load points, and the values inside the matrix are the improvements in the reliability index in the load point d after placing the component c in the system

Continuous Variables

$\hat{c}^B_m$	Bidding for electricity price from MG m
p^L_l	Active power flow through transmission line l
p^G_g	Active power produced by generating unit *g*
$p_g^{G^{max}}$	Active power capacity of unit *g*

$p_{e/n}^{E}$	Active power output of the EENS unit *e* / located at bus n
p_{d}^{D}	Total active load of demand *d*
$p_{d,t,t_d}^{D_{nc,ctl,df}}$	Active load portion (non-controllable, controllable, and deferrable) of demand *d*
p_{d}^{LS}	Active load shedding of demand *d*
$\widehat{pr}_j$	Priority criterion for MG seller j
$q_{cp/n}^{SH}$	Reactive power for capacitor n / located at bus n
$\hat{r}_m^{B\|S}$	Energy bought/sold by the MG
$\widehat{rv}^T$	Total revenue received by all MG
$\widehat{rv}_m$	Revenue received by MG m
r^{BS}, r^{TS}	Total energy bought/sold in the system
soc_e	State of charge in the ESS unit *e*
η	Auxiliary variable to reconstruct the generation and load shedding costs of the objective function in the first stage of the adaptive robust optimization problem
v_n	Voltage at bus n
v_{sr}	Voltage magnitude difference between bus *s* and bus *r*
θ_n	Voltage angle at bus n, period *t*, and time t_d
θ_{sr}	Voltage angle difference between bus *s* and bus *r*
$\mathscr{p}_{\mathscr{s}}^{\mathcal{S}}$	True probability distribution for scenario from data bin $\mathscr{s}$
$\mathscr{p}_{\mathscr{s}}^{\mathcal{S}_0}$	Estimated probability distribution for scenario from data bin $\mathscr{s}$
$\mathscr{p}_{\mathscr{s}}^{\mathcal{S}\pm}$	Deviation between $\mathscr{p}_{\mathscr{s}}^{\mathcal{S}}$ and $\mathscr{p}_{\mathscr{s}}^{\mathcal{S}_0}$
$\Delta\hat{P}_m$	Net active power from MG m

PS.: The variables regarding the reactive power are not described in this section, they are defined by Q.

Additional Notation

$\widetilde{\blacksquare}$	Represents that the variable ■ is subject to uncertainties
$\dot{\blacksquare}$	Represents that the variable ■ is fixed

$\hat{\blacksquare}$	Represents that the variable ■ is exclusively for a microgrid, used in the model considering energy trading market
ϕ	Dual variable related to inequality constraints
λ	Dual variable related to equality constraints

*Most variables are in lowercase letters, while parameters are in uppercase letters.

TABLE OF CONTENTS

1 INTRODUCTION 22

1.1 RESEARCH OBJECTIVES 27

1.2 CONTRIBUTIONS 28

1.3 PUBLICATIONS 29

1.4 DOCUMENT STRUCTURE 31

2 LITERATURE REVIEW 33

2.1 METHODOLOGY 33

2.2 WORKS FROM THE LITERATURE REVIEW 34

2.3 SUMMARY OF THE LITERATURE REVIEW 39

3 THEORETICAL BACKGROUND 43

3.1 EXPANSION PLANNING FOR ELECTRIC POWER SYSTEMS 43

3.2 DERs AND THE REPRESENTATION OF 24H-OP 44

3.3 RELIABILITY IN ELECTRICAL POWER SYSTEMS 46

3.4 CONTINGENCY IN ELECTRICAL POWER SYSTEMS 48

3.5 DEMAND RESPONSE 48

3.6 OPTIMAL POWER FLOW 50

3.7 MULTIPLE MICROGRIDS 52

3.8 ENERGY TRADING IN MULTIPLE MICROGRIDS' ENVIRONMENTS 54

3.9 UNCERTAINTIES 56

3.9.1 Deterministic Methods 58

3.9.2 Stochastic and Probabilistic Methods 58

3.9.3 Info-Gap Decision Theory (IGDT) 59

3.9.4 Adaptative Robust Optimization 59

3.9.5 Data-Driven Approach 68

3.9.6 Data-Driven Distributionally Approach 70

3.10 CONCLUDING REMARKS FOR THE CHAPTER 73

4 A RELIABILITY-CONSTRAINED ROBUST MODEL FOR THE EXPANSION PLANNING OF ADNs 75

4.1 INTRODUCTION 75

4.2 CONTEXT AND ASSUMPTIONS 76

4.3 PROPOSED MODEL 76

4.3.1 Formulation 77

4.3.2 Algorithm and solution approach 82

4.4 CASE STUDY 93

4.4.1 SIMULATION RESULTS 95

4.4.2 Expansion proposal in different uncertainty budgets 95

4.4.3 Expansion proposal details for uncertainty budget of 25% 97

4.4.4 Processing time and iterations 99

4.4.5 Effects on processing time and total cost due to changing EENS target, neglecting faults' extension, and neglecting switches 100

4.4.6 Comparisons of the proposed model not considering some components ... 102

4.5 SUMMARY 103

5 A CONTINGENCY-CONSTRAINED ROBUST MODEL FOR EXPANSION PLANNING OF ACTIVE DISTRIBUTION NETWORKS AND MULTIPLE MICROGRIDS 105

5.1 INTRODUCTION 105

5.2 CONTEXT AND ASSUMPTIONS 106

5.3 PROPOSED MODEL 108

5.3.1 Formulation 108

5.3.2 Algorithm and solution approach 113

5.4 CASE STUDY 119

5.5 SIMULATION RESULTS 120

5.5.1 Multi-period expansion planning decision 120

5.5.2 DERs' coordination 123

5.5.3 MG's power flow 124

5.5.4 Voltage and power flow analysis 125

5.5.5 Contingencies and MG's isolated operation 127
5.5.6 Cases neglecting contingency, demand response, and the representation of the 24H-OP 129
5.5.7 Comparison among models 132
5.6 SUMMARY 132
6 A DATA-DRIVEN DISTRIBUTIONALLY ROBUST MODEL FOR EXPANSION PLANNING OF ACTIVE DISTRIBUTION NETWORKS WITH MULTIPLE MICROGRIDS 134
6.1 INTRODUCTION 134
6.1.1 Historical data and ambiguity sets in DDDRO models 134
6.2 CONTEXT AND ASSUMPTIONS 137
6.3 PROPOSED MODEL 138
6.3.1 Formulation 139
6.3.2 Algorithm and solution approach 141
6.4 CASE STUDY 144
6.5 SIMULATION RESULTS 144
6.5.1 Expansion Planning Decision 144
6.5.2 DERs' coordination 146
6.5.3 Evolution of the data bin's probabilities 147
6.5.4 Comparison between DDDRO and ARO models 147
6.5.5 Comparison among models 149
6.6 SUMMARY 149
7 A DATA-DRIVEN DISTRIBUTIONALLY ROBUST MODEL FOR EXPANSION PLANNING OF ADNs CONSIDERING ENERGY TRADING STRATEGY BASED ON GAME THEORY 151
7.1 INTRODUCTION 151
7.2 CONTEXT AND ASSUMPTIONS 153
7.3 PROPOSED MODEL 155
7.3.1 Formulation 155
7.3.2 Algorithm and solution approach 160

7.4 CASE STUDY 165
7.5 SIMULATION RESULTS 165
7.5.1 Expansion Planning Decision 165
7.5.2 DER's Coordination 169
7.5.3 Price Strategy 170
7.5.4 Comparison among models 171
7.6 SUMMARY 172
8 CONCLUSIONS 173
8.1 FUTURE WORKS 174
8.2 ACKNOWLEDGMENTS 175
A. APPENDIX – Additional information and data used in the case study 176
B. APPENDIX – Summary of all constraints 179
C. APPENDIX – Summary of formulation of all models 184
REFERENCES 185

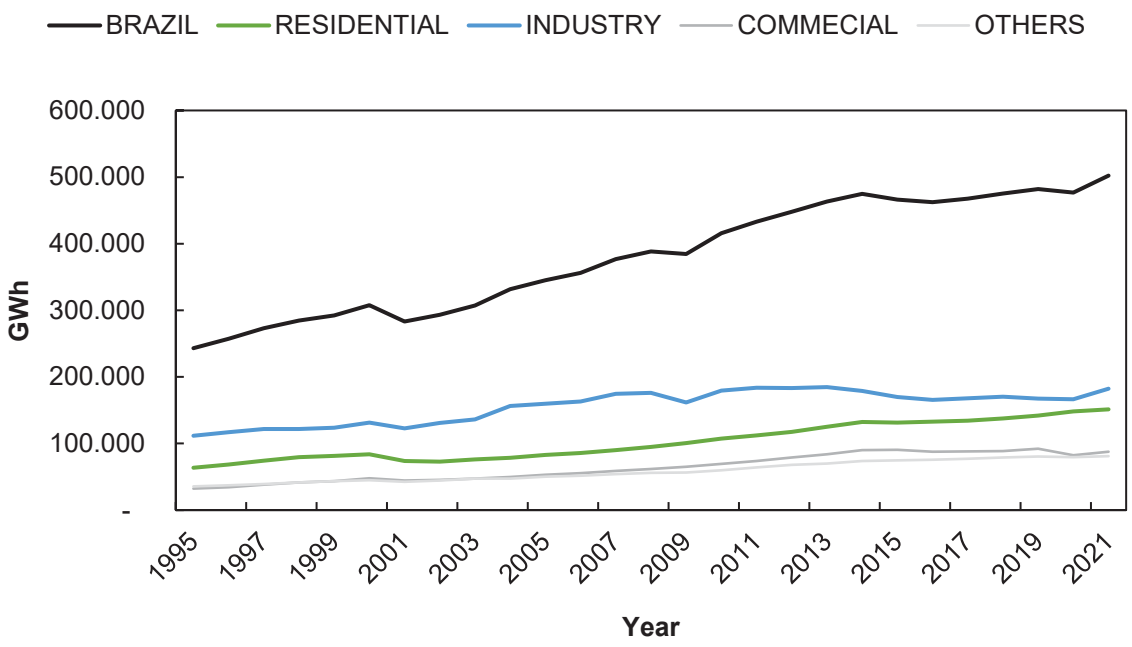
1 INTRODUCTION

Electricity is an essential component of modern life, and transitioning away from fossil fuels in favor of low-carbon energy sources is crucial for the preservation of our planet. In 2015, the Paris Agreement marked a major step forward in the push for a climate-neutral world. Power grids play a vital role in this transition, as they are essential for meeting energy demand and integrating renewable energy into the power system. The shift towards a low-carbon and digital economy is heavily dependent on electricity and is driven by three key factors: decarbonization, digitalization, and decentralization, which pose new challenges for distribution systems.

The growing popularity of distributed energy resources (DERs) is seen as both a challenge and an opportunity for energy providers. DER integration requires an upgraded grid capable of handling bi-directional power flow and increased energy consumption, availability, uncertainty, and potentially higher capacity of feeders to ensure that the new resources do not cause network congestion. At the same time, distributed energy can be deployed as a viable solution with various benefits for customers, utilities, wholesale energy markets, and the environment. In particular, DERs can serve as non-wired alternatives (NWAs) to delay, reduce or avoid traditional network investments. States are developing laws, regulatory processes, or initiatives to require the inclusion of DERs as NWAs in technology and development planning. This introduces new complexities for planning and evaluating unconventional alternatives to increase grid capacity, photovoltaic hosting capacity, and reliability (MASIELLO and KHODAEI, 2022).

Furthermore, as new technologies appear and society's financial conditions increase, electricity consumption tends to rise. For example, as shown in Figure 1, the total amount of energy consumed in Brazil from 1995 to 2021 increased by 106%.

FIGURE 1 – HISTORICAL ELECTRICITY CONSUMPTION IN BRAZIL



SOURCE: EPE (2022a)

Although the total electricity consumption in Brazil has constantly increased from 1995 to 2019, Figure 1 shows some years with unexpected behaviors. For example, in 2009, 2015, and 2016 the power consumption decreased by 1% in Brazil compared to the previous year. Moreover, some years had rates of increase higher than the yearly average of 3%; for example, in 2004 and 2010, this rate was 8%.

The different behaviors in electricity consumption over the years are usually due to economic and political changes, which are difficult, if not impossible, to predict. Thus, the concept of uncertainty is defined as scenarios where something is not known or certain, impacting the decision-making in the power system expansion planning.

According to the Empresa de Pesquisa Energética (EPE), the total electricity consumption in 2022 was 570,000 GWh in Brazil, with an estimated growth rate of 3.4% per year from 2022 to 2031, reaching 792,000 GWh in this year (EPE, 2022b).

The increase in electricity consumption, insertion of new power generation, and the entry of new technologies may require replacing or installing components in the power system to ensure safety, quality, reliability, and reduction in operational costs.

The general objective of the power system expansion planning aims to place/replace components in the network, ensuring the best investments that would

provide the lowest costs and losses, meet the growing demand, and allow the entry of new players, services, and businesses.

The expansion planning problem is typically divided into three groups:

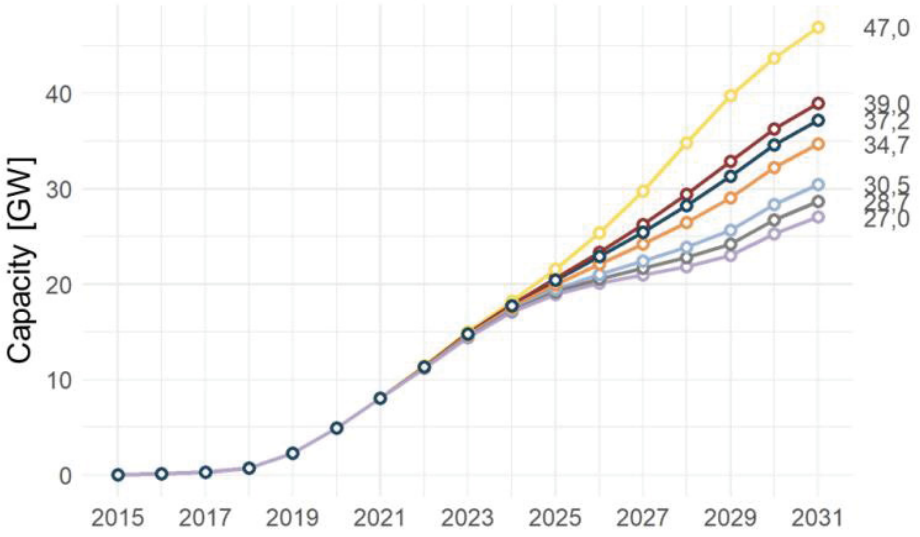
- Generation: conversion of a form of primary energy form (hydro, thermal, solar, wind) into electrical energy;
- Transmission: transportation of the energy from generation to consumption centers. Typically, in very long distances and high amounts of voltage magnitude;
- Distribution: fulfilling the consumers' demand at a certified voltage level.

Each group has specific types of equipment, quality and safety standards, and particular challenges. Modern distribution networks include distributed generation (DG), which are decentralized small-scale generation units. In Brazil, DG connections grew exponentially after the introduction of the Normative Resolution 482/2012 from ANEEL. In 2012, only ten power plants were established as mini- or micro-power distributed generation in the country; this number was 1.871 in 2016 and 337.553 in 2020 (ANEEL, 2021). In October 2022, Brazil reached an installed capacity of 14 GW of distributed generation, composed of 99% photovoltaic sources (ABSOLAR, 2022).

Figure 2 presents the projection of the installed capacity of DGs in Brazil until 2031 for different scenarios (EPE, 2022c), which reaches between 27 and 47 GW. It shows the importance and relevance of models considering these components in the power system expansion planning.

Expansion planning problems considering DGs may be a hard task. The power generation units from DGs are generally related to uncertainties, such as solar or wind power generation. Moreover, predictions used in planning also incorporate uncertainties. The representation of uncertainties in the expansion planning can change the investment decisions since more components may be required to supply the uncertain scenario, or the investment in a new component may not be economically feasible. In high levels of uncertainty, the demand generally increases, and more generation is required, for example. On the other hand, high levels of uncertainty reduce the confidence in the generation power capacity of DG units, and the investment in these components may not be worth its economic benefits to the system once their cost remains the same.

FIGURE 2 – PROJECTION FOR INSTALLED CAPACITY OF DGs IN BRASIL (2015-2031)



SOURCE: EPE (2022c)

The traditional distribution network was designed to deliver power from the substation to consumers, and the Distribution Network Operator (DNO) was responsible for this operation. The rules for the DNO may change from one country to another; for example, in Brazil, the DNO is a concessionaire accountable for the distribution system's operation, maintenance, and expansion. They are also responsible for connecting new customers to the grid and are regulated by the national electric power agency, Aneel (Agência Nacional de Energia Elétrica).

The classic DNO model is changing with the introduction of distributed generation, renewable sources, energy storage, microgrids, automation, and communication. These technologies impose consequences for the design, operation, maintenance, and improvement of distribution networks, which are a more complex system in this context, where consumers are no longer passive; they can generate power, store energy, and sell it to other consumers. In this context emerge the Distribution System Operator (DSO) and the Active Distribution Network (ADN). The DSO is responsible for operating the network and coordinating the system's automation, communication, and distributed energy resources. The ADN is the modernization of grid functionalities with high penetration and control of DERs (KAZMI et al., 2017).

In an ADN, consumers can decide to install DG or other components seeking their own benefits. They would follow regulations and rules imposed by the government and the DSO, but they are generally free to decide about such investments. Thus, the DSO must operate a complex system highly impacted by the customer's actions. To overcome these challenges, the DSO constantly studies scenarios considering different customer actions.

A consumer or a group of consumers can have more autonomy than just generating and storing energy if they are inside a microgrid (MG). The MG is similar to an ADN but on a small scale; thus, MG is a group of DERs that includes DG units, ESSs, it may include controllable loads, it may operate isolated from the main grid, and incorporate other technologies. The concept has gained popularity due to renewable energy resources and trending new technologies (SAHOO and KISHORE, 2017).

An MG is a concept that can have different structures, such as townhouses, parks, buildings, condo districts, military bases, ports, or any civilian facility that can conglomerate more than one consumer. These MGs can be owned by private investors or by the DSO. For the first case, where investors own the MG, the DSO is responsible for delivering power and ensuring security up to the connection point of the ADN and the MG; the investors or operators chosen by them are responsible for the internal operation of the MG. If the DSO owns the MG, he is responsible for delivering power, operating the internal network, and coordinating its DERs. These definitions are important since the DSO has different rules and decision-making power in each scenario.

In ADNs and MGs, load demand can have different portions, such as critical/non-controllable, deferrable, and controllable (VARASTEH et al., 2019). The deferrable and controllable portions require a certain amount of energy within a given time period, but the exact timing is not defined. These different aspects of the load must be observed during the expansion planning design since the distribution system operator (DSO) only directly controls the controllable portion of the load. In contrast, deferrable loads can be shifted over time, but the DSO does not control them.

In emerging distribution systems, ADNs may incorporate multiple microgrids (MMG), increasing the complexity of the expansion planning problem. In this case, it is necessary to observe requirements in the coordination of the DERs, coordination of the isolated operation of the MGs, choice of the best investment decisions in the expansion planning, and yet seeking the global best solution.

MMGs are complex systems in which a single player can operate all MGs, or multiple players can have different objectives seeking their own benefits. Thus, networks with MMGs may create competitive environments in which pursuing a unique best global solution is not possible.

In this context, it is essential to develop new operational and expansion planning methods for ADNs that are more compatible with the massive implementation of DERs than with radial feeders designed for unidirectional power flow (PINTO et al, 2021 and MONTENEGRO et al., 2022). Since these aspects are modern, complex, and few works consider them jointly, this work was developed to address optimization models for the expansion planning of active distribution networks with multiple microgrids under uncertainties.

The models presented in this work are designed from the DSO's perspective; in other words, they can be used in studies where the DSO seeks to minimize the total cost of investment and operation in modern ADNs. These studies may consider a centralized investment decision, where the DSO selects the best components and locations, or a competitive scenario where consumers and MGs' owners seek their own benefits. Models considering centralized decision-making in MMG systems may be impractical in real-life contexts but are important to point out what would be best for the DSO, since he can create incentive programs to motivate investors to follow what is best for him. On the other hand, robust models considering competitive aspects help the DSO to understand the best decision if investors do not follow those incentive programs.

1.1 RESEARCH OBJECTIVES

This dissertation aims to develop computational methodologies to solve the expansion planning problem for ADNs under uncertainties considering modern aspects of these networks, such as demand response, DERs, MMG, reliability indexes, contingencies, daily 24-hour operation, and energy trade market.

It is important to note that different approaches can be used to deal with uncertainties and competitive aspects of MMGs scenarios, depending on who controls the MGs (if they are single or multiple players) and on governmental regulations. Therefore, this work explores different optimization models for expansion planning problems.

At the end of the work, the reader will have access to modern models and approaches to solve contemporary problems in distribution expansion planning models.

To achieve this objective, the following specific objectives are pursued:

- evaluate techniques for including uncertainty in the expansion planning problem;
- evaluate/develop approaches to incorporate reliability and contingency in the expansion planning problem;
- evaluate demand response formulations;
- evaluate methods to model the competitive aspects of MMGs;
- develop mathematical models and computational implementations to solve proposed formulations;
- apply the methodologies in test systems;
- analyze the results among different uncertainty levels;
- discuss the importance of including uncertainty, reliability/contingency, ESS, demand response, and the competitive aspect of MMGs in the ADN expansion planning problem.

1.2 CONTRIBUTIONS

The ADN expansion planning in multiple microgrid environments, including uncertainty, contingency, demand response, and energy trade, is a complex problem. Therefore, this work is motivated by these challenges, and its main contributions are:

1) Novel multi-level robust models for different cases of expansion planning problems of ADNs with multiple microgrids, including reliability and contingency.
2) The inclusion of demand response in robust models, where the load is represented by three different portions (non-controllable, controllable, and deferrable).
3) Representation of competitive energy trade markets in MMGs using game theory inside a data-driven robust approach.
4) Consideration of the MMG's internal network integrated with the above contributions.

The literature review shows that most works only consider the subjects presented in this dissertation separately; only BiazarGhadikolaei et al. (2019) includes most of this work's aspects but using a stochastic approach and not considering the energy trade market.

Thus, the novelty of this work is to consider these subjects inside robust models. Moreover, this work is motivated by problems where the distribution system operator seeks the best investment decisions for the ADN expansion planning considering uncertainties, reliability/contingencies, demand response, and DERs, in an MMG environment, which are modern subjects in ADNs. It is not known by the author a previous work considering a similar problem using a robust approach.

1.3 PUBLICATIONS

The following publications have been published as part of the research carried out for or related to this work.

- **PINTO, R. S.**; UNSIHUAY-VILA, C.; TABARRO, F. H. Reliability-constrained robust expansion planning of active distribution networks. *IET Generation, Transmission & Distribution*. 2021. https://doi.org/10.1049/gtd2.12263

- **PINTO, R. S.**; UNSIHUAY-VILA, C.; TABARRO, F. H. Coordinated operation and expansion planning for multiple microgrids and active distribution networks under uncertainties. *Applied Energy*, 2021. https://doi.org/10.1016/j.apenergy.2021.117108.

- **PINTO, R. S.**; UNSIHUAY-VILA, C.; FERNANDES, T. S. P.; BARAN JR, A. R. Linear AC Three-Phase OPF Model for Active Distribution Networks with Unbalanced ZIP Loads. *Brazilian Archives of Biology and Technology*, 2022. https://www.scielo.br/j/babt/a/3kvZxJxyDW9G9Yhqmj6cSmq/

- BLASI, T. M.; DE AQUINO, C. C. C. B.; **PINTO, R. S.**; et al. Active Distribution Networks with Microgrid and Distributed Energy Resources Optimization Using Hierarchical Model. *Energies*, 2022. https://doi.org/10.3390/en15113992

- LARA FILHO, M. O. DE; **PINTO, R. S.**; AQUINO, C. C. C. B. DE; UNSIHUAY-VILA, C.; TABARRO, F. H. A Data-driven Robust Model for Day-ahead Operation Planning of Microgrids Considering Distributed Energy Resources and Demand Response. *Brazilian Archives of Biology and Technology*, 2022**.** https://doi.org/10.1590/1678-4324-2023220245

- LARA FILHO, M. O.; **PINTO, R. S**.; DE CAMPOS, A. C.; VILA, C. U.; TABARRO, F. H. Day-Ahead Robust Operation Planning of Microgrids Under Uncertainties Considering DERs and Demand Response. *IEEE PES Innovative Smart Grid Technologies Conference - Latin America (ISGT Latin America),* 2021. https://doi.org/10.1109/ISGTLatinAmerica52371.2021.9543063

- DE CAMPOS, A. C.; **PINTO, R. S.**; DE LARA FILHO, M. O.; UNSIHUAY-VILA, C. A Linear AC Three-Phase Optimal Power Flow Model for Active Distribution Networks and Microgrids. *IEEE PES Innovative Smart Grid Technologies Conference - Latin America (ISGT Latin America*), 2021. https://doi.org/10.1109/ISGTLatinAmerica52371.2021.9543035

- CEREZOLLI, P.; MUTHEMBA, L. J.; **PINTO, R. S.**; UNSIHUAY-VILA, C. Robust Model for Network-constraint Hydro-thermal-wind Operation Planning Considering Uncertainties. *Anais do Simpósio Brasileiro de Sistemas Elétricos*, 2020. https://doi.org/10.48011/sbse.v1i1.2404

1.4 DOCUMENT STRUCTURE

This work presents four models to solve distribution expansion planning problems using distinct approaches to deal with uncertainties and different considerations of the multiple microgrids, reliability, operation, and market aspects. Thus, these models are presented and discussed in separate chapters (from 4 to 7), each describing the method, context/assumptions, formulations, case study, and simulation results.

Chapter 2 presents a literature review, describing works in the literature that are similar or relevant to at least one of the main subjects of this work. A literature review summary is presented at the end of the chapter to facilitate comparing the works.

Chapter 3 introduces the required theoretical background related to the subjects discussed in this dissertation. The chapter does not provide deep information or formulations about these topics but the understanding of their concepts, a description of the methods/approaches typically used by other authors, and an important introduction for the following chapters.

Chapter 4 presents a robust model to solve expansion planning problems of active distribution networks considering uncertainties and a reliability index target. MGs and historical data are not considered in this model.

Chapter 5 shows a robust model similar to the proposal from Chapter 4 but including multiple microgrids and replacing the reliability indexes with a contingency-constrained approach. The model described in this chapter considers only one player owning the ADN and the MGs, the DSO; in other words, a centralized decision-making.

Chapter 6 describes a model to solve problems similar to Chapter 5 but using a data-driven approach to deal with uncertainties. The model also considers only one player owning the ADN and the MGs, which neglects competitive aspects of MMG systems.

Chapter 7 proposes a new model to solve the expansion planning problem of active distribution networks with multiple microgrids, including a data-driven approach to deal with uncertainties and the competitive aspects of MMGs based on game theory. In this model, private investors own the MGs and seek their own benefits.

Finally, the last section presents the conclusions of the work along with the Appendixes and References.

To facilitate the reading, this work uses the notation $\Psi^{constraint}$ to represent a specific set of constraints during the formulation of the computational models. These sets are only defined during their first appearance and in the Appendix of this work.

Appendix A details the information used to reproduce the results in the simulations of this work. Appendix B shows all constraints for the formulations proposed in this work, described in each chapter.

2 LITERATURE REVIEW

The current challenges in active distribution networks have encouraged many studies, including uncertainties, DERs, demand response, reliability, contingency, multiple microgrids, and energy trading. This literature review also considers works that model some of these subjects individually, since few works consider them jointly. This review is extended to transmission and generation works since some approaches from these areas can inspire their use in distribution systems, such as uncertainties and reliability formulations.

This chapter outlines the methodology used to gather and organize the studies for the literature review, provides an overview of the highlights for each study, and includes a summary table that highlights the main contributions of this dissertation.

2.1 METHODOLOGY

During the literature review, two groups of keywords were selected, one related to the main problem and the other associated with specific aspects of the problem. Table I presents the keywords chosen for each group.

TABLE I – GROUPS OF KEYWORDS

Group 1 - Problem	Group 2 – Specific Aspects
Distribution expansion planning	Distributed energy resources
Active distribution expansion planning	Demand response
Microgrid expansion planning	Uncertainties
Robust expansion planning	Reliability
Robust expansion model	Contingency
	Energy trading
	Game theory

The keywords presented in Table I were mixed between the two groups. Different searches were made using the software *Harzing Publish or Perish* with the *Google Scholar* database, limited to 100 works from the last 10 years. Subsequently,

the titles of the works were evaluated, and the database was defined using 300 works from this first filter. From this database were analyzed the abstracts and conclusions, and 100 works were selected for a full reading. Lastly, the final portfolio was defined with 30 works for the literature review.

2.2 WORKS FROM THE LITERATURE REVIEW

This subsection presents some details for each work selected for the literature review, including the type of the problem, main contribution, and highlights. A comparison among these works is presented in the next subsection.

Traditionally, deterministic models were used to solve expansion planning problems, and uncertainties were studied as case studies. With the emergence of technologies that provide accurate historical data and the improvement in computational processing power, stochastic and probabilistic models arise. However, modern networks are too complex and with many uncertainties that make it hard to evaluate probabilistic scenarios for expansion problems. Thus, modern approaches and research started to incorporate the concept of robust optimization in these problems, in which the expansion planning seeks the best decisions under the worst realization of uncertainties. If an expansion decision is robust to the worst-case, it will also be to all other cases.

Qaeini et al. (2019) propose an expansion planning model for active distribution networks considering uncertainties, microgrids, and reliability. The authors calculate reliability indexes, model uncertainties using stochastic programming, and define the price strategy of multiple players through a coordinated bidding approach. The work's main contribution is encountering the conditional value at risk (CVaR) criterion to explore the trading risks of ADN with the wholesale market. Since the model uses stochastic programming, the processing time was approximately 1.5 hours to solve a 33-node case study.

Munoz-Delgado et al. (2016) propose a multistage network expansion planning model for distribution systems considering uncertainty and reliability, using stochastic programming to solve the problem. The proposed formulation does not include microgrids or the representation of the hours of the day. Moreover, the authors consider the proposed algorithm having an effective performance for a stochastic approach, which required 16h to solve a 138-node case study.

Martins and Borges (2011) use a multiobjective approach to solve an ADN expansion planning problem with demand response and uncertainties. The main contribution is using a genetic algorithm to solve the problem, where different scenarios are evaluated inside the algorithm. The proposed formulation does not include microgrids or the representation of the hours of the day.

Zheng et al. (2019) propose a robust model to solve transmission expansion planning problems incorporating demand response and N-1 generation contingencies. The problem is solved using stochastic programming, where the algorithm evaluates the contingency cases. Although the case study is not a distribution system or microgrid, the method and key findings from the results can be extended to distribution problems. The authors conclude that uncertainties can considerably increase the expansion decision costs in extreme scenarios and demand response programs are a helpful approach to reducing these costs.

Munoz-Delgado et al. (2020) formulate a model to solve transmission and distribution expansion planning problems considering uncertainties. The problem is solved using stochastic programming. The authors show the impact on the processing time when increasing the number of operating conditions (defined as the number of different load levels). The algorithm could not solve the 15-node case study when considering the 8.760 hours of a year. The authors conclude that DGs can substantially reduce the total cost of expansion planning problems.

Zakernezhad et al. (2021) propose a multi-level optimization framework for the expansion planning problem of distribution systems with DERS. The main contributions of the work are the inclusion of uncertainties in electricity price, candidates' location, generation, and external shocks' location. The proposed algorithm required 1,961 seconds to solve a 123-bus test system.

Hemmati et al. (2017) present a two-level stochastic microgrid planning tool using stochastic programming. The authors show the importance of including some operational aspects in the long-term expansion planning when DERs are included in the system, which can reduce the planning cost.

BiazarGhadikolaei et al. (2019) also use stochastic programming to solve expansion planning of energy storages in microgrids under uncertainties and demand response. The authors demonstrate that installing storage devices in microgrid cause cost reduction while improving system adequacy.

Wang et al. (2019) solve a robust distribution expansion planning with multiple microgrids considering energy trading and uncertainties. The authors' main contribution is using a methodology with aspects from Stochastic Programming (SP) and Adaptative Robust Optimization (ARO). The conclusion shows a limitation of the model in not considering MGs' individual decisions, which may affect the DSO's decision.

Wu et al. (2018) propose a robust model to solve transmission expansion planning problems under uncertainties, including contingencies. The work's main contribution is the inclusion of N-k contingencies for line failures inside an ARO model. The proposed algorithm required 2.878 seconds to solve a 96-bus test system having its maximum value for the uncertainty budget. The authors show that the uncertainty budget inside ARO models highly affects the expansion plan.

Amjady et al. (2018a) propose an ARO model to solve distribution expansion planning problems with DERs. The framework designed by the authors decomposes the problem into three levels. The first level solves the expansion planning problem, the second level defines the worst-case realization of the uncertainties using a linearized AC optimal power flow (AC-OPF) formulation, and the third level solves a non-linear AC-OPF. Dual cuts are generated among the levels for each iteration until the algorithm reaches convergence. The work's main contribution is the introduction of a non-linear AC-OPF in an ARO model; since these models are computationally expensive, non-linear formulations can become intractable. The results show a highly efficient model, solving a 123-bus test system in less than 17 minutes for a 10-years expansion plan.

Dehghan and Amjady (2016) present a robust generation and transmission expansion planning model considering reliability indexes. The authors propose a tri-level ARO framework, in which the first level solves the expansion planning problem, the second level finds the worst-case realization of the uncertain parameters, and the third stage estimates the reliability indexes using Monte Carlo Simulation. The proposed algorithm took up to 47 hours to solve a 73-bus test system.

Wu, Liu et al. (2018) show a bi-level model for distribution expansion planning problems considering N-1 contingencies in AC-DC hybrid systems. The first level of the problem optimizes the total investment and operational costs, while the second level minimizes the curtailment of DGs under the worst contingency. The authors only considered contingencies in the DC part of the system. They used a genetic algorithm

to solve the problem, which required nearly 4,000 seconds to solve a case study with 31 buses.

Baringo et al. (2020) present a robust expansion planning for distribution systems with electric vehicles, storage, and renewable units. The authors use a bi-level framework to solve the problem. The first level optimizes the expansion planning problem, and the second level finds the worst-case realization of the uncertain parameters. The main contributions of the work are the inclusion and analysis related to electric vehicles (EV), such as quantifying the amount of CO_2 saved with the utilization of EV.

Wu, M. et al. (2019) also propose a bi-level robust planning model for distribution networks under uncertainties. The main contributions of the work are the inclusion of on-load tap changers, capacitor banks, and static VAR compensation. The non-linear terms in the proposed formulation are linearized using a big-M approach or reformulated as a second order conic programming.

Xie et al. (2020) show a two-stage robust optimization model for expansion planning of active distribution systems coupled with urban transportation networks. The work includes the coordination of DERs along with public transportation considering generation and load uncertainties, which is the work's main contribution. Results show the efficiency of the two-stage model, converging in a few iterations in all test cases.

Zhang et al. (2021) propose a data-driven distributionally robust model to solve transmission expansion planning problems. The authors use a contingency-constrained approach for generation. The main contribution of the work is the proposed framework. The problem is solved using a two-stage decomposition, in which the first stage optimizes the expansion planning problem, and the second stage is divided into three subproblems (A, B, and C). Subproblem A detects the worst-case for the contingencies, subproblem B optimizes the power flow, and subproblem C defines the worst-case probabilities for the uncertain parameters.

Wu, T. et al. (2019) present a data-driven approach based on a tri-level formulation for generation and transmission expansion planning problems with high wind penetration. The tri-level problem is solved using a two-stage framework. The first stage solves the expansion planning problem, and the second stage finds the worst distribution probabilities for the uncertain parameters. The authors conclude that data-driven approaches make the best use of the historical data compared to SP models and avoid the over-conservativeness of ARO models.

Shavandi et al. (2018) develop a data-driven model generation expansion planning. The authors cluster the data according to the four seasons of the year. The work's main contribution is the inclusion of the 24 hours of the day and representation of short-term constraints inside a data-driven generation expansion planning model.

Bagheri et al. (2017) present a data-driven transmission expansion planning model. The work's main contribution is the introduction of a data-driven distributionally model for transmission problems. The authors clearly show the comparison between SP, ARO, and DDDRO (data-driven distributionally robust optimization) models. The results present that ARO models are over-conservative, while SP models are highly dependent on a high volume of historical data. On the other hand, DDDRO models are closer to ARO models if there is little historical data available and closer to SP models if a high volume of historical data is available.

Dehghan et al. (2020) show a data-driven distributionally model for the robust planning of microgrids. The proposed model is decomposed into two stages. The first stage solves the expansion planning problem, and the second stage finds the worst case for the distribution probability of the uncertain parameters.

Gao et al. (2020) propose a data-driven distributionally model for active distribution expansion planning jointly with DERs planning. The work's main contributions are: (i) the proposal of a model to solve the expansion planning problem along with the planning of DERs' coordination; (ii) a comparison that shows that DDDRO models can achieve better optimal solutions compared to traditional ARO models and it is more robust than SP models.

Although the model proposed by Masoumi-Amiri et al. (2021) does not include uncertainties or energy trade markets, it formulates the solution for expansion planning problems with MMG considering a cooperative environment between the DSO and private MGs. Results show that cooperative environments benefit both MG's owners and the DSO.

Aschidamini et al. (2022) propose a framework for reliability assessment in distribution expansion planning problems. The proposed method clusters the network in zones according to switches and safety equipment, evaluating the effects of faults on each zone. Since analytical reliability assessments are important due to more easily integrating with other studies, the authors show that the framework can guide the location of the installation and automation of switches by determining zones in which the faults most contribute to the reliability indices.

Boloukat and Foroud (2018) formulate an expansion planning problem for MMG environments, including a local energy market. The proposed model also includes the minimization of reliability indexes and DER, and it is solved using the reformulation of a mixed integer non-linear bilevel programming. Uncertainties are neglected.

Nazari et al. (2021) present a model to solve joint investment of community energy storage systems in distribution networks using modified Nash bargaining theory. The authors do not include uncertainty in their formulation. The work's main contribution is the proposal of a framework to find an optimal point of investment for multiple players (microgrids and DSO). The proposed formulation considers that all players cooperate to reach the optimal point of investment and operation.

Nazari and Keypour (2019) also propose a cooperative expansion planning model based on a bargaining framework. Uncertainties and reliability indexes are incorporated using a stochastic approach. The bargaining framework is created using a two-stage decomposition and a Nash equilibrium point. The work's main contributions are: (i) a model including reliability and energy trading strategy for multiple microgrid systems and (ii) a comparison between non-cooperative and cooperative approaches for energy trade.

Navidi; Moghaddas-Tafreshi (2021) present an agent-based Stackelberg framework for joint expansion planning for microgrid's private owners. The proposed model does not include uncertainties or reliability/contingency, but it considers multiple microgrids and the main grid.

Liang et al. (2021) propose a novel framework for energy trading strategy for multiple microgrids based on a non-cooperative game theory. The authors model the problem considering the gap between the availability of power generation and the load demand; thus, the electricity price is defined throughout a competitive game. The problem is solved using a Particle Swarm Optimization (PSO) algorithm within a few seconds.

2.3 SUMMARY OF THE LITERATURE REVIEW

Active distribution networks face various complex challenges, including distributed generation, energy storage systems, microgrids, uncertainties, demand response, energy trade, and others. Despite the importance of these trends, there is a

limited number of studies that address these challenges jointly in a comprehensive manner in the context of expansion planning for power systems..

Table II summarizes the works reported in the literature compared to the proposed models in chapters 4, 5, 6, and 7 in this work (PM4, PM5, PM6, and PM7, respectively). The comparison shows if the work is related to generation, transmission, or distribution systems (G/T/D), the approach used to deal with uncertainty, if it considers energy trade, includes reliability or contingency in its formulation, DERs, MGs, MMGs, demand response, and if the representation of the hours of the day (24H-OP) is considered in the formulation.

TABLE II – COMPARISON OF THE LITERATURE REVIEW WITH THE PROPOSED MODEL

Ref	G/T/D	Uncertainty Approach	Energy Trade	Reliability / Contingency	DERs	MG	MMG	DR	24H-OP
[1]	D	SP	Y	Reliability	Y	Y	Y	Y	Y
[2]	D	SP	-	Reliability	-	-	-	-	-
[3]	D	SP	-	Reliability	-	-	-	-	-
[4]	T	SP	-	Contingency	-	-	-	Y	-
[5]	T/D	SP	-	-	-	-	-	-	-
[6]	D	SP	-	Contingency	Y	-	-	Y	Y
[7]	D	SP	-	-	Y	Y	-	Y	Y
[8]	D	SP	-	-	Y	Y	Y	Y	Y
[9]	D	SP	Y	Reliability	Y	Y	Y	-	Y
[10]	D	ARO	Y	-	Y	Y	Y	-	Y
[11]	T	ARO	-	Contingency	-	-	-	-	-
[12]	G/T	ARO	-	Reliability	-	-	-	-	-
[13]	D	ARO	-	-	Y	-	-	-	-
[14]	D	ARO	-	Reliability	Y	-	-	-	Y
[15]	D	ARO	-	Contingency	Y	-	-	-	-
[16]	D	ARO	-	-	Y	-	-	-	Y
[17]	D	ARO	-	-	Y	Y	-	-	-
[18]	D	ARO	-	-	Y	Y	-	-	Y
[19]	T	DDDRO	-	Contingency	-	-	-	-	-
[20]	G/T	DDDRO	-	-	Y	-	-	-	-
[21]	G	DDDRO	-	-	-	-	-	-	Y
[22]	T	DDDRO	-	-	-	-	-	-	-
[23]	D	DDDRO	-	-	Y	Y	-	-	Y
[24]	D	DDDRO	-	-	Y	-	-	-	Y
[25]	D	-	-	-	Y	Y	Y	-	Y

Ref	G/T/D	Uncertainty Approach	Energy Trade	Reliability / Contingency	DERs	MG	MMG	DR	24H-OP
[26]	D	-	-	Reliability	-	-	-	-	-
[27]	D	-	Y	Reliability	Y	Y	Y	-	Y
[28]	D	-	Y	-	Y	Y	Y	-	Y
[29]	T	-	Y	-	Y	Y	Y	-	-
[30]	D	-	Y	-	Y	Y	Y	-	Y
PM4	**D**	**ARO**	**-**	**Reliability**	**Y**	**-**	**-**	**-**	**Y**
PM5	**D**	**ARO**	**-**	**Contingency**	**Y**	**Y**	**Y**	**Y**	**Y**
PM6	**D**	**DDDRO**	**-**	**Contingency**	**Y**	**Y**	**Y**	**Y**	**Y**
PM7	**D**	**DDDRO**	**Y**	**Contingency**	**Y**	**Y**	**Y**	**Y**	**Y**

Y: yes, Ref: reference, PM: proposed model, ARO: Adaptative Robust Optimization, SP: Stochastic Programming, DDDRO.: Data-Driven Distributionally Robust Optimization, DR: Demand Response.

The references in Table II are listed below.

[1] Qaeini et al. (2019)

[2] Munoz-Delgado et al. (2016)

[3] Martins and Borges (2011)

[4] Zheng et al. (2019)

[5] Munoz-Delgado et al. (2020)

[6] Zakernezhad et al. (2021)

[7] Hemmati et al. (2017)

[8] BiazarGhadikolaei et al. (2019)

[9] Nazari and Keypour (2019)

[10] Wang et al. (2019)

[11] Wu; Liu, Y.; et al. (2018)

[12] Dehghan et al. (2016)

[13] Amjady et al. (2018a)

[14] Dehghan; Amjady (2016)

[15] Wu; Liu, P.; et al. (2018)

[16] Baringo et al. (2020)

[17] Wu, M. et al. (2019)

[18] Xie et al. (2020)

[19] Zhang et al. (2021)

[20] Wu, T. et al. (2019)

[21] Shavandi et al. (2018)

[22] Bagheri et al. (2017)

[23] Dehghan et al. (2020)
[24] Gao et al. (2020)
[25] Masoumi-Amiri et al. (2021)
[26] Aschidamini et al. (2022)
[27] Boloukat and Foroud (2018)
[28] Nazari et al. (2021)
[29] Navidi and Moghaddas-Tafreshi (2021)
[30] Liang et al. (2021)

Table II highlights that:

- Works solving distribution problems typically includes the hours of the day (24H-OP) in their formulation;
- Works using SP models tend to incorporate more subjects;
- Works using ARO models normally do not include all the aspects considered in this dissertation;
- Few works using DDDRO include contingency and reliability;
- Even few works include energy trade along with uncertainties or reliability/contingency.

This literature review did not find the following:

- An ARO model for distribution expansion planning considering reliability/contingency, DERs, MMGs, and 24H-OP;
- A DDDRO model for distribution expansion planning considering the same aspects;
- The inclusion of energy trading strategy in the same problem.

Given the findings of the literature review, the models proposed in this dissertation aim to address the gaps in the existing research. Since Zakernezhad et al. (2021) and Nazari and Keypour (2019) cover some of the main aspects cited in the literature reviews throughout an SP model, this dissertation does not include SP algorithms in the proposed models.

3 THEORETICAL BACKGROUND

This work uses many concepts from distribution systems, and this chapter aims to clarify these subjects and present the considerations applied to the proposed models. The following subsections of this chapter provide theoretical background focusing on the concept of each subject; thus, a few formulations and technical understanding are provided, which are detailed in the next chapters of this dissertation.

3.1 EXPANSION PLANNING FOR ELECTRIC POWER SYSTEMS

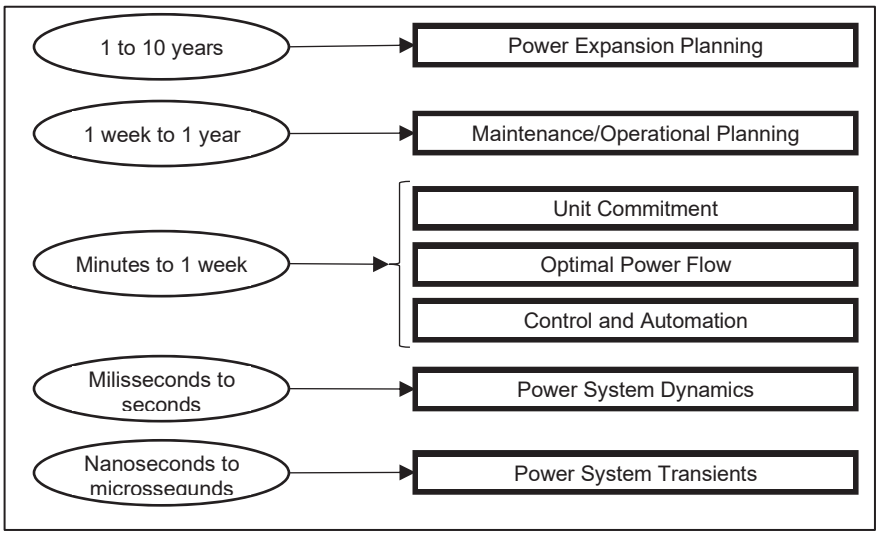
The use of new technologies has constantly increased in electric power systems, and the operation and planning of the greatest system created by mankind are complex tasks. The inclusion of new technologies in power systems provides the ability for real-time monitoring, quick response to anomalies, reduction of costs, and improvement in the safety and reliability of the system. These challenges have motivated studies aiming to achieve the best (or near the best) solutions to these problems.

There are different sorts of studies regarding electric power systems. The main feature that differentiates them is the time horizon considered in the study, but not limited to it. Seifi and Sepasian (2011) present a classification for power system studies, reproduced in Figure 3.

Figure 3 shows that power expansion planning problems are typically on a horizon from 1 to 10 years. The main objective of these problems is to determine the best investments to improve safety, reliability, reduce costs, and meet demand growth.

The power expansion planning problem is divided into generation, transmission, and distribution. The primary function of a distribution network is to transfer energy from the transmission system to end customers carrying out the required voltage transformations. This part of the power system is also responsible for integrating power supply from distributed generators and maintaining the voltage level and power quality within given limits.

FIGURE 3 – CLASSIFICATION FOR POWER SYSTEM STUDIES



SOURCE: adapted from Seifi and Sepasian (2011)

Thus, distribution networks are the most impacted by consumers' actions, such as installing batteries and generators. In modern distribution networks, the DSO constantly faces uncertainties regarding the future amount of power required by consumers while maintaining reliability indexes at standard levels. Therefore, the distribution network is the scope of the study of this dissertation.

Expansion planning models considering periods over 5 years are typically used to redesign networks, relocate loads, or build new substations. Since the proposed models do not include these aspects and consider the addition of components such as DG, ESS, capacitors, and the reinforcement of existing lines, the periods in the expansion models are defined as 3 years for the models presented in chapters 4 to 6 and 5 years for the model presented in chapter 7.

3.2 DERS AND THE REPRESENTATION OF 24H-OP

The concept of distributed energy resources has been widely discussed in recent works due to its importance in distribution networks. Traditionally, distribution networks are connected to a substation, the primary power source for the entire grid, increasing the risk of faults interrupting the power supply for loads. On the other hand, systems incorporating DERs can supply their loads even if a fault occurs.

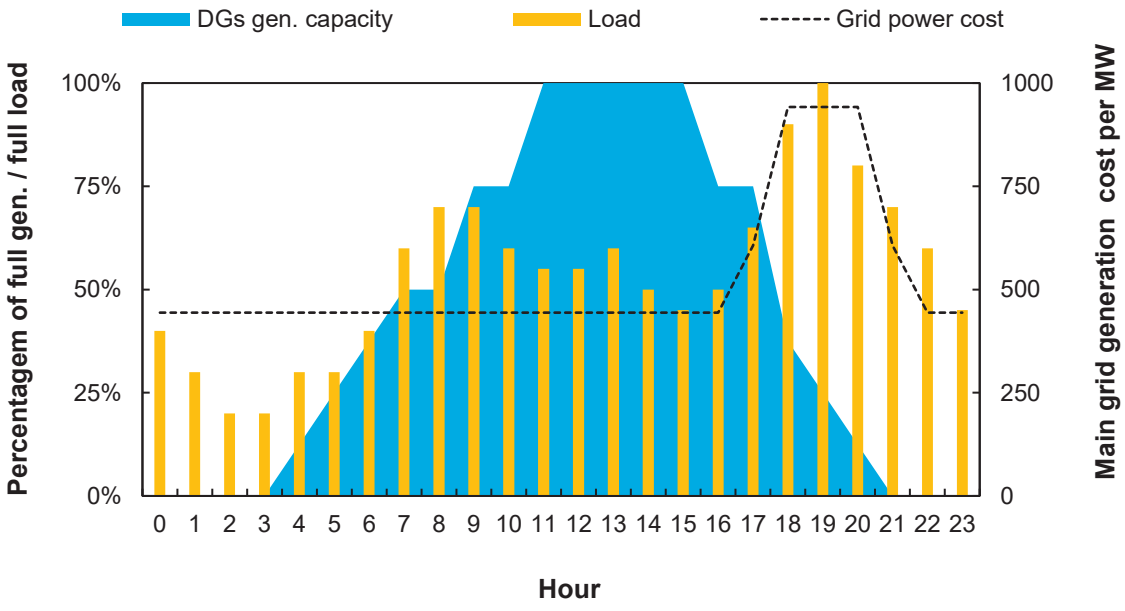
Since distribution expansion planning aims to determine the best investments in the system for a long-term operation, most works in distribution expansion planning

model the generation and load as constant for its daily operation. This approach provides reasonable results for traditional distribution expansion problems; however, it may not precisely represent the DERs.

The decision to install DGs and ESSs is overly sensitive to the main grid's generation capacity, load levels, and power generation cost throughout the hours of the day (24H-OP).

To illustrate the importance of representing the 24H-OP in systems with DERs, Figure 4 shows a generic representation of the generation capacity of a solar-based DG unit, a load profile, and the grid power cost for a 24-hour horizon, such as modeled in Dehghan et al (2020), Nazari et al. (2021), Liang et al. (2021), and others.

FIGURE 4 – EXAMPLE OF 24-HOUR REPRESENTATION OF GENERATION CAPACITY, LOAD PROFILE, AND GRID POWER COST



SOURCE: the author (2021)

If an expansion planning formulation does not consider the 24H-OP, the DGs generation capacity, load profile, and grid power cost would be represented as a unique value for the entire day of operation. Thus, the model would not consider the overnight unavailability of solar-based DG units, the different load levels during the day, or the grid's power cost at different hours of the day.

Furthermore, the benefits of installing ESS units are usually associated with the electricity price at peak level hours and the unavailability of DGs at specific hours

of the day. Moreover, the importance of including the 24H-OP representation in the expansion planning problem is directly related to the need to represent DERs' coordination in the model. The downside of incorporating the 24H-OP is that the complexity and the number of variables of the problem considerably increase; thus, methodologies to effectively solve these problems are relevant for ADN's studies.

3.3 RELIABILITY IN ELECTRICAL POWER SYSTEMS

Electrical power systems are the largest systems created by mankind (Chen, 2004), and they have evolved over decades, including the presence of technologies, real-time monitoring, and new components to ensure continuity and quality in the power supply. Reliability indexes are essential to measure the system's reliability and maintain high standards in power systems.

Regulatory authorities in many countries impose penalties (or rewards) related to these indexes, which introduce a component of financial risk to the investor due to the uncertainty associated with preserving a specific level of system reliability (Da Silva et al., 2006).

The reliability indexes may be calculated using historical data of the system or estimated by simulations using each component's failure rate and repair time. Some of the most used indexes in power systems are:

- **SAIDI** – System Average Interruption Duration Index;
- **SAIFI** – System Average Interruption Frequency Index;
- **CAIDI** – Customer Average Interruption Duration Index;
- **CAIFI** – Customer Average Interruption Frequency Index;
- **EENS** – Expected Energy Not Supplied;

Although these indexes are internationally known, some countries have their corresponding indexes; for example, in Brazil, SAIDI is defined as DEC, SAIFI is FEC (Da S. PINTO et al., 2009).

In expansion planning problems considering reliability indexes, the objective function of the problem aims to improve these indexes or ensure that the system achieves desired levels. Historical data on failure and repair time help to understand the current level of reliability. However, only historical data does not provide enough

information to estimate these indexes when placing a new component in the system. There are several techniques in the literature to estimate reliability indexes, among which stand out the following:

- *Minimal Cut Set* (Billinton and Allan, 1992) is an analytical and deterministic approach used to estimate reliability indexes in power systems. The method evaluates a set of components that connect the power source to the loads, and if one or more members of this set fail, the power supply is interrupted for that specific load. By using the failure rate and repair time of these components, the reliability indexes can be calculated. In the Minimal Cut Set concept, there are different orders of cuts, with a first-order cut being defined as a component that interrupts the load's power supply if just one member fails. A second-order cut is a set of components that, if just one fails, the power supply continues, but if two or more components fail, the power supply is interrupted. The concept of cut order is essential in reliability studies because cuts of second-order or higher have small contributions to reliability indexes and, generally, they may be neglected (DA SILVA et al., 2006 and BILLINTON et al., 1998). This method is efficient as it does not explore all component failures, and the computational performance is much higher.
- *Monte Carlo Simulation (MCS)*: this method is widely used in any problem with chances for events to occur. Kagan et al. (2009) present an MCS along with an optimal power flow algorithm. The approach performs an extensive number of simulations and, for each iteration, estimates the random chances that the components have to fail. If a component fails, it is removed from the system, and the effects are computed. Thus, the reliability indexes can be calculated after the convergence of the process. Da Silva et al. (2006) propose a chronological MSC assessment for distribution system reliability, which defines each component's operating state along the expansion planning horizon according to their failure rate.

There are other approaches to estimating reliability indexes, and each technique has advantages. For example, Aschidamini et al. (2022), presented in the literature review, propose a novel framework for reliability assessment, which creates zones that help to guide expansion decisions.

For the Minimal Cut Set, the reliability is computed without exploring all component failures, and the computational performance is much higher. On the other hand, MCS provides useful information regarding the chances of different scenarios over a probability density function, and it is more flexible to introduce analisys or action during the faults.

This dissertation uses the chronological MSC to estimate the reliability indexes, detailed in chapter 4.

3.4 CONTINGENCY IN ELECTRICAL POWER SYSTEMS

Since components from second-order cuts (or higher) used in the Minimal Cut Set approach have small contributions to reliability indexes, their failure rates may be neglected (DA SILVA et al., 2006). Modeling contingencies is an approach that can complement the estimation of reliability indexes inside the optimization model for distribution systems, which is very expensive in computational manners.

The most popular formulation considers the N-1 contingency in the network's operation, which requires the system to operate normally if one component is off, as presented in Lin et al. (2019), Wu; Liu Y.; et al. (2018), and Zheng et al. (2019).

Including N-1 generation contingency in the ADN expansion planning problem is essential for a reliable isolated operation of MGs, enabling the maintenance of any DG unit inside an MG without interrupting the isolated operation and improving reliability indexes.

Similarly to reliability indexes, contingencies can also be introduced into ADN expansion planning models by using MSC. However, the most common methods are constrained approaches, where contingencies are modeled as constraints in the problem, making it possible to use exact models to solve the optimization problem. In contingency-constrained approaches, contingencies are defined as constraints in the problem formulation, and multiple cases of contingencies are imposed on the expansion decision.

3.5 DEMAND RESPONSE

A reliable operation of power systems requires a balance between supply and demand. Operating these systems is a complex task since the load and generation

levels can change rapidly and unexpectedly due to many reasons, such as generation unit outages, line outages, and sudden load change (ALBADI and El-SAADANY, 2007). Moreover, load peak levels can require a surplus generation capacity for the system, increasing the investment cost. In this context, ESSs and demand response help to reduce the overload in the main grid or DG units.

Albadi and El-Saadany (2007) define demand response as changes in electricity usage by end-use customers from their normal consumption patterns over time. Further, demand response can also be seen as incentive payments designed to induce lower electricity consumption at times of high wholesale market prices or when system reliability is jeopardized.

Demand response can be used as a tool to shift the load consumption away from peak levels and reduce system overload or total cost. However, if the DSO does not have control over this process and the load is shifted, it can result in unexpected behaviors, such as being shifted to peak-level hours.

Thus, demand response is commonly used as a tool to represent expected behaviors from the consumers that would benefit the DSO as a response to incentive programs, such as financial benefits for using energy at lower-level hours; however, this optimistic point of view does not fit in a robust approach.

To overcome this situation, Varasteh et al. (2019) propose the division of the load into three different portions: critical/non-controllable, controllable, and deferrable. The non-controllable portion is defined as loads that cannot be shifted in time and are subject to uncertainties. Both controllable and deferrable portions of the load require a certain amount of energy within a given time period, but the exact timing is not defined. The controllable loads are controlled by the DSO and are easier to predict, and are scheduled for periods of the day that are most suitable for the DSO. On the other hand, the deferrable loads are expected to be shifted due to financial motivations or agreements, but there is high uncertainty regarding this information since the DSO has no control over it.

Assuming that deferrable loads are placed only during the best hours of the day is overly optimistic and unrealistic. Due to the high uncertainty in the behavior of the deferrable portion of the loads, this dissertation also proposes a robust model considering this aspect, seeking the best investments for the worst-case realization of the load shifting. Therefore, it considers controllable and deferrable loads, using a single formulation.

3.6 OPTIMAL POWER FLOW

In a load flow problem, the system is analyzed in steady-state operation. Some variables are specified and fixed, such as real and reactive power at *PQ* buses, real powers and voltages at *PV* buses, and voltages and angles at slack buses. However, it does not always lead to optimal operating conditions, as infinitely variable choices exist in specifying a balanced steady-state load flow situation (DAS, 2017).

The optimal power flow (OPF) problem traditionally emphasizes the optimization of the system's operation costs; however, this problem can become quite complex. The OPF problem can be generally described as the minimization of power generation or any type of cost, as well as the maximization of profits or any economic variable, in an interconnected system where real and reactive power, transformer taps, and phase-shift angles are controllable within a wide range of inequality constraints (DAS, 2017).

In the OPF formulation, the most complex equations model the lines' power flow. There are several different mathematical representations for these equations, some non-linear, others linear but representing only the active portion of the power flow, and some linear representing both active and reactive portions.

The choice of adequately representing the power flow in the lines is essential, if not crucial, in the ADN formulation. Radial distribution systems may have problems regarding voltage levels in buses at the end of the network, and some simplifications in their formulations may provide inaccurate results, such as neglecting the reactive portion of the power flow. On the other hand, the complexity imposed in modern ADN by including DGs, ESSs, and demand response requires a fast and scalable formulation that can handle its size, complexity, and representation of modern components (LIU, 2020).

The non-linear representation of the power flow in the lines can be defined as follows.

$$p_l^L = v_s^2 G_l - v_s v_r G_l \cos(\theta_{sr}) - v_s v_r B_l \sin(\theta_{sr}) \quad (1)$$

$$q_l^L = -v_s^2 B_l - v_s v_r B_l \cos(\theta_{sr}) + v_s v_r G_l \sin(\theta_{sr}) \quad (2)$$

where p_l^L and q_l^L are the active and reactive power in the lines; G_l and B_l are the conductance and susceptance in the lines; v_s, v_r, and θ_{sr} are the voltage in bus *s*, voltage in bus *r*, and the difference of the angle between buses *s* and *r*.

Equations (1) and (2) are accurate and the most used equations in power flow studies; however, they are non-linear equations and can turn problems into intractable for some ADN studies (considering reasonable computational time).

One of the most used simplifications in the OPF problem is the linearization in the power flow equations. The linear direct current (DC) OPF has been widely used to solve complex expansion planning problems. The following equation represents the formulation used in the DC power flow to represent the power flow in the lines.

$$p_l^L = -B_l \theta_{sr} \tag{3}$$

The linear DC power flow is a consistent simplification for bus angles near zero and voltage levels near 1 pu. However, this formulation does not provide information on voltage magnitudes and reactive power flow in the lines, which may be crucial information for ADN systems. Although the DC power flow can be applied in distribution systems, its application is more common in transmission expansion planning problems.

To properly represent the active and reactive power flow in ADN systems, some works have proposed the linear AC OPF, which provides the necessary information on voltage magnitudes and reactive power flow in the lines. Yang et al. (2017) propose the following linear AC formulation for power flow in the lines.

$$p_l^L = G_l v_{sr} - B_l \theta_{sr} \tag{4}$$

$$q_l^L = -G_l \theta_{sr} - B_l v_{sr} \tag{5}$$

The linear AC power flow for the lines presented in equations (4) and (5) provides simplicity and accurate results (YANG et al., 2017), while voltage levels and the reactive power in the lines are obtained.

The choice of which power flow formulation should be used depends on many factors such as the horizon, type, objective of the problem, and many other aspects. Due to the simplicity, practicality, and accuracy of the results presented in Yang et al. (2017), this work uses the linear AC power flow formulation.

3.7 MULTIPLE MICROGRIDS

According to Nawaz et al. (2022), microgrid is the basic building block of the smart grid concept, which provides a controlled environment for efficient control and utilization of distributed renewable resources and consumer load demand. MG can operate autonomously in an islanded mode as well as a controlled entity in grid-connected mode. However, due to the associated uncertainties with DERs and related control and management challenges, it is a hard task to plan and control them. With recent advancements in power electronics and fast improvement in communication infrastructure, interest has been shifted towards the networked operation of multiple microgrids (MMGs) for more efficient utilization of DERs and coping with uncertainty challenges (ALAM et al., 2019).

In MMGs concept, multiple individual MGs are physically interconnected through a distribution bus in a remotely close area and functionally networked to achieve cooperative benefits with adjacent MGs. MMGs can provide features such as increasing the penetration ratio of DERs into MGs and distribution networks, ensuring MGs' stable and efficient operation, and delivering backup power to prioritized critical loads. The stability and reliability of the entire system can be improved with MMGs through efficient mutual coordination and cooperative energy exchange among individual MGs and the main grid (ZOU et al.2019). This also helps reduce the main grid's burden and minimize distributed transmission line congestion. With the capability of energy sharing among MGs, the operation cost is reduced, and load demand is met with more efficient utilization of DERS.

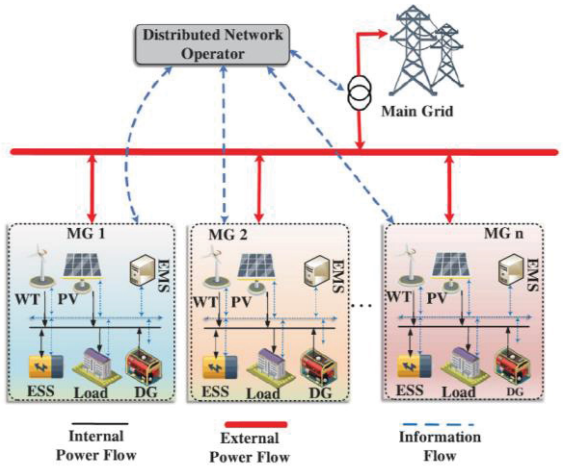
The energy management system (EMS) is critical in achieving stable and cost-effective MMG operations by managing and coordinating dispatchable distributed generation, energy storage systems, and energy trading among microgrids to achieve power supply-demand balances and reduce consumer dissatisfaction. High penetration of DERs and time-variable consumer load with uncertainties inflect intermittent in MMGs, significantly impacting energy management (MOHAN et al., 2017). Thus, the energy scheduling decision of one MG will be substantially affected by other neighboring MGs (ZARGAR et al., 2021).

MMG's systems have several different architectures regarding the direction of their power flow, information, and control (NAWAZ et al., 2022). In radial architectures, the MGs are only connected to the main grid and do not exchange power or information

among them, as illustrated in Figure 5. Figure 6 shows the daisy-chain architecture, where the adjacent MGs can exchange energy and information. Figure 7 presents the mesh architecture, in which each MG can exchange power and data with any other MGs; moreover, mesh architectures can have variations in the connections, such as, only the exchange of information among all MGs and power among the neighbors.

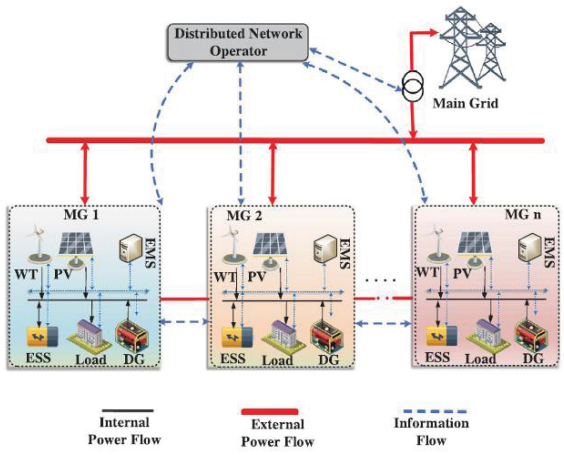
Depending on the architecture, governmental regulation, and who owns the MGs, the MMG system's environment can have different behaviors, such as a cooperative or non-cooperative environment, centralized or decentralized decision, and even a local energy trading market.

FIGURE 5 – RADIAL ARCHITECTURE OF MMG



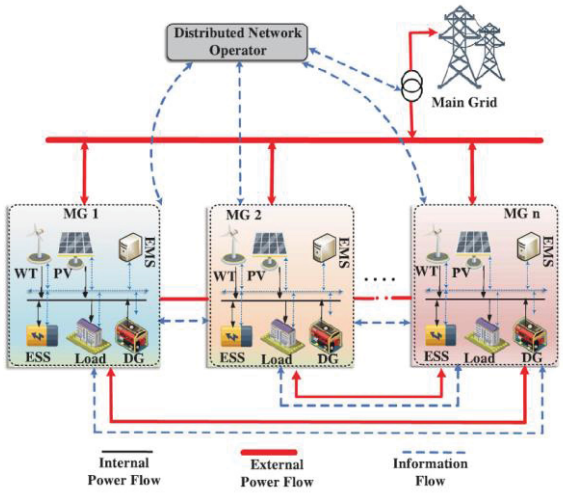
SOURCE: Nawaz et al. (2022)

FIGURE 6 – DAISY-CHAIN ARCHITECTURE



SOURCE: Nawaz et al. (2022)

FIGURE 7 – MESH ARCHITECTURE OF MMG



SOURCE: Nawaz et al. (2022)

Before creating an expansion planning model for ADN with MMG, it is essential to define its architecture, who controls the MGs, and the plan's objective. These aspects drive the decision-making. In this context, this dissertation explores three different circumstances:

- In chapter 4: an ADN without MGs.
- In chapter 5 and 6: an ADN having 3 MGs owned by the DSO. The MGs are physically connected and can exchange power, but the DSO centralizes the data processing and decision.
    - This circumstance can also be seen as a case where private investors own the MGs, and the DSO wishes to study the MG's decisions that would best benefit him to create incentive programs. However, the MGs cannot trade energy among themselves, only sell/buy from the main grid.
- In chapter 7: an ADN having 3 MGs owned by private investors. In this case, the MGs can trade energy among themselves, and a local energy trading market is considered. It is assumed a mesh architecture where any MG can trade energy with another.

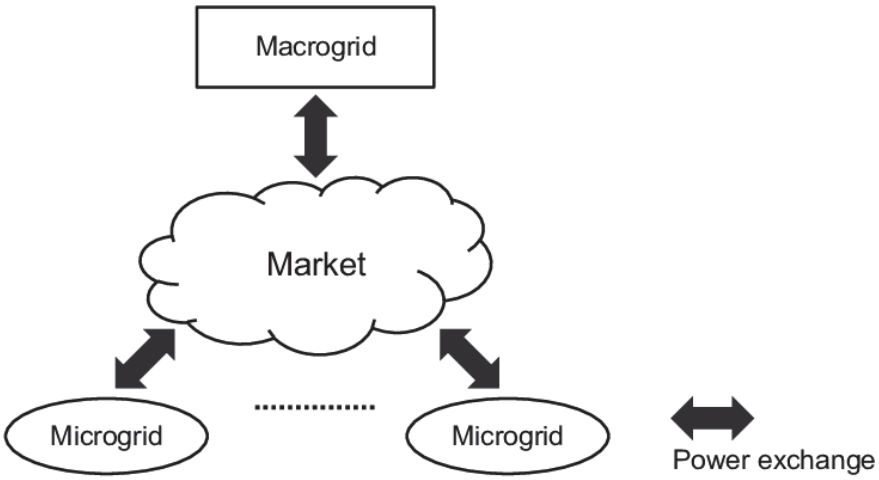
3.8 ENERGY TRADING IN MULTIPLE MICROGRIDS' ENVIRONMENTS

In scenarios where private investors own the MGs and can exchange power, the players may buy/sell energy among themselves, creating a local energy trade market illustrated in Figure 8. Typically, a macrogrid is represented by the ADN and the system has two or more MGs.

Since each MG makes individual investment and operational decisions, its strategy is divided into cooperative and non-cooperative (or competitive) approaches (KARIMI et. Al, 2021).

In cooperative strategies, all microgrids cooperate to maximize the overall benefit of the MMG's environment. Generally, the energy transaction with minor power loss should be prioritized. A price mechanism based on auction models provides a more reasonable trading price among microgrids through optimal biddings (MOVAHEDNIA et al., 2022).

FIGURE 8 – DISTRIBUTED ENERGY TRADING AMONG MULTIPLE INTERCONNECTED MICROGRIDS



SOURCE: Lee et al. (2015)

In non-cooperative strategies, each microgrid aims to maximize its own profit without concern for other microgrids. Generally, the energy trading mechanisms in MMGs are designed to satisfy the demand locally. Each buyer/seller microgrid hopes to purchase/sell power from/to seller/buyer microgrids as much as possible. Thus, competitions usually exist among microgrids, and various non-cooperative game models are employed to formulate competitive strategies. The simultaneous trade-off between the DSO and microgrids can also be resolved with two-level game models (NAWAZ et al., 2022).

The non-cooperative strategy is more common since it represents a free market where the players seek personal benefits. From the perspective of the DSO, this increases the complexity of expansion planning problems, since there are infinite possibilities of decisions by the MGs' owner. Game theory algorithms are commonly used to find a Nash equilibrium point, which occurs when none of the players can increase their profit by changing their strategy unilaterally (NAEBI et al., 2020).

Microgrids are expected to have motivations and benefits to store energy in a market with fluctuating energy prices. In such a context, those microgrids as sellers may choose to keep part of the superfluous energy. Likewise, those microgrids as buyers may wish to buy and store extra energy if available because they can use or resell it at a later time (LEE et al., 2015).

Despite the endless number of possibilities, if the DSO is prepared for the worst case or can rely on probabilities of scenarios, it can define the best decisions considering this environment of uncertainties.

3.9 UNCERTAINTIES

The development of power systems with the introduction of new technologies and concepts, such as DERs and MGs, has caused significant challenges in the scheduling and operation of these networks, such as the increase in uncertainties for generation and load demand (ALEEM et al., 2020).

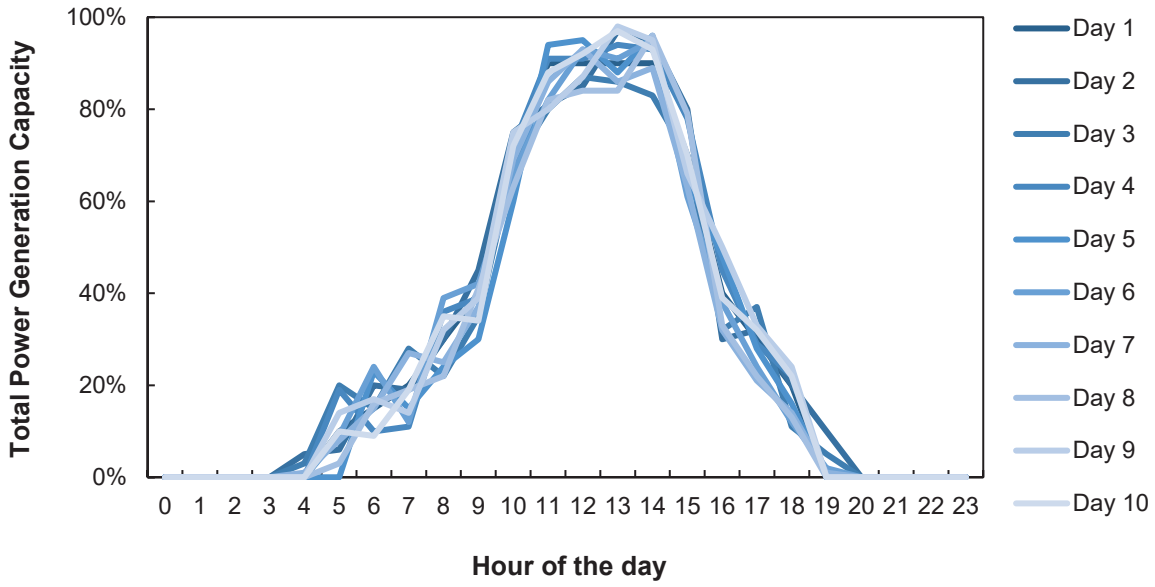
Any system operation or planning does not have all variables as deterministic parameters in real-world problems. Also, any planning uses predictions to determine future values for system parameters. Conventional prediction approaches use average historical values or models to forecast such parameters. However, these methods typically provide deterministic values for the future or estimated values within error ranges. Therefore, the process of evaluating the future value of the system parameters is subject to uncertainty.

Figure 9 presents an example of historical data for the generation capacity of a generic solar-based DG unit. For any specific hour of the day, the DG's total power generation capacity has an average expected value, but its exact value cannot be defined due to its stochastic nature. Then, the predicted value for the generation capacity at any hour of the day cannot be described as a deterministic parameter.

Although the generation capacity of a solar-based DG unit cannot be defined as a deterministic parameter, it has an expected value and bounders, noteworthy information for models considering uncertainties.

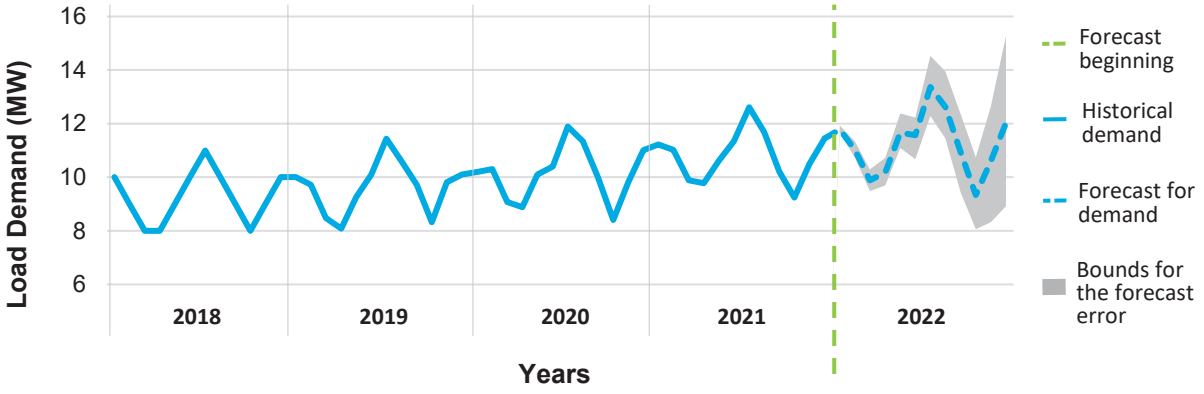
Figure 9 represents uncertainties for a generation unit, and Figure 10 shows an example of historical data and forecast for a generic load.

FIGURE 9 – EXAMPLE OF UNCERTAINTY IN POWER GENERATION



SOURCE: the author (2021)

FIGURE 10 – EXAMPLE OF UNCERTAINTY IN LOAD DEMAND



SOURCE: the author (2021)

The historical data presented in Figure 10 shows the same pattern as Figure 9, where different values are observed for the same month over the years. The forecast of this data shows an expected value within a tolerable error range. Statistic techniques provide this predicted value within the error limits (bounds for the forecast error), representing uncertainties in the parameter's future value. Further predictions from the current date have greater ranges for tolerable error.

There are several methods to deal with uncertainties in optimization problems in power systems, such as stochastic programming (SP), Info-Gap Decision Theory (IGDT), robust optimization (RO), data-driven models, and others.

3.9.1 Deterministic Methods

Deterministic methods are the most used formulations to solve classical power system problems; however, it does not model the many scenarios that uncertainties could create. These models only provide the results for a single case; thus, it is necessary to define an exact value for the future value of all system parameters.

Deterministic models can be used in scenarios containing uncertainties by creating different cases and studying the impact of forecasted parameter variation. However, the definition of these scenarios can produce cases far from the worst case and result in over-optimistic solutions.

3.9.2 Stochastic and Probabilistic Methods

Stochastic and probabilistic methods are one of the simple and earliest methods, which assume all uncertain parameters as random variables (ALEEM et al., 2020). In these methods, each variable may take any stochastic value within a range and respect its probability density function. Three main techniques are used for uncertainty management in this case: Monte Carlo Simulation (MCS), point estimation method (PEM), and scenario-based optimization method (ALEEM et al., 2020).

In the MCS, samples for each uncertain parameter are generated according to the nature of the variable (stochastic/probabilistic). For each sample, a deterministic model solves the problem, and the results are computed. The process is repeated for many iterations until it reaches a convergence point. The PEM is based on the concept of statistical moments for uncertain parameters. Unlike the MCS, the PEM only generates two samples for each parameter. Decision-making based on scenarios is another technique that is based on stochastic/probability theory. A scenario list is generated using each uncertain parameter's corresponding set and probability. In this case, it is performed an extensive exploration of scenarios.

The stochastic and probabilistic methods have the advantage of exploring many scenarios, providing detailed information on each case and probabilistic density

curves. The main disadvantages of these methods are the need for probability distribution functions, which may not be available in some problems, and the high computational effort.

3.9.3 Info-Gap Decision Theory (IGDT)

The IGDT was first proposed by Ben-Haim (2006), and it is a non-probabilistic and non-fuzzy method for quantification of uncertainty. In this method, the uncertainty is defined as the distance between what is known (or predicted) and what may happen in reality (SOROUDI and EHSAN, 2013). One of this method's applications is helping decision-makers maximize the robustness of their decisions against uncertainties.

Aleem et al. (2020) define that when the value of the uncertain parameter is not equal to the predicted value, and this is unknown, IGDT is implemented to find a good solution that gives the robustness feature to the value of the objective function against the predicting error.

The IGDT relies on what is known, and any other variables and parameters (that are unknown) are outputs from the method. An example for ADN expansion problems is using the investment budget as a known parameter and input for the problem. At the same time, it is desired to identify the worst-case realization of the uncertainty that would fit into this budget. This approach does not require extensive exploration of scenarios as the stochastic and probabilistic methods.

The IGDT approach has the advantage of only using known parameters as inputs, and the unknown parameters are outputs of the process. Although IGDT is an efficient approach to studying the maximum level of uncertainties supported by a given investment budget, it does not provide the required investment for different levels of uncertainty.

3.9.4 Adaptative Robust Optimization

The origins of robust optimization date back to the establishment of modern decision theory in the 1950s with the use of worst-case analysis and Wald (1945)'s maximin model as a tool for treating severe uncertainty. Over the years, the theory has been applied in statistics, operations research, power system problems, control theory, finance, and many other fields. Recently, Robust Optimization (RO)

achieved great advances in optimization under uncertainty, in which the uncertainty model is not stochastic, but rather deterministic and set-based. Instead of seeking to immunize the solution in some probabilistic sense to stochastic uncertainty, in the RO, the decision-maker constructs a solution that is feasible for any realization of the uncertainty in a given set.

Thus, the RO provides the best solution for the worst-case realization of uncertainties without searching all possible scenarios. The motivation for this approach is twofold. First, the model of set-based uncertainty is simple and effective in representing possible uncertainty cases. Second, computational tractability is also a primary motivation and goal (BERTSIMAS et al., 2011).

The Adaptive Robust Optimization (ARO) models cases where the decision-makers make two types of decisions: “here-and-now” decisions that must be made immediately, and “wait-and-see” decisions that can be made at some point in the future (YANIKOĞLU et al., 2019). ARO improves the robust optimization framework by accounting for any information the decision-maker does not know now, but may learn before making future decisions. ARO is applicable in the real world whenever past decisions and new information influence future decisions (BEN-Tal et al., 2004).

Adaptative Robust Optimization (ARO) has been one of the most used methods to solve power system expansion problems including uncertainties. The concept of the ARO relies on finding the best decisions for the worst-case realization of the uncertainty, which makes any system robust against uncertainties.

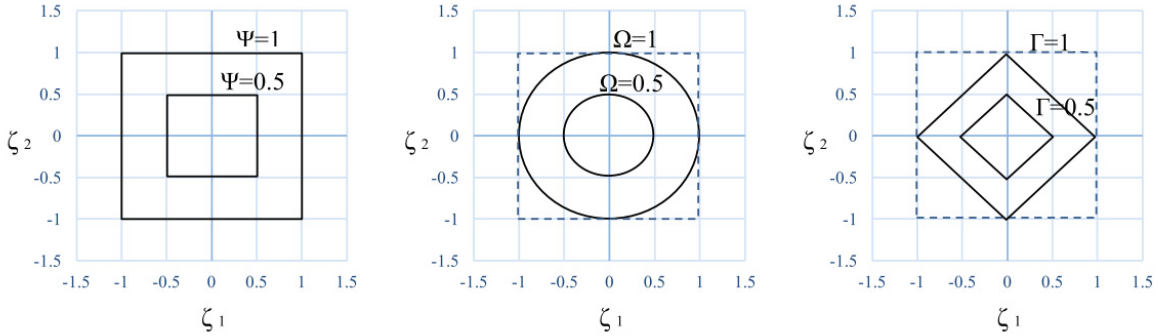
An example in distribution expansion problems is finding the best investment that would minimize the investment and operation costs for the worst-case realization of generation and load demand, which is a scenario that may occur. Moreover, if the system is immune to the worst uncertainty case, it is robust to all other cases.

The great advantage of ARO models is that it is unnecessary to explore all cases, and historical data are not required, like in the stochastic/probabilistic approaches. Compared to the IGDT, the ARO provides the required budget for the worst-case scenario, while the IGDT provides the uncertainties to fit the expected budget.

The ARO method represents the uncertainties through robust sets, which are generally easier to obtain than probability distribution functions. Moreover, robust models are comparatively less complex than stochastic programming models and require less computational effort.

The representation of uncertainty can be performed in many forms through robust sets. Figure 11 presents the three main robust sets used in the power system (JALILVAND-NEJAD et al., 2016).

FIGURE 11 – GENERIC UNCERTAINTY ROBUST SETS



SOURCE: Jalilvand-Nejad et al. (2016)

The representation of uncertainty robust sets denotes the relation between different uncertainty variables of the problem. If the historical data of this variable is available, this set can be adapted to fit this data best; otherwise, the three sets presented in Figure 11 are the most used, mainly the polyhedral set for distribution expansion planning problems.

The uncertainty sets in Figure 11 shows two variables (ξ_1 and ξ_2), and the values inside each set represent the possible values that these variables may assume. The uncertainty budgets ($\Psi, \Omega,$ and Γ) represent the amount of uncertainty that is tolerated, of which 1 represents 100% (or the worst possible case), and 0 is 0% (or the optimistic case). Taking Figure 9 as an example and choosing a specific hour of the day, the bounders in the sets from Figure 11 would be the same as the bounders observed in Figure 9.

It is important to observe that $\Psi, \Omega,$ or Γ should not always take extreme values such as 0 or 100%. In the generation uncertainty case, for example, $\Gamma = 100\%$ may represent that no power generation capacity is available in the DG units, which is an unrealistic and catastrophic scenario. The maximum value of the uncertainty budget should consider historical values or worst-case expected values, such as 25% of power generation unavailability.

For a better understating of the uncertainty budgets ($\Psi, \Omega,$ and Γ), uncertainty sets, and their effect on the uncertain parameters, suppose a system with two DG units (ξ_1 and ξ_2, both represented by Figure 9) and the choice of a polyhedral uncertainty set (Figure 11.c). If the uncertainty budget (Γ) is defined as equal to 1, both DG units would have no generation capacity. If Γ is defined as 0, both DG units will generate in the upper bound level (maximum value from Figure 9). Now, if Γ is defined as 0.5, the total amount of generation would be in the middle of the lower bound and the upper bound levels; however, it is not possible to easily define the generation capacity of each generating unit; this definition would be the worst-case for the system, the only information known prior to the optimization process is that the total amount of generation would be exactly in the middle of the bounders, but the specific values for each DG power generation is an output from the optimization problem.

The use of uncertainty sets is an easy and effective approach to represent uncertainties, which provides enough information for the ARO method to seek the worst-case realization of uncertainties.

3.9.4.1 Representing ARO models

ARO models have been successfully used to solve problems similar to the one presented in this work, such as in Amjady et al. (2018a), Dehghan et al. (2016), Wu et al. (2019), Wu et al. (2018) and Xie et al. (2020).

Expansion planning problems under uncertainties are generally modeled as follows:

$$\min_{x \in X} c^T x + \max_{u \in U} \min_{y \in Y} f\big(y(x,u)\big) \tag{6}$$

s.t.

$$g_X(x) = 0 \tag{7}$$

$$h_X(x) \geq 0 \tag{8}$$

$$u \in U \tag{9}$$

$$g_Y(x,y,u) = 0 \tag{10}$$

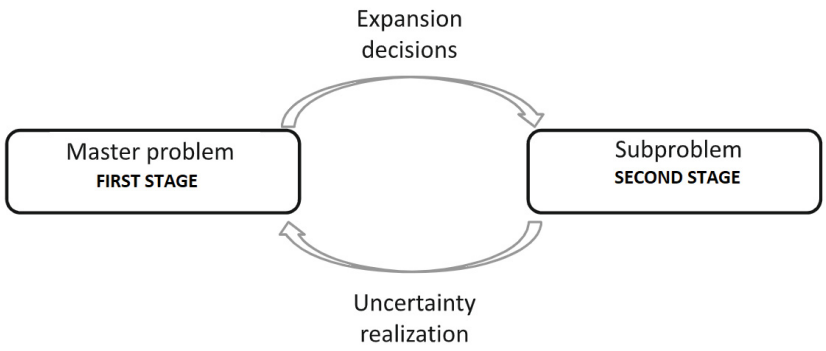
$$h_Y(x,y,u) \geq 0 \tag{11}$$

where x represents the decisions on the expansion planning problem, c^T is the investment cost for x, u are the variables related to the uncertainty parameters, y pertains to the operational decisions in the power system. $f\big(y(x,u)\big)$ is the portion of the objective function that depends on the investment (x) and the uncertainties (u), represented by operational variables (y). $g_X(x)$ and $h_X(x)$ are constraints related to the expansion decision and $g_Y(x,y,u)$ and $h_Y(x,y,u)$ are the constraints pertaining to the operational decisions. U represents the uncertainty set, which may be modeled in different forms.

In the generic problem presented in (6), the decision over x may be interpreted as the “here-and-now” decisions, and the decisions over $y(x,u)$ are the “wait-and-see” decisions.

The objective function (6) is a three-level problem (min-max-min) that can be solved using the ARO approach through a two-stage decomposition framework representation of the problem. Figure 12 shows a generic representation of the ARO approach.

FIGURE 12 – ADAPTIVE ROBUST OPTIMIZATION APPROACH: INTERACTIONS BETWEEN MASTER PROBLEM AND SUBPROBLEM



SOURCE: adapted from Conejo et al. (2016)

The interactions between the master problem and the subproblem in Figure 12 occur continuously until convergence is reached. This convergence is defined as the difference between a cost upper bound (UB) from the subproblem and a cost lower bound (LB) from the master problem.

The Column-and-Constraint Generation is one of the methods most used to solve the two-stage problem represented in Figure 12.

3.9.4.2 The Column-and-Constraint Generation (C&CG) method

Two techniques are commonly used to solve the problem represented in Figure 12: Bender's Decomposition and Column-and-Constraint Generation (C&CG). The C&CG is preferable for problems similar to (6) since Bender's Decomposition may require more iterations to convergence, as presented in Zeng; Zhao (2013).

The C&CG method applied to Figure 12 solves the generic problem (6), where the master problem (first stage) is defined as follows.

$$\min_{x \in X} c^T x + \eta \tag{12}$$

s.t.

$$g_X(x) = 0 \tag{13}$$

$$h_X(x) \geq 0 \tag{14}$$

$$\eta \geq f\big(y(x, \dot{u})\big) \qquad \forall k \tag{15}$$

$$g_Y(x, y, \dot{u}) = 0 \qquad \forall k \tag{16}$$

$$h_Y(x, y, \dot{u}) \geq 0 \qquad \forall k \tag{17}$$

where k is the number of iterations between the first and the second stages, η is an auxiliary variable to reconstruct the operational decisions of the objective function in the master problem of the ARO. $\dot{u}$ represents the fixed values of the uncertainty parameters defined in the subproblem (second stage).

Constraints (15)-(17) are defined for all k; and for each k, $\dot{u}$ is defined in the second stage of the decomposition. For the first iteration, $\dot{u}$ can be calculated running the second stage of the decomposition prior to the expansion decision or it can be defined using its optimistic values.

Constraint (15) is one of the most important equations in the C&CG method, it represents that the auxiliary variable η is defined as the worst value of $y(x, \dot{u})$, among all $\dot{u}$ calculated in the second stage.

After finding the best expansion decisions (x) in the first stage of the decomposition, the second stage is solved, which is described as:

$$\max_{u \in U} \min_{y \in Y} f\big(y(\dot{x}, u)\big) \tag{18}$$

s.t.

$$g_Y(\dot{x}, y, u) = 0 \tag{19}$$

$$h_Y(\dot{x}, y, u) \geq 0 \tag{20}$$

$$u \in U \tag{21}$$

where $\dot{x}$ represents the expansion decisions from the first stage of the decomposition and is fixed at this stage.

Note that (18) is a bi-level problem (max-min), which can be converted into a single-level max problem using the KKT conditions if $f\big(y(\dot{x}, u)\big)$ is continuos and linear.

After solving the second stage of the decomposition, it is required to check the convergence of the process. If necessary, a new iteration is performed, in which the first stage is solved again but adds solutions from the second stage.

In the C&CG method, for each iteration (k), new values for u (which represent the uncertainty variables) are calculated in the second stage of the decomposition. All values of u are kept at the first stage, creating new “scenarios” that must be handled by the expansion planning problem. For each new expansion proposal (from the first stage), the second stage will seek the worst realization of u.

Note that for each iteration k, constraints (15)-(17) are replicated.

Therefore, the generic steps for the C&CG are:

a) Initiate $k = 0$.
b) Calculate an **initial value for $\boldsymbol{u}$** prior to the expansion planning decision. In this step, the second stage of the problem can be solved before the expansion planning problem to provide the initial value.
c) Fix the values of u.
d) Solve the **first stage** of the decomposition considering that constraints (15)-(17) are replicated for each k, and u has different values for each k. Moreover, x is the main output from the first stage
e) Calculate a Lower Bound (**LB**) for the problem and fix the values of x.
f) Solve the **second stage** of the decomposition, using the fixed values of x (solution from the first stage).
g) Calculate an Upper Bound (**UB**) for the problem.

h) Check the **convergence**: If UB-LB is lower than tolerance, the algorithm ends; otherwise, it continues.
i) Update $k = k + 1$.
j) **Fix the values of $\boldsymbol{u}$** and keep them for all iterations.
k) Go back to step (d).

The definition of LB and UB depends on each problem and can be defined in different forms, generally calculated as follows:

$$\mathrm{LB} = c^T x + \eta \tag{22}$$

$$\mathrm{UB} = \min\{UB,\ c^T \dot{x} + f\big(y(\dot{x}, u)\big)\} \tag{23}$$

where LB uses outputs from the first stage and UB outputs from the second stage within the fixed values of $\dot{x}$.

3.9.4.3 Solving the MAXMIN subproblem

The subproblem (18) is a maxmin problem and can be converted into a single-level max problem using the KKT conditions. This is only possible because all decision variables (binaries) are in the master problem from Figure 12 and are fixed in the subproblem. Thus, $f\big(y(\dot{x}, u)\big)$ is linear and continuos.

In order to understand how to solve maxmin problems, consider the generic problem in (18). Since $\dot{x}$ is fixed and y is impacted by u, to simplify the notation, $f\big(y(\dot{x}, u)\big)$ is now defined as $f(y)$, $g_Y(\dot{x}, y, u)$ is $g(y)$ and $h_Y(\dot{x}, y, u)$ is $h(y)$.

If $f(y)$ is continuous and linear, the Lagrange function of the problem is:

$$\mathcal{L}(y, \lambda, \phi) = f(y) - \lambda g(y) - \phi h(y) \tag{24}$$

where $\mathcal{L}$ is the Lagrange function, and λ and ϕ are dual variables from the problem.

From the KKT conditions, the following equation must be satisfied.

$$\nabla f(y^*) - \sum_i \lambda_i \nabla g_i(y^*) - \sum_j \phi_j \nabla h_j(y^*) = 0 \tag{25}$$

where i and j denote the number of constraints in $g(y)$ and $h(y)$, respectively. And y^* is an optimal solution of $f(y)$.

Thus, the set of constraints related to the Lagrange function (Ψ^{KKT}) is defined:

$$\frac{\partial \mathcal{L}}{\partial y} = 0 \quad \forall y \in Y \tag{26}$$

In addition, from the KKT conditions, the dual variables of the problem or the inequality constraints must be activated (different from 0). Thus, $\phi = 0$ and $h(y) \geq 0$, or $\phi \geq 0$ and $h(y) = 0$. Therefore, the following complementarity constraints are defined for all $h(y)$ constraints in (20).

$$0 \leq \phi \perp h(y) \geq 0 \tag{27}$$

which can be represented through the following equations:

$$\phi \geq 0 \tag{28}$$

$$h(y) \geq 0 \tag{29}$$

$$\phi\, h(y) = 0 \tag{30}$$

The equation (27) is nonlinear because of (30), but it can be replaced by the following equivalent mixed-integer linear expressions, as demonstrated in Fortuny-Amat and McCarl (1981).

$$\phi \geq 0 \tag{31}$$

$$h(y) \geq 0 \tag{32}$$

$$\phi \leq M\mu \tag{33}$$

$$h(y) \leq M(1 - \mu) \tag{34}$$

where μ is an auxiliary binary variable and M is a large enough positive constant. Note that μ is unique for each constraint $h(y)$ of the problem.

Thus, the set of constraints related to the complementary equations (Ψ^{compt}) is defined as:

$$0 \leq \phi \perp h(y) \geq 0 \quad \forall y \in Y \tag{35}$$

where ϕ is the dual variable of constraint $h(y)$.

Finally, the bi-level max-min problem is converted into a single-level max problem, which can be solved using MILP.

$$\max f\big(y(\dot{x},u)\big) \tag{36}$$

s.t.

$$g(\dot{x},y,u) = 0 \tag{37}$$

$$h(\dot{x},y,u) \geq 0 \tag{38}$$

$$u \in U \tag{39}$$

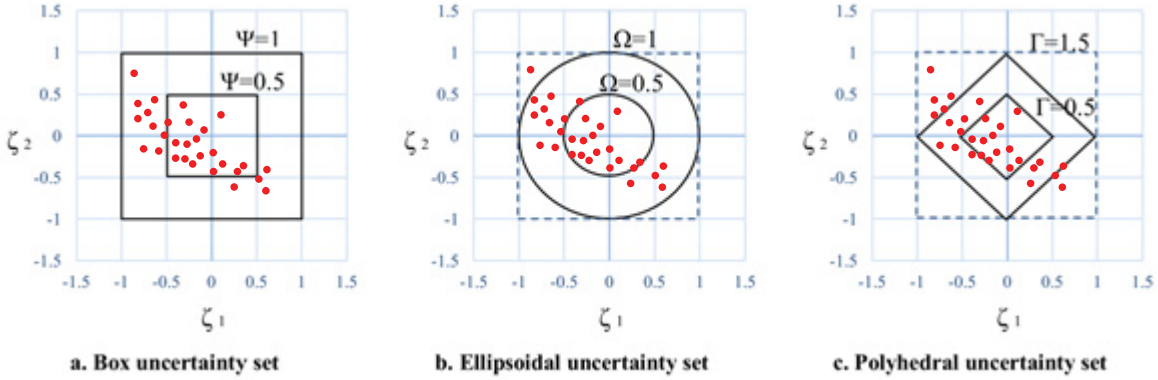
$$\Psi^{KKT} \rightarrow \partial\mathcal{L}/\partial y = 0 \qquad \forall y \in Y \tag{40}$$

$$\Psi^{compt} \rightarrow 0 \leq \phi \perp h(y) \geq 0 \qquad \forall y \in Y \tag{41}$$

3.9.5 Data-Driven Approach

The robust sets presented in Figure 11 are generic approaches and may not accurately represent some problems. As an example, Figure 13 shows the generic uncertainty sets and historical data of two variables (ξ_1 and ξ_2), which are represented by red dots.

FIGURE 13 – UNCERTAINTY ROBUST SETS WITH HISTORICAL DATA



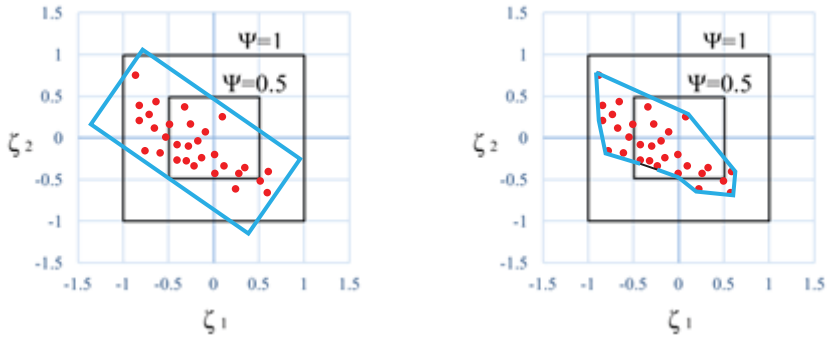
a. Box uncertainty set b. Ellipsoidal uncertainty set c. Polyhedral uncertainty set

SOURCE: Adapted from Jalilvand-Nejad et al. (2016)

Note that the generic sets cannot precisely represent the historical data (red dots). Using these sets in the expansion planning problem would provide over-conservative solutions (for the case of the box uncertainty set), or it may not consider a scenario that has occurred in the past (for the polyhedral uncertainty set).

Thus, data-driven approaches create robust sets that are not over-conservative and represent historical data. Figure 14 presents how would be a data-driven robust set for the historical data presented in Figure 13.

FIGURE 14 – DATA-DRIVEN ROBUST SET (IN BLUE)



SOURCE: The author (2022)

Figure 14 shows two different approaches for the data-driven robust set: the data-driven robust set is in blue, the historical data is in red, and the generic box uncertainty set is in black.

There are several different techniques for data-driven approaches since this is a concept in which historical data is used to seek a robust plan. The most common techniques are reshaping the robust set according to the historical data, linear combinations of historical cases, and a distributionally approach.

Regarding the reshaping approach of robust sets, the set on the left side of Figure 14 shows the result from an approach that models the robust set to fit most of the historical data, but keeping the box shape of the set, this approach may neglect outliers from the historical data. Typically, machine learning algorithms are applied to model the robust set and fit most of the historical data (NING and YOU, 2019).

The robust set on the right side of Figure 14 represents the result of a technique that shapes the uncertainty set based on historical data, creating a hollow polyhedron. Although Machine learning algorithms may also be applied to create this

set, a linear combination of historical data is easier and provide faster results, as presented in (VELLOSO,et al., 2020).

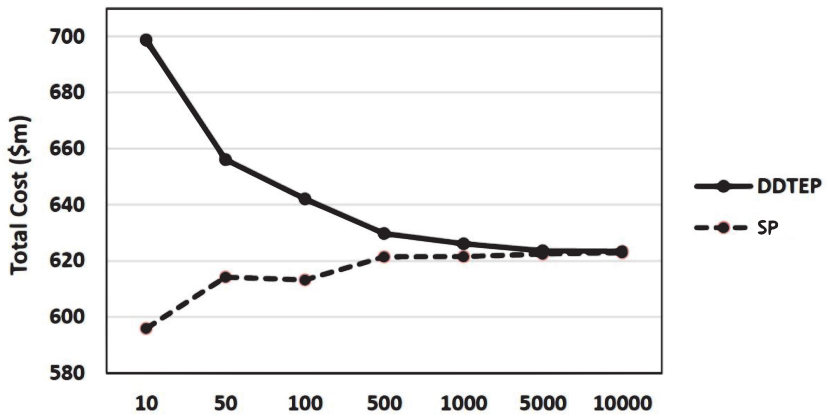
Although both cases in Figure 14 provide more realistic results for problems considering uncertainty compared to generic sets, they require historical data on the uncertainty parameters of the system. And historical data may not precisely represent the future for long-term planning, such as in expansion planning problems. For example, the historical load demand does not provide reliable information for the load demand for the next 3 years. Therefore, for expansion planning problems, a distributionally approach is more indicated.

3.9.6 Data-Driven Distributionally Approach

In order to overcome the limitations of stochastic programming (SP), ARO, and traditional data-driven (DDRO) approaches, the data-driven distributionally robust optimization (DDDRO) uses historical information to create different scenarios considering the worst-possible probabilities for them.

Bagheri et al. (2017) show that for cases having little historical data available, the DDDRO would provide more conservative solutions compared to SP. While if, hypothetically, the available historical data represents the real probability distribution, then the solutions from DDDRO and SP would be the same; however, DDDRO requires less computational time. Figure 15 shows the results presented in Bagheri et al. (2017), which represent the effects of the size of historical data on the total cost for the expansion planning of transmission systems.

FIGURE 15 – EFFECTS OF THE SIZE OF HISTORICAL DATA ON TOTAL COST.



SOURCE: Bagheri et al. (2017)

DDDRO models attenuate over-conservativism if the size of historical data is increased. Figure 15 shows that if a small amount of data is available, the DDDRO model will behave as an ARO model; otherwise, it will be close to an SP model. This is the main advantage of DDDRO models since they can be applied in cases with a large amount of data.

The main objective of DDDRO models is to convert historical data into stochastic scenarios and find the probability of each scenario that will provide the worst result for the objective function of the proposed model. In practical terms, the historical data is converted into data bins, representing scenarios. These data bins have an initial probability of occurrence based on historical data. The DDDRO will adjust these probabilities according to the amount of historical data and its confidence level.

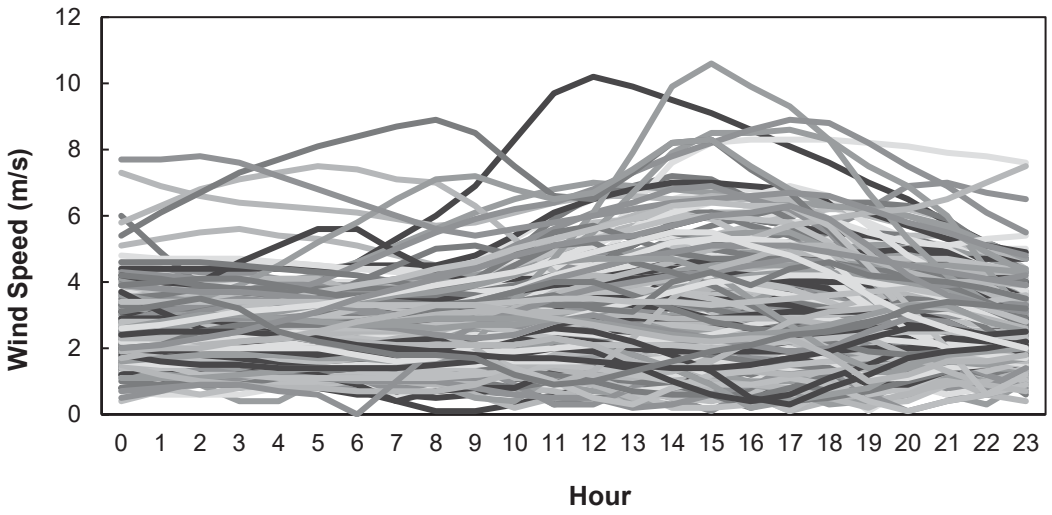
Although historical data is not always available or applicable to estimate future behavior, alternative information can adequately estimate future values of the variable of interest. For example, historical data on wind power generation may not be available if the system does not have these generator units; however, wind speed can be used to estimate future wind power plants' capacity values. The same can be applied to solar power units, where irradiance can be used to estimate future values of power solar plants’ capacity.

Figure 16 shows historical data for wind speed for São Paulo city, from 2017 to 2021, available in Solcast (2021). The information in Figure 16 demonstrates that it is not easy to define a deterministic value for wind speed based on historical data. Thus, as mentioned before, the DDDRO approach converts this information into data bins. Figure 17 shows 6 data bins created for the information in Figure 16, containing the expected wind speed and frequency.

The frequency in Figure 17 can be converted into a probability for each data bin. Thus, DDDRO optimizes the problem for the worst-case of the probability of each data bin, considering the amount of historical data and its confidence level.

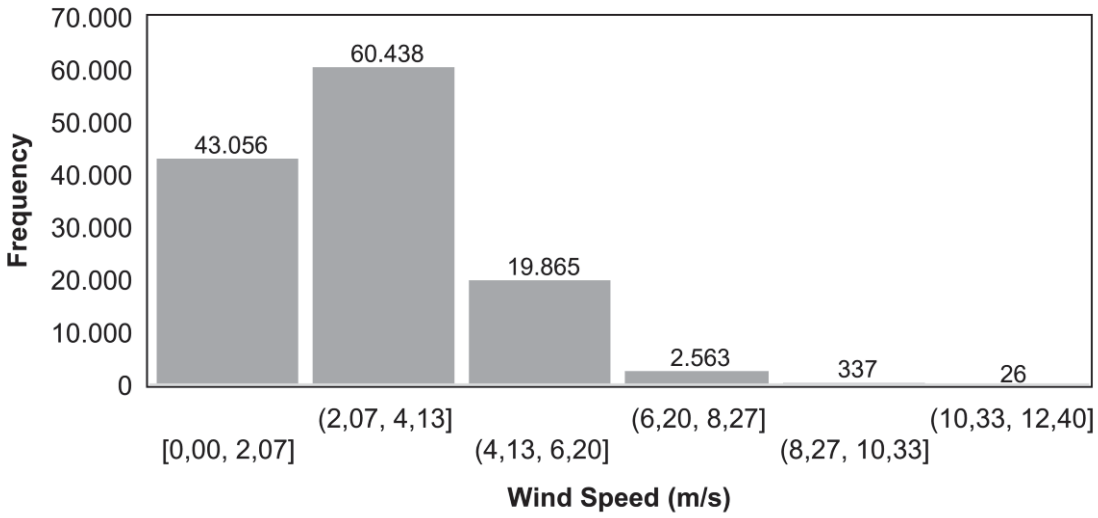
If there is a considerable amount of historical data available, the confidence level of the data bin’s probability is high; thus, their current probability levels are trustful. Otherwise (if little historical data is available), the confidence level of the data bin’s probability is low, and the worst scenarios will increase their probabilities in the DDDRO approach.

FIGURE 16 – HISTORICAL DATA FOR WIND SPEED FOR SAO PAULO, BRAZIL (2017-2021)



SOURCE: Solcast (2021)

FIGURE 17 – DATA BINS FOR THE HISTORICAL DATA FOR WIND SPEED FOR SAO PAULO, BRAZIL (2017-2021)



SOURCE: the author (2022)

DDDRO can be seen as a hybrid approach of SP, ARO, and DDRO. It has the advantage of each method while it deals with problems with little or a lot of historical data. However, if historical data is not available, SP, DDRO, and DDDRO cannot be used, and ARO is indicated.

More details and formulation for the DDDRO is presented in subsection 6.1.

3.10 CONCLUDING REMARKS FOR THE CHAPTER

Microgrids are generally related to DERs and are expected to operate isolated from the main grid. Thus, representing the 24H-OP in the ADN expansion planning problem is essential due to the requirement for an accurate representation of the unavailability of DGs and the demand response.

To operate isolated from the main grid, MGs should be able to deal with contingencies, since any system's component is subject to failure. The robustness against contingencies also improves the system's reliability and allows maintenance in the DG units during the regular operation of the MG. Also, the inclusion of DGs with renewable sources increases the uncertainties in the system.

The demand response can be considered a tool to increase or deal with uncertainties. It depends if the DSO has (or not) total control over the shiftable portion of the load.

Regarding uncertainties, many methodologies have been applied in different works. Robust, data-driven, and stochastic models can be used depending on the objective and availability of historical data. Problems with sufficient historical data can be solved using stochastic or data-driven models; if historical data is unavailable, robust models are indicated. Data-driven distributionally models are intermediate approaches that provide results near robust models if little historical data is available and results near stochastic models if there is enough data.

Therefore, this work proposes four complementary models to solve AND expansion planning problems as follows:

- Chapter 4: An ARO model to solve ADN expansion planning problems, including reliability, uncertainties, and demand response. Indicated for problems where historical data is not available, and MMGs are not presented in the system.
- Chapter 5: An ARO model to solve ADN expansion planning problems, including contingencies, demand response, uncertainties, and MMG. Indicated if historical data is not available and MMGs are presented in the system but owned by the DSO.
- Chapter 6: A DDDRO model to solve ADN expansion planning problems, including contingencies, demand response, uncertainties, and MMG. Indicated if historical data is available and MMGs are

presented in the system but owned by the DSO (or they are subject to the DSO / governmental pricing regulations).

- Chapter 7: A DDDRO model to solve ADN expansion planning problems, including contingencies, demand response, uncertainties, and MMG with energy trading. Indicated if historical data is available, MMGs owned by private investors are presented in the system, and energy trading is allowed.

Each model can be applied to different cases where data is available, if the system has MMG, if the MGs are owned/regulated by the DSO/government, and if energy trading is allowed among the MGs.

This work does not explore pure stochastic models since DDDRO provides the same results if enough historical data is available. DDDRO models are modern approaches that give robustness to problems having little historical data.

4 A RELIABILITY-CONSTRAINED ROBUST MODEL FOR THE EXPANSION PLANNING OF ADNs

4.1 INTRODUCTION

Modern distribution networks do not only contain lines, transformers, capacitors, and loads. They also have DERs and automated equipment to ensure quality and safety. Thus, designing new active distribution networks or proposing their expansion plans are more complex than traditional distribution expansion planning problems. Moreover, uncertainties and minimum quality standards increase this complexity.

Distributed generation units are often associated with renewable power sources, making it hard to predict their generation capacity due to uncertainties. The power consumption profile is also uncertain since it increases over time, and changes in consumer behaviors may occur due to the appearance of new technologies, such as electric vehicles.

Governments generally impose minimum quality standards in power delivery services, typically measured by reliability indexes. These indexes measure the frequency and duration of faults, not supplied load, and many other aspects related to delivering power to consumers.

Therefore, modern distribution networks are complex, and the distribution expansion planning problem must properly represent its current features, such as uncertainty, reliability issues, and the presence of DERs.

The installation of DG and most of the ESS units in distribution systems are typically defined and performed by customers and not the DSO. Thus, the inclusion of these components in the DSO's expansion planning decision can be seen as a study to create incentive programs that would benefit those customers that follow the DSO's desired strategy.

In this context, this chapter presents a new model to solve the distribution expansion planning problem of ADNs considering uncertainty, reliability, and DERs.

The main contribution of this chapter is the introduction of reliability indexes in a novel three-stage robust framework along with more realistic representations of ADN aspects, such as 24H-OP and self-healing capacity.

4.2 CONTEXT AND ASSUMPTIONS

This chapter assumes that the DSO desires to solve a distribution expansion planning problem, defining where and when to install distributed generator units, energy storage system units, capacitors, switches, and install/rewire lines.

The DSO determines a minimum acceptable level for the EENS reliability index, and the expansion planning decision must meet this requirement. It aims to minimize the total cost of investment and operation (generation cost), while meeting the reliability index level desired.

In addition, the following definitions are considered in the model:

- The technologies used for DG units are wind turbines and photovoltaic modules. These types of technologies have uncertainty in production due to the dependence on renewable energy source and have the flexibility required for generation curtailment (AMJADY et al., 2018a).
- The degradation of energy storage system units by charging/discharging and their efficiency are ignored. Active losses in lines are also ignored. Similar simplifications have been used in other expansion planning problems, such as by Baringo et al. (2020).
- Uncertainties in generation and load are considered, but historical data is unavailable. Thus, an ARO approach is indicated.
- The loads and DG's generation capacities are represented by a typical operational day, which changes per period t_y. In the simulations presented in this work, t_y are years, which is not a limitation but a consideration for the case study.

4.3 PROPOSED MODEL

Since this chapter assumes that historical data of generation or load is unavailable, the problem is modeled using robust optimization to deal with uncertainties.

Aiming to solve a robust expansion planning problem including uncertainties and reliability, a min-max-min model is proposed along with a Monte Carlo Simulation (MCS) to estimate the reliability indexes.

The three-level (min-max-min) problem uses the linear AC power flow formulation, presented in (4) and (5), to represent the power flow inside the first and second levels; while it uses the nonlinear AC power flow equations, presented in (1) and (2), in the third level.

4.3.1 Formulation

This subsection describes the objective function and each constraint of the problem individually to facilitate the reader's comprehension.

4.3.1.1 Objective function

For a deterministic model, the objective function of the problem would be defined as:

$$\min \sum_{t_y} \sum_{c} \frac{I_c^C x_{c,t_y}^C}{(1+R)^{t_y}} + \sum_{t_y} \sum_{t_h} \left[\sigma \left(\sum_{g} C_{g,t}^G p_{g,t}^G + \sum_{d} C_{d,t}^{LS} p_{d,t}^{LS} \right) \right] \tag{42}$$

The first part of the equation (42) represents the investment in the expansion proposal, where *C* represents a generic set of all candidates, I_c^C is the annualized investment in candidate c, x_{c,t_y}^C is a binary variable that denotes if a candidate c is installed or not (1 or 0) at year t_y, R is the rate of return. The second and third parts of equation (42) contain the generation and load shedding costs ($C_{g,t}^G, C_{d,t}^{LS}$) and the generation power and load shedding values ($p_{g,t}^G$, $p_{d,t}^{LS}$). The load shedding ($p_{d,t}^{LS}$) represents an undesirable interruption in the supply of a load. The index t represents a set of $\{t_y, t_h\}$.

To include uncertainties in the expansion decision, the objective function in equation (42) can be rewritten as:

$$\min_{x_{c,t_y}^C} \max_{\Delta Smax} \min_{\Delta Smin} \sum_{t_y} \sum_{c} \frac{I_c^C x_{c,t_y}^C}{(1+R)^{t_y}} + \sum_{t_y} \sum_{t_h} \left[\sigma \left(\sum_{g} C_{g,t}^G p_{g,t}^G + \sum_{d} C_{d,t}^{LS} p_{d,t}^{LS} \right) \right] \tag{43}$$

where $\Delta Smax$ is the set with variables subject to uncertainties $\{\tilde{p}_{g,t}^{G^{max}}, \tilde{p}_{d,t}^{D}\}$ and $\Delta Smin$ represents all variables except $\{x_{c,t_y}^{C}, \tilde{p}_{g,t}^{G^{max}}, \tilde{p}_{d,t}^{D}\}$.

The objective function (43) minimizes the total investment and operation cost in the expansion planning horizon for the worst-case realization of generation and load uncertainties. The min-max-min formulation can be seen as a wait-and-see approach, in which investment decisions are made at the first level of the problem (min), the second level (max) defines the worst-case for the uncertainties, the third level (min) calculates the best operational response for the uncertainties.

4.3.1.2 Constraints

In addition to the objective function, the model is defined by the following constraints. The variables λ and ϕ are dual variables, defined for each constraint and used in the decomposition approach of the problem.

Reliability target constraint ($\boldsymbol{\Psi^{rel}}$):

$$f_{EENS}\left(x_{c,t_y}^{C}\right) \leq EENS^{TG} \qquad (\phi^{EENS}) \qquad (44)$$

where f_{EENS} is a function that calculates the EENS index using Monte Carlo Simulation (MCS) and $EENS^{TG}$ is a target (parameter) for the reliability index. The function f_{EENS} is used to simplify the representation in constructing the EENS index, detailed in subsection 4.3.2.5 of this chapter.

This constraint imposes that the EENS of the system must be less or equal to the target. Different investment decisions (x_{c,t_y}^{C}) would require different simulations using MCS, what is intractable without a decomposition approach.

AC power flow constraints ($\boldsymbol{\Psi^{Lflow}}$):

$$p_{l,t}^{L} = x_{l,t_y}^{L}\left(G_l v_{rs(l),t} - B_l \theta_{rs(l),t}\right), \ \forall l, \forall t \qquad \left(\lambda_{Lp}\right) \qquad (45)$$

$$q_{l,t}^{L} = x_{l,t_y}^{L}\left(-G_l \theta_{sr(l),t} - B_l v_{sr(l),t}\right), \ \forall l, \forall t \qquad \left(\lambda_{Lq}\right) \qquad (46)$$

These equations were presented in subsection 3.6 and are defined in Yang et al. (2017). They provide the active ($p^L_{l,t}$) and reactive ($q^L_{l,t}$) power flowing in the network's lines. In addition to the voltage angle ($\theta_{l,t}$), they provide the voltage magnitute ($v_{l,t}$). x^L_{l,t_y} represents if line l is actived or not at year y. The notation $v_{rs(l),t}$ is the same as $v_{r(l),t} - v_{s(l),t}$, where $r(l)$ is the receiving node of line l and $s(l)$ is the sending node.

Although equations (45) and (46) are non-linear due to the multiplication of x^L_{l,t_y} and $v_{l,t}/\theta_{l,t}$, they can be linearized using the BigM approach. The linearization for equation (45) is:

$$-x^L_{l,t_y} P^{Lmax}_l \leq p^L_{l,t} \leq x^L_{l,t_y} P^{Lmax}_l \qquad \forall l, \forall t \qquad (47)$$

$$-\left(1 - x^L_{l,t_y}\right) M \leq p^L_{l,t} + B_l \theta_{sr(l),t} - G_l v_{sr(l),t} \leq \left(1 - x^L_{l,t_y}\right) M \qquad \forall l, \forall t \qquad (48)$$

where M is a large enough positive constant.

Power balance constraints (Ψ^{bal}):

$$\sum_{g \in \Omega^G_n} p^G_{g,t} - \sum_{l \in \Omega^L_{n(s)}} p^L_{l,t} + \sum_{l \in \Omega^L_{n(r)}} p^L_{l,t} + p^E_{n,t} = \sum_{d \in \Omega^D_n} \left(\tilde{p}^D_{d,t} - p^{LS}_{d,t}\right), \quad \forall n, \forall t \quad (\lambda_{np}) \qquad (49)$$

$$\sum_{g \in \Omega^G_n} q^G_{g,t} - \sum_{l \in \Omega^L_{n(s)}} q^L_{l,t} + \sum_{l \in \Omega^L_{n(r)}} q^L_{l,t} + q^{SH}_{n,t} = \sum_{d \in \Omega^D_n} \left(\tilde{q}^D_{d,t} - q^{LS}_{d,t}\right), \forall n, \forall t_t \quad (\lambda_{nq}) \qquad (50)$$

where $p^G_{g,t}$, $p^L_{l,t}$, $p^E_{n,t}$, $\tilde{p}^D_{d,t}$, and $p^{LS}_{d,t}$ are the generation power, line's power flow, stored/supply energy of ESS units, load demand, and load shedding for the active power balance in the equation (49). The same is applied to the reactive power balance in the equation (50), adding $q^{SH}_{n,t}$ as the reactive power provided by the capacitor located at node n. The notations Ω^G_n and Ω^D_n represent the set of all generators and all loads placed at bus n, $\Omega^L_{n(r)}$ and $\Omega^L_{n(s)}$ are the set of all lines provinding power to node n and all lines sending power from node n to another node.

Equation (49) represents the active power balance, while (50) is the reactive power balance. Each constraint is defined for all nodes and time periods.

Energy storage system constraints (Ψ^{ess}):

$$soc_{n,t} = soc_{n,(t-1)} - p^{E}_{n,t},\ \forall n, \forall t \qquad (\lambda_{st}) \qquad (51)$$

$$x^{E}_{n,t_y}\, SOC^{min}_{n} \leq soc_{n,t} \leq\ x^{E}_{n,t_y}\, SOC^{max}_{n},\ \forall n, \forall t \qquad (\phi_{st}) \qquad (52)$$

$$x^{E}_{n,t_y}\, P^{Emin}_{n} \leq p^{E}_{n,t} \leq\ x^{E}_{n,t_y}\, P^{Emax}_{n},\ \forall n, \forall t \qquad (\phi_{pt}) \qquad (53)$$

where $soc_{n,t}$ is the state of charge of the ESS unit placed at node n, $p^{E}_{n,t}$ the power provided or stored by this unit, and P^{Emin}_{n}/ P^{Emax}_{n} its limits.

Equation (51) represents the state of charge (SOC) for the ESS unit placed in bus n at each time period, which depends on the charging/discharging ($p^{E}_{n,t}$) and the SOC in the previous period ($soc_{n,(t-1)}$). Constraints (52) and (53) are the bounds for the SOC and $p^{E}_{n,t}$.

Operational constraints (Ψ^{op}):

$$0 \leq p^{LS}_{d,t} \leq \tilde{p}^{D}_{d,t},\ \forall d, \forall t \qquad (\phi_{DP}) \qquad (54)$$

$$tan\left(pf_{d,t}\right)\left(\tilde{p}^{D}_{d,t} - p^{LS}_{d,t}\right) = \tilde{q}^{D}_{d,t} - q^{LS}_{d,t},\ \forall d, \forall t \qquad (\lambda^{pf}_{d}) \qquad (55)$$

$$x^{G}_{g,t_y} p^{G^{min}}_{g,t} \leq p^{G}_{g,t} \leq x^{G}_{g,t_y} \tilde{p}^{G^{max}}_{g,t},\ \ \forall g, \forall t \qquad (\phi_{GP}) \qquad (56)$$

$$x^{G}_{g,t_y}\, Q^{G^{min}}_{g,t_d} \leq q^{G}_{g,t} \leq x^{G}_{g,t_y}\, \tilde{q}^{G^{max}}_{g,t_d},\ \forall g, \forall t \qquad (\phi_{GQ}) \qquad (57)$$

$$q^{SH}_{n,t} = x^{CP}_{n,t_y} Q^{SH}_{n},\ \forall n, \forall t \qquad (\lambda_{Q}) \qquad (58)$$

$$-P^{Lmax}_{l} \leq p^{L}_{l,t} \leq P^{Lmax}_{l},\ \forall l, \forall t \qquad (\phi_{L}) \qquad (59)$$

$$V^{min}_{n} \leq v_{n,t} \leq V^{max}_{n},\ \forall n, \forall t \qquad (\phi_{V}) \qquad (60)$$

$$-\pi \leq \theta_{n,t} \leq \pi,\ \forall n, \forall t \qquad (\phi_{\theta}) \qquad (61)$$

$$\theta_{n,t} = 0,\ \ n\text{: ref}\,, \forall t \qquad (\lambda^{ref}_{\theta}) \qquad (62)$$

This set of constraints represents the limit for load shedding in (54), a constant power factor for the load shedding in (55), generation power limits in (56) and (57), power provided by capacitors in (58), power flow limits in the lines in (59), voltage magnitude limits in (60), voltage angle limits in (61), definition of a slack node in (62).

Investment constraints (Ψ^{inv}):

$$\sum_{t_y}\left(\sum_{c\in\Omega^{C+}}\left(I_c^C x_{c,t_y}^C\right)/(1+R)^{t_y}\right)\leq I^{max} \tag{63}$$

$$x_{c,t_y}^C=\sum_{t_i=1}^{t_y}\alpha_{c,t_i}^C,\ \ \forall c,\forall t_y \tag{64}$$

$$\sum_{t_y\in\Omega^{Ty}}\alpha_{c,t_y}^C\leq 1,\ \ \forall c \tag{65}$$

$$\alpha_{c,t_y}^C, x_{c,t_y}^C\ as\ binary,\ \ \forall c,\forall t_y \tag{66}$$

where α_{c,t_y}^C represents the year when a candidate c is installed in the system.

Equation (63) is the investment budget, a limit for all investments; equation (64) defines that a candidate is activated in the year t_y if its installation decision has been made up to that year; constraint (65) defines that the decision on installing a new component can only be made in one period.

Uncertainty constraints (Ψ^{unc}):

$$P_{g,t}^{G^{min}}\leq\tilde{p}_{g,t}^{G^{max}}\leq\bar{P}_{g,t}^{G^{max}},\ \ \forall g,\forall t \tag{67}$$

$$\underline{P}_{d,t}^D\leq\tilde{p}_{d,t}^D\leq\bar{P}_{d,t}^D,\ \ \forall d,\forall t \tag{68}$$

$$\frac{\sum_g x_{g,t_y}^G\left(\bar{P}_{g,t}^{G^{max}}-\tilde{p}_{g,t}^{G^{max}}\right)}{\sum_g x_{g,t_y}^G\left(\bar{P}_{g,t}^{G^{max}}-P_{g,t}^{G^{min}}\right)}\leq\ \Gamma^G,\forall t \tag{69}$$

$$\frac{\sum_d\left(\tilde{p}_{d,t}^D-\underline{P}_{d,t}^D\right)}{\sum_d\left(\bar{P}_{d,t}^D-\underline{P}_{d,t}^D\right)}\leq\ \Gamma^D,\forall t \tag{70}$$

$$\tilde{p}_{g,t}^{G^{max}}=\tilde{q}_{g,t}^{G^{max}}\left(\bar{P}_{g,t}^{G^{max}}/\bar{Q}_{g,t}^{G^{max}}\right),\ \ \forall g,\forall t \tag{71}$$

$$\tilde{p}_{d,t}^{D^{max}}=\tilde{q}_{d,t}^D\left(\bar{P}_{d,t}^D/\bar{Q}_{d,t}^D\right),\ \ \forall d,\forall t \tag{72}$$

Variable $\tilde{p}_{g,t}^{G^{max}}$ is the generation capacity of DG unit g and $\tilde{p}_{d,t}^D$ is the load demand, both subject to uncertainties, represented by the accent ~. Parameters $\bar{P}_{g,t}^{G^{max}}$

and $\bar{P}_{d,t}^{D}$ are the upper bounds for generation and load uncertainties, $P_{g,t}^{G^{min}}$ and $\underline{P}_{d,t}^{D}$ are the lower bounds. Γ^{G} and Γ^{D} are the uncertainty budget for generation and load.

Constraints (67) and (68) define the bounds for the variables subject to uncertainties. Equations (69) and (70) represent the polyhedral uncertainty set introduced in subsection 3.9.4. Equations (71) and (72) define the reactive power for generation and load according to the uncertainty sets.

Set Ψ^{unc} models the uncertainty sets of the problem, which are modeled as polyhedral sets and bounded by uncertainty budgets, same approach used to solve distribution expansion planning problems in Conejo et al. (2016).

The model proposed in this chapter is a min-max-min problem, and it is solved through a decomposition approach, described and detailed in the following subsection, along with the calculation of the reliability index in $f_{EENS}\left(x_{c,t_y}^{C}\right)$.

4.3.2 Algorithm and solution approach

Adaptative robust optimization (ARO) models have been successfully used to solve similar problems in Attarha et al. (2018), Amjady et al. (2018a), and Dehghan et al. (2016). Since this model assumes that no historical data is available, the uncertainty budget from equations (69) and (70) can be used to study the best investment decisions under different levels of uncertainty. Figure 18 presents the three-stage algorithm used to solve the min-max-min problem in (43).

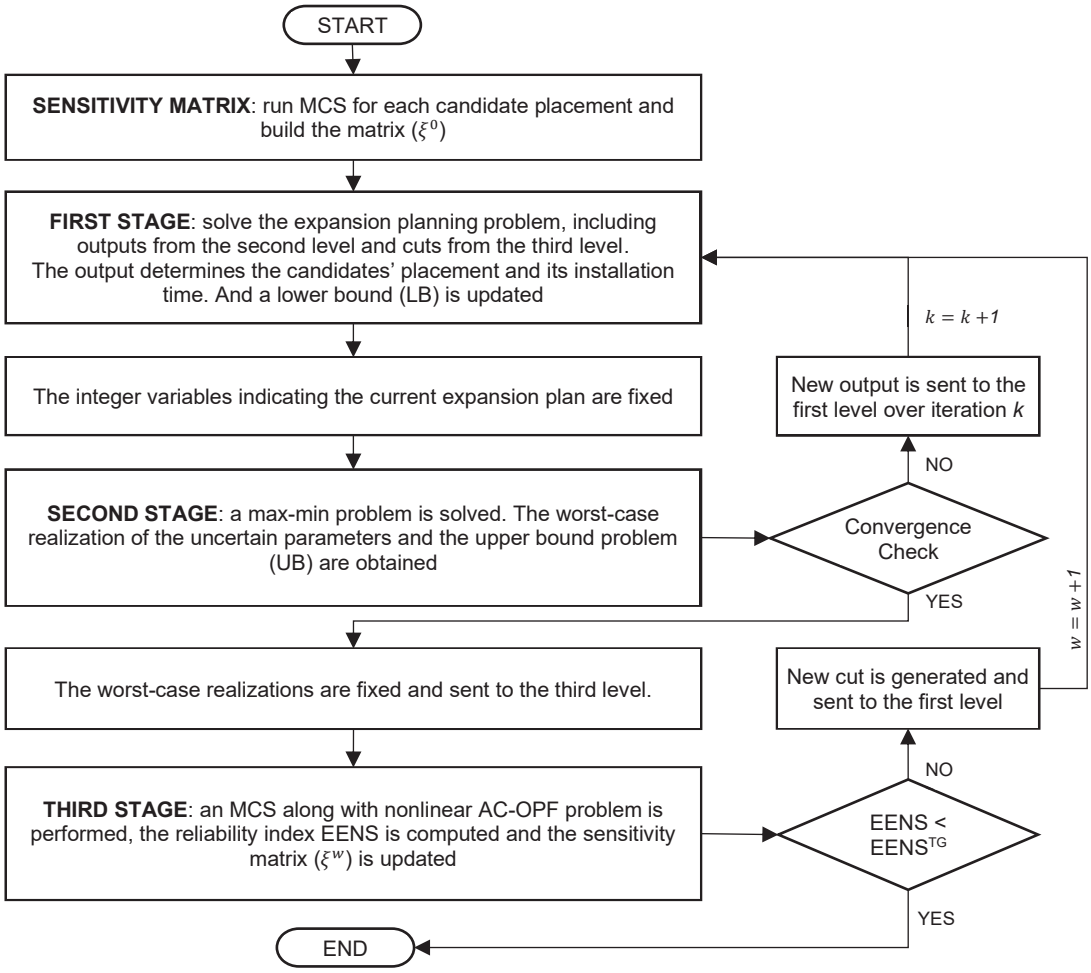
The first and second stages are formulated using contributions from Dehghan et al. (2016), and the third stage uses contributions from Dehghan et al. (2016) and Amjady et al. (2018a).

The algorithm seeks the best investment proposal that would meet the EENS target and minimize the total cost of the problem (investment, generation, and load shedding costs) for the worst-case realization of the uncertainties.

The first step in the algorithm is the definition of a sensitivity matrix, which is used to guide the investments that would meet the EENS target ($EENS^{TG}$).

After the sensitivity matrix has been created, the iterations for the three-stage decomposition start. The first stage defines the best investment decisions; the second stage, the worst-case realization for the uncertainties and the best operational point, which is a maxmin problem; and the third stage updates the sensitivity matrix.

FIGURE 18 – TRI-STAGE DECOMPOSITION MODELING.



The interaction between the first and second stages uses the column-and-constraint generation algorithm (C&CG), the same presented in Zeng and Zhao (2013). The third stage generates new cuts in the master problem (first stage). Thus, after converging, the iteration process among the stages provides a global solution.

The sensitivity matrix and the three stages from Figure 18 are detailed in the following subsections. For this algorithm, *k* denotes the iterations among the first and second levels, and *w* the iterations including the third level of the decomposition.

4.3.2.1 Sensitivity Matrix

The first step in the algorithm is to build the sensitivity matrix. Reliability index calculations generally require high computational time, especially if techniques such

as MCS are used (PINTO, 2018). Thus, the inclusion of reliability inside a robust model may result in prohibitive computational time.

Thus, this method uses a sensitivity matrix to estimate reliability indexes and guide investment decisions in the expansion planning formulation. The sensitivity matrix is updated during the iterations; thus, estimation errors of this step are corrected in the decomposition's third stage.

The sensitivity matrix is built by placing new components in the system, one at a time. Then, an MCS is performed using a nonlinear AC-OPF (non-linear optimal power flow) formulation. For each component placed in the system, the improvement in the EENS index is computed; this process is illustrated in Figure 19.

FIGURE 19 – ALGORITHM TO BUILD THE SENSITIVITY MATRIX

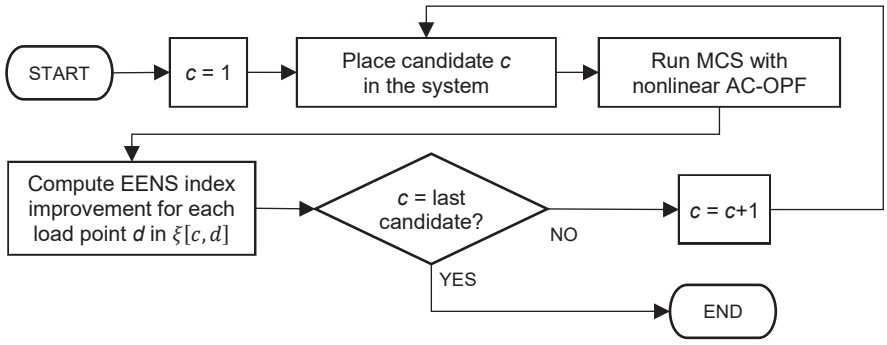


Figure 19 shows an iterative process in which a candidate component *c* is placed in the system, the MCS computes the EENS index, and the sensitivity matrix ($\xi[c, d]$) is defined.

4.3.2.1.1 Details for "Run MCS with nonlinear AC-OPF" step presented in Figure 19

The steps of the MCS are adapted from Da Silva et al. (2006):

(i) Create the time step of the simulation for the whole planning horizon.

(ii) Define the operating state of each component by generating random numbers and comparing them with the components' failure rate. Thus, the faults in the system are estimated for the current iteration.

(iii) For each fault in the system:

(a) Compute the fault extension by finding the switches that must be triggered and the lines for self-healing that must be selected.

(b) Define the simulation duration (Ω^{Tmcs}) as equal to the time of the fault and run the nonlinear AC-OPF.

(c) Compute the load shedding.

(iv) Compute the EENS for the entire simulation.

(v) Evaluate the coefficient of variation ω for the EENS. If ω is less than the tolerance (5%), the algorithm provides the expected value of EENS; otherwise, it returns to step (ii).

Step (iii)-(a) is critical, since many works remove the faulted components from the system, while the proposed model considers the extension of the fault and the activation of switches and lines for self-healing. In this step, switches closest to the fault are triggered, and the faulted area is isolated.

Lines for self-healing are lines not used in normal operation; however, if a fault occurs, these components are activated and may supply an isolated area or improve the power flow balance (PINTO, 2018).

The time step in (iii)-(b) is given by the shortest repair time of the components

Step (iii)-(c) computes the total load shedding using the following model:

$$\min \sum_{t\in\Omega^{Tmcs}} \left(\sum_{g} C^{G}_{g,t} p^{G}_{g,t} + \sum_{d} C^{LS}_{d,t} p^{LS}_{d,t} \right) \tag{73}$$

subject to Ψ^{bal}, Ψ^{ess}, Ψ^{op}, and Ψ^{NLflow}

$\boldsymbol{\Psi^{NLflow}}$: nonlinear power flow constraints

$$p^{L}_{l,t} = \dot{x}^{L}_{l,t_y}\left(v^{2}_{s(l),t} G_l - v_{s(l),t} v_{r(l),t} G_l \cos\left(\theta_{sr(l),t}\right) - v_{s(l),t} v_{r(l),t} B_l \sin\left(\theta_{sr(l),t}\right)\right), \quad \forall l, \forall t \tag{74}$$

$$q^{L}_{l,t} = \dot{x}^{L}_{l,t_y}\left(-v^{2}_{s(l),t}\left(B_l + B^{sh}_{l}\right) - v_{s(l),t} v_{r(l),t} B_l \cos\left(\theta_{sr(l),t}\right) + v_{s(l),t} v_{r(l),t} G_l \sin\left(\theta_{sr(l),t}\right)\right), \quad \forall l, \forall t \tag{75}$$

The objective function (73) seeks to minimize the generation and load shedding costs.

Constraints (74) and (75) represent the nonlinear AC power flow equations. $\dot{x}_{l,t}^{L}$ denotes that the candidate l is fixed in this process, since the placement of the components is defined as described in Figure 19.

The sets of constraints Ψ^{bal}, Ψ^{ess}, and Ψ^{op} are defined in equations (49)-(62).

The load shedding is the key output of each iteration in step (iii)-(c), and it is obtained from $p_{d,t}^{LS}$, which is the required information to create the EENS index; thus, EENS is the same as $p_{d,t}^{LS}$ (BILLINTON and ALLAN, 1984).

In step (v), the coefficient of variation ω is computed as:

$$\omega = \sqrt{V(EENS)}/EENS \tag{76}$$

where $V(EENS)$ is the variance of the EENS index.

After the convergence of the process, where ω is less than the tolerance, the MCS is finished, and the expected value of the EENS index is computed.

4.3.2.1.2 Details for “Compute EENS index improvement for each load point d” step presented in Figure 19

After placing each candidate *c* in the system and estimating the EENS index, the improvement in the reliability index is computed for all load points *d* ($\Delta EENS_d^0$), as presented in equation:

$$\xi[c,d] = \Delta EENS_d^0 \tag{77}$$

where $\Delta EENS_d^0$ is the difference between the EENS index before the installation of candidate *c* and this index after the placing of the same candidate for load point *d*.

Since this matrix expresses the improvement in the EENS index for the individual placement of new components, it may not accurately estimate this index when placing multiple components in the system. Thus, the matrix is updated in the third stage of this decomposition.

4.3.2.2 First Stage and LB Definition

The first and second stages are solved using the same approach presented in subsection 3.9.4.

After creating the sensitivity matrix, the algorithm starts the iteration process, and the index *k* represents iterations among the first and second stages, while iterations over index *w* include the third stage.

The first stage solves the expansion planning problem and finds the best investment proposal that satisfies the EENS defined as the target, meets the demand, and minimizes the total cost. Moreover, the variables with uncertainties are fixed in this stage; they are calculated in the second stage of the decomposition.

This first stage is formulated as a MILP (mixed-integer linear programming) problem. The objective function is defined as:

$$min \sum_{t_y} \left[\sum_{c \in \Omega^C} \frac{\left(I_c^C x_{c,t_y}^C \right)}{(1+R)^{t_y}} \right] + \eta \tag{78}$$

Subject to Ψ^{η}, Ψ^{rel}, Ψ^{Lflow}, Ψ^{bal}, Ψ^{ess}, Ψ^{op}, Ψ^{inv}

The sets of constraints Ψ^{Lflow}, Ψ^{bal}, Ψ^{ess}, Ψ^{op}, Ψ^{inv} were defined in subsection 4.3.1.2 and Ψ^{η} and Ψ^{rel} are described below.

The objective function seeks to minimize the total cost of investment, generation, and load shedding. Variable η represents the worst-case operational costs for all *k* iterations, and it is defined inside the set Ψ^{η}, defined as:

$$\eta \geq \sum_{t_y} \sum_{t_h} \left[\sigma \left(\sum_{g} C_{g,t}^G p_{g,t}^G + \sum_{d} C_{d,t}^{LS} p_{d,t}^{LS} \right) \right], \qquad \forall k \tag{79}$$

The sensitivity matrix is used in this stage to correlate the placement of new components with the improvement in the EENS index, aiming at meeting the EENS target. Therefore, set Ψ^{rel} is defined as:

$$EENS_{t_y}^{w} \leq EENS_{t_y}^{TG} - \sum_{d} \sum_{c \in \Omega^C} \left(\xi_{t_y}^{w}[c,d]\, x_{c,t_y}^{C} \right), \qquad \forall w, \forall t_y \tag{80}$$

w represents the algorithm iterations that include the third stage of the decomposition. $EENS_{t_y}^{w}$ is the EENS index at year t_y and iteration *w*. If $w = 0$, $EENS_{t_y}^{0}$ denotes the value of the index prior to the expansion decision. $EENS_{t_y}^{TG}$ is the EENS target, which may be defined by the DSO or by government authorities.

For the next iterations in *w*, the value of $EENS_{t_y}^{w}$ and the matrix $\xi_{t_y}^{w}$ are computed in the third stage of the decomposition.

Equation (80) shows that $f_{EENS}\left(x_{c,t_y}^{C}\right)$ is defined as

$$f_{EENS}\left(x_{c,t_y}^{C}\right) = EENS_{t_y}^{w} + \sum_{d} \sum_{c \in \Omega^C} \left(\xi_{t_y}^{w}[c,d]\, x_{c,t_y}^{C} \right) \tag{81}$$

Following the same approach used in the C&CG algorithm, all the variables subject to uncertainty are fixed in this stage, and all variables that are not related to the expansion planning decision must be defined for all *k*.

The key outputs in this first level are investment decisions (x_{c,t_y}^{C}) and a cost lower bound (LB), calculated as:

$$LB = \sum_{t_y} \left[\sum_{c \in \Omega^C} \frac{\left(I_c^C \dot{x}_{c,t_y}^{C} \right)}{(1+R)^{t_y}} \right] + \dot{\eta} \tag{82}$$

where $\dot{x}_{c,t}^{C}$ and $\dot{\eta}$ are the solutions from this stage.

4.3.2.3 Second Stage and UB Definition

The second stage is formulated as a max-min problem, and the investment decisions are fixed as $\dot{x}_{c,t_y}^{C}$. Its objective function is:

$$\max_{\Delta Smax} \min_{\Delta Smin} \sum_{t_y} \sum_{t_h} \left[\sigma \left(\sum_{g} C_{g,t}^{G} p_{g,t}^{G} + \sum_{d} C_{d,t}^{LS} p_{d,t}^{LS} \right) \right] \quad (83)$$

Subject to Ψ^{Lflow}, Ψ^{bal}, Ψ^{ess}, Ψ^{op}, Ψ^{unc}

The objective function (83) seeks to minimize the generation and load shedding costs in the worst-case of load demand and generation capacity.

Although (83) is a bi-level problem, it can be converted into an equivalent single-level problem. All integer variables are fixed at this stage, since they are defined in the first stage.

The lower-level subproblem (min) is continuous and linear (and thus convex) in its decision variables. Therefore, it can be replaced by its Karush–Kuhn–Tucker conditions, and the max-min problem becomes a max problem, as presented in Conejo et al. (2016).

Thus, the problem in (83) is reformulated as follows:

$$\max \sum_{t_y} \sum_{t_h} \left[\sigma \left(\sum_{g} C_{g,t}^{G} p_{g,t}^{G} + \sum_{d} C_{d,t}^{LS} p_{d,t}^{LS} \right) \right] \quad (84)$$

Subject to Ψ^{Lflow}, Ψ^{bal}, Ψ^{ess}, Ψ^{op}, Ψ^{unc}, Ψ^{KKT}, Ψ^{compt}

The KKTs conditions constraints (set Ψ^{KKT}) are presented below and formulated as presented in subsection 3.9.4:

$$\sigma C_{g,t}^{G} - \lambda_{np(g),t} - \phi_{GPmin,t} + \phi_{GPmax,t} = 0, \ \forall g, \forall t \quad (85)$$

$$-\lambda_{nq(g),t} - \phi_{GQmin,t} + \phi_{GQmax,t} = 0, \ \forall g, \forall t \quad (86)$$

$$\sigma C_{d,t}^{LS} - \lambda_{np(d),t} + \lambda_{d,t}^{pq} tan\left(pf_{d,t}\right) - \phi_{DPmin,t} + \phi_{DPmax,t} = 0, \ \forall d, \forall t \quad (87)$$

$$-\lambda_{nq(d),t} - \lambda_{d,t}^{pq} = 0, \ \forall d, \forall t \quad (88)$$

$$\lambda_{np(s),t} - \lambda_{np(r),t} - \lambda_{Lp,t} - \phi_{LPmin,t} + \phi_{LPmax,t} = 0, \ \forall l, \forall t \quad (89)$$

$$\lambda_{nq(s),t} - \lambda_{nq(r),t} - \lambda_{Lq,t} = 0, \ \forall l, \forall t \quad (90)$$

$$\sum_{l \epsilon \Omega^L | n(s)} \dot{x}_{l,t}^{L} \left(\lambda_{Lp,t} G_l - \lambda_{Lq,t} B_l\right) + \sum_{l \epsilon \Omega^L | n(r)} \dot{x}_{l,t}^{L} \left(-\lambda_{Lp,t} G_l + \lambda_{Lq,t} B_l\right) - \phi_{Vmin,t} + \phi_{Vmax,t} = 0, \ \forall n, \forall t \quad (91)$$

$$\sum_{l\epsilon\Omega^L|n(s)} \dot{x}_{l,t}^{L}\left(-\lambda_{Lp,t}B_l - \lambda_{Lq,t}G_l\right) + \sum_{l\epsilon\Omega^L|n(r)} \dot{x}_{l,t}^{L}\left(\lambda_{Lp,t}B_l + \lambda_{Lq,t}G_l\right) - \phi_{\theta min,t} + \phi_{\theta max,t} = 0,\ \forall n \backslash n{:}\,ref, \forall t \quad (92)$$

$$\sum_{l\epsilon\Omega^L|n(s)} \dot{x}_{l,t}^{L}\left(-\lambda_{Lp,t}B_l - \lambda_{Lq,t}G_l\right) + \sum_{l\epsilon\Omega^L|n(r)} \dot{x}_{l,t}^{L}\left(\lambda_{Lp,t}B_l + \lambda_{Lq,t}G_l\right) - \phi_{\theta min,t} + \phi_{\theta max,t} - \lambda_{\theta,t}^{ref} = 0,\ n{:}\,ref, \forall t \quad (93)$$

The complementarity constraints (set Ψ^{compt}) are described as follows and formulated as presented in subsection 3.9.4:

$$0 \le \phi_{GPmin} \perp p_{g,t}^{G} - \dot{x}_{g,t}^{G} P_{g,t}^{G^{min}} \ge 0,\ \forall g, \forall t \quad (94)$$

$$0 \le \phi_{GPmax} \perp \dot{x}_{g,t}^{E} \tilde{p}_{g,t}^{G^{max}} - p_{g,t}^{G} \ge 0,\ \forall g, \forall t \quad (95)$$

$$0 \le \phi_{GQmin} \perp q_{g,t}^{G} - \dot{x}_{g,t}^{G} Q_{g,t}^{G^{min}} \ge 0,\ \forall g, \forall t \quad (96)$$

$$0 \le \phi_{GQmax} \perp \dot{x}_{g,t}^{G} \tilde{q}_{g,t}^{D} - q_{g,t}^{G} \ge 0,\ \forall g, \forall t \quad (97)$$

$$0 \le \phi_{DPmin} \perp p_{d,t}^{LS} \ge 0,\ \forall d, \forall t \quad (98)$$

$$0 \le \phi_{DPmax} \perp \tilde{p}_{d,t}^{D} - p_{d,t}^{LS} \ge 0,\ \forall d, \forall t \quad (99)$$

$$0 \le \phi_{LPmin} \perp p_{l,t}^{L} + P_{l}^{Lmax} \ge 0,\ \forall l, \forall t \quad (100)$$

$$0 \le \phi_{LPmax} \perp P_{l}^{Lmax} - p_{l,t}^{L} \ge 0,\ \forall l, \forall t \quad (101)$$

$$0 \le \phi_{Vmin} \perp v_{n,t} - V_{n}^{min} \ge 0,\ \forall n, \forall t \quad (102)$$

$$0 \le \phi_{Vmax} \perp V_{n}^{max} - v_{n,t} \ge 0,\ \forall n, \forall t \quad (103)$$

$$0 \le \phi_{\theta min} \perp \theta_{n,t} + \pi \ge 0,\ \forall n, \forall t \quad (104)$$

$$0 \le \phi_{\theta max} \perp \pi - \theta_{n,t} \ge 0,\ \forall n, \forall t \quad (105)$$

The dual variables used in Ψ^{KKT} are defined in equations (44)-(62). The generic constraint $0 \le a \perp b \ge 0$ presented in Ψ^{COMP} represents the set of constraints $a \ge 0,\ \ b \ge 0$ and $ab = 0$, which are nonlinear, but can be replaced by the following equivalent linear expressions (FORTUNY-AMAT and MCCARL, 1981).

$$a \ge 0,\quad b \ge 0,\quad a \le M\mu \ \text{ and } \ b \le M(1-\mu) \quad (106)$$

where μ is an auxiliary binary variable and M is a large enough positive constant. Thus, each nonlinear equation in constraints Ψ^{COMP} can be replaced by the three linear equations in (106).

The key outputs in this second stage are the load demand ($\tilde{p}_{d,t}^{D}, \tilde{q}_{d,t}^{D}$), the generation capacities for the DGs ($\tilde{p}_{g,t}^{G^{max}}, \tilde{q}_{g,t}^{G^{max}}$), and a UB (upper bound) of the cost, calculated as:

$$UB = \min\left\{UB, \sum_{t_y}\left[\sum_{c\in\Omega^C}\frac{\left(I_c^C \dot{x}_{c,t_y}^C\right)}{(1+R)^{t_y}} + \sigma\sum_{t_d}\left(\sum_{g} C_{g,t}^{G}\dot{p}_{g,t}^{G} + \sum_{d} C_{d,t}^{LS}\dot{p}_{d,t}^{LS}\right)\right]\right\} \quad (107)$$

where $\dot{x}_{c,t_y}^C$ is the solution from the first stage and $\dot{p}_{g,t}^G$ and $\dot{p}_{d,t}^{LS}$ are solutions from the second stage.

4.3.2.4 Convergence of First and Second Stages

Before starting the third stage, the first and second stages must converge, as they provide the best investments for the worst-case load demand and generation capacity.

Computing (UB-LB)/LB checks the convergence. If this gap is lower than a given tolerance (10^{-4}), the algorithm continues at the third level; otherwise, it goes back to the first stage.

4.3.2.5 Third stage and Sensitivity Matrix Update

Stage one uses a sensitivity matrix to estimate the EENS index. This index value helps to improve the computational time for the optimization process in the first stage of the decomposition; however, the estimation of this index may not be accurate enough when placing multiple components since the sensitivity matrix is created by placing the candidates individually.

The third stage updates the sensitivity matrix by using an MCS to accurately calculate the EENS index using the solution found in the convergence of stages one

and two. The calculation of EENS using MCS is the same approach described in subsection 4.3.2.1.1.

The new EENS index is compared with the $EENS_{t_y}^{TG}$. If the target is met, the algorithm ends; otherwise, the new EENS value is saved in $EENS_{t_y}^{w}$ and the sensitivity matrix ($\xi_{t_y}^{w}$) is updated, and the algorithm returns to the first stage.

The updated sensitivity matrix ($\xi_{t_y}^{w}$) is defined as:

$$\xi_{t_y}^{w}[c,d] = \xi_{t_y}^{0}[c,d] \ \left(1 - \dot{x}_{c,t_y}^{C}\right), \qquad \forall c, \forall d \tag{108}$$

where $\xi_{t_y}^{0}$ is the sensitivity matrix before the expansion decision.

The new values for the EENS index and the sensitivity matrix are kept for all w iterations in $EENS_{t_y}^{w}$ and $\xi_{t_y}^{w}$, respectively.

Note that $\xi_{t_y}^{w}$ is a copy of $\xi_{t_y}^{0}$ with null values in the positions of the proposed expansion planning in the current iteration. Since $EENS_{t_y}^{w}$ provides the exact EENS index for the current expansion decision, the sensitivity matrix in these positions is ignored.

This approach creates a new cut in the first stage and provides, in the next iterations, the correct value of the EENS index for the current expansion decision.

The new cut in the first stage is created using constraint (80):

$$EENS_{t_y}^{w} \leq EENS_{t_y}^{TG} - \sum_{t_y} \sum_{d \in \Omega_n^D} \left(\xi_{t_y}^{w}[c,d] \ x_{c,t_y}^{C}\right)$$

After updating the sensitivity matrix in (180), constrain (80) from the first stage of the decomposition properly represents the correct EENS index for the components placed in the current algorithm's iteration.

4.3.2.6 Convergence after the third stage

If the new EENS calculated in the third stage is less or equal to the target, the algorithm ends; otherwise, it updates the $\xi_{t_y}^{w}[c,d]$ matrix and returns to the first stage of the decomposition.

4.3.2.7 Overview of the proposed model

The proposed approach embodies the reliability index in the expansion decision in the first stage. It seeks to minimize the total cost for the worst-case realization of uncertainty in the second stage. An MCS with nonlinear AC-OPF is performed in the third level, which updates the sensitivity matrix, if necessary.

The model provides simplicity at each level to enable the solution of such a complex problem.

This model uses the EENS reliability index. Other indexes also can be used in the same methodology by adapting the creation of the sensitivity matrix, and equations (44) and (80).

The uncertainties are controlled by the uncertainty budget (Γ). $\Gamma = 1$ represents the worst possible scenario, and $\Gamma = 0$ represents an optimistic case, from the perspective of the uncertainty levels. Both cases ($\Gamma = 1,\ \Gamma = 0$) may be seen as unrealistic scenarios; one has over-conservatism decisions that lead to over-investment costs; the other is too optimistic. Therefore, the proposed model must be seen as a tool to study different uncertainty budgets, and investors can discuss the acceptable levels of uncertainty and investments.

Using a sensitivity matrix in a mixed-integer linear approach can lead to suboptimal solutions, while using nonlinear formulations can result in a long computing time. Moreover, the installation of switches along with distributed generation can provide very different results in reliability indexes if compared to the placement of these components individually. Thus, this work proposes the third stage in the decomposition of the problem to update the sensitivity matrix using MCS and a nonlinear formulation, which overcomes these issues related to the use of sensitivity matrices.

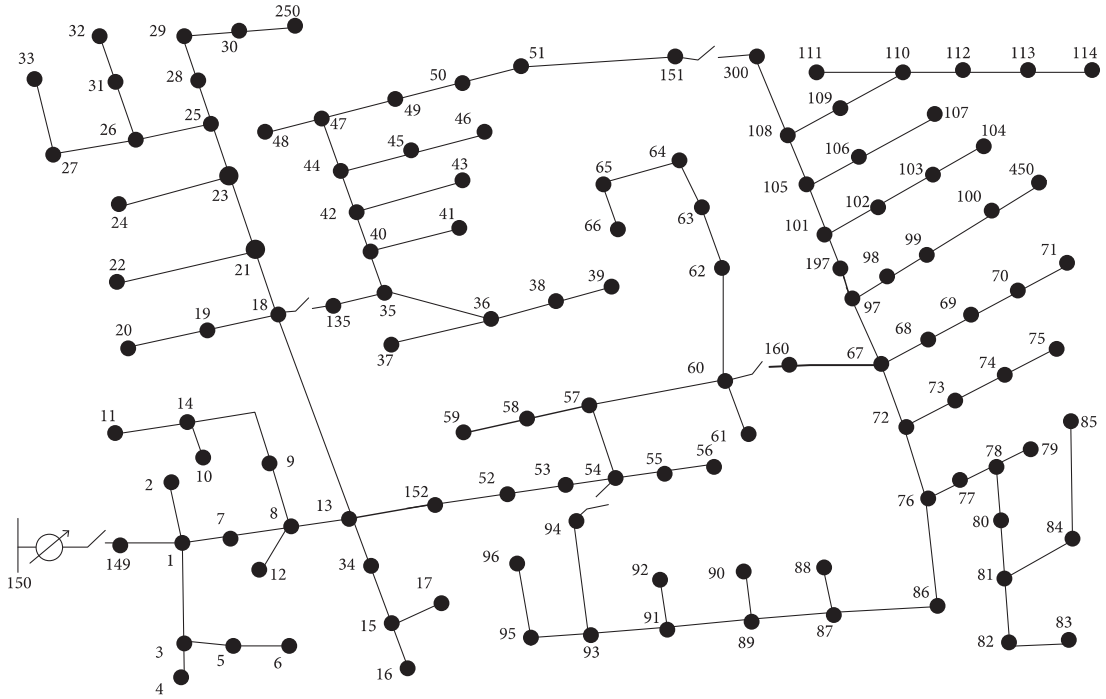
4.4 CASE STUDY

The proposed model is illustrated using a modified version of the IEEE 123-bus test system, represented by a 24.9/4.16 kV system with 3.4 MW of load demand, proposed in Kersting (1991).

The expansion plan horizon is defined as 3 years, and all load points are assumed to increase at a rate of 10%/year with 20% of uncertainty range (varying from

80 to 120% of its estimated value). Figure 20 shows the test system before the expansion decisions.

FIGURE 20 – IEEE 123-BUS TEST SYSTEM Kersting (1991)



The availability of the power sources, the load profile throughout the hours of the day, and their uncertainty range are obtained from Alam et al. (2020).

The additional required data for this test system has been taken from Kersting (1991), including line lengths, conductor characteristics, switch configurations, and capacitor types.

The existing lines have a failure/year rate of 10^{-1} and repair time of 5h, while new lines have 10^{-4} failures/year and repair time of 1h. These values were defined based on average values presented in Pinto et al. (2019).

The EENS target is set to 25% of its original value, 14.2 MWh/year, representing a goal defined by the DSO.

The candidate lines have characteristics similar to the existing lines from the original system but with lower failure rates and 50% less resistance/reactance.

More details of the test system are presented in appendix A.

4.4.1 SIMULATION RESULTS

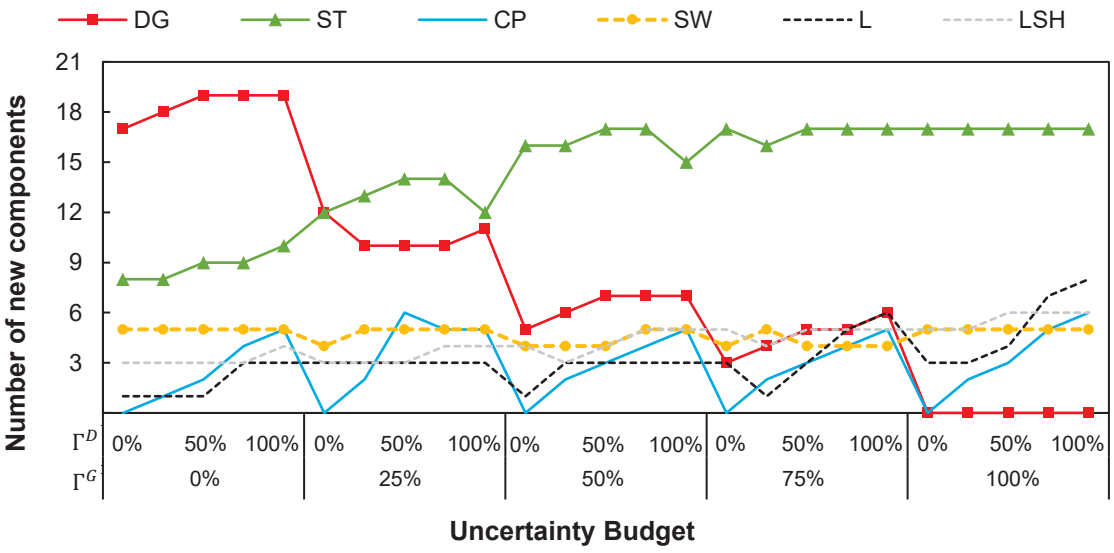
Studies including uncertainties require exploring different scenarios so the investor can evaluate the accepted risk level. This section presents expansion proposals for different uncertainty budgets, some operational results provided by the model, processing time, impacts varying the EENS target, and a discussion on including or not some of the aspects considered in this chapter.

The numerical experiments were carried out with Gurobi to solve the first/second stages (MILP) and IPOPT to solve the third stage (NLP), in a machine with 8 cores and 32GB of RAM, with Python.

4.4.2 Expansion proposal in different uncertainty budgets

The proposed model was applied in the IEEE 123-bus test system for 25 different cases, in which the uncertainty budget of demand and generation capacity were set as 0, 25, 50, 75, and 100%, independently. Figure 21 shows the number of components placed in the system for each case.

FIGURE 21 – NUMBER OF COMPONENTS PLACED IN THE IEEE 123-BUS TEST SYSTEM VARYING UNCERTAINTY BUDGETS



DG: distributed generation, ST: energy storage system, CP: capacitors, SW: switches, L: lines, LSH: lines for self-healing

Figure 21 shows that if the uncertainty in the load demand increases, the number of DGs placed in the system slightly increases. In the same case, ESS units and capacitors increase considerably. That occurs because, if the demand increases, more generation power is required, and the capacitors are needed to compensate the increment in the reactive power.

The increasement in the uncertainty budget for generation negatively impacts the placement of DGs, going from 20 to 0 components in the system. That occurs because the investments in DGs remain the same, while their total capacity decreases; thus, the investment may not be worthwhile. On the other hand, the number of ESS units increases within the uncertainty for generation because ESS does not depend exclusively on the DGs for storing the energy, and they are good alternatives if a fault occurs, as it improves the EENS index.

The switches and lines for self-healing are exclusively used in improving the reliability indexes, and they are not significantly impacted by the changes in the uncertainty budget in this case study. These components only complete the investment to meet the EENS target, and they do not provide a reduction in operational costs.

In this case study, the number of lines is not significantly affected as well; however, this may not occur in cases where their power flow limits do not support the increase in load.

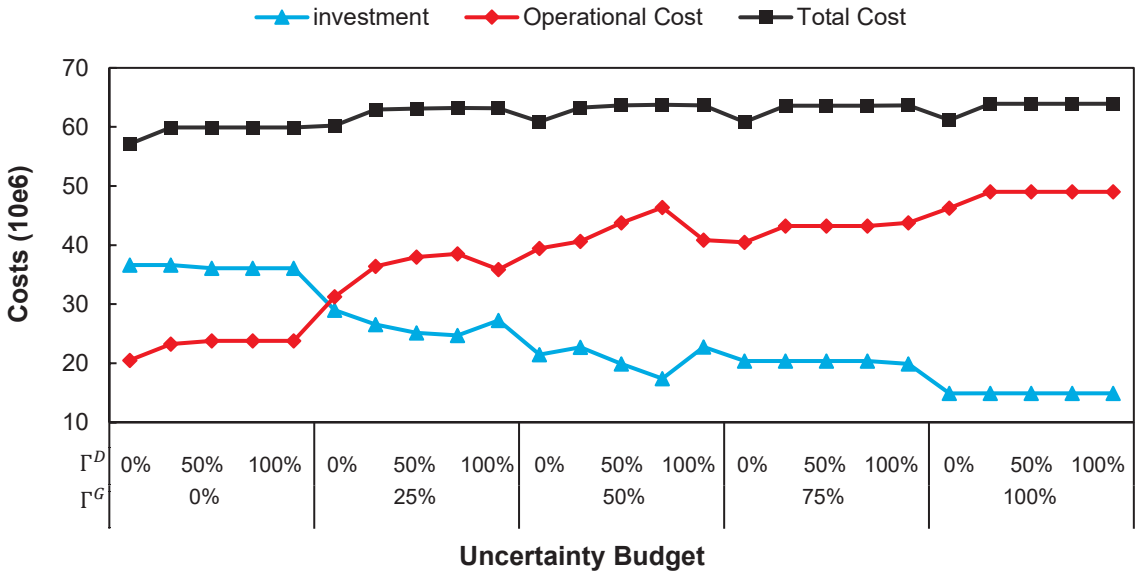
Figure 21 shows the impacts of different uncertainty budgets over the number of components placed in the system. It is also important to observe the expansion plan’s cost in different cases, shown in Figure 22.

Figure 22 shows that the investment cost decreases if the generation uncertainties increase, which is expected since Figure 21 shows that the number of DG units is reduced for the same case, and these components are the most expensive.

At higher uncertainty levels, operational costs increase for two reasons: fewer DG units in the system and higher load demand. If the generation uncertainty is high, DG units are not worth it; thus, the operational cost increases while the investment decreases. If the load uncertainty is high, the load demand increases.

Furthermore, the results show that most of the investments are not economically viable in high levels of uncertainty for this case study.

FIGURE 22 – INVESTMENT, OPERATIONAL, AND TOTAL COST IN THE IEEE 123-BUS TEST SYSTEM VARYING UNCERTAINTY BUDGETS



For this case study, the Total Cost slightly increases when varying the uncertainty budget from 57e6 to 64e6. This occurs because the proposal method seeks the lowest total cost; however, this behavior may change for other case studies, since it may have cases where load shedding is inevitable.

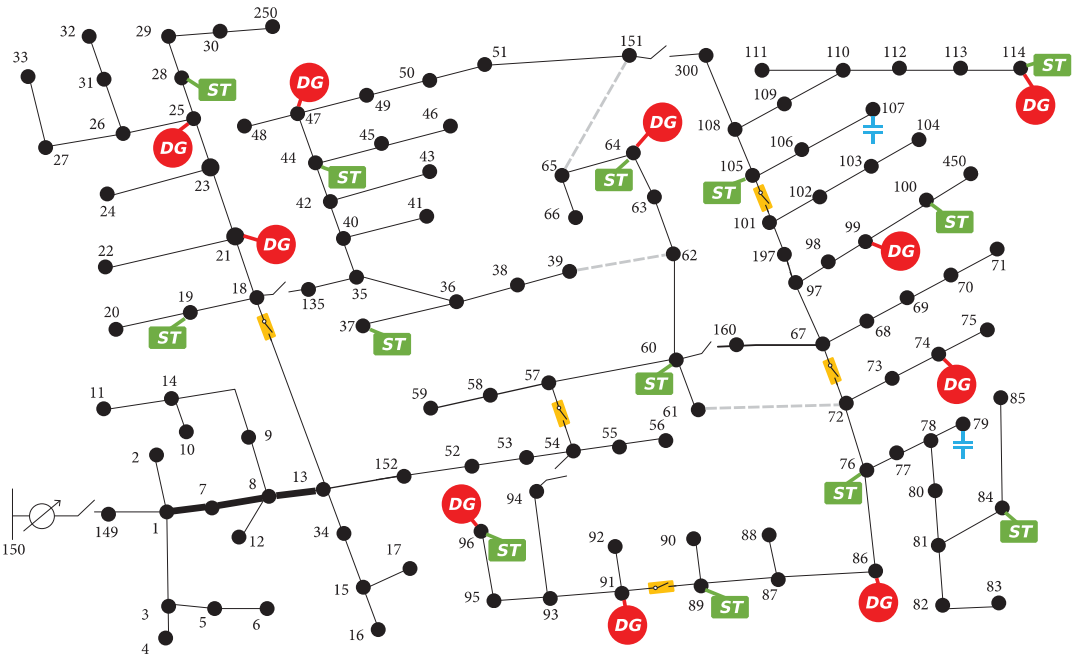
4.4.3 Expansion proposal details for uncertainty budget of 25%

To illustrate the expansion planning decisions obtained by the proposed model, Figure 23 shows the candidates' location in the last year of the expansion planning considering the case with 25% of uncertainty for generation and demand.

Most of the DG and ESS units were placed near the system's end nodes, which helps to improve the voltage profile in these areas and supply the demand in case of faults. The same occurs with all capacitors, but DGs and ESSs are distributed along the system, which helps to supply loads during faults.

The switches were placed in branches that, if necessary, could isolate specific areas. This is important when evaluating reliability indexes because if a fault occurs in a zone delimited by those switches, they may isolate this region. As an example, if a fault occurs in the line between buses 23-25, the switches near bus 18 would switch off, and part of the system would still be supplied during the repair time of the faulted component.

FIGURE 23 – EXPANSION PLANNING DECISION AT THE LAST YEAR OF THE EXPANSION PLANNING DECISION CONSIDERING UNCERTAINTY BUDGET OF 25%



Moreover, the branches between buses 65-151, 39-62, and 61-72 are lines for self-healing. These branches can be activated at any time, if that would reduce the load shedding during the repair time. For example, a fault near bus 21 would activate the switch in bus 18, and the region of buses 35-51 would be disconnected from the main grid. At the same time, the DSO would activate the branches 65-151 and 39-62; thus, the region would be connected to the main grid again. This self-healing capacity is only possible in modern ADNs with the proper technology and automation.

Furthermore, the placement of ESS units, along with distributed generation, switches, and lines for self-healing, creates a scenario where the DSO can isolate specific areas during faults and reduce the impact on the rest of the system, improving the EENS index.

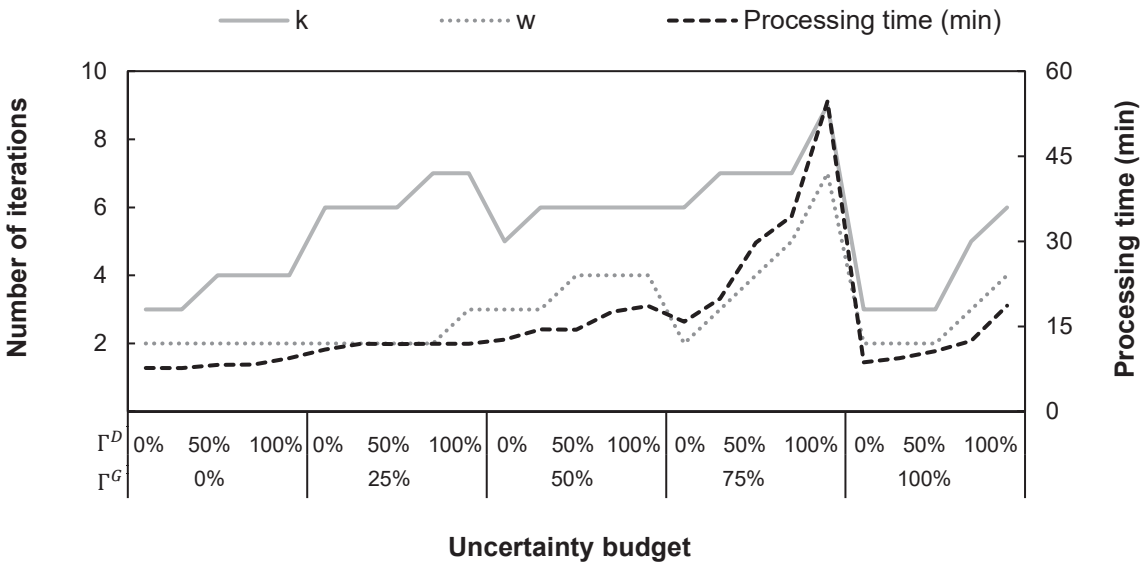
The branches connecting buses 1-7, 7-8, and 8-13 were reinforced. They are the main branches to connect to the substation in node 1, and most of the power from the substation flows on these branches. Reinforcing these branches reduces the risk of faults that disconnect the entire system from the substation.

4.4.4 Processing time and iterations

Robust models can become hard to solve in viable computational time, and including reliability increases its complexity. Figure 24 presents the number of iterations and the processing time for each case of the uncertainty budget. Parameter *k* represents the number of iterations in the first and second stages, and *w* is the iteration including the third stage.

The processing time presented in Figure 24 does not consider the time to create the sensitivity matrix. This step can be performed once and used for all simulations. The test system's time to run the sensitivity matrix was 132 minutes. It is fair to compare the processing time neglecting this step since the matrix represents the benefit of adding a single component to the system, and if new components are desired to be included, it can be evaluated just their benefits and this value added to the matrix.

FIGURE 24 – NUMBER OF ITERATIONS (k AND w) AND PROCESSING TIME FOR THE TEST SYSTEM VARYING THE UNCERTAINTY BUDGETS



If *w* is equal to 1, the initial sensitivity matrix has accurately estimated the EENS index in the first iteration. The increase in *w* shows the number of iterations required to update the matrix.

As expected, the processing time depends mostly on the number of iterations in the third stage (w) due to the MCS. Moreover, the processing time for the uncertainty

budgets of 0% is about 7 minutes, which is reasonable for this case study including reliability. The processing time increases up to 55 minutes if both uncertainty budgets are set as 75%. Additionally, if the generation uncertainty budget is 100%, the processing time declines more than 50% because the DGs are not even considered in this case.

In addition, compared to other works, the processing time of the proposed work is attractive. Reference Dehghan et al. (2016) also proposes a three-stage decomposition using MCS and a sensitivity matrix to estimate reliability indexes. The work shows simulation time from 1.5 hours to 47 hours for a similar test system, while this work shows simulation time from 7 minutes to 55 minutes. This reference proposes a different type of cut in the first stage of the problem, which requires more time for the algorithm to converge; it also does not include some important elements from active distribution networks, such as ESS.

4.4.5 Effects on processing time and total cost due to changing EENS target, neglecting faults' extension, and neglecting switches

In order to study the effects on the processing time and total cost changing some aspects of the proposed model, the uncertainty budgets are fixed at 25% for generation and demand uncertainties, and the following three cases are defined:

Case A: changing EENS target from 14.2 to 7.1 MWh/year (less 50% compared to the base case)

Case B: changing EENS target from 14.2 to 10.7 MWh/year (less 25% compared to the base case)

Case C: changing EENS target from 14.2 to 21.3 MWh/year (more 50% compared to the base case)

Case D: neglecting faults' extension in the MCS (Step (iii)-(a) in the MCS process defined in subsection 4.3.2.1.1).

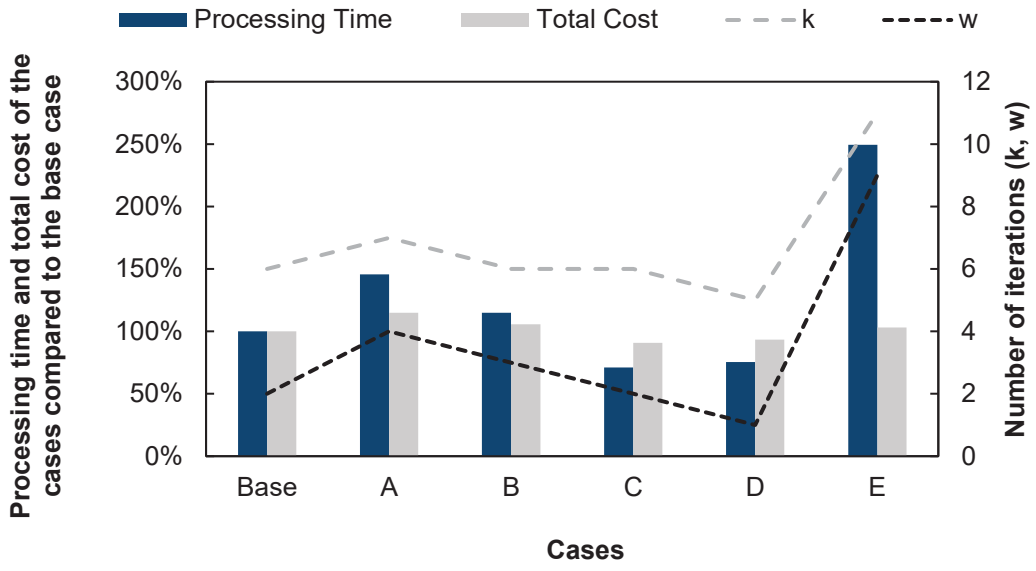
Case E: neglecting original switches of the IEEE-123 bus test system

Cases A to C are used to understand the effects of changing the EENS target in the computing time and total cost of the problem, the values for the EENS target are 50%, 75%, and 150% of the value of the base case. Case D shows the importance of considering the fault's extension in reliability studies. Case E presents a case where

the test system has no switches placed in its initial configuration, but switch candidates are considered in the expansion planning.

Figure 25 shows the computing time and total cost of each case compared to the case base.

FIGURE 25 - PROCESSING TIME, TOTAL COST, AND NUMBER OF ITERATIONS FOR CASES A TO E



The processing time increases for the cases where the EENS target is tight: 146% for case A and 115% for case B, compared to the base case. This time decreases for the case where the index is loose, 71% for case C. Moreover, the total cost increases if the EENS index is tighter.

Case D shows that if the faults' extension is neglected, processing time and total cost decrease. The processing time is lower because the complexity of the problem is reduced. The reduction in the total cost shows that less investment is required for this case; however, this representation does not truly represent faults in practical systems. This shows the importance of considering faults' extension in the model; otherwise, the proposed expansion planning would not provide practical results.

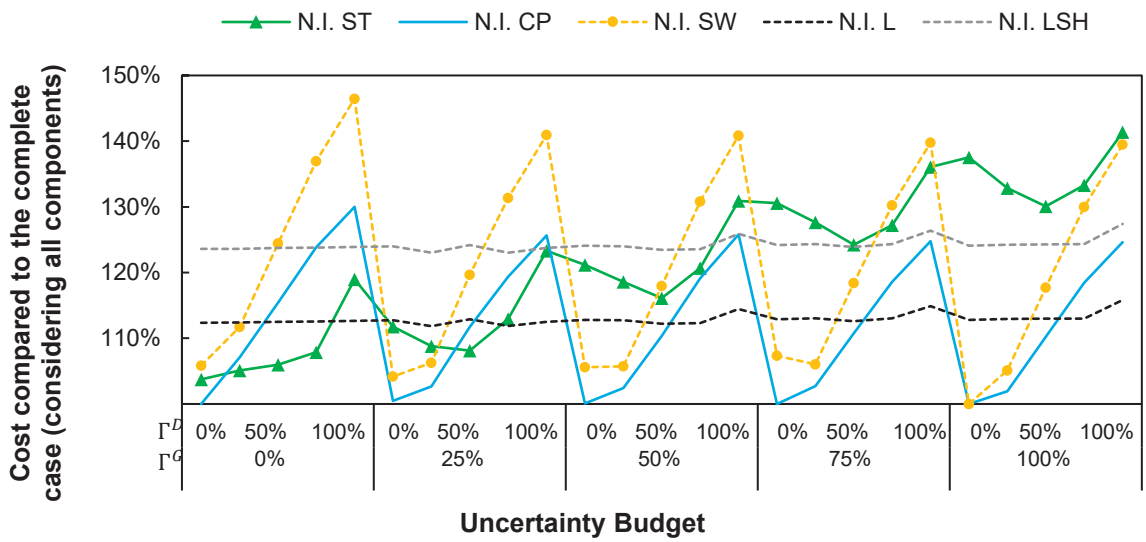
Case E presents a scenario where the original system has no switch installed. In this case, more iterations are required due to the sensitivity matrix. The processing time is near 250% of the base case, and the total cost is similar (103%). The use of a sensitivity matrix has limitations in cases where the single installation of DG or ESS unit does not provide the expected improvement in the reliability index due to the

extension of a fault, which cannot be isolated if switches do not exist; thus, more iterations are required.

4.4.6 Comparisons of the proposed model not considering some components

In order to understand the importance of formulating the problem with all aspects presented in this chapter, Figure 26 shows the variation in total cost (objective function) using the IEEE 123-bus test system, but not including (N.I.) some type of components (individually).

FIGURE 26 – COMPARISON OF THE TOTAL COST OF THE COMPLETE CASE STUDY WITH CASES NOT INCLUDING (N.I.) SOME COMPONENTS



ST: ESS units, CP: capacitors, SW: switches, L: branches, LSH: lines for self-healing

Figure 26 shows that the objective function is up to 147%, compared to the complete case, if not considering switches, which are even more important for higher uncertainty budgets of demand.

The objective function is up to 143% when not including ESS units. The impact of this component in the total cost increases within both uncertainty budgets.

In the simulation, the increase in capacitors installed in the system was only related to the demand uncertainty. This was expected since they are used to compensate the increment in the reactive power of the loads.

The branches and lines for self-healing present some impact in the objective function; however, they do not significantly correlate with the uncertainty levels. This is

true for the case study; however, this might be different if the power flow in a line is too close to its transmission capacity.

Figure 26 does not present the case not including DG, because generation uncertainty would not apply in this case, and the comparison would not be consistent.

Therefore, the aspects presented in this chapter are essential and should be adequately represented for a suitable expansion planning decision.

4.5 SUMMARY

This chapter presented a model to solve the expansion planning problem for active distribution networks, including uncertainty, reliability, and DERs. The model considers distributed generation, ESS, lines, self-healing, capacitors, and switches. The model uses an adaptive robust optimization approach to determine the best investment times and locations for all expansion candidates.

A novel sensitivity matrix method is introduced in the C&CG algorithm to improve computational time significantly. This matrix proved to be very effective in the cases studied, providing fast and consistent results. Compared to similar works, the proposed model shows up to 90% less processing time.

The solution approach uses a three-stage decomposition based on the C&CG algorithm. The first stage seeks the best investment to minimize the total cost while meeting an EENS index target using the sensitivity matrix; the second stage defines the worst-case realization of the uncertainties; the third stage updates the sensitivity matrix using an MCS.

The results show that the number of DGs installed in the system is inversely proportional to the generation uncertainty budget. In contrast, the number of ESS units increases with the uncertainty levels.

Moreover, simulations show that the EENS index target impacts the proposed model's processing time and total cost. Considering reliability indexes in the expansion planning model (or similar approaches that would improve quality/safety) is important to understand the required investment to reach the desired target.

Switches and the lines for self-healing are components related mostly to the reliability indexes. The variation in the uncertainty budgets does not significantly impact the number of these components placed in the system. Yet, their inclusion improves the objective function of the problem.

Simulations demonstrate that not including ESS units, capacitors, switches, or DGs may increase the total cost of the expansion planning up to 147% compared to the case considering all these aspects. These components help reduce the operation cost while improving the reliability indexes.

5 A CONTINGENCY-CONSTRAINED ROBUST MODEL FOR EXPANSION PLANNING OF ACTIVE DISTRIBUTION NETWORKS AND MULTIPLE MICROGRIDS

5.1 INTRODUCTION

Chapter 4 presented an expansion planning model for ADNs, including uncertainties and reliability. In addition to the concepts of modern distribution networks, microgrids and demand response also stand out.

The microgrid (MG) concept is similar to an ADN but on a small scale; thus, MG is a group of DERs that includes DG units, ESSs, it may include controllable loads, and it may operate isolated from the main grid. The concept has gained popularity due to renewable energy resources and trending new technologies (SAHOO and KISHORE, 2017).

More complex ADNs may incorporate multiple microgrids (MMG), creating a big challenge for expansion planning problems. Its complexity is mainly due to simultaneously defining the coordination of DERs, working with controllable and deferrable loads, finding the best investment decisions, and yet seeking the best global solution.

Regarding demand response, most works on robust expansion planning have represented the load demand as a unique portion. Reference Varasteh et al. (2019) proposes the representation of the load into three different portions: critical/non-controllable (NC), deferrable (DF), and controllable (CTL). The deferrable and controllable portions require a certain amount of energy within a given period, but the exact timing is not defined. The representation of the load in different portions is important in robust approaches since some parts of the load may be subject to uncertainties, while the system operator totally controls other parts.

Moreover, to effectively design an isolated operation of MGs, generation contingency should be considered. This plays an important role in the reliability level of MGs because any equipment is subject to failure during its operation. Since MGs are supposed to operate isolated from the main grid if necessary, the contingency approach guarantees enough power generation inside an MG to meet the load demand even if a fault occurs.

Furthermore, the power source of DGs is generally related to uncertain sources, such as solar and wind, which impact investment decisions. Thus, the investment in DG units is not consistent if uncertainties are not considered.

Therefore, the model presented in this chapter includes MMG, demand response, and contingencies in the ADN expansion planning problem under uncertainties, which is also its main contribution.

5.2 CONTEXT AND ASSUMPTIONS

The model presented in this chapter considers the following:

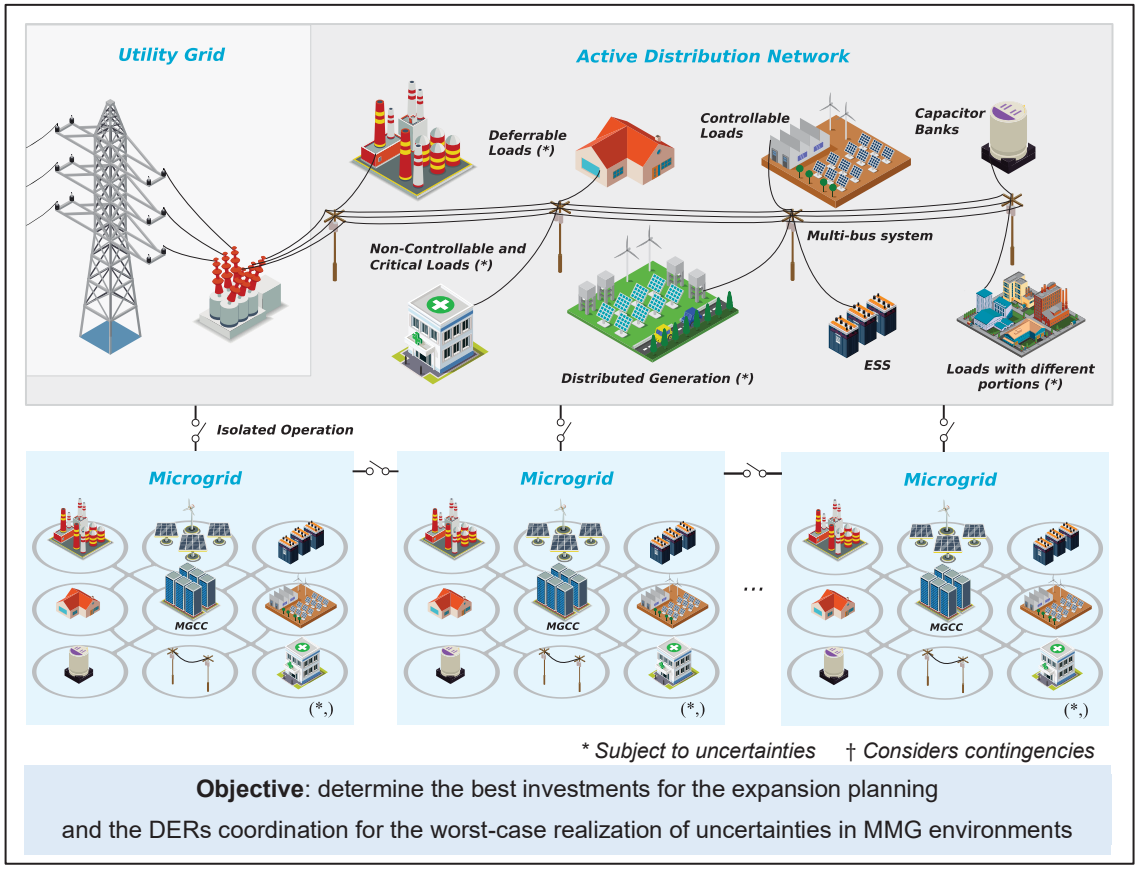
- The DSO desires to minimize the total cost of investment and operation (generation and load shedding).
- The DSO owns or controls the investment in all MGs. Thus, the DSO decides on whether install or not a new component inside the MGs.
- The candidates for the expansion planning problem are distributed generator units, energy storage system units, capacitors, and installation/reconductoring of lines.
- Loads have three portions: non-controllable; controllable, controlled directly by the DSO; deferrable, which may be shifted over time, but the DSO does not control it.
- All MGs must be able to operate with N-1 generation contingency. The generation contingency is defined as the capacity of each MG to operate isolated from the main grid even if one of the generator units has failed (N-1 contingency).
- Historical data is unavailable; thus, an ARO is the best approach.
- The degradation of ESSs by charging/discharging and their efficiency are ignored, as well as active power losses in lines.
- Any MG of the system may operate isolated from the main grid at any hour of the day. The decision on operating/not-operating isolated is related to the operational constraints and their benefits to the system.

In addition, reliability indexes are not directly represented in this chapter (and the next ones) since N-1 contingencies are included in the model. Cuts of second-order

or higher have small contributions to reliability indexes, and, generally, they may be neglected (DA SILVA et al., 2006 and BILLINTON et al., 1998).

Figure 27 illustrates the scope of the model proposed in this chapter, in which the main goal is to find the best investment decisions and the DERs coordination under the worst-case of uncertainties in MMG systems. The main components considered in this work are also presented in Figure 27, in which MGCC stands for Microgrid Central Controller.

FIGURE 27 – SCOPE AND OBJECTIVE OF THE MODEL IN THIS CHAPTER USING A GENERIC STRUCTURE OF MMG SYSTEMS.



SOURCE: Pinto et al. (2021)

Figure 27 shows the complexity of systems with ADN and MMGs. The Utility Grid, the ADN, and all MGs are connected, and they can exchange power. The networks inside the ADN and MGs are considered with multiple load points defined as multi-bus. The MGCC is responsible for controlling the DERs coordination and the isolated operation of the MGs.

This chapter proposes a model for scenarios that the distribution system operator (DSO) owns the network and its investment decisions. Although the

expansion decisions in the ADN and the MGs are made directly by the DSO, the decisions inside the MGs can be seen as areas where the DSO should encourage the investment of those components by private investors or invest by itself.

5.3 PROPOSED MODEL

Similar to chapter 4, assuming that historical data of generation or load is unavailable, this chapter models the problem using robust optimization to deal with uncertainties and a contingency-constrained approach.

The model seeks the best investments and operational conditions (generation, DERs coordination, and load shedding costs) for the worst-case realization of the uncertainties in the ADN and MGs.

The model is formulated as a tri-level optimization problem and solved using a two-stage robust optimization approach formulated as a MILP problem. Reformulation procedures are proposed to reconstruct the problem using the C&CG.

The following subsections show the problem formulation and the solution approach.

5.3.1 Formulation

5.3.1.1 Objective function

Generally, the distribution expansion planning problem aims to minimize the total cost of investment and operation in the planning horizon. Considering a robust optimization approach to deal with uncertainties, the proposed model is defined as follows.

$$\min_{x^C_{c,t_y}} \max_{\Delta Smax} \min_{\Delta Smin} \sum_{t_y} \sum_{c} \frac{I^C_c x^C_{c,t_y}}{(1+R)^{t_y}} + \sum_{t_y} \sum_{t_h} \left[\sigma \left(\sum_{g} C^G_{g,t} p^G_{g,t} + \sum_{d} C^{LS}_{d,t} p^{LS}_{d,t} \right) \right] \qquad (109)$$

subject to Ψ^{Lflow}, Ψ^{bal}, Ψ^{ess}, Ψ^{op}, Ψ^{inv}, Ψ^{unc}, Ψ^{dr}, Ψ^{cont}, Ψ^{bsw}, Ψ^{uncCTL}

The structure of the objective function in (109) is the same presented in chapter 4, where x^C_{c,t_y} represents the expansion planning decision for each component *c*.

$\Delta Smax$ is the subset of variables related to the uncertainties $\{\tilde{p}_{g,t}^{G^{max}}, \tilde{p}_{d,t}^{D_{nc}}, \tilde{p}_{d,t}^{D_{df}}\}$, and $\Delta Smin$ is the subset of all variables, except $\{x_{c,t_y}^{C}, \tilde{p}_{g,t}^{G^{max}}, \tilde{p}_{d,t}^{D_{nc}}, \tilde{p}_{d,t}^{D_{df}}\}$. This is a three-level problem, in which the first level seeks the best investments, the second level defines the worst-case realization of uncertainties, and the third level represents the operational conditions of the power system.

There are two variables representing the time. The first variable is t_y, which is used to define the period of the installation of new components in the system and load levels per year (or period). The second variable is t_h that represents the hours of the daily 24-hour operation (24H-OP), which is used to define the DERs' coordination.

5.3.1.2 Constraints

The set of constraints Ψ^{Lflow}, Ψ^{bal}, Ψ^{ess}, Ψ^{op}, Ψ^{inv}, and Ψ^{unc} are the same as defined in chapter 4, subsection 4.3.1.2. And sets Ψ^{dr}, Ψ^{cont}, Ψ^{bsw}, and Ψ^{uncCTL} are defined below.

Demand response constraints (Ψ^{dr}):

The load demand can be represented by three different portions. A non-controllable portion ($p_{d,t}^{D_{nc}}$) that cannot be shifted over time and is subject to uncertainty. A controllable portion ($p_{d,t}^{D_{ctl}}$) that may be shifted over time and is directly controlled by the DSO. And a deferrable portion ($p_{d,t}^{D_{df}}$), which may be shifted over time, but the DSO has no decision over it and is subject to uncertainty.

The following constraints represent the demand response.

$$p_{d,t}^{D} = \tilde{p}_{d,t}^{D_{nc}} + \tilde{p}_{d,t}^{D_{df}} + p_{d,t}^{D_{ctl}} \qquad \forall d, \forall t \qquad (110)$$

$$q_{d,t}^{D} = \tilde{q}_{d,t}^{D_{nc}} + \tilde{q}_{d,t}^{D_{df}} + q_{d,t}^{D_{ctl}} \qquad \forall d, \forall t \qquad (111)$$

$$p_{d,t}^{D} \leq \sum_{t_h} p_{d,t}^{D} / (Lfac_d \, T_h) \qquad \forall d, \forall t \qquad (112)$$

$$\sum_{t_h} p_{d,t}^{D_{ctl}} = P_{d,t}^{D_{ctl}^{total}} \qquad \forall d, \forall t_y \qquad (113)$$

$$p_{d,t}^{D_{ctl}} \leq \overline{P}_{d,t}^{D_{ctl}} \qquad \forall d, \forall t \qquad (114)$$

$$p_{d,t}^{D_{ctl}} = q_{d,t}^{D_{ctl}} \left(P_{d,t}^{D_{ctl}^{total}} / Q_{d,t}^{D_{ctl}^{total}} \right) \qquad \forall d, \forall t \qquad (115)$$

Constraints (110) and (111) represent the total active and reactive loads for each load point, period, and time. $p_{d,t}^{D}$ and $q_{d,t}^{D}$ are the total active and reactive load in load point d.

Constraint (112) defines a minimum value of load factor ($Lfac$) for all load points. This is important to provide consistent results; otherwise, the load portions with uncertainties may have nonsense peaks. T_h is the number of hours in one day. Since the deferrable portion of the load is included in the max subproblem presented in the objective function, the load factor control helps to provide more realistic results.

Constraint (113) defines the total amount of controllable loads for a daily operation $\left(P_{d,t}^{D_{ctl}^{total}} \right)$. It does not fix the specific time for this portion; thus, it may be allocated at any hour of the day.

Constraint (114) represents a limit for controllable loads for each hour of the daily operation $\left(\overline{P}_{d,t}^{D_{ctl}} \right)$. This constraint prevents the controllable load from being allocated in undesired hours of the day, such as overnight. Lastly, constraint (115) keeps constant the load power factor.

The proposed approach is a generic formulation. If the DSO wishes to ignore the minimum load factor or the limit for controllable loads, constraints (112) and (114) can be ignored.

Note that some constraints for the controllable loads are not replicated to the deferrable loads because they are defined in the set of uncertainty constraints. Thus, some of the constraints presented in the Uncertainty Constraints (Ψ^{uncCTL}) are related to the demand response.

Generation contingency constraints (Ψ^{cont}):

This model assumes that all MGs are able to operate isolated from the main grid and with N-1 generation contingency. Thus, the following constraints are defined:

$$\sum_{g_c \epsilon \Omega_m^G \setminus g} x_{g_c,t_y}^{G} \tilde{p}_{g_c,t}^{G^{max},m} + \sum_{e} p_{e,t}^{E,m} \geq \sum_{d} \left(p_{d,t}^{D,m} - p_{d,t}^{LS,m} \right) \qquad \forall m, \forall g \epsilon \Omega_m^G, \forall t \qquad (116)$$

$$\sum_{g_c \epsilon \Omega_m^G \backslash g} x_{g_c,T}^G \tilde{q}_{g_c,t}^{G^{max},m} + \sum_{cp} q_{cp,t}^{SH,m} \geq \sum_{d} \left(q_{d,t}^{D,m} - q_{d,t}^{LS,m}\right) \qquad \forall m, \forall g \epsilon \Omega_m^G, \forall t \qquad (117)$$

The notation $\sum_{g_c \epsilon \Omega_m^G \backslash g} x_{g_c,t_y}^G \tilde{p}_{g_c,t}^{G^{max},m}$ in (116) represents the total active power generation capacity of the generator units allocated in the MG m, excluding the generator g. Ω_m^G represents all generator units inside MG m. The notation $g_c \epsilon \Omega_m^G \backslash g$ shows that g_c is the index representing all generators from MG m (Ω_m^G), except the generator g ($\backslash g$). This constraint is set for all microgrids ($\forall m$), all generators' units inside the MG m ($\forall g \epsilon \Omega_m^G$), and the hours in a day.

Thus, constraint (116) defines that the total active power generation capacity plus the charging/discharging power of the ESSs inside the microgrid m must be greater or equal to the total amount of active load inside the same microgrid, even if the generator unit g has failed. This is defined for all generators inside the MG ($\forall g \epsilon \Omega_m^G$). Constraint (117) is similar to (116), but for the reactive power.

This formulation is an exhaustive failure analysis, in which a constraint is defined for each case of generation fault (since it is defined $\forall m, \forall g \epsilon \Omega_m^G, \forall t$). The approach ensures that inside each MG there is enough power generation capacity to meet the load demand even if one of the generator units has failed.

Although the network is ignored in these constraints for the sake of tractability, the operational constraints (Ψ^{op}) formulate the network and ensure that the power limit in the lines and voltage limits are respected during the operation.

MGs' isolated operation constraints (Ψ^{bsw}):

MGs are expected to operate isolated from the main grid if necessary, which improves the system's reliability and guarantees independence from any event that may occur externally of the MG. Furthermore, the increase in load or generation levels may create an infeasible point of operation in the main grid, and the isolated operation would help in these cases.

This model proposes the possibility of isolating the MG at any hour of the daily operation. Thus, the following constraints are defined:

$$p_{l,t}^{L,m} = x_{l,t_y}^L bsw_{l,t}^{con(m)} \left(G_l v_{sr(l),t} - B_l \theta_{sr(l),t}\right) \qquad \forall m, \forall l \epsilon \Omega_{m,adn}^L, \forall t \qquad (118)$$

$$q_{l,t}^{L,m} = x_{l,t_y}^{L} bsw_{l,t}^{con(m)} \left(-G_l \theta_{sr(l),t} - B_l v_{sr(l),t}\right) \qquad \forall m, \forall l \epsilon \Omega_{m,adn}^{L}, \forall t \qquad (119)$$

$bsw_{l,t}^{con(m)}$ is a binary variable that defines if the microgrid m is connected/not-connected with the ADN through the line l at period t. And $l \epsilon \Omega_{m,adn}^{L}$ represents all lines l that connect the microgrid m to the ADN. The remaining variables and parameters follow the same notation and representation of Ψ^{Fflow} in chapter 4.

Constraints (118) and (119) contain the multiplication of two binary variables ($x_{l,t}^{L} bsw_{l,t}^{con(m)}$), which can be linearized replacing $x_{l,t}^{L} bsw_{l,t}^{con(m)}$ by $z_{l,t}$, an auxiliar binary variable defined as:

$$z_{l,t} \leq x_{l,t_y}^{L} \qquad \forall l, \forall t \qquad (120)$$

$$z_{l,t} \leq b_{l,t}^{con(m)} \qquad \forall l, \forall t \qquad (121)$$

$$z_{l,t} \geq x_{l,t_y}^{L} + b_{l,t}^{con(m)} - 1 \qquad \forall l, \forall t \qquad (122)$$

The constraint (118) still nonlinear even after replacing $x_{l,t}^{L} bsw_{l,t}^{con(m)}$ by $z_{l,t}$. And the equation can be yet linearized by the following sets of constraints:

$$-z_{l,t}^{L} P_l^{Lmax} \leq p_{l,t}^{L} \leq z_{l,t}^{L} P_l^{Lmax} \qquad \forall l, \forall t \qquad (123)$$

$$-\left(1 - z_{l,t}^{L}\right) M \leq p_{l,t}^{L} + B_l \theta_{sr(l),t} - G_l v_{sr(l),t} \leq \left(1 - z_{l,t}^{L}\right) M \qquad \forall l, \forall t \qquad (124)$$

where M is a large enough positive constant.

The same approach can be applied to constraint (119).

This formulation allows the decision on investing (or not) in a new line through x_{l,t_y}^{L} and allows the decision on operating (or not) the MG isolated from the main grid through $b_{l,t}^{con(m)}$.

Uncertainty for deferrable load constraints (Ψ^{uncCTL}):

In this chapter, the uncertainties are modeled as a polyhedral set and bounded by an uncertainty budget (CONEJO et al., 2016). The generation uncertainty is

represented in Ψ^{unc}, defined in chapter 4. Since the load in this model has three portions, its uncertainty set is modeled as follows:

$$\frac{\sum_d \left(\tilde{p}_{d,t}^{D_{nc}} - \underline{P}_{d,t}^{D_{nc}}\right)}{\sum_d \left(\bar{P}_{d,t}^{D_{nc}} - \underline{P}_{d,t}^{D_{nc}}\right)} \leq \Gamma_t^{D_{nc}} \qquad \forall t \qquad (125)$$

$$\underline{P}_{d,t}^{D_{nc}} \leq \tilde{p}_{d,t}^{D_{nc}} \leq \bar{P}_{d,t}^{D_{nc}} \qquad \forall d,t \qquad (126)$$

$$\tilde{p}_{d,t}^{D_{nc}} = \tilde{q}_{d,t}^{D_{nc}} \bar{P}_{d,t}^{D_{nc}} / \bar{Q}_{d,t}^{D_{nc}} \qquad \forall d,t \qquad (127)$$

$$\frac{\sum_d \left(\sum_{t_h} \tilde{p}_{d,t}^{D_{df}} - \sum_{t_h} \underline{P}_{d,t}^{D_{df}}\right)}{\sum_d \left(\sum_{t_h} \bar{P}_{d,t}^{D_{df}} - \sum_{t_h} \underline{P}_{d,t}^{D_{df}}\right)} \leq \Gamma_{t_y}^{D_{df}} \qquad \forall t_y \qquad (128)$$

$$\tilde{p}_{d,t}^{D_{df}} \leq \overline{P}_{d,t}^{D_{df}} \qquad \forall d,t \qquad (129)$$

$$\tilde{p}_{d,t}^{D_{df}} = \tilde{q}_{d,t}^{D_{df}} \sum_{t_h} \bar{P}_{d,t}^{D_{df}} \Big/ \sum_{t_h} \bar{Q}_{d,t}^{D_{df}} \qquad \forall d,t \qquad (130)$$

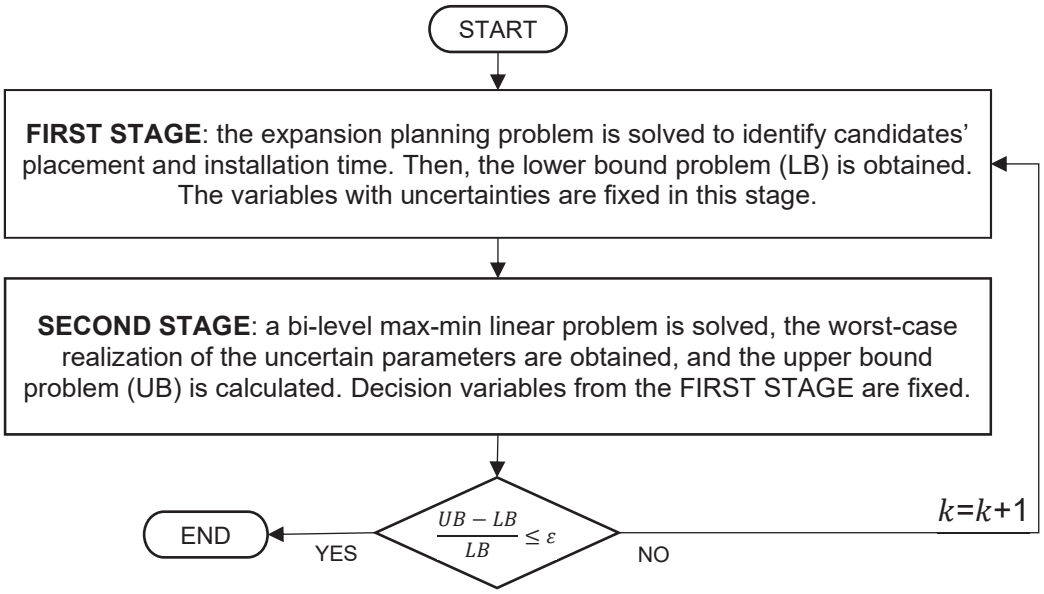
The main difference between the non-controllable and the deferrable portions in the uncertainty constraint is that the first has maximum and minimum limits for every hour of the day in the constraint (126). In contrast, the second has only an upper bound limit in constraint (129). Constraints (127) and (130) keep the power factor of the non-controllable and deferrable loads, respectively.

This formulation provides a generic approach where different portions of the load may be controlled by the DSO ($p_{d,t}^{D_{ctl}}$) or considered unpredictable in time ($\tilde{p}_{d,t}^{D_{nc}}$). The proposed model finds the worst-case realization of uncertainties since it seeks a robust solution.

5.3.2 Algorithm and solution approach

The proposed model is a tri-level optimization problem and is solved using a two-stage robust optimization approach. Figure 28 presents the decomposition used to solve the problem.

FIGURE 28 – TWO-STAGE DECOMPOSITION TO SOLVE THE TRI-LEVEL FORMULATION



The following subsections provide more details on the two-stage decomposition of the problem presented in Figure 28. The algorithm is an iterative process, and the number of variables and constraints increases for each iteration.

5.3.2.1 First Stage and LB Definition

The first stage is formulated as a MILP problem. The variables related to uncertainties are fixed and updated at the second stage of the decomposition; they represent the power generation capacity of the DGs, the non-controllable portion of the loads, and the deferrable portion of the loads ($\tilde{p}_{g,t}^{G^{max}}$, $\tilde{p}_{d,t}^{D_{nc}}$, and $\tilde{p}_{d,t}^{D_{df}}$).

Since this first stage seeks the best investments for the worst-case realization of the uncertainties defined/updated at the second level of the decomposition, its objective function is:

$$\min \sum_{t_y} \left[\sum_{c} \frac{\left(I_c^C x_{c,t_y}^C \right)}{(1+R)^{t_y}} \right] + \eta \tag{131}$$

Subject to Ψ^{η}, Ψ^{Lflow}, Ψ^{bal}, Ψ^{ess}, Ψ^{op}, Ψ^{inv}, Ψ^{dr}, Ψ^{cont}, Ψ^{bsw}

Variable η represents the worst-case for generation and load shedding costs for all *k* scenarios of the C&CG algorithm, and it is defined in the following constraint (Ψ^{η}):

$$\eta \geq \sum_{t_y}\sum_{t_h}\left[\sigma\left(\sum_{g} C_{g,t}^{G} p_{g,t}^{G} + \sum_{d} C_{d,t}^{LS} p_{d,t}^{LS}\right)\right], \qquad \forall k \tag{132}$$

where k represents the number of iterations of the algorithm. Thus, η represents the worst-case of realization of the generation and load shedding costs under uncertainties.

Important to note that, by using C&CG, all the variables subject to uncertainty are fixed in this stage, and all variables that are not related to the expansion planning decision must be defined for all k.

The key outputs in this first stage are the binary decisions (x_{c,t_y}^{C}, $bsw_{l,t}^{con(m)}$) and a cost lower bound (LB), which is the value of the objective function of this stage:

$$LB = \sum_{t_y}\left[\sum_{c}\frac{\left(I_c^C \dot{x}_{c,t}^{C}\right)}{(1+R)^{t_y}}\right] + \dot{\eta} \tag{133}$$

5.3.2.2 Second Stage and UB Definition

The second stage computes the worst-case realization for the uncertainties. The decision variables from the first stage (x_{c,t_y}^{C} and $bsw_{l,t}^{con(m)}$) are fixed. Thus, the objective function and constraints in the second stage are defined as follows:

$$\max_{\Delta Smax}\min_{\Delta Smin}\sum_{t_y}\sum_{t_h}\left[\sigma\left(\sum_{g} C_{g,t}^{G} p_{g,t}^{G} + \sum_{d} C_{d,t}^{LS} p_{d,t}^{LS}\right)\right] \tag{134}$$

Subject to Ψ^{Lflow}, Ψ^{bal}, Ψ^{ess}, Ψ^{op}, Ψ^{dr}, Ψ^{unc}, Ψ^{uncCTL}

Although the objective function (134) is a bi-level max-min problem, the lower-level subproblem is continuous and linear (and thus convex) in its decision variables.

Therefore, it can be replaced by its Karush–Kuhn–Tucker (KKT) conditions, and the objective function may be reformulated as a max problem, as follows.

$$\max \sum_{t_y} \sum_{t_h} \left[\sigma \left(\sum_{g} C_{g,t}^{G} p_{g,t}^{G} + \sum_{d} C_{d,t}^{LS} p_{d,t}^{LS} \right) \right] \tag{135}$$

Subject to Ψ^{Lflow}, Ψ^{bal}, Ψ^{ess}, Ψ^{op}, Ψ^{dr}, Ψ^{unc}, Ψ^{uncCTL}, Ψ^{KKT}, Ψ^{compt}

The set of constraints Ψ^{KKT} and Ψ^{compt} are formulated as presented in subsection 3.9.4. Ψ^{KKT} is detailed below:

$$-\sigma C_{g,t}^{G} + \lambda_{n(g),t}^{np} - \phi_{g,t}^{G^{min}} + \phi_{g,t}^{G^{max}} = 0 \qquad \forall g, \forall t \tag{136}$$

$$\lambda_{n(g),t}^{nq} = 0 \qquad \forall g, \forall t \tag{137}$$

$$-\lambda_{n(e),t}^{np} - \lambda_{e,t}^{SOC} - \phi_{e,t}^{P_e^{min}} + \phi_{e,t}^{P_e^{max}} = 0 \qquad \forall e, \forall t \tag{138}$$

$$-\lambda_{n(e),t,T_0}^{np} - \lambda_{e,t,T_0}^{SOC_0} - \phi_{e,t,T_0}^{P_e^{min}} + \phi_{e,t,T_0}^{P_e^{max}} = 0 \qquad \forall e, \forall t \tag{139}$$

$$-\lambda_{e,t,t_h}^{SOC} + \lambda_{e,t,(t_h+1)}^{SOC} - \phi_{e,t,t_h}^{SOC^{min}} + \phi_{e,t,t_h}^{SOC^{max}} = 0 \qquad \forall e, \forall t \tag{140}$$

$$-\lambda_{e,t,T_h}^{SOC} + \lambda_{e,t,T_0}^{SOC_0} - \phi_{e,t,t_h}^{SOC^{min}} + \phi_{e,t,t_h}^{SOC^{max}} = 0 \qquad \forall e, \forall t \tag{141}$$

$$-\lambda_{e,t,T_0}^{SOC_0} + \lambda_{e,t,(T_0+1)}^{SOC} - \phi_{e,t,t_d}^{SOC^{min}} + \phi_{e,t}^{SOC^{max}} = 0 \qquad \forall e, \forall t \tag{142}$$

$$\sigma C_{d}^{LS} - \lambda_{n(d),t}^{np} + \lambda_{d,t}^{LS} - \phi_{d,t}^{P_d^{LS,min}} + \phi_{d,t}^{P_d^{LS,max}} = 0 \qquad \forall d, \forall t \tag{143}$$

$$-\lambda_{n(d),t}^{nq} - \lambda_{d,t}^{LS} \bar{P}_{d,t}^{D} / \bar{Q}_{d,t}^{D} = 0 \qquad \forall d, \forall t \tag{144}$$

$$\lambda_{n(s(l)),t}^{np} - \lambda_{n(r(l)),t}^{np} - \lambda_{l,t}^{l_p} - \phi_{l,t}^{P_l^{min}} + \phi_{l,t}^{P_l^{max}} = 0 \qquad \forall l, \forall t \tag{145}$$

$$\lambda_{n(s(l)),t}^{nq} - \lambda_{n(r(l)),t}^{nq} - \lambda_{l,t}^{l_q} = 0 \qquad \forall l, \forall t \tag{146}$$

$$-\lambda_{n(cp),t}^{nq} - \lambda_{cp,t}^{SH} = 0 \qquad \forall cp, \forall t \tag{147}$$

$$\sum_{l(n_s)} \dot{x}_{l,t}^{L} \left(\lambda_{l,t}^{l_p} G_l - \lambda_{l,t}^{l_q} B_l \right) + \sum_{l(n_r)} \dot{x}_{l,t}^{L} \left(-\lambda_{l,t}^{l_p} G_l + \lambda_{l,t}^{l_q} B_l \right) - \phi_{n,t}^{V^{min}} + \phi_{n,t}^{V^{max}} = 0 \qquad \forall n \backslash \left(n: ref, n \epsilon \Omega_{m,adn}^{L} \right), \forall t \tag{148}$$

$$\sum_{l(n_s)} \dot{x}_{l,t}^{L} \left(\lambda_{l,t}^{l_p} G_l - \lambda_{l,t}^{l_q} B_l\right) + \sum_{l(n_r)} \dot{x}_{l,t}^{L} \left(-\lambda_{l,t}^{l_p} G_l + \lambda_{l,t}^{l_q} B_l\right) - \phi_{n,t}^{V^{min}} + \phi_{n,t}^{V^{max}} - \lambda_{n,t}^{Vref} = 0 \quad n: \text{ref}, \forall t \quad (149)$$

$$\sum_{l(n_s)} \dot{x}_{l,t}^{L} b\dot{s}w_{l,t}^{con(m)} \left(\lambda_{l,t}^{l_p} G_l - \lambda_{l,t}^{l_q} B_l\right) + \sum_{l(n_r)} \dot{x}_{l,t}^{L} b\dot{s}w_{l,t}^{con(m)} \left(-\lambda_{l,t}^{l_p} G_l + \lambda_{l,t}^{l_q} B_l\right) - \phi_{n,t}^{V^{min}} + \phi_{n,t}^{V^{max}} = 0 \quad \forall n \epsilon \Omega_{m,adn}^{L}, \forall t$$

$$\sum_{l(n_s)} \dot{x}_{l,t}^{L} \left(-\lambda_{l,t,t_d}^{l_p} B_l - \lambda_{l,t,t_d}^{l_q} G_l\right) + \sum_{l(n_r)} \dot{x}_{l,t}^{L} \left(\lambda_{l,t,t_d}^{l_p} B_l + \lambda_{l,t,t_d}^{l_q} G_l\right) - \phi_{n,t,t_d}^{\theta^{min}} + \phi_{n,t}^{\theta^{max}} = 0 \quad \forall n \backslash \left(n: ref, n \epsilon \Omega_{m,adn}^{L}\right), \forall t \quad (150)$$

$$\sum_{l(n_s)} \dot{x}_{l,t}^{L} \left(-\lambda_{l,t}^{l_p} B_l - \lambda_{l,t}^{l_q} G_l\right) + \sum_{l(n_r)} \dot{x}_{l,t}^{L} \left(\lambda_{l,t,t_d}^{l_p} B_l + \lambda_{l,t}^{l_q} G_l\right) - \phi_{n,t}^{\theta^{min}} + \phi_{n,t}^{\theta^{max}} - \lambda_{n,t,t_d}^{\theta ref} = 0 \quad n: \text{ref}, \forall t \quad (151)$$

$$\sum_{l(n_s)} \dot{x}_{l,t}^{L} b\dot{s}w_{l,t}^{con(m)} \left(-\lambda_{l,t}^{l_p} B_l - \lambda_{l,t}^{l_q} G_l\right) + \sum_{l(n_r)} \dot{x}_{l,t}^{L} b\dot{s}w_{l,t}^{con(m)} \left(\lambda_{l,t}^{l_p} B_l + \lambda_{l,t}^{l_q} G_l\right) - \phi_{n,t}^{\theta^{min}} + \phi_{n,t}^{\theta^{max}} = 0 \quad \forall n \epsilon \Omega_{m,adn}^{L}, \forall t \quad (152)$$

And the set of constraints Ψ^{compt} is defined as:

$$0 \leq \phi_{d,t}^{G^{min}} \perp p_{g,t}^{G} \geq 0 \quad \forall g, \forall t \quad (153)$$

$$0 \leq \phi_{d,t}^{G^{max}} \perp -p_{g,t,t_d}^{G} + \tilde{p}_{d,t,t_d}^{G^{max}} \geq 0 \quad \forall g, \forall t \quad (154)$$

$$0 \leq \phi_{n,t}^{V^{min}} \perp -V_n^{min} + v_{n,t} \geq 0 \quad \forall n, \forall t \quad (155)$$

$$0 \leq \phi_{n,t}^{V^{max}} \perp -v_{n,t} + V_n^{max} \geq 0 \quad \forall n, \forall t \quad (156)$$

$$0 \leq \phi_{n,t}^{\theta^{min}} \perp \pi + \theta_{n,t} \geq 0 \quad \forall n, \forall t \quad (157)$$

$$0 \leq \phi_{n,t}^{\theta^{max}} \perp -\theta_{n,t} + \pi \geq 0 \quad \forall n, \forall t \quad (158)$$

$$0 \leq \phi_{l,t}^{P_l^{min}} \perp \dot{x}_{l,t}^{L} b\dot{s}w_{l,t}^{con(m)} P_l^{Lmax} + p_{l,t}^{L} \geq 0 \quad \forall l \epsilon \Omega_{m,adn}^{L}, \forall t \quad (159)$$

$$0 \leq \phi_{l,t}^{P_l^{max}} \perp -p_{l,t}^{L} + \dot{x}_{l,t}^{L} b\dot{s}w_{l,t}^{con(m)} P_l^{Lmax} \geq 0 \quad \forall l \epsilon \Omega_{m,adn}^{L}, \forall t \quad (160)$$

$$0 \leq \phi_{l,t}^{P_l^{min}} \perp \dot{x}_{l,t}^{L} P_l^{Lmax} + p_{l,t}^{L} \geq 0 \quad \forall l, \forall t \quad (161)$$

$$0 \leq \phi_{l,t}^{P_l^{max}} \perp -p_{l,t}^{L} + \dot{x}_{l,t}^{L} P_l^{Lmax} \geq 0 \quad \forall l, \forall t \quad (162)$$

$$0 \leq \phi_{d,t}^{P_d^{LS,min}} \perp p_{d,t}^{LS} \geq 0 \quad \forall d, \forall t \quad (163)$$

$$0 \leq \phi_{d,t}^{P_d^{LS,max}} \perp -p_{d,t}^{LS} + p_{d,t}^{D} \geq 0 \quad \forall d, \forall t \quad (164)$$

$$0 \leq \phi_{e,t}^{P_e^{min}} \perp \dot{x}_{e,t}^{E} P_e^{E_{max}} + p_{e,t}^{E} \geq 0 \qquad \forall e, \forall t \qquad (165)$$

$$0 \leq \phi_{e,t}^{P_e^{max}} \perp -p_{e,t}^{E} + \dot{x}_{e,t}^{E} P_e^{E_{max}} \geq 0 \qquad \forall e, \forall t \qquad (166)$$

$$0 \leq \phi_{e,t}^{SOC^{min}} \perp -\dot{x}_{e,t}^{E} SOC_{e,t}^{min} + SOC_{e,t} \geq 0 \qquad \forall e, \forall t \qquad (167)$$

$$0 \leq \phi_{e,t}^{SOC^{max}} \perp -SOC_{e,t} + \dot{x}_{e,t}^{E} SOC_{e,t}^{max} \geq 0 \qquad \forall e, \forall t \qquad (168)$$

The key outputs in this second stage are the non-controllable portion ($\tilde{p}_{d,t}^{D_{nc}}, \tilde{q}_{d,t}^{D_{nc}}$), the deferrable portion ($\tilde{p}_{d,t}^{D_{df}}, \tilde{q}_{d,t}^{D_{df}}$), the generation capacities for the DGs ($p_{g,t}^{G^{max}}, \tilde{q}_{g,t}^{G^{max}}$), and an upper bound (UB) of the cost, calculated as:

$$UB = \sum_{t_y} \left[\sum_{c} \frac{\left(I_c^C x_{c,t_y}^C \right)}{(1+R)^{t_y}} \right] + \sum_{t_y} \sum_{t_h} \left[\sigma \left(\sum_{g} C_{g,t}^{G} p_{g,t}^{G} + \sum_{d} C_{d,t}^{LS} p_{d,t}^{LS} \right) \right] \qquad (169)$$

5.3.2.3 Convergence

For each iteration k, the convergence is checked by computing (*UB-LB)/LB*. If this gap is less than a given tolerance (10^{-4}), the algorithm ends; otherwise, it goes back to the first stage and new values for the uncertainty variables are kept.

5.3.2.4 Overview of the proposed model

The proposed model solves the expansion planning problem of ADN with MMG under uncertainties, including N-1 contingency, isolated operation of MGs, and demand response.

The problem is formulated as a three-level min-max-min and solved using a two-stage decomposition. The first stage seeks the best investment decisions, defines the isolated operation of the microgrids, and guarantees the N-1 generation contingency. The second stage is formulated as a maxmin problem that is converted to a single-level max problem using the KKTs conditions.

Since the model seeks the best solution from the DSO perspective, it is recommended for cases where the DSO owns the MMG or wishes to create incentive

programs for its owners. It is also recommended for cases where historical data is not available.

5.4 CASE STUDY

The proposed model is illustrated using the same test case used in chapter 4. Additionally:

- Three MGs were defined in the test, which is presented in Figure 29.
- The daily load profile is defined in Figure 30, and its non-controllable, controllable, and deferrable portions are defined as 90, 3, and 7%, respectively.
- The generation cost from the main grid throughout the hours of the day is also shown in Figure 30.
- The expansion planning horizon is 3 years.
- Contingencies are only considered in the last year of the expansion planning. It is not a limitation of the model but a consideration that allows a better understanding of its impacts on the results.
- More details of the test system are presented in appendix A.

FIGURE 29 – MODIFIED VERSION OF THE IEEE 123-BUS TEST SYSTEM WITH THREE MICROGRIDS

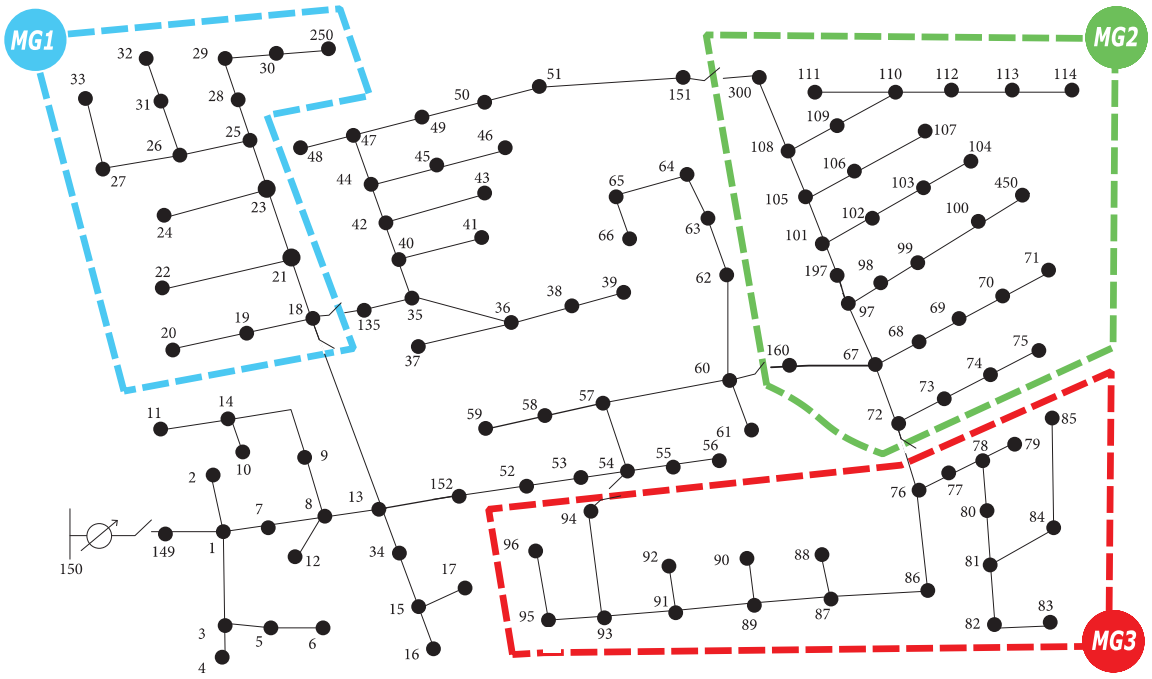
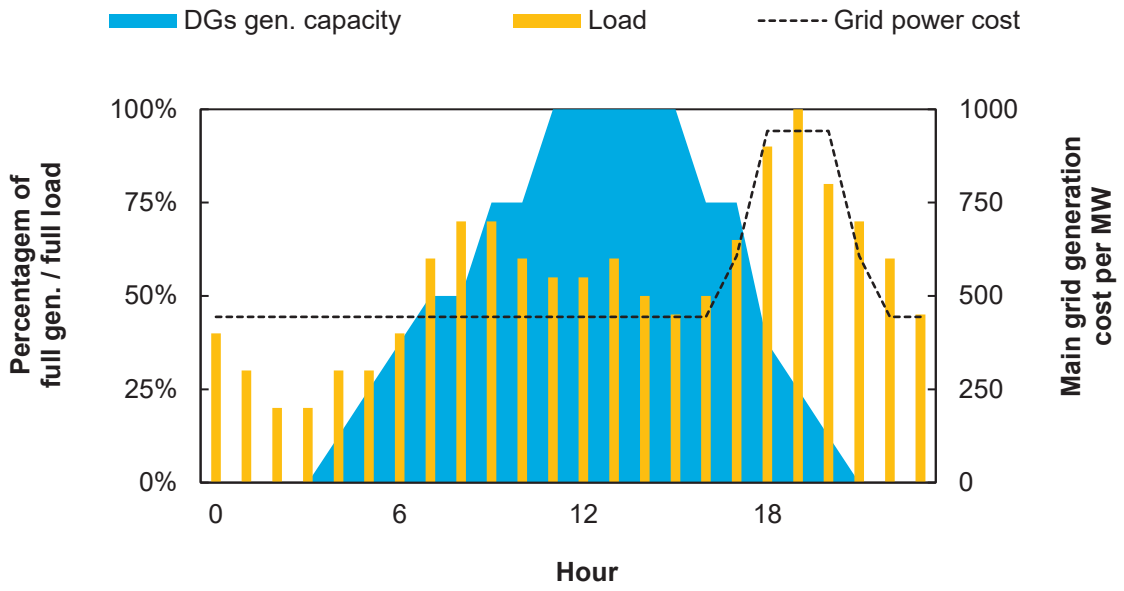


FIGURE 30 – DAILY POWER GENERATION CAPACITY OF DGS, LOAD PROFILE, AND MAIN GRID POWER PRODUCTION COST (GEN.: GENERATION)



5.5 SIMULATION RESULTS

This section presents expansion proposals for two cases of uncertainty budgets, DER's coordination, some operational results provided by the model, contingency results, a discussion on neglecting some of the contributions of the chapter, and a comparison between this model and the one presented in the previous chapter.

The numerical experiments are carried out with Gurobi, in a machine with 8 cores and 32GB of RAM, with Python.

5.5.1 Multi-period expansion planning decision

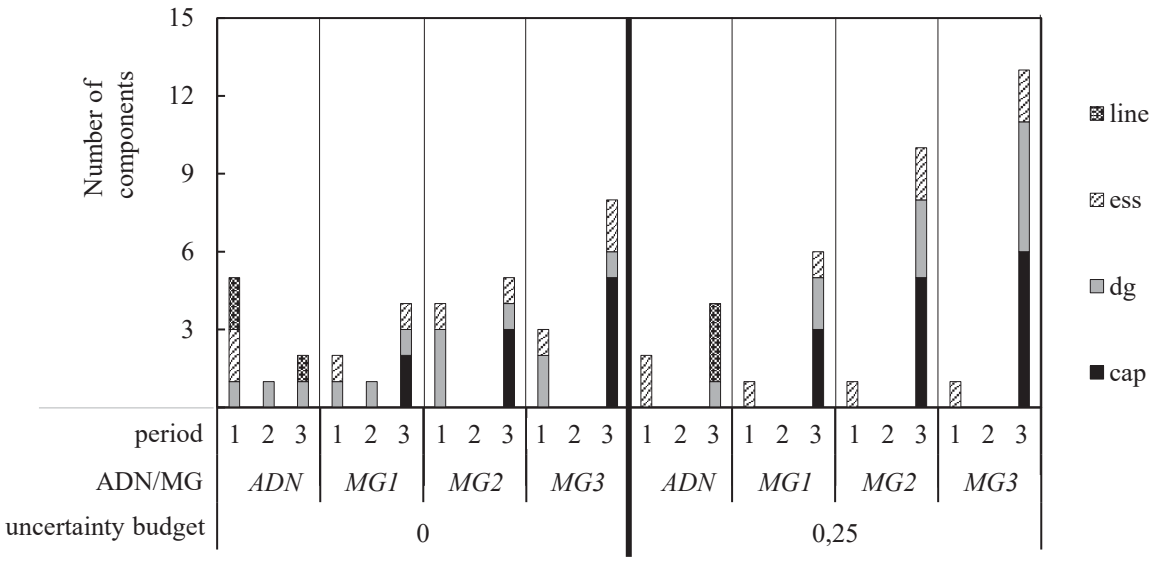
The test system was simulated for two cases of uncertainties. The first case has uncertainty budgets equal to 0 (for generation and loads), which represents an optimistic scenario. The second case uses an uncertainty budget of 0.25, which is characterized as a risk-averse scenario. The processing time was 1.1 minutes for the case with uncertainty budgets equal to 0, and 18 minutes for the other case.

Cases with an uncertainty budget greater than 0.25 were not explored since they may be unrealistic scenarios. For example, an uncertainty budget of 0.5 would

represent that 50% of the power generation capacity is unavailable. This is not a limitation of the model but a consideration in studying the results.

Figure 31 shows the expansion decision for both cases of the test system, indicating the number of components (lines, ESSs, DGs, and capacitors) placed in each microgrid and in the ADN (part of the network that is not inside an MG), for each period (year).

FIGURE 31 – NUMBER OF COMPONENTS PLACED IN THE IEEE-123 BUS TEST SYSTEM



Using the uncertainty budget of 0, DGs are placed in periods 1 and 2; however, for the case with 0.25, all DGs are placed in the last period. The increase in generation uncertainty decreases the power generation capacity in the DGs, reducing these components' economic viability. Thus, the DGs are only placed in the last period due to the contingency constraints. Behavior similar to what was observed in the results from chapter 4.

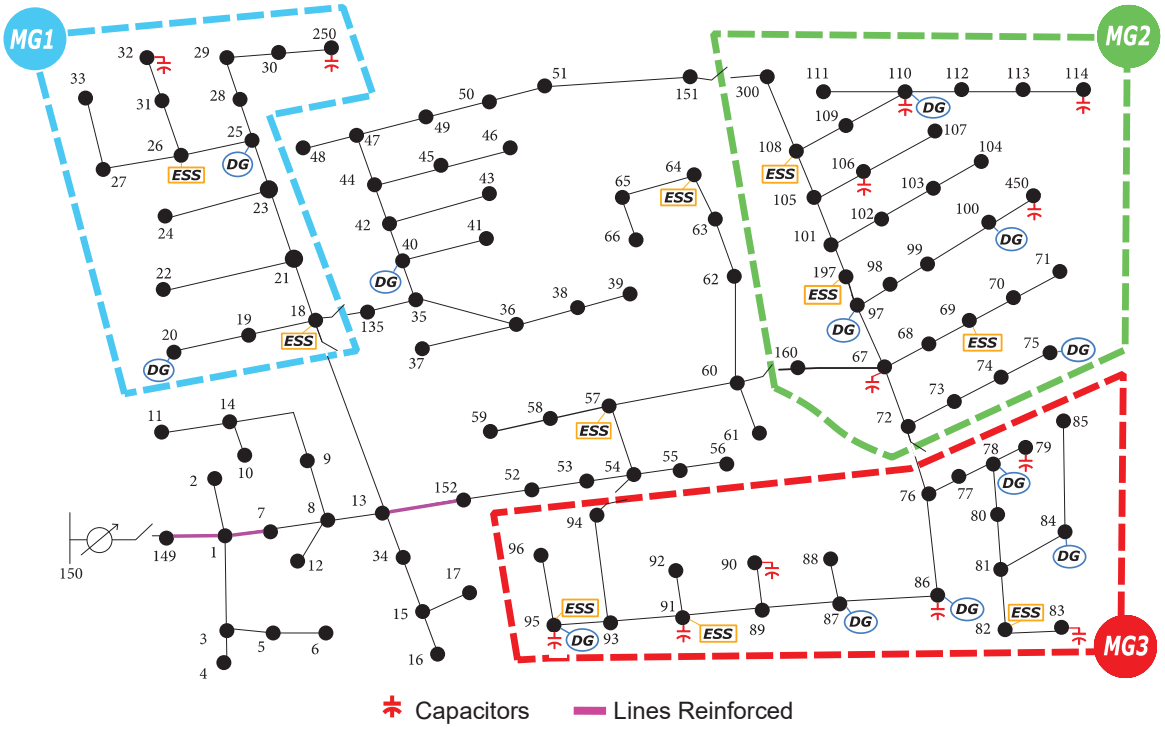
In MG1, the number of DGs has reduced if the uncertainty budget increases; on the other hand, the number of this component increases in MG3 for the same case. For Γ=0.25, MG3 requires more DG units to keep the N-1 contingency operation, since the load demand would increase, while MG1 has a lower demand level.

The number of ESSs and capacitors do not reduce when the uncertainty budget increases. Uncertainties do not negatively impact these components, and their number of components would either keep the same or increase within the uncertainty.

The results show that some components are placed in the system only to satisfy the contingency constraints, which is evident for high levels of uncertainty. Moreover, the computational effort is most related to the contingency constraints since the proposed formulation exhaustively explores all possible failures.

Figure 32 illustrates the components placed in the system for the expansion planning decision in the last period of the expansion planning for the case with an uncertainty budget equal to 0.25.

FIGURE 32 – EXPANSION PLANNING DECISIONS FOR THE TEST SYSTEM UNDER UNCERTAINTY BUDGET OF 0.25 IN THE LAST PERIOD



Lines connecting buses 149-1 and 1-7 were reinforced. These lines are one of the main lines to connect the substation (bus 150) to the MGs, most of the power from the substation flows through them. Besides, results show that lines were reinforced to allow the use of the surplus power generation of the DGs in the substation.

The expansion planning slightly impacts the ADN because the contingency constraints force the placement of components inside the MGs, which provides enough benefits for the system because the MGs export power to the ADN.

5.5.2 DERs' coordination

One of the main contributions of this model is regarding the inclusion of the 24H-OP in the expansion planning using a robust approach, which allows the study of DERs. Thus, Figure 33 and Figure 34 show the power balance of the entire system for uncertainty budgets of 0 and 0.25, respectively. They describe the DERs coordination for each hour of the worst day at the last period of the expansion planning horizon.

FIGURE 33 – DERS COORDINATION FOR THE 24-HOUR OPERATION AT THE LAST PERIOD AND UNCERTAINTY BUDGET OF 0

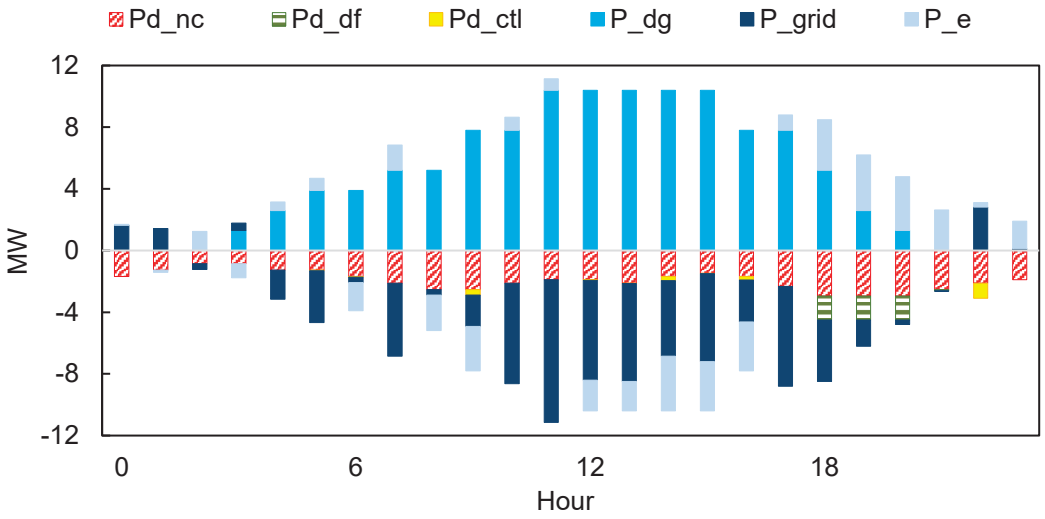
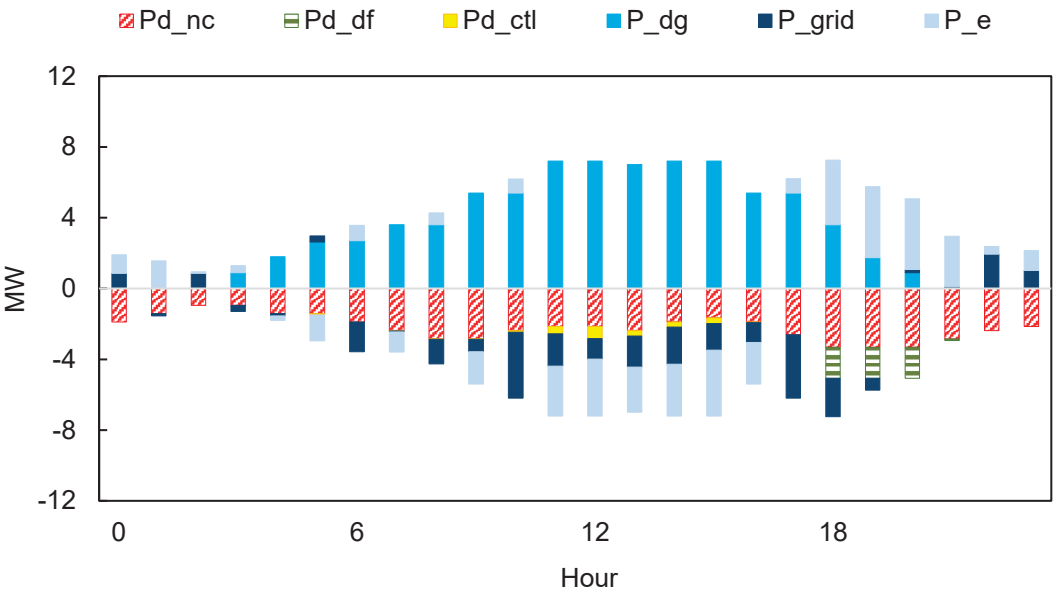


FIGURE 34 – DERS COORDINATION FOR THE 24-HOUR OPERATION AT THE LAST PERIOD AND UNCERTAINTY BUDGET OF 0.25



In both cases, the deferrable portion of the load (Pd_df) is placed at the hours that the generation cost from the main grid and load level are at higher levels. As long as the DSO has no control over this portion of the load, this would be the best approach for a robust plan. Moreover, the controllable portion of the load (Pd_ctl) is placed during the hours the load is on the lowest levels and there is enough power generation capacity in the DGs. The load peak levels occur from 17h to 22h, and the ESSs are mostly used at these hours and during the night (positive values of P_e), when the DGs' power generations are not fully available.

The power generation capacities for the DGs (P_dg) are greater than the load demand at some hours of the day. The surplus generation is sold to the main grid for the same price bought as an incentive for the installation of the candidates, which is represented by the negative values in the P_grid.

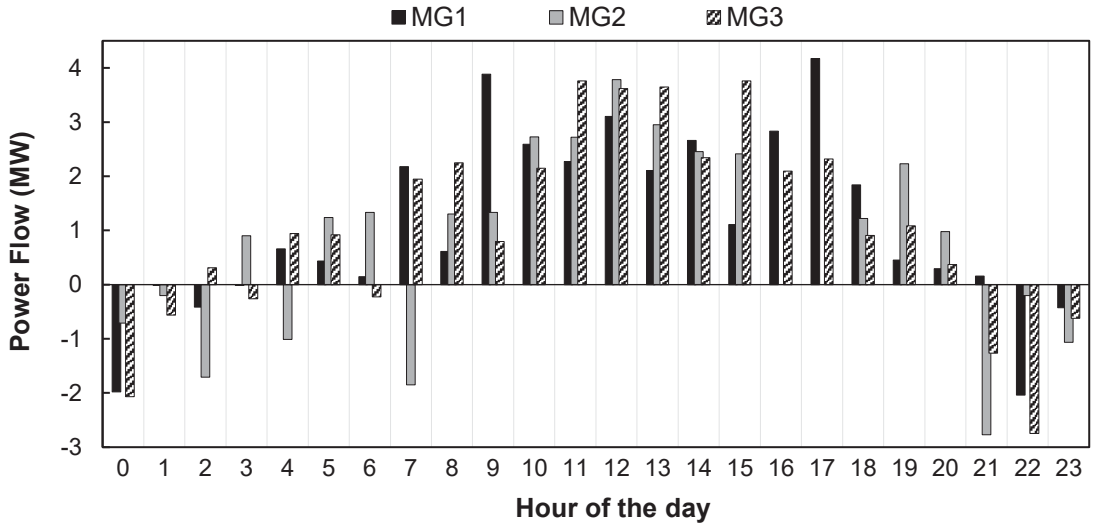
Comparing both cases with uncertainty budgets of 0 and 0.25, the power generation from the DGs decreases while the demand increases, which is consistent.

If the demand response is neglected, the results of the expansion plan could be unrealistic since the load would be defined as predictable at each hour of the day. Thus, the demand response proposed in this chapter provides a model representing controllable loads that may be shifted in time but are not controlled by the DSO, which are very hard to predict.

5.5.3 MG's power flow

Power flow analyses are hard to perform since this case study has 124 lines, 3 years, 24 hours, and 2 cases of uncertainties. These numbers provide 17,856 different cases for the power flow in the lines. To illustrate the power flow in the system, the lines connecting the ADN and the MGs were selected. Figure 35 shows the total power flow that each MG exports or imports at the last period of the expansion planning horizon.

FIGURE 35 – NET POWER FLOW IN LINES CONNECTING THE ADN AND THE MGS AT THE LAST PERIOD OF THE EXPANSION PLANNING CONSIDERING AN UNCERTAINTY BUDGET OF 0.25



In Figure 35, positive values of the power flow show hours that the MGs are exporting power, and negative values represent that the MGs are importing power from other MG or the main grid.

During the hours of unavailability of the DG units, the MGs generally import power from the grid or other MGs, for example, from hours 21 to 2. During hours from 9 to 16, all MGs are providing power to external sources, which means that the ADN and the substation are consuming the surplus power from the MGs. This behavior shows that the ESS units inside the MGs are storing power during hours when load levels and the grid power cost are lower, while they are exporting power when the load levels and grid power cost are higher.

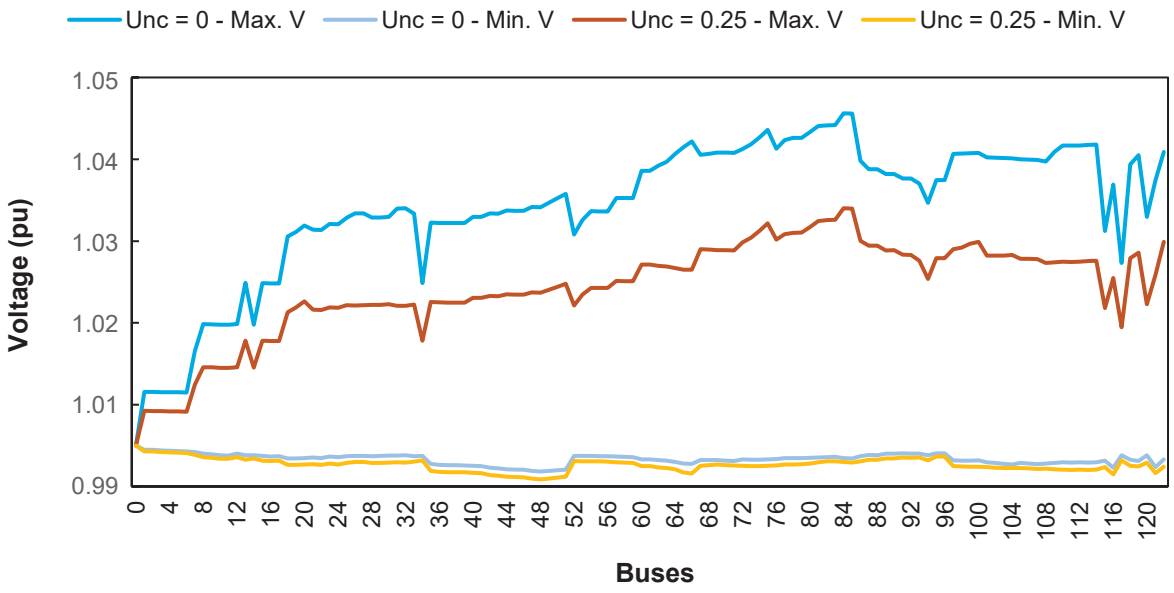
Furthermore, at hours 16 and 17, MG2 is operating isolated ($bsw_{l,t}^{con(m)} = 0$), which can be observed in Figure 35, since the net power flow from this MG is 0. The isolated operation occurs when it is best to store all the surplus generation inside the MG or if some constrains are not met in a connected operation, such as voltage limits.

5.5.4 Voltage and power flow analysis

The voltage profile in distribution systems is important since radial systems may have problems with loads in the end nodes of the network or in points with generation units. All models proposed in this work provide information on the voltage

profile, and Figure 36 shows the maximum and minimum value of the voltage for all buses in the IEEE 123-bus test system for the two cases of uncertainties studies, 0 and 0.25. The maximum and minimum values represent the values throughout the hours of the day. The voltage limits were defined as 1.05 and 0.95 pu for this test system.

FIGURE 36 – MINIMUM AND MAXIMUM VALUES FOR VOLTAGE IN THE BUSES DURING THE DAILY OPERATION FOR THE LAST YEAR OF THE EXPANSION PLANNING HORIZON



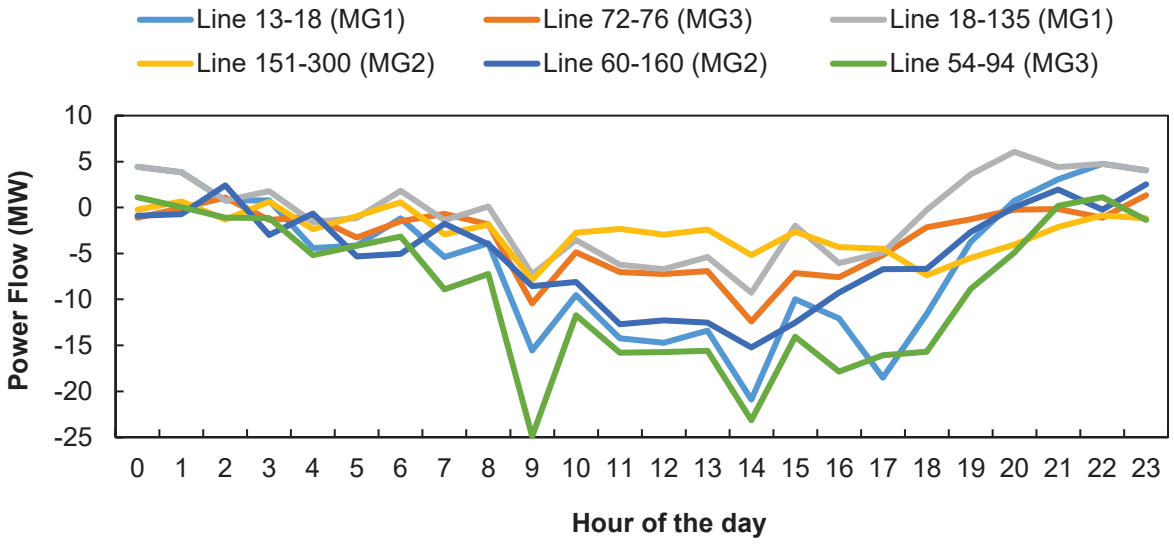
The first bus is the one connected to the main substation, and its voltage is 1 pu. Voltage deviations from 1 pu are greater for the case with an uncertainty budget of 0. This occurs because in this case, there is more power generation in the DG units.

To illustrate the power flow in the problem, the lines connecting the ADN and the MGs were chosen, and Figure 37 shows the power flow in these lines at the last period of the expansion planning horizon.

The positive values of power flow in Figure 37 show hours that the MGs are consuming external power, and negative values represent hours that the MGs are providing power to other MG or to the main grid.

During the unavailability of DG units, the power flowing in the lines is at lower levels, for example, from hours 21 to 5.

FIGURE 37 – POWER FLOW IN THE LINES CONNECTING THE ADN AND THE MGs AT THE LAST PERIOD OF THE EXPANSION PLANNING HORIZON



At specific hours, lines from an MG consume power, while other lines from the same MG provide power. For example, at hour 19, line 18-135 imports power to MG1 while line 13-18 exports power from the same MG. This is possible because the MGs can have more than one connection, and it benefits the system by delivering power from DGs to neighbor nodes.

During the hours from 8 to 17, all MGs are providing power to external sources, which means that the ADN and the substation are consuming the surplus power from the MGs during these hours.

Figure 37 shows why the voltages in Figure 36 are closer to higher values (1.05 pu) than to lower values (0.95 pu). The direction of the power flow is mainly from the DGs inside the MGs to the ADN. Opposite of traditional networks, where all power flows from the substation to the loads.

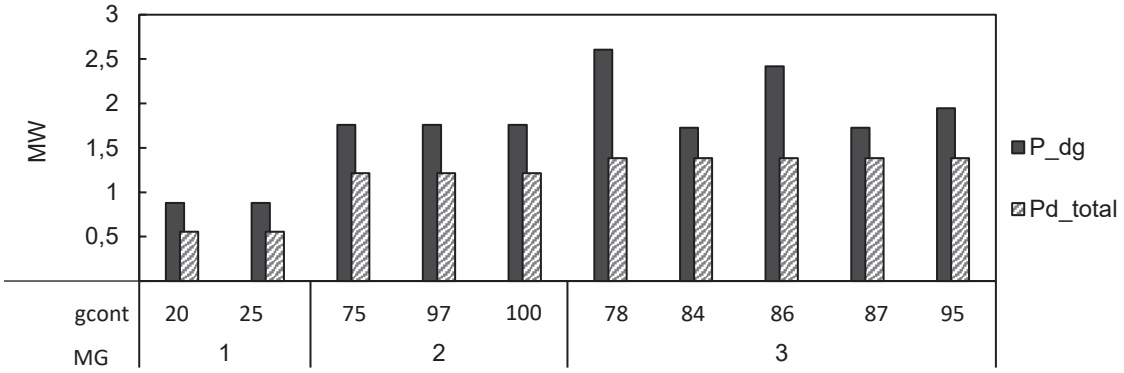
5.5.5 Contingencies and MG's isolated operation

The N-1 generation contingency is described as the capacity of power generation greater than load demand at any hour of the day, even if a component fails.

Figure 38 shows the total amount of power generation capacity and load for all MGs in different cases of contingencies for an uncertainty budget of 0.25 during the last period of the expansion planning. *gcont* represents the bus where a generator unit

is off during the contingency analysis. All cases are for the isolated operation of the MGs.

FIGURE 38 – POWER AVAILABLE AND LOAD FOR THE N-1 GENERATION CONTINGENCY CASES FOR ALL MGS OPERATING ISOLATED FROM THE GRID AT THE LAST PERIOD AND UNCERTAINTY BUDGET OF 0.25



There is more generation capacity (P_dg) than load (Pd_total) in all MGs even if any generator (*gcont*) is off. For *gcont*=20, for example, Figure 38 shows that inside MG1 there is more generation capacity than load demand even if the generator unit located in bus 20 is off.

Figure 39 presents the total load (Pd), power generation capacity of DGs (P_dg), and the charging/discharging power from ESS units (P_e) for each MG in an isolated operation during a contingency *gcont*.

FIGURE 39 – ISOLATED OPERATION FOR ALL MGS UNDER CONTINGENCIES "*GCONT*" AT THE LAST PERIOD AND UNCERTAINTY BUDGET OF 0.25

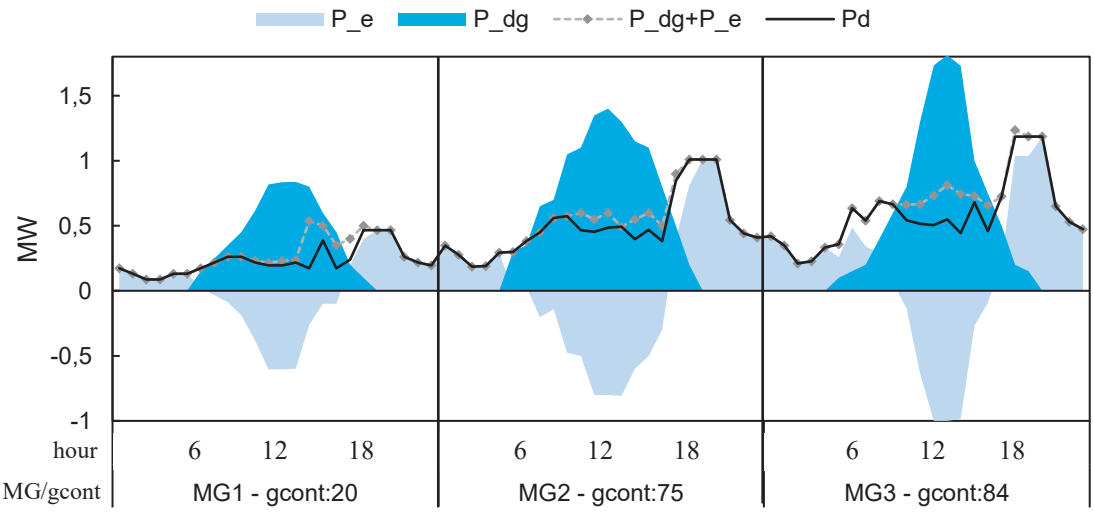


Figure 39 shows that, inside each MG, the total available power (P_dg + P_e) is greater than or equal to the total load at any hour of the day, during a generation contingency case and for the worst-case of uncertainties. Besides, during some hours, P_dg + P_e is greater than Pd, which represents that the system could even support higher load levels.

When P_dg is unavailable, P_e is the only power source available. The MGCC stores energy from the DGs into the ESS units during the day, which is represented by negative values of P_e; thus, this power is used overnight, when no power is available in the DGs.

Solar-power-based DGs are the most difficult power sources for isolated operation planning. The results show the robustness of the proposed model in this work, in which the DGs and ESS units were able to provide energy for an entire day of operation under contingency and the worst-case of uncertainty.

The MGCC is responsible for the control and automation of the MGs operation. The investment must provide the required technology to operate the DERs coordination and the isolated operation. Moreover, disconnecting an MG in an MMG environment is not harmful to the system if proper technologies are used since this operation is expected in many MG projects.

5.5.6 Cases neglecting contingency, demand response, and the representation of the 24H-OP

To illustrate the importance of contingency, demand response (DR), and the 24H-OP in the expansion planning problem, the following five cases are presented in this section:

- A: base case of the IEEE 123-bus test system: not considering contingency, DR, 24H-OP.
- B: the base case with the generation contingency.
- C: the base case with the representation of the 24H-OP.
- D: the base case with the representation of the 24H-OP and DR.
- E: the complete case.

Cases A to E are simulated using an uncertainty budget of 0.25 and their results are presented in Table III, which shows the total cost, expansion cost, operational cost, number of components installed in the system, and the EENS index for each case.

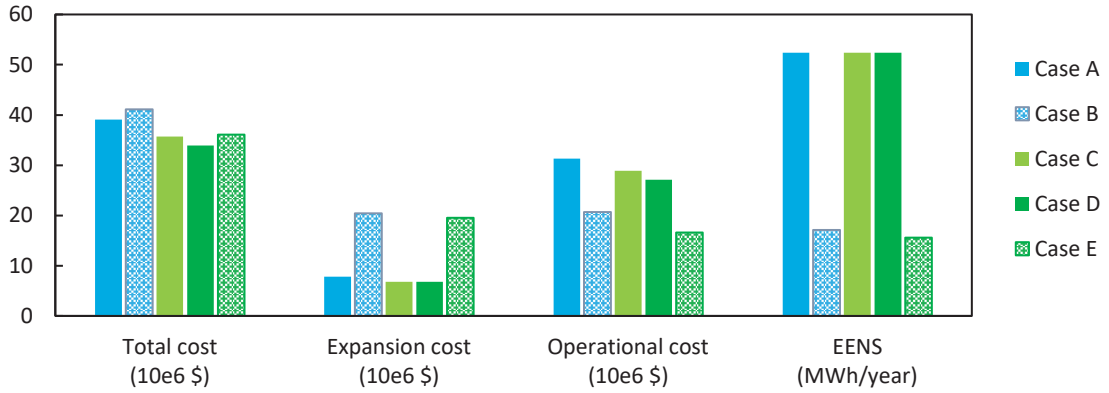
TABLE III – RESULTS FOR DIFFERENT CASES USING AN UNCERTAINTY BUDGET OF 0.25

CASE	A	B	C	D	E
Total cost (10^6)	39.1	41.1	35.7	33.9	36.1
Expansion cost (10^6)	7.8	20.4	6.8	6.8	19.5
Operational cost (10^6)	31.3	20.7	28.9	27.1	16.6
Number of lines	0	2	0	0	3
Number of ESSs	0	0	7	7	10
Number of DGs	4	13	2	2	11
Number of capacitors	3	9	4	4	14
EENS (MWh/year)	52	17	52	52	15

For practicality and comparison purposes, Table III shows the estimated EENS index, calculated after the expansion proposal defined by the model for each case. The failure rates and repair time are the same as in chapter 4.

Figure 40 shows the same costs and EENS presented in Table III. The EENS index is considered only for the last period of expansion planning.

FIGURE 40 – TOTAL EXPANSION AND OPERATIONAL COSTS FOR DIFFERENT CASES USING AN UNCERTAINTY BUDGET OF 0.25



The results show that the total cost of the expansion planning may reduce up to 13% if including demand response and the representation of the 24H-OP (comparing cases A and D).

Figure 40 shows that the system's operational cost decreases after considering the 24H-OP, contingencies, and demand response. Cases C and D reduce the total cost because the ESSs can provide additional benefits if the 24H-OP is considered. Additionally, the demand response is only feasible in cases considering the 24H-OP; otherwise, the shiftable load could not be placed during the appropriate hours of the day.

In the cases considering contingency (B and E), the total cost is increased if compared with the previous cases (A and D); however, in these cases, the system is tolerant against N-1 faults, and its reliability is improved. Comparing case E with D, the total cost increases by 6.5% while the EENS index decreases by 70%. And comparing case B with A, the total cost increases by 5.1%, and the EENS index also decreases by 70%. Thus, the inclusion of contingency substantially improves the system's reliability, while the total cost slightly increases.

The EENS index is greater than zero in cases B and E because the contingencies modeled in this chapter are only for power generation, and faults in the lines of the system may still occur. Even though faults in lines may impact the system, the isolated operation in the MGs protects them. The N-1 contingency approach ensures enough power generation to supply the load demand inside each MG; thus, the reliability index inside the MGs is improved.

The inclusion of the contingency greatly impacts the number of DGs. Thus, for cases B and E, the inclusion of DGs is related to the improvement in the system's reliability, through the contingency constraints, and not to its financial benefits. Besides, the number of ESSs is substantially impacted by the inclusion of the 24H-OP since they can provide power at hours with power generation unavailability in the DGs.

Comparing cases B and E, case B is far less complex, and both consider contingencies. On the other hand, case E has a total cost of 12.2% less than case B and more details on the system operation, such as DERs coordination. When it comes to expansion planning, many works simplify the system operation for tractability; the proposed model includes some operational details in the expansion planning, reducing the total cost, which is relevant for such investments. Besides, case E properly represents loads that are shiftable in time.

Therefore, the inclusion of the 24H-OP and demand response improves the quality of the distribution expansion planning and reduces its total cost. Including contingencies provides additional benefits to the system, which becomes tolerant against N-1 faults. Comparing cases E and A, the complete case considers all aspects of this work and reduces the total cost by 7.7%, while the reliability index is improved.

5.5.7 Comparison among models

Comparing different models may be impossible due to particular aspects and the context of each one of them. Table IV compares the main aspects of the models presented up to this chapter.

TABLE IV – COMPARISON AMONG MODELS FROM CHAPTERS 4 AND 5

	Model Chapter 4	**Model Chapter 5**
Uncertainty approach	ARO	ARO
DG, ESS, capacitors, and line placement	✓	✓
Self-healing and reliability	✓	
N-1 contingency		✓
Demand response		✓
MMG		✓

Compared to the previous model, the model presented in this chapter adds contingencies, demand response, and an MMG formulation, while reliability is not considered in the formulation. Note that it is important to consider the context of each model and not compare if one considers more aspects than the other.

5.6 SUMMARY

This chapter presented a model to solve a robust multi-period expansion planning problem for ADN with multiple microgrids, DERs, demand response, and N-1 generation contingency. Lines and capacitors are also considered in the expansion planning problem. The proposed model determines the best investment periods and

locations for all expansion candidates, considering the optimal coordination of DERs with hourly steps of the day.

The model is designed for cases where the DSO owns the MMG or wishes to create incentive programs for MG's private owners. Also, the model is more appropriate for cases with unavailable historical data; thus, robust sets are indicated to represent uncertainties.

Regarding the solution approach, the load is decomposed into three different portions (non-controllable, controllable, and deferrable). This load's representation shifts the controllable portion of the load to minimize the objective function of the problem, while the deferrable portion is placed for the worst-case of uncertainties. This approach makes the system robust against the uncertainties in the load's portion that the system operator does not control.

Simulations show that the increase in generation uncertainty reduces the economic viability of DGs. In other words, installing DGs may not provide the expected financial benefits for the system in high uncertainties; thus, some of these components may not be chosen in expansion decisions for high uncertainties. The same observation was made in the previous chapter.

Results show that the introduction of DERs and the representation of the 24H-OP may reduce the total cost of the problem by 13%.

Although the total cost in the expansion planning increases with the inclusion of N-1 contingencies, the system's reliability is substantially improved. In this comparison, simulations show that the total cost increases by about 6% when considering contingencies, while the EENS reliability index reduces by 70%.

Moreover, the results show that the total cost of the expansion plan considering contingencies, the hourly steps of the day, and demand response is 7.7% lower than the case not considering these aspects.

Therefore, considering contingencies along with demand response and the 24-hour operation reduces the total cost, and the system's reliability is substantially improved.

6 A DATA-DRIVEN DISTRIBUTIONALLY ROBUST MODEL FOR EXPANSION PLANNING OF ACTIVE DISTRIBUTION NETWORKS WITH MULTIPLE MICROGRIDS

6.1 INTRODUCTION

As shown in Figure 13 from subsection 3.9.5, the generic robust set used in ARO may be over-conservative, considering cases that are not practical or very rare, for example, a case where both generation and load are in high levels of uncertainty budget.

Many different data-driven approaches have been used in the literature; however, most of them are only practical in operational planning, such as using historical data to model the robust set or to determine the worst-case based on a linear combination of this data.

The data-driven distributionally robust optimization (DDDRO) approach, as mentioned in subsection 3.9.6, can be seen as a hybrid stochastic and robust method, where historical data is used to create data bins (or scenarios) with probabilities. Thus, rare cases are also considered in the DDDRO but have weights related to their frequency.

Two aspects are fundamental in DDDRO models, historical data and ambiguity sets. The main objective of a DDDRO model is converting historical data into stochastic scenarios and finding the probability of each scenario that would provide the worst result for the objective function of the proposed model. Ambiguity sets are used for this purpose, which relates the true probability distribution function (T-PDF) with the estimated distribution function (E-PDF), as presented in subsection 3.9.6.

6.1.1 Historical data and ambiguity sets in DDDRO models

Figure 41 shows the historical data for solar irradiance, wind speed, and load demand for the city of Sao Paulo, Brazil, from January 2007 to June 2021. The same information is presented in Figure 42 but within a 24-hour window. The data is available in Solcast (2021) and ONS (2021). This is the historical data used in the DDDRO model from this chapter.

FIGURE 41 – HISTORICAL DATA FOR SOLAR IRRADIANCE, WIND SPEED, AND LOAD DEMAND FOR SAO PAULO, BRAZIL (2017-2021)

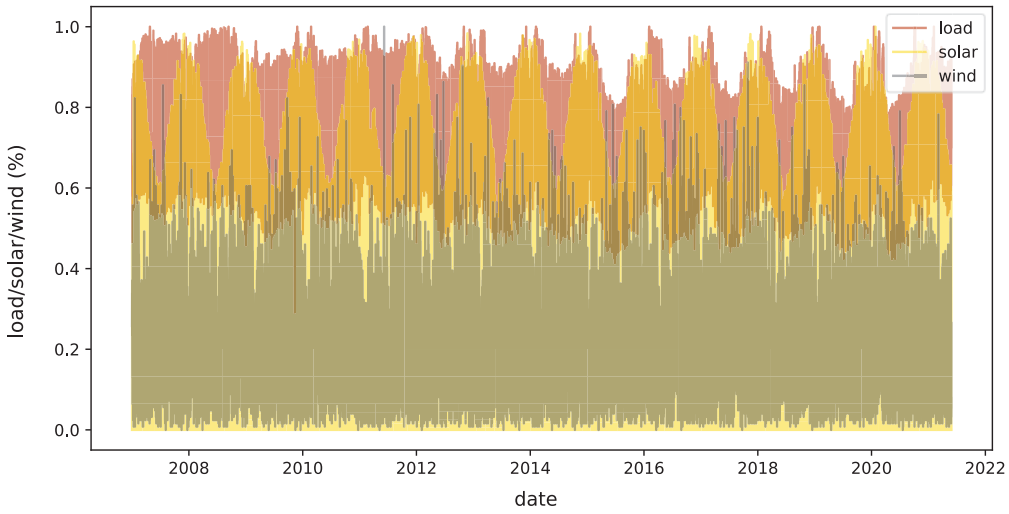


FIGURE 42 – HISTORICAL DATA IN 24 HOUR HORIZON FOR SOLAR IRRADIANCE, WIND SPEED, AND LOAD DEMAND FOR SAO PAULO, BRAZIL (2017-2021)

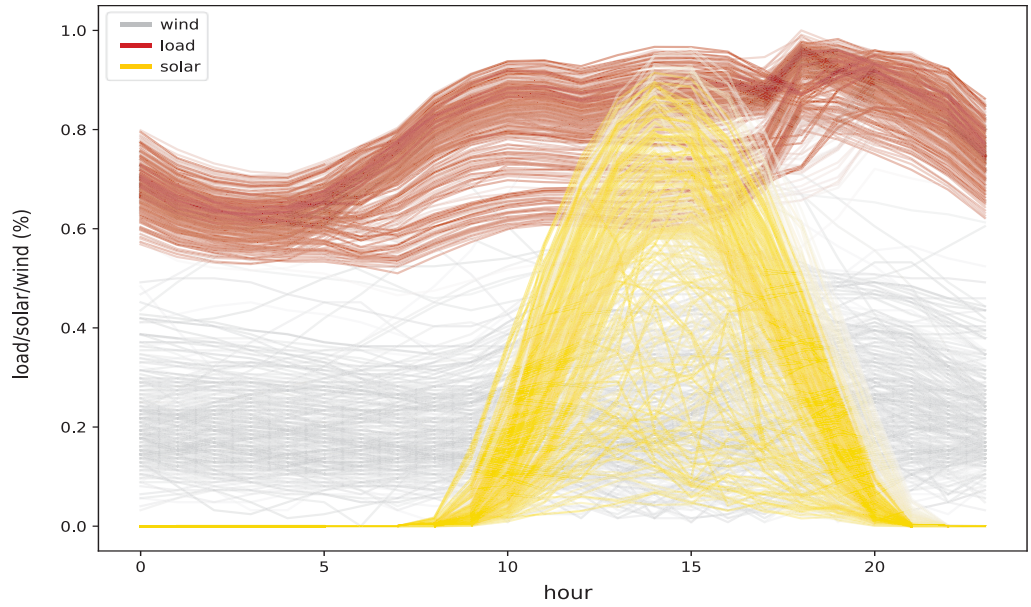
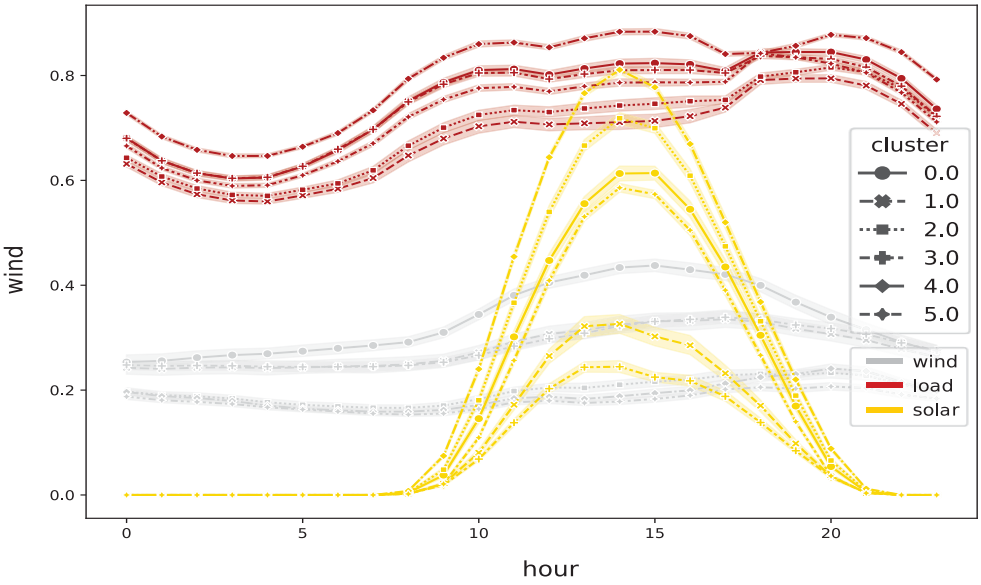


Figure 42 shows that is not possible to define a deterministic value for these variables, in other words, the variables are subject to uncertainties. Since the historical data is available, the information from Figure 42 can be converted into data bins, where an expected value for the variables and the probability of the scenario are defined.

In this context, Figure 43 shows 6 clusters (scenarios) defined using the historical data from Figure 42 with the machine learning algorithm k-means from the

package scikit-learn in Python (PEDREGOSA et al., 2012) using 6 clusters and 100 different centroids.

FIGURE 43 – CLUSTER OF 6 SCENARIOS USING K-MEANS



In the DDDRO concept, the true probability distribution function (T-PDF) is unknown, but an estimated distribution (E-PDF) is defined from the available historical data. Thus, the T-PDF can be defined from the E-PDF within a tolerance range.

The relation between T-PDF (p_s^S) and E-PDF ($p_s^{S_0}$) is defined by the ambiguity set (Ψ^{amb}) below (ZHANG et al., 2021).

$$\Psi^{amb} = \left\{ \begin{array}{c} \left\| p_s^S - p_s^{S_0} \right\|_1 = \sum_s \left| p_s^S - p_s^{S_0} \right| \le \delta_1 \\ \left\| p_s^S - p_s^{S_0} \right\|_\infty = \max_s \left(p_s^S - p_s^{S_0} \right) \le \delta_\infty \\ \sum_s p_s^S = 1 \\ p_s^S \ge 0, \forall s \end{array} \right\} \quad (170)$$

For notation brevity, the E-PDF and T-PDF distributions are defined as $p_s^{S_0}$ and p_s^S. Moreover, $\|\cdot\|_1$ and $\|\cdot\|_\infty$ indicate norm L1 and norm L∞, which can be defined as the summation and maximum forms in (170), as defined and used in Zhang et al. (2021).

Note that the right-hand thresholds δ_1 and δ_∞ in (170) refer to tolerance coefficients associated with given confidence level and historical data. As more historical data is inserted, the uncertainty set shrinks, and the E-PDF gets closer to the T-PDF. If the confidence levels of two norms are described as φ_1 and φ_∞, the tolerance coefficients can be defined as follows (ZHANG et al., 2021):

$$\delta_1 = \frac{M_D}{2N}\ln\frac{2M_D}{1-\varphi_1}, \delta_\infty = \frac{1}{2N}\ln\frac{2M_D}{1-\varphi_\infty} \tag{171}$$

where M_D is the number of data bins and N the number of historical data available. Thus, the probability $p_s^{\delta_0}$ of case s from the E-PDF is defined as $p_s^{\delta_0} = N_s/N$, in which N_s is the number of data inside the case s. As N gets close to infinity, the tolerances δ_1 and δ_∞ get close to zero; thus, if infinity historical data is available, $p_s^{\delta_0}$ is the same as p_s^{δ}.

The ambiguity set provides information to reconstruct the T-PDF within a confidence level. Inside the DDDRO, the T-PDF is optimized for the worst-case given the tolerance calculated from the E-PDF (ZHANG et al., 2021).

The Ψ^{amb} can replace the Ψ^{unc} from chapters 4 and 5. Thus, the E-PDF is used to estimate the T-PDF based on the confidence level of the historical data, instead using generic robust sets; and, the Ψ^{amb} is part of the formulation.

6.2 CONTEXT AND ASSUMPTIONS

The model presented in this chapter considers the following:

- The DSO desires to minimize the total cost of investment and operation (generation and load shedding).
- The DSO owns or controls the investment in all MGs. Thus, the DSO decides whether to install a new component inside the MGs. Although the expansion decisions in the ADN and the MGs are made directly by the DSO, the decisions inside the MGs can be seen as areas where the DSO should encourage the investment of the components by private investors or invest by itself.

- The candidates for the expansion planning problem are distributed generator units, energy storage system units, capacitors, and installation/rewiring of lines.
- Loads may have three portions: non-controllable; controllable, controlled directly by the DSO; deferrable, which may be shifted over time, but the DSO does not control it.
- All MGs must be able to operate with N-1 generation contingency.
- Historical data is available
- The degradation of ESSs by charging/discharging and their efficiency are ignored, as well as active power losses in lines.
- Any MG of the system may operate isolated from the main grid at any hour of the day. The decision on operating/not-operating isolated is related to the operational constraints and their benefits to the system.

The main difference between the model proposed in this chapter compared to the one from chapter 5 is the availability of historical data. Thus, DDDRO is used instead of ARO. In addition, its main contribution is the incorporation of contingencies and demand response inside a DDDRO model.

6.3 PROPOSED MODEL

The model seeks the best investments and operational conditions (generation, DERs coordination, and load shedding costs) for the worst-case realization of the uncertainties in the ADN and MGs, considering historical data for generation and load.

The model is formulated as a tri-level optimization problem and solved using a two-stage robust optimization approach using MILP. Reformulation procedures are proposed to reconstruct the problem using the C&CG. The following subsections show the problem formulation and the solution approach.

6.3.1 Formulation

6.3.1.1 Objective function

The model's objective function aims to minimize the cost of investment in new lines, DG units, ESSs units, and capacitors for the worst-case probability density function of the historical data. At the same time, it defines the operating condition to minimize the total cost. Thus, the objective function of the problem is defined as:

$$\min_{x^C_{c,t_y}} \max_{p^S_{s,t_y}} \min_{\Delta Smin} \sum_{t_y} \sum_{c} \frac{I^C_c x^C_{c,t_y}}{(1+R)^{t_y}} + \sum_{s} p^S_{s,t_y} \left[\sum_{t_y} \sum_{t_h} \sigma \left(\sum_{g} C^G_{g,t} p^G_{g,t} + \sum_{d} C^{LS}_{d,t} p^{LS}_{d,t} \right) \right] \quad (172)$$

subject to Ψ^{Lflow}, Ψ^{bal}, Ψ^{ess}, Ψ^{op}, Ψ^{inv}, Ψ^{dr}, Ψ^{cont}, Ψ^{bsw}, Ψ^{amb}

The set $\Delta Smin$ is represented by all variables in the problem, except $\left\{x^C_{c,t_y}, p^S_{s,t_y}\right\}$, in which $x^C_{c,t}$ is the expansion planning decision for each component c (lines, capacitors, ESSs, DGs) and p^S_{s,t_y} is the true probability of each data bin s. σ is the number of days in year t_y. And $C^G_{g,t} p^G_{g,t}$ is the cost of generating power for generator unit g, in the hour t_h of year t_y.

Compared to the problem in chapter 5, the three-level problem in (172) maximizes the objective function over the variable p^S_{s,t_y}, instead of the uncertainty variables directly ($\tilde{p}^{G^{max}}_{g,t}$, $\tilde{p}^{D_{nc}}_{d,t}$, $\tilde{p}^{D_{df}}_{d,t}$).

6.3.1.2 Constraints

The set of constraints Ψ^{Lflow}, Ψ^{bal}, Ψ^{ess}, Ψ^{op}, and Ψ^{inv} are the same as defined in chapter 4, subsection 4.3.1.2. Constraints Ψ^{dr}, Ψ^{cont}, and Ψ^{bsw} are described in chapter 5, subsection 5.3.1.2. And constraint Ψ^{amb} is defined in this chapter.

Ambiguity Set for Uncertainties (Ψ^{amb})

DDDRO models require the construction of the ambiguity set for the uncertainties, which was defined in the introduction subsection of this chapter, equations (170) and (171), replicated below:

$$\Psi^{amb} = \left\{ \begin{array}{c} \left\| p_s^{\delta} - p_s^{\delta_0} \right\|_1 = \sum_s \left| p_s^{\delta} - p_s^{\delta_0} \right| \le \delta_1 \\ \left\| p_s^{\delta} - p_s^{\delta_0} \right\|_\infty = \max_s \left(p_s^{\delta} - p_s^{\delta_0} \right) \le \delta_\infty \\ \sum_s p_s^{\delta} = 1 \\ p_s^{\delta} \ge 0, \forall s \end{array} \right\}$$

$$\delta_1 = \frac{M_D}{2N} \ln \frac{2M_D}{1-\varphi_1}, \delta_\infty = \frac{1}{2N} \ln \frac{2M_D}{1-\varphi_\infty}$$

As mentioned before, if the number of historical data increases (N), the tolerance coefficients δ_1 and δ_∞ get close to zero. In this case, the E-PDF ($p_s^{\delta_0}$) is close to the T-PDF (p_s^{δ}).

Equation (170) is nonlinear, and Zhang et al. (2021) present a linearized proposal for this set, which is adapted in this work as follows:

$$\sum_s p_s^{\delta} = 1 \tag{173}$$

$$p_s^{\delta} \ge 0 \qquad \forall s \tag{174}$$

$$p_s^{\delta} = p_s^{\delta_0} + p_s^{\delta\pm} \qquad \forall s \tag{175}$$

$$-\delta_1 \le \sum_s p_s^{\delta\pm} \le \delta_1 \tag{176}$$

$$-\delta_1 \le p_s^{\delta\pm} \le \delta_1 \qquad \forall s \tag{177}$$

$$-\delta_\infty \le p_s^{\delta\pm} \le \delta_\infty \qquad \forall s \tag{178}$$

Equation (173) defines that the summation of the T-PDF for all data bins is 100%, and constraint (174) sets all probabilities as positive numbers.

The variable $p_s^{\delta\pm}$ is the maximum deviation allowed between the T-PDF and the E-PDF. Thus, equation (175) relates T-PDF and E-PDF.

Equations (176), (177), and (178) set the bounds for $p_s^{\delta\pm}$.

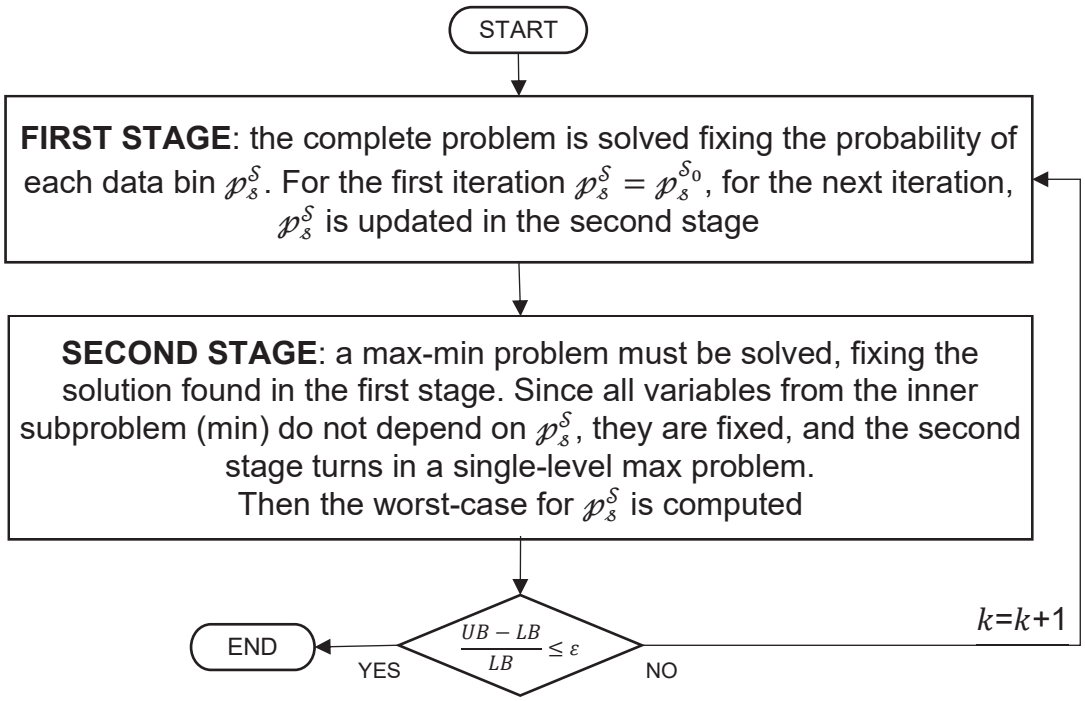
It is important to note that the parameter $p_s^{\delta_0}$ is known and defined by the probability for each data bin created from the historical data. The variable p_s^{δ} is used in the object function (172), which depends on $p_s^{\delta\pm}$.

The DDDRO approach defines the worst p_s^{δ} for each data bin; in other words, it changes the probability of historical data based on the amount of data available. If enough data is available, the confidence level is high and p_s^{δ} is close to $p_s^{\delta_0}$.

6.3.2 Algorithm and solution approach

The proposed model in this chapter is formulated as a tri-level problem, and it is solved using a two-stage robust approach using the C&CG algorithm. Figure 44 presents the proposed algorithm to solve the problem.

FIGURE 44 – TWO-STAGE DECOMPOSITION TO SOLVE THE TRI-LEVEL FORMULATION



The two-stage decomposition presented in Figure 44 is detailed in the following subsections. For each algorithm iteration, the number of variables and constraints is increased according to the iteration variable k.

6.3.2.1 First Stage and LB Definition

The first stage is solved using MILP. The variables related to uncertainties ($\mathscr{p}^{\mathcal{S}}_{s,t_y}$) are fixed and updated in the second stage, representing each data bin's probability.

The first stage seeks the best investments considering all data bins and their probabilities. The objective function is:

$$\min \left[\sum_{t_y} \sum_{c} \frac{I^C_c x^C_{c,t_y}}{(1+R)^{t_y}} + \eta \right] \tag{179}$$

subject to $\Psi^{\eta 2}$,Ψ^{Lflow}, Ψ^{bal}, Ψ^{ess}, Ψ^{op}, Ψ^{inv}, Ψ^{dr}, Ψ^{cont}, Ψ^{bsw}

Variable η reconstructs the maxmin subproblem from the original objective function of the problem and the set of constraints $\Psi^{\eta 2}$ is:

$$\eta \geq \sum_{s} \dot{\mathscr{p}}^{\mathcal{S}}_{s,t_y} \left[\sum_{t_y} \sum_{t_h} \sigma \left(\sum_{g} C^G_{g,t} p^G_{g,t} + \sum_{d} C^{LS}_{d,t} p^{LS}_{d,t} \right) \right], \qquad \forall k \tag{180}$$

where k represents the number of iterations of the algorithm.

In this stage, all variables (except x^C_{c,t_y}) and constraints must be replicated for all k. And, since the uncertainties are fixed, constraints Ψ^{amb} are not included in this stage.

Only $\mathscr{p}^{\mathcal{S}}_{s,t_y}$ is fixed in this stage; thus, all other variables are outputs. Moreover, the lower bound (LB) is defined as:

$$LB = \sum_{t_y} \sum_{c} \frac{I^C_c x^C_{c,t_y}}{(1+R)^{t_y}} + \eta \tag{181}$$

6.3.2.2 Second Stage and UB Definition

The second stage computes the worst-case realization for the T-PDF from the ambiguity set. Thus, the objective function in the second stage is defined as:

$$\max_{\mathcal{P}^{\mathcal{S}}_{s,t_y}} \min_{\Delta Smin} \sum_{s} \mathcal{P}^{\mathcal{S}}_{s,t_y} \left[\sum_{t_y} \sum_{t_h} \sigma \left(\sum_{g} C^{G}_{g,t} p^{G}_{g,t} + \sum_{d} C^{LS}_{d,t} p^{LS}_{d,t} \right) \right] \quad (182)$$

subject to Ψ^{Lflow}, Ψ^{bal}, Ψ^{ess}, Ψ^{op}, Ψ^{dr}, Ψ^{amb}

Since $p^{G}_{g,t}$ is defined for all data bin s and does not depend on the value of $\mathcal{P}^{\mathcal{S}}_{s,t_y}$, the inner subproblem (min) of this stage can be removed, because it is constant. Therefore, the objective function of the second stage is reduced to:

$$\max \sum_{s} \sum_{t_y} \sum_{t_h} \sigma \mathcal{P}^{\mathcal{S}}_{s,t_y} \left(\sum_{g} C^{G}_{g,t} \dot{p}^{G}_{g,t} + \sum_{d} C^{LS}_{d,t} \dot{p}^{LS}_{d,t} \right) \quad (183)$$

subject to Ψ^{amb}

All variables, except $\mathcal{P}^{\mathcal{S}}_{s,t_y}$, are fixed at this stage, and only the constraint Ψ^{amb} is defined. This is only possible because the values of all variables in the second stage are not affected by the $\mathcal{P}^{\mathcal{S}}_{s,t_y}$ value, what is not valid in the first stage of the problem, where the expansion decision x^{C}_{c,t_y} depends on $\mathcal{P}^{\mathcal{S}}_{s,t_y}$.

The problem is solved using MILP, and the key outputs are the T-PDF of each data bin ($\mathcal{P}^{S}_{s,t_y}$) and an upper bound (UB) of the cost, calculated as:

$$UB = \sum_{t_y} \sum_{c} \frac{I^{C}_{c} \dot{x}^{C}_{c,t_y}}{(1+R)^{t_y}} + \sum_{s} \dot{\mathcal{P}}^{\mathcal{S}}_{s,t_y} \left[\sum_{t_y} \sum_{t_h} \sigma \left(\sum_{g} C^{G}_{g,t} \dot{p}^{G}_{g,t} + \sum_{d} C^{LS}_{d,t} \dot{p}^{LS}_{d,t} \right) \right] \quad (184)$$

6.3.2.3 Convergence

For each iteration k, the convergence is checked by computing (*UB-LB)/LB*. If this gap is less than a given tolerance (10^{-4}), the algorithm ends; otherwise, it goes back to the first stage and new values for the $\mathcal{P}^{\mathcal{S}}_{s,t_y}$variables are kept.

6.4 CASE STUDY

The proposed model is demonstrated using the modified version of the IEEE 123-bus test system presented in subsection 5.4. In addition:

- The historical data for solar and wind power generation was taken from Solcast (2021) for the city of Sao Paulo, Brazil, from 2008 to 2021, illustrated in Figure 42.
- The historical data for the load was taken from ONS (2021) for the city of Sao Paulo, Brazil, from 2008 to 2021, also presented in Figure 42.
- The test system is defined as an MMG system with three MGs, which is presented in Figure 29.
- The confidence levels (φ_1, φ_∞) are defined as 99% as in Zhang et al. (2021), which uses less historical data.
- $M_D = 6$, number of data bins, the same presented in Figure 43.
- $N = 5{,}255$, number of historical data.

6.5 SIMULATION RESULTS

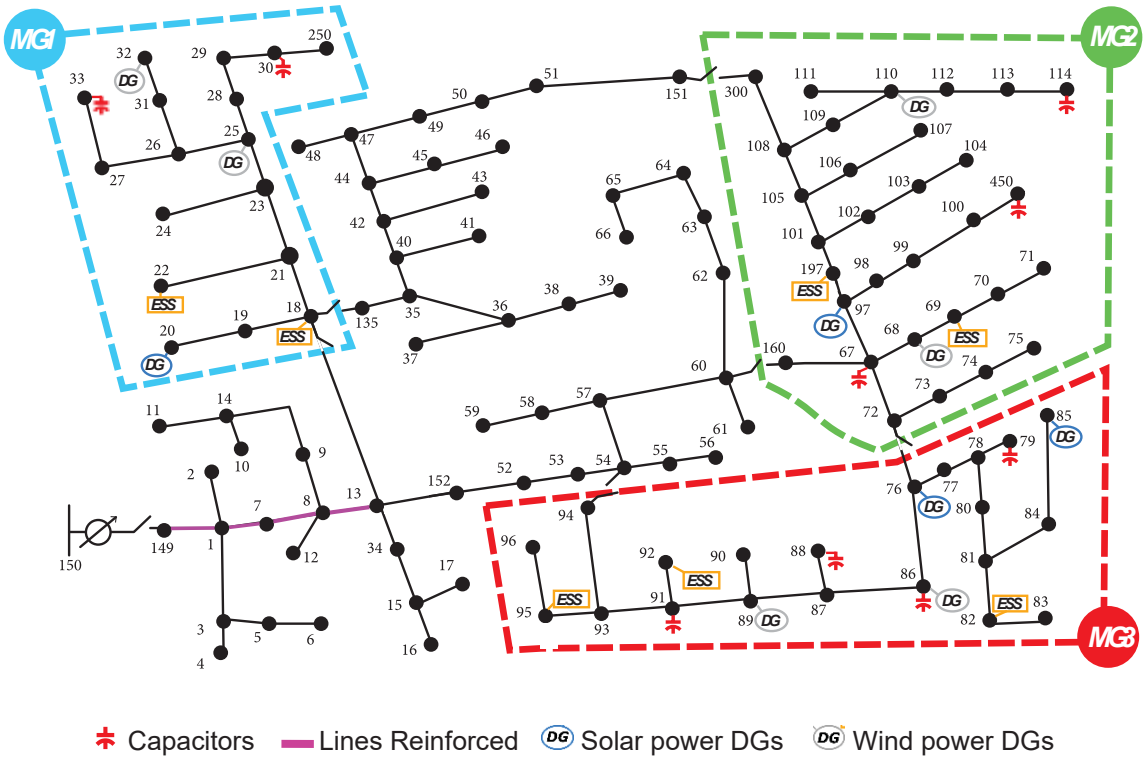
This section presents expansion proposals for two cases of uncertainty budgets, DER's coordination, some operational results provided by the model, contingency results, a discussion on neglecting some of the chapter's contributions, and a comparison between this model and the one presented in the previous chapter.

The numerical experiments are carried out with Gurobi, in a machine with 8 cores and 32GB of RAM, with Python.

6.5.1 Expansion Planning Decision

Even though the proposed model provides information for the operation of the power system, the expansion planning decision is its main output. Figure 45 illustrates the components placed in the system for the expansion planning decision in the last period of the planning horizon.

FIGURE 45 – EXPANSION PLANNING DECISIONS FOR THE TEST SYSTEM AT THE LAST PERIOD (YEAR 3)



Lines connecting buses 149-1, 1-7, 7-8, and 8-13 were reinforced. These lines are the main lines connecting the substation (bus 150) to the MGs, and most of the power from the substation flows through them. Besides, the results show that the lines were reinforced to allow the use of the surplus power generation of the DGs in the substation.

Capacitors, DGs, and ESS units were placed inside the microgrid to reduce the expansion planning cost and provide enough power inside the microgrid, even for contingency cases.

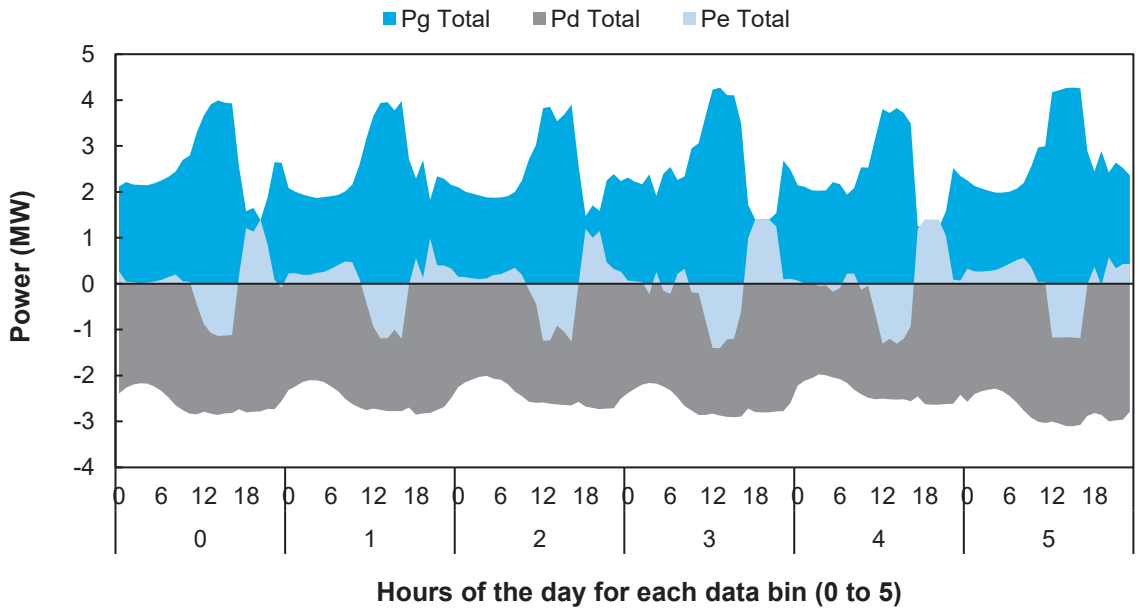
The expansion planning slightly impacts the ADN because the contingency constraints force the placement of components inside the MGs, which provides enough benefits for the system because the MGs export power to the ADN.

The expansion planning decision is unique, considering all data bins. The decisions in DDDRO models consider the probability of all scenarios, which drives the best expansion decision.

6.5.2 DERs' coordination

This model also includes the 24H-OP in the expansion planning using a DDDRO approach. Thus, Figure 46 shows the power balance of the entire system for each data bin. It describes the DERs' coordination for each hour of the day at the last period of the expansion planning horizon. *Pg Total* is the total power generated, *Pd Total* is the total load, and *Pe Total* is the total charging/discharging power of the ESS units.

FIGURE 46 – DERS' COORDINATION FOR THE 24-HOUR OPERATION AT THE LAST PERIOD (YEAR 3)



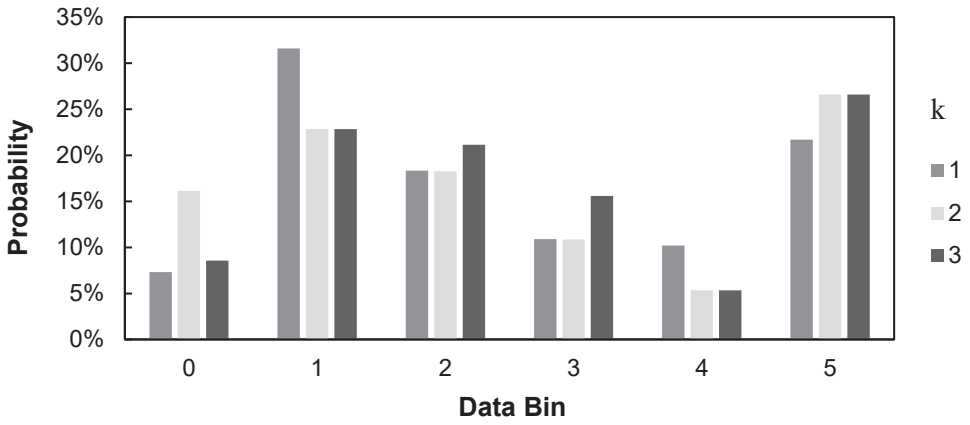
The load presented in Figure 46 is the lowest in case 4 and the highest in case 5. Each of these cases is related to the data bin. Moreover, case 3 has a load level near case 5 and little generation power capacity near hour 18.

The power generation in Figure 46 clearly shows the contribution of ESS units when used along with solar power-based DGs. During near hour 12, the ESS units store power from the DGs; near hour 18, it discharges the power to be used by the loads. Also, the ESS units are used overnight to complement the unavailability of solar power-based DGs.

6.5.3 Evolution of the data bin's probabilities

The algorithm required only 3 iterations and 25 minutes to converge for the test system. Figure 47 shows the evolution of the data bin scenario probabilities for each iteration k.

FIGURE 47 – EVOLUTION OF THE DATA BIN PROBABILITIES FOR EACH ITERATION (K)



The probabilities of cases 2, 3, and 5 increase, while cases 1 and 4 decrease. The changes in the probability of each case are defined in the second stage of the proposed model, where the probabilities are calculated for the worst case of the DDDRO.

Changes from one iteration to another represent the effects of the second stage in the model. For example, looking at data bin 0, its probability prior to the optimization process is 7.3%; in the second iteration is 16.2%; in the third iteration is 8.5%.

6.5.4 Comparison between DDDRO and ARO models

To illustrate the comparison between DDDRO and ARO, Table V shows the relation of the total cost for the same problem solved using DDDRO and ARO (model from chapter 5). For a fair comparison, the RO model has its uncertainty budget (Γ) varying from 0 to 0.5 and the DDDRO model has its number of historical data varying from 500 to 5.255. The values presented in Table V show the DDDRO model's total cost divided by the RO model's total cost.

TABLE V - TOTAL COST OF DDDRO MODEL IN RELATION OF THE TOTAL COST FROM ARO MODEL

CASES	**ARO (Γ=0)**	**ARO (Γ=0.25)**	**ARO (Γ=0.5)**
DDDRO ($N = 5{,}255$)	109%	91%	81%
DDDRO ($N = 2{,}000$)	121%	94%	83%
DDDRO ($N = 1{,}000$)	145%	107%	97%
DDDRO ($N = 500$)	147%	113%	102%

Table V shows that if a high number of historical data is available ($N = 5{,}255$), the DDDRO is recommended since the total cost of the problem is lower than the ARO model for uncertainty budgets of $\Gamma = 0.25$ and $\Gamma = 0.5$. Moreover, the result from the DDDRO is even close to the optimistic case of the RO model ($\Gamma = 0$).

Cases with an uncertainty budget near 0 in ARO models are very optimistic; these cases are close to deterministic models and are expected to have lower total costs than Data-Driven models. The simulations show that the DDDRO model has 9% more of the total cost, considering the case with 5,255 historical data for the DDDRO. However, for an uncertainty budget higher than 25%, the DDDRO provides lower total costs. Therefore, DDDRO models can provide more accurate results than deterministic models and can provide more realistic results than ARO models, if historical data is available.

If little data is available ($N = 500$), the DDDRO model behaves close to the risk-averse case of the RO ($\Gamma \geq 0.5$). In this case, ARO models are preferable; however, DDDRO can also be used. ARO models should be used when there is little or no historical data available; thus, different cases varying the uncertainty budget can be studied.

The great advantage of DDDRO is reducing the over-conservativism of ARO models and realistically/appropriately representing uncertainties in power system models. On the other hand, DDDRO requires more computational effort due to the creation of different scenarios with the data bins. For this case study, the processing time is 25 minutes for the DDDRO against 18 minutes for the ARO model.

6.5.5 Comparison among models

Table VI compares the main aspects of the models presented up to this chapter.

TABLE VI – COMPARISON AMONG MODELS FROM CHAPTERS 4, 5, AND 6

	Model from chapter		
	4	**5**	**6**
Uncertainty approach	ARO	ARO	DDDRO
Historical data			✓
DG, ESS, capacitors and line placement	✓	✓	✓
Self-healing and reliability	✓		
N-1 contingency		✓	✓
Demand response		✓	✓
MMG		✓	✓

Compared to the previous model, the model presented in this chapter uses historical data through a DDDRO approach. Reliability is not considered since contingencies are incorporated into the model, in chapter 4 is shown that including contingencies also improves reliability indexes.

6.6 SUMMARY

This chapter proposes a model to solve the expansion planning for active distribution networks under uncertainties with multiple microgrids, distributed energy resources (DERs), demand response, and N-1 generation contingency using a data-driven distributionally robust approach (DDDRO). The model seeks the best investment periods and locations for all expansion candidates, considering the optimal coordination of DERs using hourly steps of the day.

The main contribution of the model is the use of DDDRO in operation and expansion planning problems for active distribution networks with multiple microgrids under uncertainties, with demand response and inclusion of N-1 generation contingencies. The results show that DDDRO models provide a lower total cost than

Adaptative Robust Models (ARO), considering that historical data is available and uncertainty budgets are greater than 0.25 for the robust model.

Moreover, the results show that DDDRO can be used when very little historical data is available, which is not the case for stochastic approaches (SP).

Therefore, ARO models are recommended when there is little or no historical data available because different cases can be studied varying the uncertainty budget. SP models are preferable if the historical data are enough to represent the true probability density function of the uncertainty variables; however, the computational effort could be high. DDRO models are indicated for cases having historical data, they have the advantage of requiring low computational effort compared to stochastic models and are not over-conservative as ARO models.

7 A DATA-DRIVEN DISTRIBUTIONALLY ROBUST MODEL FOR EXPANSION PLANNING OF ADNs CONSIDERING ENERGY TRADING STRATEGY BASED ON GAME THEORY

7.1 INTRODUCTION

The combination of DERs and multiple MGs may increase the resilience and reliability of ADNs. Compared with single MG systems, multi-MG systems not only ensure the regular operation of the system under grid-connected and island mode operation, but also consider the energy flow among the MGs in the system, so as to improve the power supply reliability and economy.

If the MGs can exchange power among themselves and private investors own them, a new concept emerges where there is a local energy trade market. Most single microgrid models consider that the MG can exchange power with ADN, and the surplus energy can be sold or used to compensate for later power consumption. In MMG models, in addition to that point, the MGs can sell/buy power among themselves.

Multi-agent power systems pose challenges that can no longer be addressed by classical centralized planning, operation, and control methods. The need for simulation of interactions among DSO, generation and distribution companies, independent investors, consumers, prosumers, and microgrids operators forced the power systems research community to develop models under the umbrella of Game Theory. The models can be classified into cooperative and noncooperative game formulations depending on the interaction assumptions (CHURKIN et al., 2021).

Cooperative strategies consider situations where players conclude binding agreements to reach mutual benefits. In cooperative games (also called coalitional games), the key questions to address are: what coalitions will form, and what should be the payoffs to the participants? An important assumption is usually made that benefits generated by cooperation may be easily distributed and shared among the players, for example, in monetary terms.

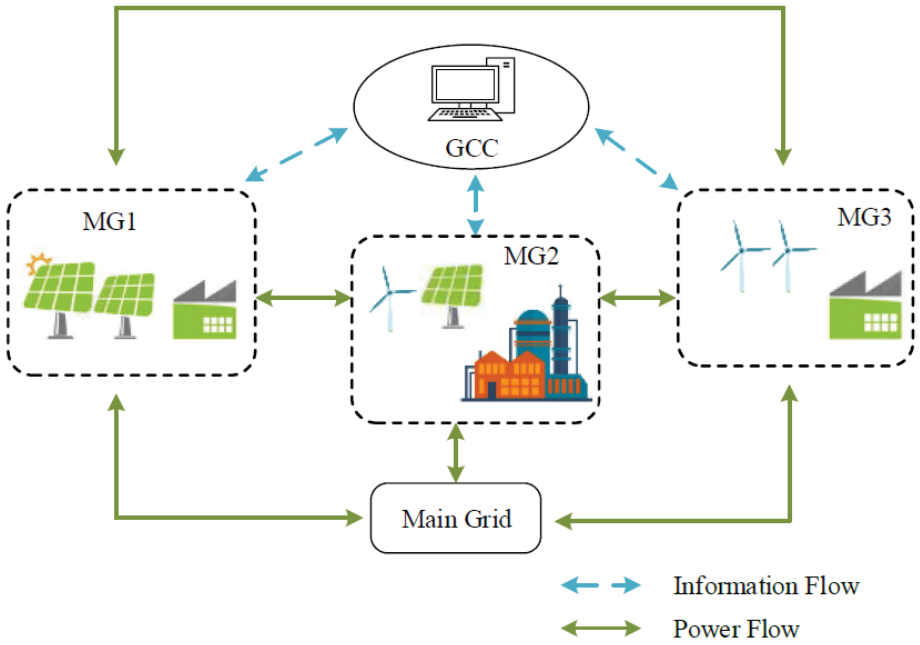
The main assumption in noncooperative games is that players act independently. That is, each player optimizes its own objective function without seeking to increase other players' benefits. The noncooperative formulation represents competition among players and is usually analyzed using equilibrium-based solution concepts. In power systems research, noncooperative games are widely used to

estimate electricity market equilibria and to model the competitive aspects of MMG systems (CHURKIN et al., 2021).

In Liang et al. (2021), MGs are divided into consumers (buyers) and providers (sellers), and the authors describe the energy flow between MGs as a game problem. Each MG obtains its own optimal operation results in the game process. A non-cooperative game model is established, and a Nash equilibrium point is obtained.

Figure 48 shows the structure of an MMG system presented by Liang et al. (2021), where the MGs can exchange power among themselves and with the main grid. The global central controller (GCC) manages the information among the MGs, which also centralizes the energy trade market decisions.

FIGURE 48 – STRUCTURE OF A MULTIPLE MICROGRIDS SYSTEM



SOURCE: Liang et al. (2021)

The introduction of game theory inside the ADN expansion planning problem under uncertainties significantly increases its complexity. In this context, while the DSO seeks investments to reduce costs in the main grid and meet demand growth, he must deal with the uncertainty of what each MG would invest in its area and how it would operate daily. Since, in this context, the MGs make decisions independently, the DSO must study cases where the MGs seek their own benefits and understand the impacts that would provide in the main grid's operation.

Thus, this chapter proposes a model incorporating all aspects of chapter 6, but including the energy trade market, and using a non-cooperative (or competitive) game theory approach.

7.2 CONTEXT AND ASSUMPTIONS

The previous chapters consider that the DSO owns the MGs or that the DSO wishes to study the investment decisions on private MGs that would benefit himself, aiming to create incentive programs. This chapter considers that private investors own the MG, and each player seeks its own benefits. The expansion planning decision is still over the DSO perspective, but now, MG's expansion and operational decisions do not necessarily benefit the DSO.

MMG systems can have different types of interaction with the main grid. In this chapter, we consider that different stakeholders control the DSO and the MGs; therefore, each MG can have its own expansion plan and trade energy among other MGs in a free market.

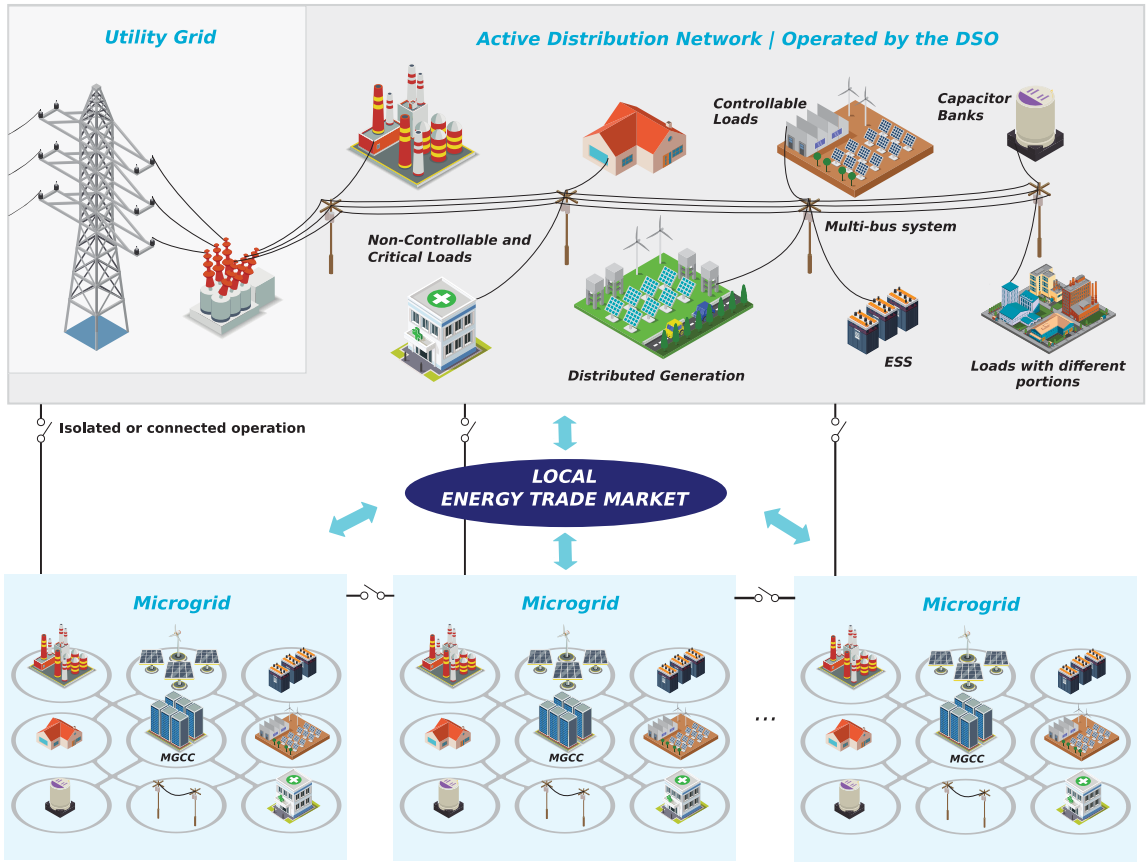
The algorithm is designed from the DSO perspective; thus, it seeks the best expansion decision for the DSO considering the following aspects and assumptions:

- The DSO aims to define the best expansion decision to minimize the investment and operation costs for the next 5 years.
- Each MG seeks to maximize its revenue from the energy trading market, while minimizing investments and operating costs. However, each MG seeks its own benefit.
- DSO and MGs can install DG units, ESS units, and capacitors. The DSO can reinforce branches.
- Load demand and DG units are subject to uncertainties.
- The DSO controls the ADN, which has controllable and non-controllable (or critical) loads.
- All MGs must be able to operate with N-1 generation contingency.
- Historical data is available
- The degradation of ESSs by charging/discharging and their efficiency are ignored, as well as active power losses in lines.

- Any MG of the system may operate isolated from the main grid at any hour of the day.
- There is a local energy trade market where MGs can offer to buy or sell energy. The DSO only defines the bounds for the price strategy, minimum and maximum price allowed.
- Since this chapter considers a context where each MG seeks its own benefit, it uses a competitive game theory approach.

Figure 49 illustrates the context above and the application of the proposed model in this work

FIGURE 49 – REPRESENTATION OF THE SCOPE OF THIS CHAPTER USING A GENERIC STRUCTURE OF MMG SYSTEMS.



SOURCE: the author (2022)

The main contribution of this model is to include an energy trading strategy based on game theory in a DDDRO model for the expansion planning of modern

distribution systems. Both subjects are complex and are typically not jointly addressed in the literature.

In addition, it incorporates the impact of the MG's individual expansion decision on the DSO (distribution system operator). Thus, this chapter proposes a new model to solve the expansion planning problem, from the DSO perspective, in a scenario where the MGs are individual players seeking their own benefits.

7.3 PROPOSED MODEL

Historical data on generation and load are available; thus, the DDDRO model is used to solve the proposed problem.

The model seeks the best investments and operational conditions (generation, DERs coordination, and load shedding costs) for DSO, considering the worst-case realization of the uncertainties in the ADN and the individual decisions of the MGs' owners.

The model is formulated as a tri-level optimization problem and solved using a four-stage robust optimization approach. The first stage converts the historical data into data bins used in the DDDRO formulation through a machine-learning approach. The second and third stages are solved using MILP. And the fourth stage is modeled as a non-cooperative game theory and solved using a genetic algorithm (GA).

The following subsections show the problem formulation and the solution approach.

7.3.1 Formulation

The objective function and constraints of the problem are detailed in this subsection. Since this formulation is complex, the algorithm and solution approach are presented in the following subsection.

7.3.1.1 Objective function

The objective function of the proposed model is defined as:

$$\min_{x^C_{c,t_y}} \max_{\mathcal{P}^S_{s,t_y}} \min_{\Delta Smin} \sum_{t_y} \sum_{c} \frac{I^C_c x^C_{c,t_y}}{(1+R)^{t_y}} + \sum_{s} \mathcal{P}^S_{s,t_y} \left[\sum_{t_y} \sum_{t_h} \sigma \left(\sum_{g} C^G_{g,t} p^G_{g,t} + \sum_{d} C^{LS}_{d,t} p^{LS}_{d,t} \right) \right. \quad (185)$$

$$\text{subject to} \left\{ \begin{matrix} \Psi^{Lflow}_{adn}, \Psi^{bal}_{adn}, \Psi^{ess}_{adn}, \Psi^{op}_{adn}, \Psi^{inv}_{adn}, \Psi^{dr}_{adn} \\ \Psi^{Lflow}_{mg}, \Psi^{bal}_{mg}, \Psi^{ess}_{mg}, \Psi^{op}_{mg}, \Psi^{inv}_{mg}, \Psi^{dr}_{mg}, \Psi^{cont}_{mg}, \Psi^{bsw}_{mg} \\ \Psi^{amb}, \Psi^{balConn}, \Psi^{game} \end{matrix} \right\}$$

Compared to chapter 6, Ψ^{game} and $\Psi^{balConn}$ are incorporated in this new model. The problem has the same objective function presented in chapter 6; however, the introduction of constraint Ψ^{game} changes everything, it represents the solution of the non-cooperative game theory. This constraint is, in fact, an optimization subproblem.

The constraints and variables of this chapter have some special notations:

- There are some constraints used in both ADN and MG (Ψ^{Lflow}, Ψ^{bal}, Ψ^{ess}, Ψ^{op}, Ψ^{inv}, Ψ^{dr}, Ψ^{amb}, Ψ^{game}, $\Psi^{balConn}$) and others used only in the MG (Ψ^{cont}, Ψ^{bsw}).
- The indexes adn and mg used in the constraints do not change the equations presented in the previous chapters; they denote that the components used to build the equations are from the ADN or from MGs, which is important for the decomposition approach that is presented in the following subsections.
- The accent ̂ is used in variables of MGs. For example, x^C_{c,t_y} is the expansion planning decision for the ADN and $\hat{x}^C_{c,t_y}$ is for the MGs.

7.3.1.2 Constraints

The sets of constraints Ψ^{Lflow}, Ψ^{bal}, Ψ^{ess}, Ψ^{op}, and Ψ^{inv} are defined in chapter 4, subsection 4.3.1.2. Sets Ψ^{dr}, Ψ^{cont}, and Ψ^{bsw} are described in chapter 5, subsection 5.3.1.2. Set Ψ^{amb} defines the ambiguity set used in the DSO and it is presented in chapter 6, subsection 6.3.1.2. And constraints Ψ^{game} and $\Psi^{balConn}$ are defined in this subsection.

Set of constraints of power balance in nodes connecting ADN and MGs ($\Psi^{balConn}$):

$$\sum_{g\epsilon\Omega_n^G} p_{g,t}^G + \sum_{e\epsilon\Omega_n^E} p_{e,t}^E - \sum_{l\epsilon\Omega_{n(s)}^L} p_{l,t}^L + \sum_{l\epsilon\Omega_{n(r)}^L} p_{l,t}^L = \sum_{d\epsilon\Omega_n^D} \tilde{p}_{d,t}^D - p_{d,t}^{LS} + \frac{\hat{r}_{m(n)}^{B|S}}{\Delta t_h} \qquad \forall n\epsilon\Omega_{m,adn}^N, \forall t \quad (186)$$

$$\sum_{g\epsilon\Omega_n^G} q_{g,t}^G + \sum_{cp\epsilon\Omega_n^{CP}} q_{cp,t}^{SH} - \sum_{l\epsilon\Omega_{n(s)}^L} q_{l,t}^L + \sum_{l\epsilon\Omega_{n(r)}^L} q_{l,t}^L = \sum_{d\epsilon\Omega_n^D} \tilde{q}_{d,t}^D - q_{d,t}^{LS} + \hat{q}_{m(n),t}^{MG} \qquad \forall n\epsilon\Omega_{m,adn}^N, \forall t \quad (187)$$

Equations in $\Psi^{balConn}$ are specific for nodes connecting the ADN to the MGs, represented by the set $\Omega_{m,adn}^N$. They are similar to equations in Ψ^{Conn}, adding $\frac{\hat{r}_{m(n)}^{B|S}}{\Delta t_h}$ and $\hat{q}_{m(n),t}^{MG}$, which are the net active power and reactive power required by the MG, defined in Ψ^{game}.

$\hat{r}_{m(n)}^{B|S}$ is the amount of active energy sold/bought by the MG, Δt_h is the time step considered in the model (1h), and $\hat{q}_{m(n),t}^{MG}$ is the reactive power used by the MG. The MGs are individual players, and they have their own decisions. Thus, $\frac{\hat{r}_{m(n)}^{B|S}}{\Delta t_h}$ and $\hat{q}_{m(n),t}^{MG}$ are used to connect the MGs' decisions defined in Ψ^{game} with the ADN decision through $\Psi^{balConn}$.

Set of constraints for game theory (subproblem Ψ^{game}):

$$\hat{c}_m^B, \hat{r}_m^{B|S}, \hat{q}_m^{MG} = \text{argmax}\left\{\begin{array}{c} \widehat{rv}_m - \sum_{t_y}\sum_{c\in\Omega_m^C} \frac{I_c^C \hat{x}_{c,t_y}^C}{(1+R)^{t^y}} \\ s.t.\ \Psi_{noncoop}^{game}, \\ \Psi_{mg}^{Lflow}, \Psi_{mg}^{bal}, \Psi_{mg}^{ess}, \Psi_{mg}^{op}, \\ \Psi_{mg}^{inv}, \Psi_{mg}^{dr}, \Psi_{mg}^{cont}, \Psi_{mg}^{bsw} \end{array}\right\} \qquad \forall m \quad (188)$$

$\widehat{rv}_m$ is the revenue received by MG seller m. $\hat{c}_m^B$ is the price strategy of energy MG buyer m. $\hat{r}_m^{B|S}$ is the net active energy bought or sold by the MG. $\hat{q}_m^{MG}$ is the reactive power required/delivered by the MG. $\hat{x}_{c,t_y}^C$ is the expansion decision for MG m.

The problem in (188) is used to find the values of variables $\hat{r}_m^{B|S}$, $\hat{q}_m^{MG}$, and the price strategy ($\hat{c}_m^B$) that maximize the revenue minus investment for each MG. And, $\hat{r}_m^{B|S}$ and $\hat{q}_m^{MG}$ are used in the set of constraints $\Psi^{balConn}$, connecting the MGs' decisions with the ADN.

The subproblem Ψ^{game} is a maximization problem, where it maximizes the revenue minus the investments made by the MG. In other words, Ψ^{game} returns the price strategy and required/exported energy by the microgrids, considering the best decisions for each MG.

The constraints inside the subproblem Ψ^{game} are defined in the previous chapter, except $\Psi^{game}_{noncoop}$, which was proposed by Liang et al. (2021) and is presented in what follows:

$$\Delta\hat{P}_m = \sum_{g\epsilon\Omega_m^G} \hat{p}_g^G + \sum_{e\epsilon\Omega_m^E} \hat{p}_e^E - \sum_{d\epsilon\Omega_m^D} \hat{p}_d^D \qquad \forall m, \forall t \quad (189)$$

$$\widehat{pr}_j = \frac{\sum_{g\epsilon\Omega_{m(j)}^G} \hat{p}_g^G + \sum_{e\epsilon\Omega_{m(j)}^E} \hat{p}_e^E}{\sum_{d\epsilon\Omega_{m(j)}^D} \hat{p}_d^D} \qquad \forall j, \forall t \quad (190)$$

$$\hat{r}_i^B = \begin{cases} -\Delta\hat{P}_i, & if\ \ 0 < r^{TB} \le r^{TS}\ \ or\ \ r^{TB} > r^{TS} > 0\ \ and\ \ \frac{\hat{c}_i^B}{\sum_i \hat{c}_i^B} r^{TS} > \Delta\hat{P}_i \\ \frac{\hat{c}_i^B}{\sum_i \hat{c}_i^B} r^{TS}, & if\ \ r^{TB} > r^{TS} > 0\ \ and\ \ \frac{\hat{c}_i^B}{\sum_i \hat{c}_i^B} r^{TS} < \Delta\hat{P}_i \\ 0, & other, \quad including\ if\ MG\ is\ isolated \end{cases} \qquad \forall i, \forall t \quad (191)$$

$$\hat{r}_j^S = \begin{cases} \Delta\hat{P}_i, & if\ \ r^{TB} > r^{TS} > 0\ \ \ or\ \ r^{TS} > r^{TB} > 0\ \ and\ \ \frac{\widehat{pr}_j}{\sum_j \widehat{pr}_j} r^{TB} > \Delta\hat{P}_j \\ \frac{\widehat{pr}_j}{\sum_j \widehat{pr}_j} r^{TB}, & if\ \ r^{TS} > r^{TB} > 0\ \ and\ \ \frac{\widehat{pr}_j}{\sum_j \widehat{pr}_j} r^{TB} < \Delta\hat{P}_j \\ 0, & other, \quad including\ if\ MG\ is\ isolated \end{cases} \qquad \forall j, \forall t \quad (192)$$

$$r^{TB} = \sum_i \Delta\hat{P}_i \qquad \forall t \quad (193)$$

$$r^{TS} = \sum_j \Delta\hat{P}_j \qquad \forall t \quad (194)$$

$$\widehat{rv}^T = \sum_i \hat{r}_i^B \hat{c}_i^B \qquad \forall t \qquad (195)$$

$$\widehat{rv}_j = \frac{\hat{r}_j^S}{\sum_j \hat{r}_j^S} \widehat{rv}^T \qquad \forall j, \forall t \qquad (196)$$

$$\hat{q}_m^{MG} = \frac{\hat{r}_m^{B|S}}{\Delta t_h} \frac{\sum_{d \epsilon \Omega_m^D} \hat{q}_d^D}{\sum_{d \epsilon \Omega_m^D} \hat{p}_d^D} \qquad \forall m, \forall t \qquad (197)$$

The indexes i and j are buyers' and sellers' MGs, respectively. The definition of an MG as a buyer or seller depends on if the MG requires power (net power negative) or if it exports power (net power positive), which is calculated in $\Delta\hat{P}_m$.

Equation (189) defines the net active power in the MG ($\Delta\hat{P}_m$), which is the generation power, plus the provided/consumed power from ESS units, minus the loads. Equation (190) is a priority criterion ($\widehat{pr}_j$) defined according the available evergy and the load inside the MG.

Equation (191) calculates the amount of energy bought by each MG ($\hat{r}_i^B$). If there is more power available than load demand, the MG can buy all required energy ($\Delta\hat{P}_m$). If there is more load demand than power available, the energy bought is prorated according to the price strategy of the MG.

Equation (192) determines the amount of energy sold by each MG ($\hat{r}_j^S$). The MG can sell all surplus power generation if there is more load demand than power available. Otherwise, the energy sold is prorated according to the priority criterion ($\widehat{pr}_j$).

Equations (193) and (194) determine r^{TB} and r^{TS}. They are the total energy bought or sold by all MGs.

The total revenue received by the MG m ($\widehat{rv}^T$) is calculated as the total energy bought ($\hat{r}_i^B$) times the strategy price of all buyers' MG ($\hat{c}_i^B$), defined in (195). Equation (196) determines the revenue for each MG ($\widehat{rv}_j$), prorated by the amount of energy sold.

Equation (197) calculates the reactive power required by the MG.

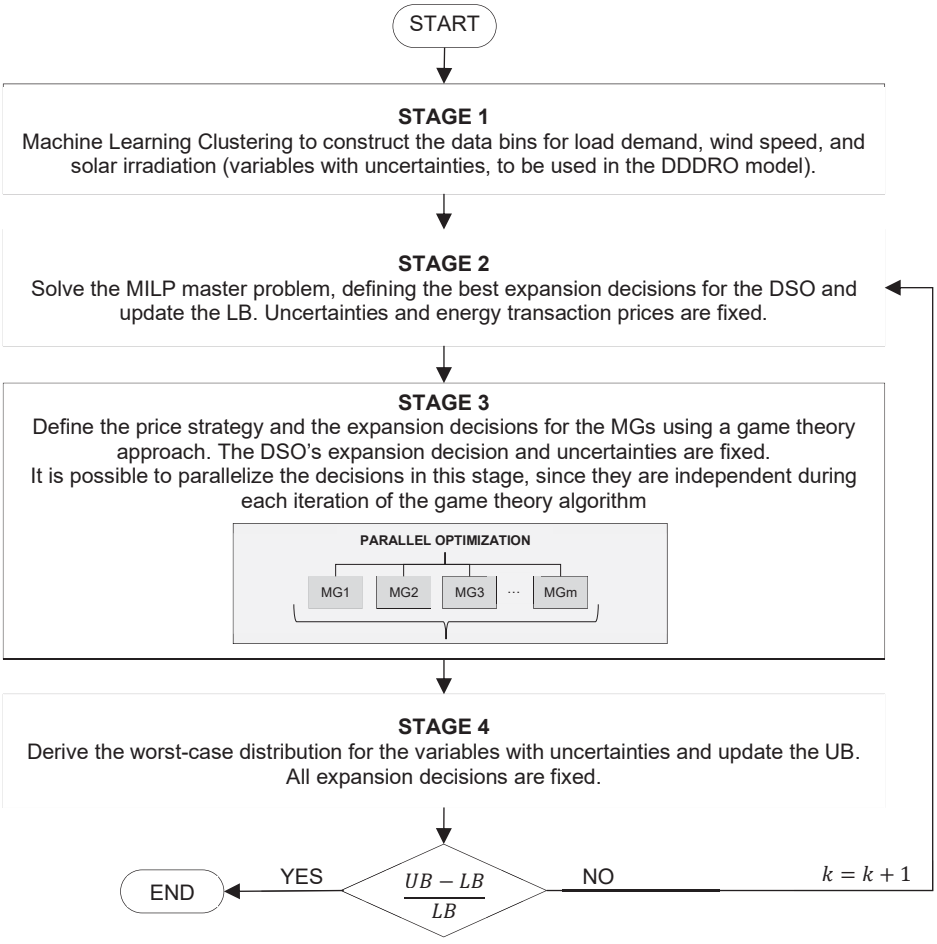
Since equations (191), (192), (195), and (196) are nonlinear, the subproblem Ψ^{game} cannot be solved using MILP. Subsection 7.3.2.3 details its solution approach.

7.3.2 Algorithm and solution approach

The algorithm proposed in this chapter seeks to minimize the total cost of investments and operation for the DSO, while the MGs independently seek their expansion plan and energy prices to increase their revenue. In addition, uncertainties are considered in load demand and DG power units.

The formulation presented in (185) is a three-level min-max-min problem in which constraint (188) is an optimization subproblem to define the decision of each MG. To solve this problem, a four-stage decomposition is proposed in Figure 50.

FIGURE 50 – FOUR-STAGE DECOMPOSITION TO SOLVE THE TRI-LEVEL FORMULATION



SOURCE: The author (2022)

The stages presented in Figure 50 are detailed below.

7.3.2.1 First Stage: clustering and representation of the Uncertainties

This stage clusters the historical data using the algorithm k-means from the package scikit-learn in Python (PEDREGOSA et al., 2012). The historical data and more details are presented in subsection 6.1.1.

7.3.2.2 Second Stage: DSO expansion plan

Stages 2 to 4 are solved using an adaptation of the column-and-constraint generation (C&CG) algorithm. In stage 2, the objective is to find the best expansion planning for the ADN, formulated as follows:

$$\min \sum_{t_y} \sum_{c} \frac{I_c^C x_c^C}{(1+R)^{t^y}} + \eta \tag{198}$$

subject to $\Psi^{\eta 2}$, Ψ_{adn}^{Lflow}, Ψ_{adn}^{bal}, Ψ_{adn}^{ess}, Ψ_{adn}^{op}, Ψ_{adn}^{inv}, Ψ_{adn}^{dr}, $\Psi^{balConn}$

Variable η reconstructs the maxmin subproblem from the original objective function and the set of constraints $\Psi^{\eta 2}$ is:

$$\eta \geq \sum_{s} \dot{p}_{s,t_y}^{S} \left[\sum_{t_y} \sum_{t_h} \sigma \left(\sum_{g} C_{g,t}^{G} p_{g,t}^{G} + \sum_{d} C_{d,t}^{LS} p_{d,t}^{LS} \right) \right], \qquad \forall k \tag{199}$$

where k represents the number of iterations of the algorithm.

In this stage, all variables (except x_{c,t_y}^C) and constraints must be replicated for all k.

Since the uncertainties are fixed, constraints Ψ^{amb} are not included in this stage. Ψ^{game} is also not considered because they are exclusively for the game theory algorithm used in the third stage. Moreover, the constraints Ψ_{adn}^{Lflow}, Ψ_{adn}^{bal}, Ψ_{adn}^{ess}, Ψ_{adn}^{op}, Ψ_{adn}^{inv}, Ψ_{adn}^{dr} are built using only components from the ADN.

This stage is solved using MILP. The value for the objective function in this stage is also defined as the C&CG algorithm's LB (lower bound):

$$LB = \sum_{t_y} \sum_{c} \frac{I_c^C x_{c,t_y}^C}{(1+R)^{t_y}} + \eta \tag{200}$$

At the end of this stage, the expansion decision for the DSO (x_c^C) and the LB are defined.

7.3.2.3 Third Stage: MGs' expansion plan and price strategy

The third stage uses the same approach presented in Liang et al. (2021), where a non-cooperative game theory solves the energy trading strategy of MMG systems.

Thus, this stage solves the constraint Ψ^{game}, represented by the subproblem (188) and replicated below:

$$\hat{c}_m^B, \hat{r}_m^{B|S}, \hat{q}_m^{MG} = \text{argmax} \left\{ \begin{array}{c} \widehat{rv}_m - \sum_{t_y} \sum_{c \in \Omega_m^C} \frac{I_c^C \hat{x}_{c,t_y}^C}{(1+R)^{t^y}} \\ s.t.\ \Psi_{noncoop}^{game}, \\ \Psi_{mg}^{Lflow}, \Psi_{mg}^{bal}, \Psi_{mg}^{ess}, \Psi_{mg}^{op}, \\ \Psi_{mg}^{inv}, \Psi_{mg}^{dr}, \Psi_{mg}^{cont}, \Psi_{mg}^{bsw} \end{array} \right\} \qquad \forall m$$

The objective function seeks to maximize the revenue ($\widehat{rv}_m$) while minimizing the total cost of investments for each MG m.

The set of constraint $\Psi_{noncoop}^{game}$ is defined in subsection 7.3.1.2 and describes the equations that create the competitive game, also detailed in Liang et al. (2021).

Since the problem presented in (188) is defined for all MG seeking the maximum revenue for all of them, it must be solved interactively for each MG until the Nash Equilibrium point is reached. As presented in Liang et al. (2021), this game theory problem can be solved as follows:

Step1: initialize the players' strategy. Because the game model has a Nash equilibrium solution, no matter how to choose the initial value, it will converge to the Nash equilibrium solution;

Step2: keep the price strategy of each player.

Step3: each participant independently optimizes its own strategy according to $\Psi_{noncoop}^{game}$ and all other constraints. The price strategy of each participant is obtained by solving the argmax subproblem in (188).

Step4: update the price strategy for all players.

Step5: if the two adjacent optimization strategies are consistent, then the combination of the strategies is the Nash equilibrium solution; otherwise, return to Step 2 and continue the optimization.

$\Psi_{noncoop}^{game}$ contains nonlinear terms, so a genetic algorithm (GA) is used to solve this stage. Also, Step 3 is solved using parallel processing in Step3 above since each MG makes decisions independently based on the information obtained in the previous iteration.

The iteration process above, including steps 1 to 5, is not related to the iterations from the C&CG algorithm. Steps 1 to 5 are exclusively used to solve the game problem among all players in this decomposition stage.

At the end of this stage, the price strategy ($\hat{c}_i^B$), the amount of energy provided/required by the MGs ($\hat{r}_m^{B|S}, \hat{q}_m^{MG}$), and the expansion decision for the MGs ($\hat{x}_{c,t_y}^C$) are stored.

7.3.2.4 Fourth Stage: Uncertainties and ambiguity set

The DDDRO uses the ambiguity set to derive the worst-case distribution probability for the data bins. Thus, the objective function is defined as:

$$\max_{p_{s,t_y}^S} \min_{\Delta Smin} \sum_{s} p_{s,t_y}^S \left[\sum_{t_y} \sum_{t_h} \sigma \left(\sum_{g} C_{g,t}^G p_{g,t}^G + \sum_{d} C_{d,t}^{LS} p_{d,t}^{LS} \right) \right] \tag{201}$$

$$\text{subject to} \left\{ \begin{matrix} \Psi_{adn}^{Lflow}, \Psi_{adn}^{bal}, \Psi_{adn}^{ess}, \Psi_{adn}^{op}, \Psi_{adn}^{dr} \\ \Psi_{mg}^{Lflow}, \Psi_{mg}^{bal}, \Psi_{mg}^{ess}, \Psi_{mg}^{op}, \Psi_{mg}^{inv}, \Psi_{mg}^{dr} \\ \Psi^{amb}, \Psi^{balConn} \end{matrix} \right\}$$

Constraints Ψ_{adn}^{inv}, Ψ_{mg}^{cont}, Ψ^{game}, and Ψ_{mg}^{bsw} are not used in this stage because they are exclusively for the decision in the second stage.

As proposed in Zhang et al. (2021) and presented in chapter 6, in this stage, the expansion decisions and price strategies are fixed; therefore, the only remaining variables are regarding the uncertainties. Since $p_{g,t}^{G}$ is defined for all data bin s and does not depend on the value of $\mathcal{p}_{s,t_y}^{\mathcal{S}}$, the inner subproblem (min) of this stage can be removed, because it is constant.

Therefore, the objective function of this stage is reduced to:

$$\max \sum_{s} \sum_{t_y} \sum_{t_h} \sigma \mathcal{p}_{s,t_y}^{\mathcal{S}} \left(\sum_{g} C_{g,t}^{G} \dot{p}_{g,t}^{G} + \sum_{d} C_{d,t}^{LS} \dot{p}_{d,t}^{LS} \right) \tag{202}$$

subject to Ψ^{amb}

All variables, except $\mathcal{p}_{s,t_y}^{\mathcal{S}}$, are fixed in this stage, and only the constraint Ψ^{amb} is used. This is only possible because the values of the variables in this stage are not affected by $\mathcal{p}_{s,t_y}^{\mathcal{S}}$. Ψ^{amb} is defined in subsection 6.3.1.2.

The problem in (202) is solved using MILP, and the key outputs are the T-PDF of each data bin ($\mathcal{p}_{s,t_y}^{\mathrm{S}}$) and an upper bound (UB) of the cost, calculated as:

$$UB = \sum_{t_y} \sum_{c} \frac{I_c^C \dot{x}_{c,t_y}^C}{(1+R)^{t_y}} + \sum_{s} \dot{\mathcal{p}}_{s,t_y}^{\mathcal{S}} \left[\sum_{t_y} \sum_{t_h} \sigma \left(\sum_{g} C_{g,t}^{G} \dot{p}_{g,t}^{G} + \sum_{d} C_{d,t}^{LS} \dot{p}_{d,t}^{LS} \right) \right] \tag{203}$$

At the end of this stage, new distribution probabilities for the data bins ($\mathcal{p}_{s,t_y}^{\mathcal{S}}$) are defined, and the UB (upper bound) for the C&CG is updated.

7.3.2.5 Convergence

After calculating UB and LB, if the distance between these bounds is lower than a given tolerance, the algorithm stops; otherwise, it returns to stage 2.

7.4 CASE STUDY

The proposed model is illustrated using the modified version of the IEEE 123-bus test system presented in subsection 5.4, having the additional details presented in subsection 6.4.

In addition, the bounds for the price strategy of each MG are defined as 0 and the price from the main grid.

7.5 SIMULATION RESULTS

The first stage uses the k-means algorithm to define clusters and the data bins. The second stage is solved using Gurobi with Python. The third stage uses the genetic algorithm from Pymoo (BLANK and DEB, 2020). And the fourth stage is also solved using Gurobi. All numerical experiments are carried out using a machine with 8 cores and 32GB of RAM.

The genetic algorithm was selected to solve the decomposition's third stage because the formulation in the game theory subproblem is nonlinear, non-continuous, and with conditional statements. Thus, exact approaches cannot be used, such as MILP and MINLP based on mathematical methods. More details of the algorithm and parameters are available at https://pymoo.org/algorithms/soo/ga.html.

The description of the test case and results are presented below.

7.5.1 Expansion Planning Decision

The proposed algorithm took 127 minutes and 3 iterations for the C&CG to solve the test case.

Figure 51 presents the number of components placed in the ADN (operated by the DSO) and in the MGs per year, where cap are capacitors, ess are energy storage system units, dg-pv represents photovoltaics' DG, dg-wt are wind power-based DGs.

The number of components placed in the system increases over the years since the load grows at a rate of 10% per year. The placement of capacitors is related to the voltage levels of buses and the compensation of reactive power, usually at the network end's nodes. ESS units are associated with the benefits of storing energy at

some hours of the day to be used later, reinforcement of lines allows more power to flow through them, and DG units provide cheap energy close to the consumption point.

FIGURE 51 – NUMBER OF COMPONENTS PLACED IN THE MGS AND IN THE AND PER YEAR

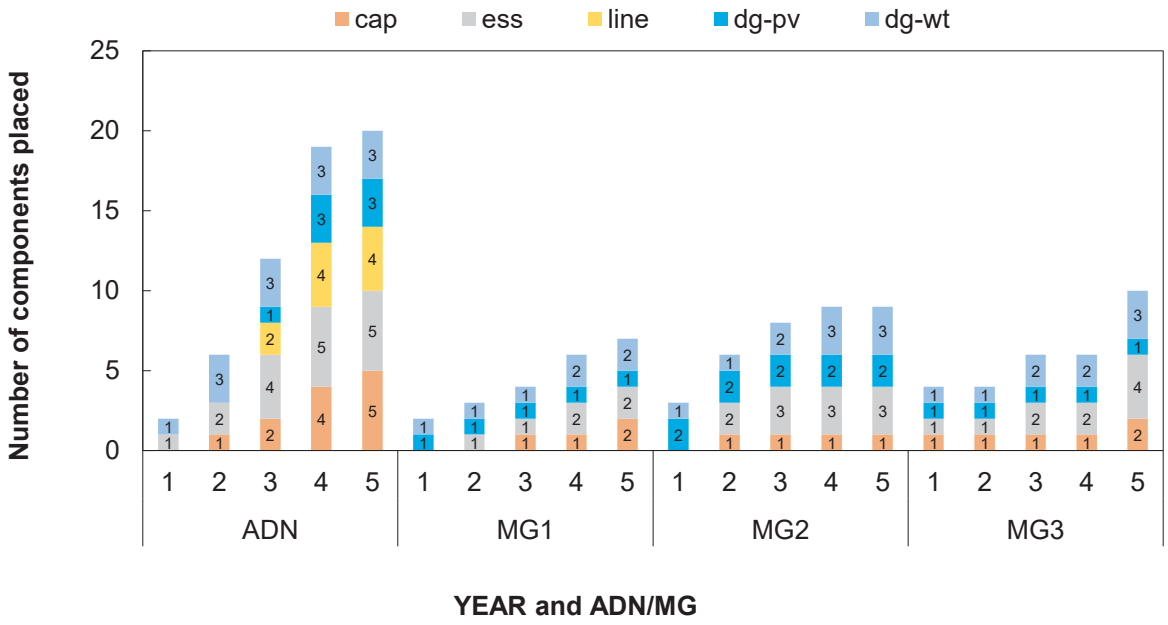


Table VII shows details of the expansion planning decision, presenting where the components were placed in the system.

TABLE VII - DETAILS ON WHERE COMPONENTS HAVE BEEN PLACED IN THE EXPANSION PLANNING DECISION

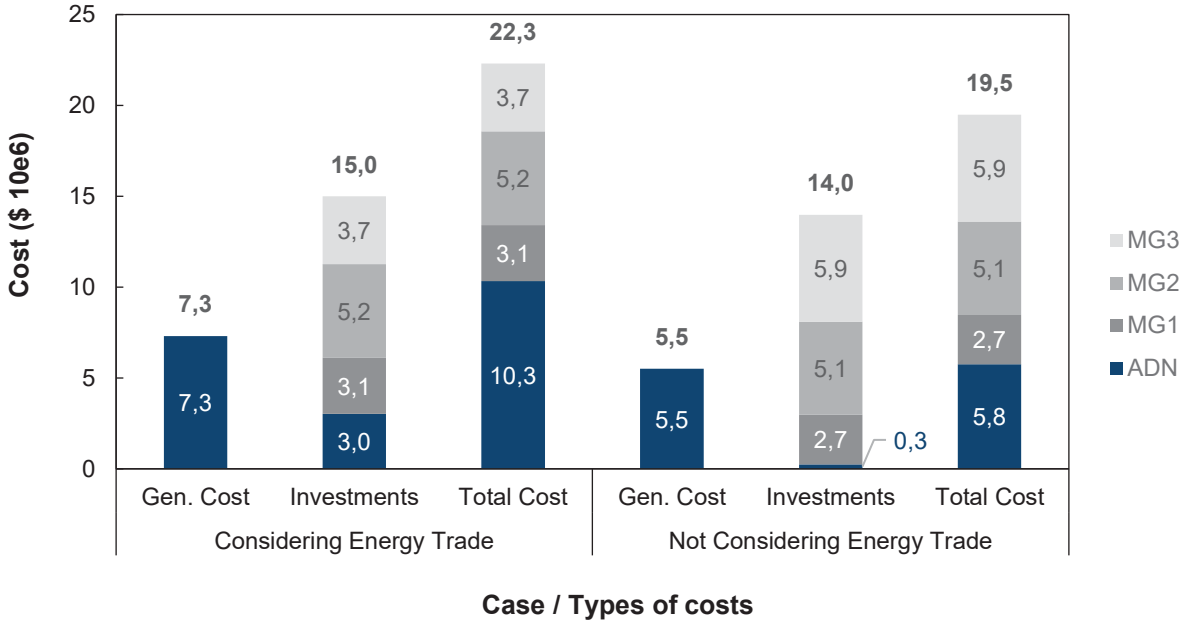
Components	**ADN, MG**	**Where components were placed**
capacitors	ADN	Buses 4, 36, 48, 56, 66
	MG1	Buses 27, 250
	MG2	Bus 101
	MG3	Buses 81, 89
ess	ADN	Buses 3, 12, 42, 55, 62
	MG1	Buses 21, 25
	MG2	Buses 70, 105, 108
	MG3	Buses 76, 84, 87, 94
line	ADN	Lines connecting buses 149-1, 1-7, 7-8, 8-13
dg	ADN	Buses 14, 15, 57, 64, 35, 47
	MG1	Buses 18, 21, 26
	MG2	Buses 67, 72, 105, 110, 160
	MG3	Buses 76, 91, 94, 95

Capacitors were placed near the end nodes of the system, ESS units were allocated along the system, the reinforced lines are the main lines connecting the ADN to the substation (node 149), and the DG units were placed in the middle of the MGs or near the connecting point with the ADN.

Chapter 6 shows that most of the DERs components are allocated in the MG areas and not in the ADN if the competitive aspect of MMG systems is neglected. On the other hand, Table VII shows that in a competitive market environment, the new resources are placed more evenly among the players, including the ADN, since the MGs' decisions seek to benefit only themselves.

Figure 52 shows the costs for two cases: the first considers energy trade among the MGs, which is the model from this chapter; the second shows the results from Chapter 6, which does not consider the energy trade market. Gen. Cost is the generation cost for the ADN, Investments are related to the placement of new components, and Total Cost is the sum of these two costs.

FIGURE 52 – COMPARISON OF COSTS FOR CASES CONSIDERING OR NOT ENERGY TRADE AMONG THE MGS



From Figure 52, note that all costs are higher if energy trade is considered since it is a competitive scenario where each MG seeks its own benefits. The total cost in the simulation is 14% higher for this case.

Considering energy trade, the DSO does not have control over the investments inside the MGs and pricing; thus, the MGs' decisions do not optimally benefit the entire system, and the ADN requires more components.

Figure 52 shows a value of $ 3e6 in investments considering energy trade and $ 0.3e6 for the other case, which are the results from the models presented in this chapter and chapter 6, respectively. In chapter 6, only lines are reconducted in the expansion decision for the ADN, and other components are only placed inside the MGs; while, in this chapter, capacitors, ESS units, and DGs are also placed in the main grid.

In the case from Chapter 6, the DSO controls the investments inside the MGs; thus, he can place and coordinate the DERs to best benefit him. In the other case, presented in this chapter, he is impacted by the investments and decisions from the MGs, and more investments inside the ADN are required to reach the optimal decision.

Although the total cost is higher for the case considering energy trade, environments where multi-players make their own decisions are beneficial since the risk is shared among them. For example, in the case considering energy trade, the DSO invests $ 3e6 in the ADN, while he invests $ 14e6 in the entire system (ADN plus MGs) in the other case. In the first case, the risk for the DSO is lower, even though the total cost for the system is higher, because private investors make part of the investments, sharing the risks.

Scenarios with competitive aspects of MMG are more practical since MGs are local networks that can operate isolated from the main grid and are more attractive to private investors. However, models considering an optimal integrated decision among MGs and the ADN are essential to study incentive programs that would benefit all players. Therefore, the models cannot be directly compared to conclude if one is better than another; they are applied to different cases and studies.

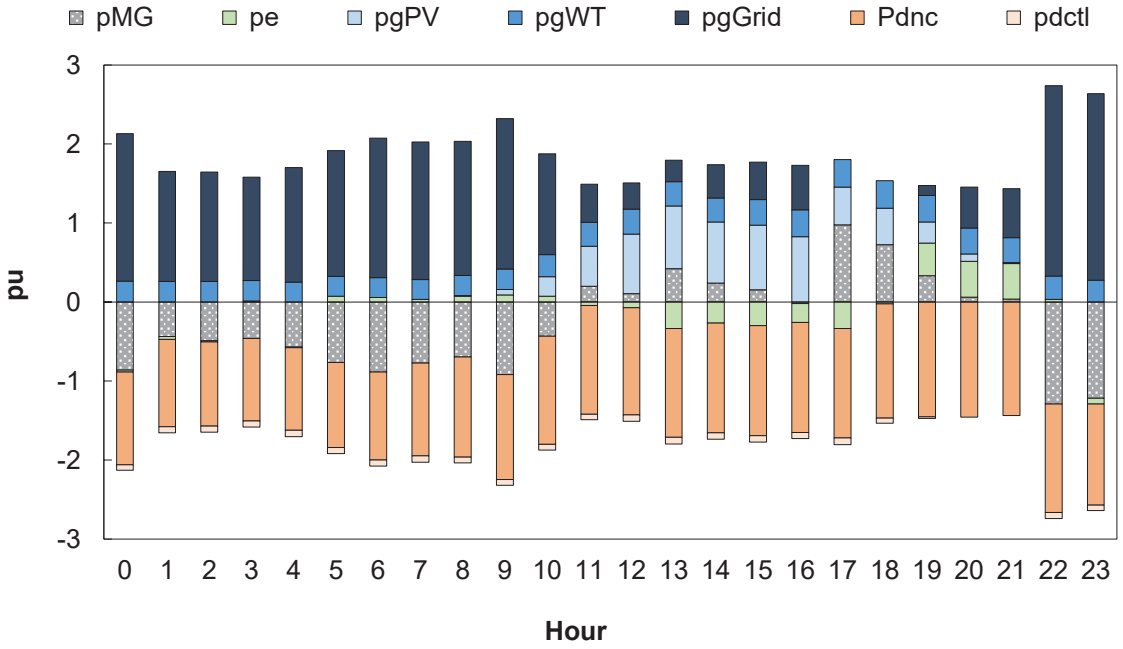
Cases where only one player makes investments and decisions, typically have cost-based electricity pricing, while cases with multi-players have bid-based pricing. The main advantages of bid-based pricing are (i) prices are updated more frequently; (ii) improvement in forecasts techniques and processes; (iii) more efficiency in risk management; (iv) more robustness against changes; and (v) the improvement in technologies due to the competitiveness aspects of supply-demand. On the other hand, models based on demand are more vulnerable to governmental regulation and

may have insufficient electricity prices to cover their costs in some specific situations (ENGIE, 2022).

7.5.2 DER's Coordination

When there is an ADN, it is important to observe the DER's coordination, which shows the use of energy resources over the hours of the day. Figure 53 shows the power balance of the entire system per hour on a typical day in the last year of the expansion planning, weighted by the data bin's probabilities.

FIGURE 53 – POWER BALANCE FOR THE ENTIRE SYSTEM IN THE LAST YEAR OF THE EXPANSION PLANNING



pMG denotes the net power of all MGs (positive values indicate that the MGs are providing energy to the ADN). pe is the power provided or stored by the ESS units. pgPV and pgWT are the power supplied by the DG units from the ADN (PV: photovoltaic, WT: wind turbine). PDnc is the non-controllable load from the ADN. Finally, pdctl is the controllable load from the ADN.

Since this chapter proposes an expansion model to be used by the DSO, Figure 53 provides information from the DSO perspective.

The MGs consume power from the ADN during hours from 0 to 10 and from 22 to 23. At other hours, the MGs are providing energy to the ADN. This behavior

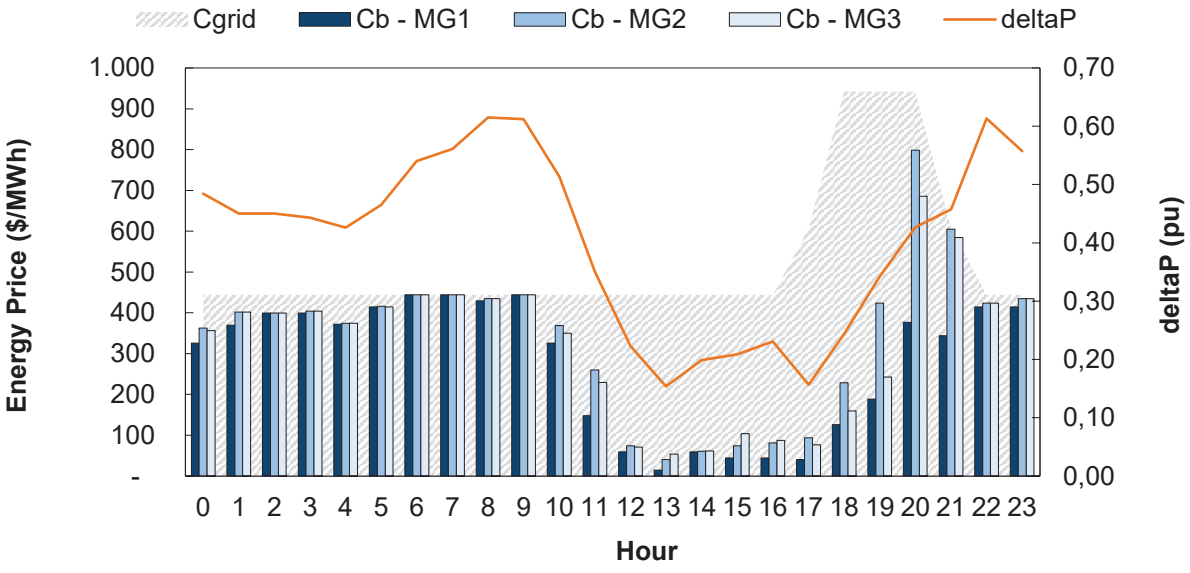
occurs because during hours 11 to 18 there is more power available in the MGs due to the photovoltaic units (pgPV).

Moreover, during hours 17 to 21 the price of the energy provided by the ADN is higher (detailed in Figure 54, next subsection); therefore, the MGs store energy before hour 18 to sell it later when the price is higher.

7.5.3 Price Strategy

This model proposes an expansion planning decision in a scenario where MGs can trade energy among themselves and with the ADN. Thus, Figure 54 shows the bid price (Cb) for each MG and the energy selling price of the ADN (Cgrid). deltaP ($\Delta\hat{P}_m$ from equation (189) represents the net power (total load minus the available generation power of the MGs).

FIGURE 54 – PRICE STRATEGY FOR EACH MG PER HOUR IN THE LAST YEAR OF THE EXPANSION PLANNING

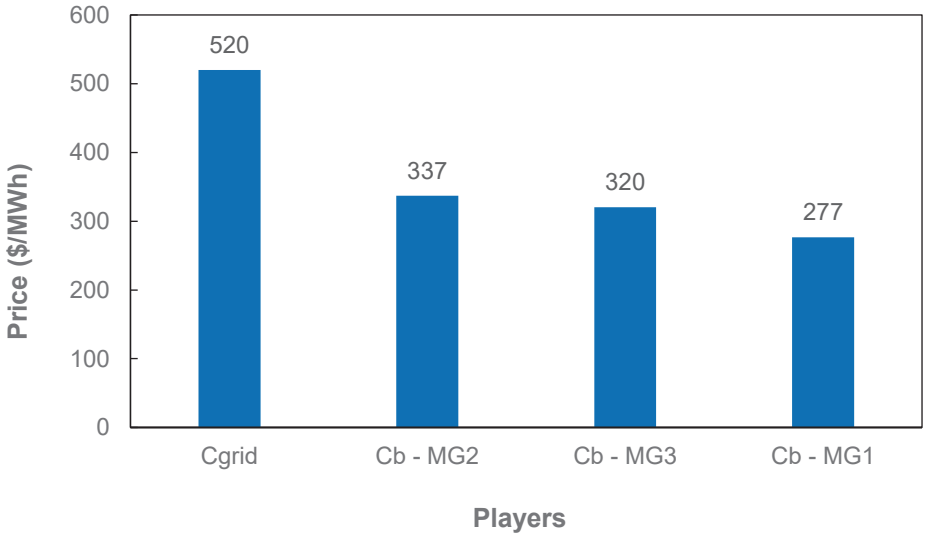


The price strategy of all MGs is very close to the ADN energy price from hours 0 to 9. After hour 10, deltaP decreases, indicating that more generation is available; thus, all players' energy price (Cb) dramatically reduces.

During hours 18 and 19, all players try to use their own energy or sell it to the ADN since the reference energy price is higher; however, at hours 20 e 21, the players increase their price because the reference (Cgrid) is high and the available power for consumption is starting to run out.

The MGs have different price strategies, and Figure 55 presents their average.

FIGURE 55 – AVERAGE PRICE STRATEGY



MG2 sells energy at higher prices among the MGs, followed by MG3. This occurs due to the number of DG and ESS units placed in the system, which can be observed in Table VII. MG2 has 5 DG units, MG3 has 4, and MG1 has 3.

7.5.4 Comparison among models

Table VIII compares the main aspects of the models presented in this work.

TABLE VIII – COMPARISON AMONG MODELS FROM CHAPTERS 4, 5, 6, AND 7

	Model from chapter			
	4	**5**	**6**	**7**
Uncertainty approach	ARO	ARO	DDDRO	DDDRO
Historical data			✓	✓
DG, ESS, capacitors and line placement	✓	✓	✓	✓
Self-healing and reliability	✓			
N-1 contingency		✓	✓	✓
Demand response		✓	✓	✓
MMG		✓	✓	✓
Energy trade market				✓

Compared to the previous model, the model presented in this chapter is similar to the model from chapter 6, including the energy trade aspect of the competitive environment among the MGs.

7.6 SUMMARY

This chapter presents a new computational framework to solve the expansion planning problem for ADNs with multiple microgrids using a data-driven, robust approach and an energy trading strategy based on game theory. The proposed method provides to the DSO a robust expansion planning against uncertainties, based on data bins created from historical data and their probabilities, considering the individual decisions of the MGs regarding price strategy and their expansion planning decisions.

Simulation results show that in a competitive game, the MGs place components that would allow them to store energy during periods when the energy is cheaper and sell it when the price is higher. Moreover, when there is a high amount of surplus energy, the energy price drops; therefore, there is an equilibrium point for the expansion decisions of the MGs and the amount of energy sold.

Different price strategies lead to further investments since some distributed generation units, such as solar-power units, are only available at specific hours of the day. Results have shown that expansion candidates are placed more evenly among the players if we consider the competitive aspect of MMG systems.

A competitive environment increases the system’s expansion planning costs since each player seeks its own benefits, but the players share the investment risks. These finds show that, in scenarios where private investors own the MGs, the expansion planning proposed by the DSO may not be the optimal response to external investments if the competitive aspect of MMG systems is neglected.

8 CONCLUSIONS

This dissertation presented four computational models to solve expansion planning problems of active distribution networks (ADN) under uncertainties. Each proposed model is designed for specific scenarios considering the availability of historical data, the existence (or inclusion or incorporation) of microgrids (MGs) in the system, and the competitive aspect of the multiple microgrids (MMG) environment.

All models are three-level problems, requiring solving a min-max-min problem. For each one, a decomposition approach in a multi-stage framework is proposed based on the column and constraint generation algorithm (C&CG).

The first model is designed for ADN problems where historical data is unavailable, and there is no MMG in the system. It includes a target for reliability indexes in the formulation, and places distributed generation (DG), energy storage systems (ESS), capacitors, and lines in the system using an adaptative robust optimization approach (ARO) to deal with uncertainties. The model introduces a new sensitivity matrix to improve computational time significantly. Compared to similar works, the proposed model shows up to 90% less processing time, mainly due to the use of the sensitivity matrix along with the C&CG. Results show that the number of DGs installed in the system is negatively impacted by high uncertainty levels, once the investment in these components is not worth it for this case. Moreover, by not including ESS units, capacitors, switches, or DGs, the total cost of the expansion plan may increase up to 147% compared to the case considering all these aspects. These components help reduce the operation cost while improving the reliability indexes.

Compared to the first model, the second one inserts MMGs in the system, replaces the reliability indexes for a contingency approach, and considers demand response using ARO for cases where historical data is unavailable, supposing no competition or energy trade among the MGs. Results show that DERs may reduce the total cost of the problem by 13%. And considering demand response and representing the 24 hours of the day in the formulation reduced the expansion plan costs by 7.7% in the simulations. Although the total cost in the expansion planning increases if contingencies are considered, the system's reliability is substantially improved. In this comparison, simulations show that the total cost increased by 6%, while the EENS reliability index reduced by 70%.

The third model uses a data-driven distributionally robust optimization approach (DDDRO) to deal with uncertainties, considering that historical data is available and there is no energy trade market. Results exhibit that DDDRO models provide a lower total cost than Adaptative Robust Models (ARO), considering that historical data is available and uncertainty budgets are greater than 0.25 for the robust model. Simulations demonstrate that DDDRO can be used when very little historical data is available, which is not the case for stochastic approaches (SP).

The fourth model introduces the energy trade market in a competitive environment among the MGs. Additional assumptions are the same as in the third model. This was expected since the players seek their own benefits and do not necessarily look for the best decision for the entire system. Simulations expose that each MG creates its own price strategy, but a similar behavior occurs; when there is a lot of surplus generation from the DG units, the price drops, while it increases when there is an energy shortage. MGs with more surplus energy have a higher priority in selling energy; while MGs that buy more energy pay more. Simulations show that the placement of components considering the competitive aspect of MMG is very different from the case not considering it. Also, the total cost increased by 14% in the case study, while players shared the investment risks.

The comparison among the models is not fair whereas they should be applied to different scenarios. Thus, it is impossible to define if one is better than the other without observing the case study and assumptions. Consequently, watching the system's characteristics is essential before choosing a model or determining a formulation.

This work's contributions help design ADN expansion planning under uncertainties and understand the relevance and impacts of consideration (or not) some modern aspects of MMGs environments, such as demand response, DGs, EES, contingencies, and energy trade market in cases having or not historical data available.

8.1 FUTURE WORKS

This work has presented different computational models for active distribution networks considering multiple microgrid scenarios. Although it includes many aspects of MGs environments, for future research, some of the following elements may be included:

- AC three-phase formulation
- Unbalanced loads
- Representation of ZIP loads
- Costs related to incentive programs for installing DGs, ESSs, and demand response.
- Load transfer
- Continuity indicators
- Non-Linear Optimal Power Flow inside the expansion planning decision
- Degradation of ESS units
- Virtual Power Plants
- Multiobjective optimization considering reliability/contingency and costs
- Electric Vehicle
- Hybrid AC/DC microgrids
- Application of Reinforcement Learning

8.2 ACKNOWLEDGMENTS

This research was funded by the Companhia Paranaense de Energia - COPEL research and technological development (RTD) program, through the PD-02866-0511/2019 project, regulated by ANEEL.

The author thanks the support of CAPES–Brazilian Federal Agency for Support and Evaluation of Graduate Education within the Ministry of Education of Brazil. We also thank the CAPES-PRINT-UFPR Project – Finance Code 001.

A. APPENDIX – Additional information and data used in the case study

This appendix provides the required data to reproduce the results in the simulation sections of this work. The proposed models are illustrated using a modified version of the IEEE 123-bus test system represented by a 4.16 kV network with 3.4 MW of load demand. The required data for this test system has been taken from Kersting (1991) and Pinto et al. (2019).

Information for expansion planning

The horizon planning is 3 years for chapters 4, 5, and 6. For chapter 7, it is 5 years. The interest rate is 10%/year, and the investment budget has been defined as infinity for this case study. The grid power cost is defined for each hour of the day as {444 $ for hours 0 to 16, 22 and 23; 607 $ for hours 17 and 21; 942 $ for hours 18 to 20}

Information for buses

All buses have voltage limits from 0.95 pu to 1.05 pu.

Information for loads

For ARO models, in the first year of the expansion planning, the lower bound (LB) for the load uncertainty is the summation of the loads in each bus, defined in Kersting (1991). The upper bound (UB) value is 150% of the LB. For the second and third year of the expansion planning, the LB and UB values of the load uncertainties are defined as 110% of the previous year.

The load shedding cost is defined as 10 times the grid power cost.

The hourly load for each bus is the average values of the loads described in Alam et al. (2020) since Kersting (1991) does not provide details for each hour of the day.

The non-controllable, deferrable, and controllable portions of the load are defined as 90, 7, and 3% of the total load for each bus, respectively.

The minimum load factor ($Lfac_d$) is defined as its same value before the expansion planning decision, and it depends on the load point.

Information for existing lines

All required information is described in Kersting (1991), such as conductors' impedance, feeders' length, and nodes connections. For the EENS reliability index calculation, existing lines have 0.01 failures per year and a repair time of 5 hours.

Definition of new candidates

ESS and capacitor candidates are defined for all buses of the system. For the sake of tractability, line and DG candidates are defined for specific buses.

DG candidates were defined through two simulations. Both simulations consider DG units for all buses of the system and only these candidates in the expansion planning. The first simulation has an uncertainty budget of 0% and the second 25%, which is considered a risk-averse scenario for this case study. Thus, the following set of buses was defined as the candidates for the expansion planning: {20, 21, 22, 25, 31, 27, 29, 97, 101, 68, 72, 75, 100, 110, 108, 76, 78, 91, 84, 86, 82, 90, 87, 95, 57, 66, 40, 50, 152}.

Information for line candidates

The existing lines have a failure/year rate of 10^{-1} and repair time of 5h, while new lines have 10^{-4} failures/year and repair time of 1h. These values were defined based on average values presented in Pinto et al. (2019).

The EENS target from the first model is set to 25% of its original value, 14.2 MWh/year, representing a goal defined by the DSO.

The candidate lines have characteristics similar to the existing lines from the original system but with lower failure rates and 50% less resistance/reactance.

The investment cost for line candidates is defined as 500,000$/km (PINTO et al., 2019).

Information for DG candidates

DGs are defined as renewable solar power sources with a maximum capacity of 0.8 MW and a constant power factor equal to 0.9, which is not a limitation of the model, but a consideration for the case study. The variation in the power generation of the DGs throughout the hours of the day has been defined as the maximum values from Alam et al. (2020), which is the UB value for the uncertainties in generation power.

The LB values are defined as 0; thus, 100% of the uncertainty budget indicates no DG power is available. The investment cost for each DG unit is 800,000$, which represents 1,000$/kW, same used in Pinto et al. (2019).

Information for ESS candidates

Each ESSs is considered with a maximum charging/discharging power of 0.4 MW, and a maximum power storage capacity of 2 MW. The investment cost for each ESS unit is 200,000$, which represents 500 $/kW. All buses of the system have one ESS unit as a candidate.

Information for capacitor bank candidates

The capacitor bank candidates are defined with 0.1 MVAr, with a cost of 17,000$. All buses of the system have one capacitor as a candidate.

Historical data for DDDRO models

The historical data for solar and wind power generation was taken from Solcast (2021) for the city of Sao Paulo, Brazil, from 2008 to 2021. The historical data for the load was taken from ONS (2021), also for Sao Paulo, Brazil.

B. APPENDIX – Summary of all constraints

Reliability target constraint (Ψ^{rel}):

$$f_{EENS}\left(x^{C}_{c,t_y}\right) \leq EENS^{TG}$$

AC power flow constraints (Ψ^{Lflow}):

$$p^{L}_{l,t} = x^{L}_{l,t_y}\left(G_l v_{rs(l),t} - B_l \theta_{rs(l),t}\right),\ \forall l, \forall t$$

$$q^{L}_{l,t} = x^{L}_{l,t_y}\left(-G_l \theta_{sr(l),t} - B_l v_{sr(l),t}\right),\ \forall l, \forall t$$

Power balance constraints (Ψ^{bal}):

$$\sum_{g\in\Omega^{G}_{n}} p^{G}_{g,t} - \sum_{l\in\Omega^{L}_{n(s)}} p^{L}_{l,t} + \sum_{l\in\Omega^{L}_{n(r)}} p^{L}_{l,t} + p^{E}_{n,t} = \sum_{d\in\Omega^{D}_{n}} \left(\tilde{p}^{D}_{d,t} - p^{LS}_{d,t}\right),\ \forall n, \forall t$$

$$\sum_{g\in\Omega^{G}_{n}} q^{G}_{g,t} - \sum_{l\in\Omega^{L}_{n(s)}} q^{L}_{l,t} + \sum_{l\in\Omega^{L}_{n(r)}} q^{L}_{l,t} + q^{SH}_{n,t} = \sum_{d\in\Omega^{D}_{n}} \left(\tilde{q}^{D}_{d,t} - q^{LS}_{d,t}\right), \forall n, \forall t_t$$

Energy storage system constraints (Ψ^{ess}):

$$soc_{n,t} = soc_{n,(t-1)} - p^{E}_{n,t},\ \forall n, \forall t$$

$$x^{E}_{n,t_y}\, SOC^{min}_{n} \leq soc_{n,t} \leq x^{E}_{n,t_y}\, SOC^{max}_{n},\ \forall n, \forall t$$

$$x^{E}_{n,t_y}\, P^{Emin}_{n} \leq p^{E}_{n,t} \leq x^{E}_{n,t_y}\, P^{Emax}_{n},\ \forall n, \forall t$$

Operational constraints (Ψ^{op}):

$$0 \leq p^{LS}_{d,t} \leq \tilde{p}^{D^{max}}_{d,t},\ \forall d, \forall t$$

$$tan\left(pf_{d,t}\right)\left(\tilde{p}^{D}_{d,t} - p^{LS}_{d,t}\right) = \tilde{q}^{D}_{d,t} - q^{LS}_{d,t}, \forall d, \forall t$$

$$x^{G}_{g,t_y} p^{G^{min}}_{g,t} \leq p^{G}_{g,t} \leq x^{G}_{g,t_y} \tilde{p}^{G^{max}}_{g,t},\ \forall g, \forall t$$

$$x^G_{g,t_y}\, Q^{G^{min}}_{g,t_d} \le q^G_{g,t} \le x^G_{g,t_y}\, \tilde{q}^{G^{max}}_{g,t_d},\ \forall g, \forall t$$

$$q^{SH}_{n,t} = x^{CP}_{n,t_y} Q^{SH}_n,\ \ \forall n, \forall t$$

$$-P^{Lmax}_l \le p^L_{l,t} \le P^{Lmax}_l,\ \ \forall l, \forall t$$

$$V^{min}_n \le v_{n,t} \le V^{max}_n,\ \ \forall n, \forall t$$

$$-\pi \le \theta_{n,t} \le \pi,\ \ \forall n, \forall t$$

$$\theta_{n,t} = 0,\ \ n\text{: ref}, \forall t$$

Investment constraints (Ψ^{inv}):

$$\sum_{t_y}\left(\sum_{c\in\Omega^C+}\left(I^C_c x^C_{c,t_y}\right)/(1+R)^{t_y}\right) \le I^{max}$$

$$x^C_{c,t_y} = \sum_{t_i=1}^{t_y} \alpha^C_{c,t_i},\ \ \forall c, \forall t_y$$

$$\sum_{t_y\in\Omega^{Ty}} \alpha^C_{c,t_y} \le 1,\ \ \forall c$$

$$\alpha^C_{c,t_y}, x^C_{c,t_y}\ \ as\ \ binary,\ \ \forall c, \forall t_y$$

Uncertainty constraints (Ψ^{unc}):

$$P^{G^{min}}_{g,t} \le \tilde{p}^{G^{max}}_{g,t} \le \bar{P}^{G^{max}}_{g,t},\ \ \forall g, \forall t$$

$$\underline{P}^D_{d,t} \le \tilde{p}^D_{d,t} \le \bar{P}^D_{d,t},\ \ \forall d, \forall t$$

$$\frac{\sum_g x^G_{g,t_y}\left(\bar{P}^{G^{max}}_{g,t} - \tilde{p}^{G^{max}}_{g,t}\right)}{\sum_g x^G_{g,t_y}\left(\bar{P}^{G^{max}}_{g,t} - P^{G^{min}}_{g,t}\right)} \le\ \Gamma^G, \forall t$$

$$\frac{\sum_d\left(\tilde{p}^D_{d,t} - \underline{P}^D_{d,t}\right)}{\sum_d\left(\bar{P}^D_{d,t} - \underline{P}^D_{d,t}\right)} \le\ \Gamma^D, \forall t$$

$$\tilde{p}^{G^{max}}_{g,t} = \tilde{q}^{G^{max}}_{g,t}\left(\bar{P}^{G^{max}}_{g,t}/\bar{Q}^{G^{max}}_{g,t}\right),\ \ \forall g, \forall t$$

$$\tilde{p}_{d,t}^{D} = \tilde{q}_{d,t}^{D}\left(\bar{P}_{d,t}^{D}/\bar{Q}_{d,t}^{D}\right),\ \ \forall d, \forall t$$

Demand response constraints (Ψ^{dr}):

$$p_{d,t}^{D} = \tilde{p}_{d,t}^{D_{nc}} + \tilde{p}_{d,t}^{D_{df}} + p_{d,t}^{D_{ctl}},\ \ \forall d, \forall t$$

$$q_{d,t}^{D} = \tilde{q}_{d,t}^{D_{nc}} + \tilde{q}_{d,t}^{D_{df}} + q_{d,t}^{D_{ctl}},\ \ \forall d, \forall t$$

$$p_{d,t}^{D} \le \sum_{t_h} p_{d,t}^{D}/(Lfac_d\, T_h),\quad \forall d, \forall t$$

$$\sum_{t_h} p_{d,t}^{D_{ctl}} = P_{d,t}^{D_{ctl}^{total}},\quad \forall d, \forall t_y$$

$$p_{d,t}^{D_{ctl}} \le \overline{P}_{d,t}^{D_{ctl}},\ \ \forall d, \forall t$$

$$p_{d,t}^{D_{ctl}} = q_{d,t}^{D_{ctl}}\left(P_{d,t}^{D_{ctl}^{total}}/Q_{d,t}^{D_{ctl}^{total}}\right),\quad \forall d, \forall t$$

Generation contingency constraints(Ψ^{cont}):

$$\sum_{g_c \epsilon \Omega_m^G \setminus g} x_{g_c,t_y}^{G}\tilde{p}_{g_c,t}^{G^{max},m} + \sum_{e} p_{e,t}^{E,m} \ge \sum_{d}\left(p_{d,t}^{D,m} - p_{d,t}^{LS,m}\right),\quad \forall m, \forall g \epsilon \Omega_m^G, \forall t$$

$$\sum_{g_c \epsilon \Omega_m^G \setminus g} x_{g_c,T}^{G}\tilde{q}_{g_c,t}^{G^{max},m} + \sum_{cp} q_{cp,t}^{SH,m} \ge \sum_{d}\left(q_{d,t}^{D,m} - q_{d,t}^{LS,m}\right),\quad \forall m, \forall g \epsilon \Omega_m^G, \forall t$$

MGs' isolated operation constraints (Ψ^{bsw}):

$$p_{l,t}^{L,m} = x_{l,t_y}^{L} bsw_{l,t}^{con(m)}\left(G_l v_{sr(l),t} - B_l \theta_{sr(l),t}\right),\ \ \forall m, \forall l \epsilon \Omega_{m,adn}^{L}, \forall t$$

$$q_{l,t}^{L,m} = x_{l,t_y}^{L} bsw_{l,t}^{con(m)}\left(-G_l \theta_{sr(l),t} - B_l v_{sr(l),t}\right),\ \ \forall m, \forall l \epsilon \Omega_{m,adn}^{L}, \forall t$$

Uncertainty for deferrable load constraints (Ψ^{uncCTL}):

$$\frac{\sum_d\left(\tilde{p}_{d,t}^{D_{nc}} - \underline{P}_{d,t}^{D_{nc}}\right)}{\sum_d\left(\bar{P}_{d,t}^{D_{nc}} - \underline{P}_{d,t}^{D_{nc}}\right)} \le\ \Gamma_t^{D_{nc}},\ \ \forall t$$

$$\underline{P}_{d,t}^{D_{nc}} \le \tilde{p}_{d,t}^{D_{nc}} \le \bar{P}_{d,t}^{D_{nc}},\ \ \forall d, \forall t$$

$$\tilde{p}_{d,t}^{Dnc} = \tilde{q}_{d,t}^{Dnc}\,\bar{P}_{d,t}^{Dnc}/\bar{Q}_{d,t}^{Dnc},\ \ \forall d, \forall t$$

$$\frac{\sum_d \left(\sum_{t_h} \tilde{p}_{d,t}^{Ddf} - \sum_{t_h} \underline{P}_{d,t}^{Ddf}\right)}{\sum_d \left(\sum_{t_h} \bar{P}_{d,t}^{Ddf} - \sum_{t_h} \underline{P}_{d,t}^{Ddf}\right)} \leq \Gamma_{t_y}^{Ddf},\ \ \forall t_y$$

$$\tilde{p}_{d,t}^{Ddf} \leq \overline{P}_{d,t}^{Ddf},\ \ \forall d, \forall t$$

$$\tilde{p}_{d,t}^{Ddf} = \tilde{q}_{d,t}^{Ddf} \sum_{t_h} \bar{P}_{d,t}^{Ddf} \Big/ \sum_{t_h} \bar{Q}_{d,t}^{Ddf},\ \ \forall d, \forall t$$

Ambiguity Set for Uncertainties (Ψ^{amb})

$$\Psi^{amb} = \left\{ \begin{array}{c} \left\| \mathscr{p}_s^{\mathcal{S}} - \mathscr{p}_s^{\mathcal{S}_0} \right\|_1 = \sum_s \left| \mathscr{p}_s^{\mathcal{S}} - \mathscr{p}_s^{\mathcal{S}_0} \right| \leq \delta_1 \\ \left\| \mathscr{p}_s^{\mathcal{S}} - \mathscr{p}_s^{\mathcal{S}_0} \right\|_\infty = \max_s \left(\mathscr{p}_s^{\mathcal{S}} - \mathscr{p}_s^{\mathcal{S}_0} \right) \leq \delta_\infty \\ \sum_s \mathscr{p}_s^{\mathcal{S}} = 1 \\ \mathscr{p}_s^{\mathcal{S}} \geq 0, \forall s \end{array} \right\}$$

$$\delta_1 = \frac{M_D}{2N} \ln \frac{2M_D}{1-\varphi_1}, \delta_\infty = \frac{1}{2N} \ln \frac{2M_D}{1-\varphi_\infty}$$

Power balance in nodes connecting ADN and MGs ($\Psi^{balConn}$):

$$\sum_{g \epsilon \Omega_n^G} p_{g,t}^G + \sum_{e \epsilon \Omega_n^E} p_{e,t}^E - \sum_{l \epsilon \Omega_{n(s)}^L} p_{l,t}^L + \sum_{l \epsilon \Omega_{n(r)}^L} p_{l,t}^L = \sum_{d \epsilon \Omega_n^D} \tilde{p}_{d,t}^D - p_{d,t}^{LS} + \frac{\hat{r}_{m(n)}^{B|S}}{\Delta t_h},\ \ \forall n \epsilon \Omega_{m,adn}^N, \forall t$$

$$\sum_{g \epsilon \Omega_n^G} q_{g,t}^G + \sum_{cp \epsilon \Omega_n^{CP}} q_{cp,t}^{SH} - \sum_{l \epsilon \Omega_{n(s)}^L} q_{l,t}^L + \sum_{l \epsilon \Omega_{n(r)}^L} q_{l,t}^L = \sum_{d \epsilon \Omega_n^D} \tilde{q}_{d,t}^D - q_{d,t}^{LS} + \hat{q}_{m(n),t}^{MG},\ \ \forall n \epsilon \Omega_{m,adn}^N, \forall t$$

Set of constraints for game theory (subproblem Ψ^{game}):

$$\hat{c}_m^B, \hat{r}_m^{B|S}, \hat{q}_m^{MG} = \text{argmax} \left\{ \begin{array}{c} \widehat{rv}_m - \sum_{t_y} \sum_{c \in \Omega_m^C} \frac{I_c^C \hat{x}_{c,t_y}^C}{(1+R)^{t^y}} \\ s.t.\ \Psi_{noncoop}^{game}, \\ \Psi_{mg}^{Lflow}, \Psi_{mg}^{bal}, \Psi_{mg}^{ess}, \Psi_{mg}^{op}, \\ \Psi_{mg}^{inv}, \Psi_{mg}^{dr}, \Psi_{mg}^{cont}, \Psi_{mg}^{bsw} \end{array} \right\},\ \ \forall m$$

Set of constraints $\Psi_{noncoop}^{game}$:

$$\Delta\hat{P}_m = \sum_{g\epsilon\Omega_m^G} \hat{p}_g^G + \sum_{e\epsilon\Omega_m^E} \hat{p}_e^E - \sum_{d\epsilon\Omega_m^D} \hat{p}_d^D, \quad \forall m, \forall t$$

$$\widehat{pr}_j = \frac{\sum_{g\epsilon\Omega_{m(j)}^G} \hat{p}_g^G + \sum_{e\epsilon\Omega_{m(j)}^E} \hat{p}_e^E}{\sum_{d\epsilon\Omega_{m(j)}^D} \hat{p}_d^D}, \quad \forall j, \forall t$$

$$\hat{r}_i^B = \begin{cases} -\Delta\hat{P}_i, & if\ \ 0 < r^{TB} \le r^{TS}\ \ or\ \ r^{TB} > r^{TS} > 0\ \ and\ \dfrac{\hat{c}_i^B}{\sum_i \hat{c}_i^B} r^{TS} > \Delta\hat{P}_i \\ \dfrac{\hat{c}_i^B}{\sum_i \hat{c}_i^B} r^{TS}, & if\ \ r^{TB} > r^{TS} > 0\ \ and\ \dfrac{\hat{c}_i^B}{\sum_i \hat{c}_i^B} r^{TS} < \Delta\hat{P}_i \\ 0, & other,\ \ including\ if\ MG\ is\ isolated \end{cases} \quad \forall i, \forall t$$

$$\hat{r}_j^S = \begin{cases} \Delta\hat{P}_i, & if\ \ r^{TB} > r^{TS} > 0\ \ or\ \ r^{TS} > r^{TB} > 0\ \ and\ \dfrac{\widehat{pr}_j}{\sum_j \widehat{pr}_j} r^{TB} > \Delta\hat{P}_j \\ \dfrac{\widehat{pr}_j}{\sum_j \widehat{pr}_j} r^{TB}, & if\ \ r^{TS} > r^{TB} > 0\ \ and\ \dfrac{\widehat{pr}_j}{\sum_j \widehat{pr}_j} r^{TB} < \Delta\hat{P}_j \\ 0, & other,\ \ including\ if\ MG\ is\ isolated \end{cases} \quad \forall j, \forall t$$

$$r^{TB} = \sum_i \Delta\hat{P}_i, \quad \forall t$$

$$r^{TS} = \sum_j \Delta\hat{P}_j, \quad \forall t$$

$$\widehat{rv}^T = \sum_i \hat{r}_i^B \hat{c}_i^B, \quad \forall t$$

$$\widehat{rv}_j = \frac{\hat{r}_j^S}{\sum_j \hat{r}_j^S} \widehat{rv}^T, \quad \forall j, \forall t$$

$$\hat{q}_m^{MG} = \frac{\hat{r}_m^{B|S}}{\Delta t_h} \frac{\sum_{d\epsilon\Omega_m^D} \hat{q}_d^D}{\sum_{d\epsilon\Omega_m^D} \hat{p}_d^D}, \quad \forall m, \forall t$$

C. APPENDIX – Summary of formulation of all models

Model 1: Chapter 4

$$\min_{x^C_{c,t_y}} \max_{\Delta Smax} \min_{\Delta Smin} \sum_{t_y}\sum_{c} \frac{I^C_c x^C_{c,t_y}}{(1+R)^{t_y}} + \sum_{t_y}\sum_{t_h}\left[\sigma\left(\sum_{g} C^G_{g,t} p^G_{g,t} + \sum_{d} C^{LS}_{d,t} p^{LS}_{d,t}\right)\right]$$

subject to Ψ^{rel}, Ψ^{Lflow}, Ψ^{bal}, Ψ^{ess}, Ψ^{op}, Ψ^{inv}, Ψ^{unc}

Model 2: Chapter 5

$$\min_{x^C_{c,t_y}} \max_{\Delta Smax} \min_{\Delta Smin} \sum_{t_y}\sum_{c} \frac{I^C_c x^C_{c,t_y}}{(1+R)^{t_y}} + \sum_{t_y}\sum_{t_h}\left[\sigma\left(\sum_{g} C^G_{g,t} p^G_{g,t} + \sum_{d} C^{LS}_{d,t} p^{LS}_{d,t}\right)\right]$$

subject to Ψ^{Lflow}, Ψ^{bal}, Ψ^{ess}, Ψ^{op}, Ψ^{inv}, Ψ^{unc}, Ψ^{dr}, Ψ^{cont}, Ψ^{bsw}, Ψ^{uncCTL}

Model 3: Chapter 6

$$\min_{x^C_{c,t_y}} \max_{p^S_{s,t_y}} \min_{\Delta Smin} \sum_{t_y}\sum_{c} \frac{I^C_c x^C_{c,t_y}}{(1+R)^{t_y}} + \sum_{s} p^S_{s,t_y}\left[\sum_{t_y}\sum_{t_h}\sigma\left(\sum_{g} C^G_{g,t} p^G_{g,t} + \sum_{d} C^{LS}_{d,t} p^{LS}_{d,t}\right)\right]$$

subject to Ψ^{Lflow}, Ψ^{bal}, Ψ^{ess}, Ψ^{op}, Ψ^{inv}, Ψ^{dr}, Ψ^{cont}, Ψ^{bsw}, Ψ^{amb}

Model 4: Chapter 7

$$\min_{x^C_{c,t_y}} \max_{p^S_{s,t_y}} \min_{\Delta Smin} \sum_{t_y}\sum_{c} \frac{I^C_c x^C_{c,t_y}}{(1+R)^{t_y}} + \sum_{s} p^S_{s,t_y}\left[\sum_{t_y}\sum_{t_h}\sigma\left(\sum_{g} C^G_{g,t} p^G_{g,t} + \sum_{d} C^{LS}_{d,t} p^{LS}_{d,t}\right)\right]$$

$$\text{subject to } \left\{\begin{array}{c} \Psi^{Lflow}_{adn}, \Psi^{bal}_{adn}, \Psi^{ess}_{adn}, \Psi^{op}_{adn}, \Psi^{inv}_{adn}, \Psi^{dr}_{adn} \\ \Psi^{Lflow}_{mg}, \Psi^{bal}_{mg}, \Psi^{ess}_{mg}, \Psi^{op}_{mg}, \Psi^{inv}_{mg}, \Psi^{dr}_{mg}, \Psi^{cont}_{mg}, \Psi^{bsw}_{mg} \\ \Psi^{amb}, \Psi^{balConn}, \Psi^{game} \end{array}\right\}$$

REFERENCES

ABSOLAR. Panorama da solar fotovoltaica no Brasil e no mundo. Disponível em: <https://www.absolar.org.br/mercado/infografico/>. Acesso em: 23/10/2022.

ALAM, M. N.; CHAKRABARTI, S.; GHOSH, A. Networked Microgrids: State-of-the-Art and Future Perspectives. **IEEE Transactions on Industrial Informatics**, v. 15, n. 3, p. 1238–1250, 2019.

ALAM, M. N.; CHAKRABARTI, S.; LIANG, X. A Benchmark Test System for Networked Microgrids. **IEEE Transactions on Industrial Informatics**, v. 16, n. 10, p. 6217–6230, 2020. IEEE. Disponível em: <https://ieeexplore.ieee.org/document/9016068/>. .

ALBADI, M. H.; EL-SAADANY, E. F. Demand Response in Electricity Markets: An Overview. 2007 IEEE Power Engineering Society General Meeting. **Anais...** . p.1–5, 2007. IEEE. Disponível em: <http://ieeexplore.ieee.org/document/4275494/>. .

ALEEM, S. A.; ALMOATAZ YOUSSEF ABDELAZIZ; AHMED ZOBAA; RAMESH BANSAL. **Decision Making Applications in Modern Power Systems**. Elsevier, 2020.

AMJADY, N.; ATTARHA, A.; DEHGHAN, S.; CONEJO, A. J. Adaptive Robust Expansion Planning for a Distribution Network With DERs. **IEEE Transactions on Power Systems**, v. 33, n. 2, p. 1698–1715, 2018a.

AMJADY, N.; ATTARHA, A.; DEHGHAN, S.; CONEJO, A. J. Adaptive Robust Expansion Planning for a Distribution Network With DERs. **IEEE Transactions on Power Systems**, v. 33, n. 2, p. 1698–1715, 2018b. Disponível em: <http://ieeexplore.ieee.org/document/8012502/>. .

ANEEL. Geração Distribuída por tempo de conexão. Disponível em: <http://www2.aneel.gov.br/scg/gd/VerGD.asp>. Acesso em: 15/1/2021.

ASCHIDAMINI, G. L.; DA CRUZ, G. A.; RESENER, M.; LEBORGNE, R. C.; PEREIRA, L. A. A Framework for Reliability Assessment in Expansion Planning of Power Distribution Systems. **Energies**, v. 15, n. 14, p. 5073, 2022. MDPI. Disponível em: <https://www.mdpi.com/1996-1073/15/14/5073>. .

ATTARHA, A.; AMJADY, N.; CONEJO, A. J. Adaptive robust AC optimal power flow considering load and wind power uncertainties. **International Journal of Electrical Power & Energy Systems**, v. 96, n. September 2017, p. 132–142, 2018. Elsevier. Disponível em: <https://linkinghub.elsevier.com/retrieve/pii/S0142061517317842>. .

BAGHERI, A.; WANG, J.; ZHAO, C. Data-Driven Stochastic Transmission Expansion Planning. **IEEE Transactions on Power Systems**, v. 32, n. 5, p. 3461–3470, 2017.

BARINGO, L.; BOFFINO, L.; OGGIONI, G. Robust expansion planning of a distribution system with electric vehicles, storage and renewable units. **Applied Energy**, v. 265, n. November 2019, p. 114679, 2020. Elsevier.

BEN-HAIM, Y. Info-Gap Decision Theory: Decisions Under Severe Uncertainty. , 2006. Academic Press.

BEN-TAL, A.; GORYASHKO, A.; GUSLITZER, E.; NEMIROVSKI, A. Adjustable robust solutions of uncertain linear programs. **Mathematical Programming**, v. 99, n. 2, p. 351–376, 2004. Disponível em: <http://link.springer.com/10.1007/s10107-003-0454-y>. .

BERTSIMAS, D.; BROWN, D. B.; CARAMANIS, C. Theory and applications of robust optimization. **SIAM Review**, v. 53, n. 3, p. 464–501, 2011.

BIAZARGHADIKOLAEI, M.; SHAHABI, M.; BARFOROUSHI, T. Expansion planning of energy storages in microgrid under uncertainties and demand response. **International Transactions on Electrical Energy Systems**, v. 29, n. 11, p. 1–20, 2019. Disponível em: <https://onlinelibrary.wiley.com/doi/abs/10.1002/2050-7038.12110>. .

BILLINTON, R.; ALLAN, R. N. **Reliability Evaluation of Engineering Systems: Concepts and Techniques**. 2º ed. New York: Springer Science+Business Media, 1992.

BILLINTON, R.; ALLAN, R. N. . **Reliability Evaluation of Power Systems**. 2º ed. New York: Plenum Press, 1984.

BILLINTON, R.; WANG, P. Distribution system reliability cost/worth analysis using analytical and sequential simulation techniques. **IEEE Transactions on Power Systems**, v. 13, n. 4, p. 1245–1250, 1998. Disponível em: <http://ieeexplore.ieee.org/document/736248/>. .

BLANK, J.; DEB, K. pymoo: Multi-Objective Optimization in Python. **IEEE Access**, v. 8, p. 89497–89509, 2020.

BOLOUKAT, M. H. S.; FOROUD, A. A. Multiperiod planning of distribution networks under competitive electricity market with penetration of several microgrids, part I: Modeling and solution methodology. **IEEE Transactions on Industrial Informatics**, v. 14, n. 11, p. 4884–4894, 2018. IEEE Computer Society.

CHEN, W. K. **The Electrical Engineering Handbook**. 2004.

CHURKIN, A.; BIALEK, J.; POZO, D.; SAUMA, E.; KORGIN, N. Review of Cooperative Game Theory applications in power system expansion planning. **Renewable and Sustainable Energy Reviews**, 1. jul. 2021. Elsevier Ltd.

CONEJO, A. J.; BARINGO MORALES, L.; KAZEMPOUR, S. J.; SIDDIQUI, A. S. **Investment in Electricity Generation and Transmission**. Cham: Springer International Publishing, 2016.

DAS, J. C. **Load Flow Optimization and Optimal Power Flow**. CRC Press, 2017.

DEHGHAN, S.; AMJADY, N. Robust Transmission and Energy Storage Expansion Planning in Wind Farm-Integrated Power Systems Considering Transmission Switching. **IEEE Transactions on Sustainable Energy**, v. 7, n. 2, p. 765–774, 2016. Disponível em: <http://ieeexplore.ieee.org/document/7345605/>. .

DEHGHAN, S.; AMJADY, N.; CONEJO, A. J. Reliability-Constrained Robust Power System Expansion Planning. **IEEE Transactions on Power Systems**, v. 31, n. 3, p. 2383–2392, 2016.

DEHGHAN, S.; NAKIGANDA, A.; ARISTIDOU, P. A data-driven two-stage distributionally robust planning tool for sustainable Microgrids. **IEEE Power and Energy Society General Meeting**, v. 2020-Augus, 2020.

ENGIE. Proposta de Metodologias para formação de preços por oferta no Brasil. , 2022. Disponível em: <https://www.engie.com.br/uploads/2021/09/PeD_Engie_Rel1_EstrategiasDeDesenho.pdf>. Acesso em: 8/11/2022.

EPE. Consumo Anual de Energia Elétrica por classe (nacional). Disponível em: <https://www.epe.gov.br/pt/publicacoes-dados-abertos/publicacoes/Consumo-Anual-de-Energia-Eletrica-por-classe-nacional>. Acesso em: 23/10/2022a.

EPE. Estudos do Plano Decenal de Expansão de Energia 2031. Disponível em: <https://www.epe.gov.br/sites-pt/publicacoes-dados-abertos/publicacoes/PublicacoesArquivos/publicacao-607/topico-591/Caderno%20de%20Demanda%20de%20Eletricidade%20-%20PDE%202031_rv1.PDF>. Acesso em: 23/10/2022b.

EPE. 2031 Ten-Year Energy Expansion Plan. Disponível em: <https://www.epe.gov.br/sites-en/publicacoes-dados-abertos/publicacoes/PublicacoesArquivos/publicacao-245/Relatorio_PDE2031_Cap09_EUS.pdf>. Acesso em: 24/10/2022c.

FORTUNY-AMAT, J.; MCCARL, B. A Representation and Economic Interpretation of a Two-Level Programming Problem. **Journal of the Operational Research Society**, v. 32, n. 9, p. 783–792, 1981. Disponível em: <https://www.tandfonline.com/doi/full/10.1057/jors.1981.156>. .

GAO, H.; WANG, R.; LIU, Y.; et al. Data-driven distributionally robust joint planning of distributed energy resources in active distribution network. **IET Generation, Transmission and Distribution**, v. 14, n. 9, p. 1653–1662, 2020.

HEMMATI, R.; SABOORI, H.; SIANO, P. Coordinated short-term scheduling and long-term expansion planning in microgrids incorporating renewable energy resources and energy storage systems. **Energy**, v. 134, p. 699–708, 2017. Elsevier Ltd. Disponível em: <http://dx.doi.org/10.1016/j.energy.2017.06.081>. .

JALILVAND-NEJAD, A.; SHAFAEI, R.; SHAHRIARI, H. Robust optimization under correlated polyhedral uncertainty set. **Computers & Industrial Engineering**, v. 92, p. 82–94, 2016. Elsevier Ltd. Disponível em: <http://dx.doi.org/10.1016/j.cie.2015.12.006>. .

KAGAN, N.; ROBBA, E.; SCHMIDT, H. **Estimação de indicadores de qualidade da energia elétrica**. 1º ed. São Paulo: Blucher, 2009.

KARIMI, H.; JADID, S. Modeling of transactive energy in multi-microgrid systems by hybrid of competitive-cooperative games. **Electric Power Systems Research**, v. 201, p. 107546, 2021.

KAZMI, S. A. A.; SHAHZAD, M. K.; KHAN, A. Z.; SHIN, D. R. Smart distribution networks: A review of modern distribution concepts from a planning perspective. Energies. **Anais...** . v. 10, 2017.

KERSTING, W. H. Radial distribution test feeders. **IEEE Transactions on Power Systems**, v. 6, n. 3, p. 975–985, 1991. Disponível em: <http://ieeexplore.ieee.org/document/119237/>. .

LEE, J.; GUO, J.; CHOI, J. K.; ZUKERMAN, M. Distributed energy trading in microgrids: A game-theoretic model and its equilibrium analysis. **IEEE Transactions on Industrial Electronics**, v. 62, n. 6, p. 3524–3533, 2015. Institute of Electrical and Electronics Engineers Inc.

LIANG, J.; WANG, P.; SUN, W.; ZHANG, J.; XU, D. A non-cooperative game theory based energy trading strategy of multi-microgrids. IOP Conference Series: Earth and Environmental Science. **Anais...** . v. 675, 2021. IOP Publishing Ltd.

LIN, Z.; HU, Z.; SONG, Y. Distribution Network Expansion Planning Considering notation N-1 Criterion. **IEEE Transactions on Power Systems**, v. 34, n. 3, p. 2476–2478, 2019.

LIU, M. Z. **Optimal Power Flow for Active Distribution Networks: Advanced Formulations, Practical Considerations and Laboratory Demonstration**, 2020. University of Melbourne.

MARTINS, V. F.; BORGES, C. L. T. Active Distribution Network Integrated Planning Incorporating Distributed Generation and Load Response Uncertainties. **IEEE Transactions on Power Systems**, v. 26, n. 4, p. 2164–2172, 2011. Disponível em: <http://ieeexplore.ieee.org/document/5743048/>. .

MASIELLO, R.; KHODAEI, A. Nonwire alternatives: Much ado about nothing? . **IEEE Power and Energy Magazine**, v. 20, n. 2, p. 10–13, 2022.

MASOUMI-AMIRI, S. M.; SHAHABI, M.; BARFOROUSHI, T. Interactive framework development for microgrid expansion strategy and distribution network expansion planning. **Sustainable Energy, Grids and Networks**, v. 27, 2021. Elsevier Ltd.

MOHAN, V.; SURESH, R.; SINGH, J. G.; ONGSAKUL, W.; MADHU, N. Microgrid Energy Management Combining Sensitivities, Interval and Probabilistic Uncertainties of Renewable Generation and Loads. **IEEE Journal on Emerging and Selected Topics in Circuits and Systems**, v. 7, n. 2, p. 262–270, 2017.

MONTENEGRO, D.; TAYLOR, J. Multidimensional method for assessing nonwires alternatives within distribution system planning. **Decentralized Frameworks for Future Power Systems**. p.81–98, 2022. Elsevier.

MOVAHEDNIA, M.; KARIMI, H.; JADID, S. A Cooperative Game Approach for Energy Management of Interconnected Microgrids. , 2022. Acesso em: 29/10/2022.

MUNOZ-DELGADO, G.; CONTRERAS, J.; ARROYO, J. M. Multistage Generation and Network Expansion Planning in Distribution Systems Considering Uncertainty and Reliability. **IEEE Transactions on Power Systems**, v. 31, n. 5, p. 3715–3728, 2016. IEEE.

MUNOZ-DELGADO, G.; CONTRERAS, J.; ARROYO, J. M.; SANCHEZ DE LA NIETA, A.; GIBESCU, M. Transmission and Distribution System Expansion Planning Considering Network and Generation Investments under Uncertainty. 2020 International Conference on Smart Energy Systems and Technologies (SEST). **Anais...** . v. 00, p.1–6, 2020. IEEE. Disponível em: <https://ieeexplore.ieee.org/document/9203430/>. .

NAEBI, A.; SEYEDSHENAVA, S. J.; CONTRERAS, J.; RUIZ, C.; AKBARIMAJD, A. EPEC approach for finding optimal day-ahead bidding strategy equilibria of multi-microgrids in active distribution networks. **International Journal of Electrical Power and Energy Systems**, v. 117, n. November 2019, p. 105702, 2020. Elsevier. Disponível em: <https://doi.org/10.1016/j.ijepes.2019.105702>. .

NAVIDI, M.; MOGHADDAS-TAFRESHI, S. M. An agent-based Stackelberg framework for joint expansion planning of privately Owned regional energy systems and sub-transmission grid. **Electric Power Systems Research**, v. 193, 2021. Elsevier Ltd.

NAWAZ, A.; ZHOU, M.; WU, J.; LONG, C. A comprehensive review on energy management, demand response, and coordination schemes utilization in multi-microgrids network. **Applied Energy**, v. 323, 2022. Elsevier Ltd.

NAZARI, A. A.; KEYPOUR, R. A cooperative expansion program for Disco and independent microgrids based on a bargaining framework. **Sustainable Energy, Grids and Networks**, v. 20, 2019. Elsevier Ltd.

NAZARI, A. A.; KEYPOUR, R.; AMJADY, N. Joint investment of community energy storage systems in distribution networks using modified Nash bargaining theory. **Applied Energy**, v. 301, 2021. Elsevier Ltd.

NING, C.; YOU, F. Data-driven adaptive robust unit commitment under wind power uncertainty: A Bayesian nonparametric approach. **IEEE Transactions on Power Systems**, v. 34, n. 3, p. 2409–2418, 2019. Institute of Electrical and Electronics Engineers Inc.

ONS. Históricos da Operação. Disponível em: <http://www.ons.org.br/paginas/resultados-da-operacao/historico-da-operacao>. Acesso em: 30/6/2021.

PEDREGOSA, F.; VAROQUAUX, G.; GRAMFORT, A.; et al. Scikit-learn: Machine Learning in Python. , 2012. Disponível em: <http://arxiv.org/abs/1201.0490>. .

PINTO, R. S. **Planejamento Multiestágio da Expansão de Sistemas de Distribuição Considerando Confiabilidade e Geração Distribuída no Contexto de Smart Grids**, 2018. Curitiba: Universidade Federal do Paraná. Disponível em: <https://acervodigital.ufpr.br/handle/1884/56589>. Acesso em: 9/10/2022.

PINTO, R. S.; UNSIHUAY-VILA, C.; FERNANDES, T. S. P. Multi-objective and multi-period distribution expansion planning considering reliability, distributed generation and self-healing. **IET Generation, Transmission & Distribution**, v. 13, n. 2, p. 219–228, 2019. Disponível em: <https://digital-library.theiet.org/content/journals/10.1049/iet-gtd.2018.5037>. .

PINTO, R. S.; UNSIHUAY-VILA, C.; TABARRO, F. H. Coordinated operation and expansion planning for multiple microgrids and active distribution networks under uncertainties. **Applied Energy**, v. 297, n. June, p. 117108, 2021. Elsevier Ltd. Disponível em: <https://doi.org/10.1016/j.apenergy.2021.117108>. .

QAEINI, S.; NAZAR, M. S.; YOUSEFIAN, M.; et al. Optimal expansion planning of active distribution system considering coordinated bidding of downward active microgrids and demand response providers. **IET Renewable Power Generation**, v. 13, n. 8, p. 1291–1303, 2019.

DA S. PINTO, C. L.; DE OLIVEIRA, C. C. B.; YUN, Y. J.; MATIOLI, L. C. Methodology to Works Prioritization in the Distribution System. 2009 15th International Conference on Intelligent System Applications to Power Systems. **Anais...** . p.1–6, 2009. IEEE.

SAHOO, S. K.; KISHORE, N. K. Coordinated control and operation of a multi-microgrid system. 2017 7th International Conference on Power Systems (ICPS). **Anais...** . p.283–288, 2017. IEEE. Disponível em: <https://ieeexplore.ieee.org/document/8387307/>. .

SEIFI, H.; SEPASIAN, MOHAMMAD SADEGH. **Electric Power System Planning Issues, Algorithms and Solutions**. 1º ed. Springer-Verlag Berlin Heidelberg, 2011.

SHAVANDI, H.; FULLER, J. D.; PIRNIA, M. An Efficient Data Driven Model for Generation Expansion Planning with Short Term Operational Constraints. , 2018.

DA SILVA, A. M. L.; CASSULA, A. M.; NASCIMENTO, L. C.; et al. Chronological Monte Carlo-Based Assessment of Distribution System Reliability. 2006 International Conference on Probabilistic Methods Applied to Power Systems. **Anais...** . p.1–7, 2006. IEEE. Disponível em: <http://ieeexplore.ieee.org/document/4202386/>. .

SOLCAST. Solar Irradiance Data. Disponível em: <http://solcast.com/>. Acesso em: 30/6/2021.

SOROUDI, A.; EHSAN, M. IGDT Based Robust Decision Making Tool for DNOs in Load Procurement Under Severe Uncertainty. **IEEE Transactions on Smart Grid**, v. 4, n. 2, p. 886–895, 2013. Disponível em: <http://ieeexplore.ieee.org/document/6338333/>. .

VARASTEH, F.; NAZAR, M. S.; HEIDARI, A.; SHAFIE-KHAH, M.; CATALÃO, J. P. S. Distributed energy resource and network expansion planning of a CCHP based active microgrid considering demand

response programs. **Energy**, v. 172, p. 79–105, 2019. Disponível em: <https://linkinghub.elsevier.com/retrieve/pii/S0360544219300179>. .

VELLOSO, A.; STREET, A.; POZO, D.; ARROYO, J. M.; COBOS, N. G. Two-stage robust unit commitment for co-optimized electricity markets: An adaptive data-driven approach for scenario-based uncertainty sets. **IEEE Transactions on Sustainable Energy**, v. 11, n. 2, p. 958–969, 2020.

WALD, A. Statistical Decision Functions Which Minimize the Maximum Risk. **The Annals of Mathematics**, v. 46, n. 2, p. 265, 1945. Disponível em: <https://www.jstor.org/stable/1969022?origin=crossref>. .

WANG, L.; ZHANG, B.; LI, Q.; SONG, W.; LI, G. Robust distributed optimization for energy dispatch of multi-stakeholder multiple microgrids under uncertainty. **Applied Energy**, v. 255, 2019. Elsevier Ltd.

WU, M.; KOU, L.; HOU, X.; et al. A bi-level robust planning model for active distribution networks considering uncertainties of renewable energies. **International Journal of Electrical Power and Energy Systems**, v. 105, n. September 2018, p. 814–822, 2019.

WU, T.; XIE, K.; HU, B.; et al. Data-Driven Approach based Tri-Level Generation and Transmission Expansion Planning Model with High Wind Penetration. **iSPEC 2019 - 2019 IEEE Sustainable Power and Energy Conference: Grid Modernization for Energy Revolution, Proceedings**, p. 1858–1863, 2019.

WU, Z.; LIU, P.; GU, W.; HUANG, H.; HAN, J. A bi-level planning approach for hybrid AC-DC distribution system considering N-1 security criterion. **Applied Energy**, v. 230, n. August, p. 417–428, 2018. Elsevier. Disponível em: <https://doi.org/10.1016/j.apenergy.2018.08.110>. .

WU, Z.; LIU, Y.; GU, W.; WANG, Y.; CHEN, C. Contingency-constrained robust transmission expansion planning under uncertainty. **International Journal of Electrical Power & Energy Systems**, v. 101, n. March, p. 331–338, 2018. Elsevier. Disponível em: <https://doi.org/10.1016/j.ijepes.2018.03.020>. .

XIE, S.; HU, Z.; WANG, J. Two-stage robust optimization for expansion planning of active distribution systems coupled with urban transportation networks. **Applied Energy**, v. 261, n. January, p. 114412, 2020. Elsevier.

YANG, J.; ZHANG, N.; KANG, C.; XIA, Q. A State-Independent Linear Power Flow Model With Accurate Estimation of Voltage Magnitude. **IEEE Transactions on Power Systems**, v. 32, n. 5, p. 3607–3617, 2017. Disponível em: <http://ieeexplore.ieee.org/document/7782382/>. .

YANIKOĞLU, İ.; GORISSEN, B. L.; DEN HERTOG, D. A survey of adjustable robust optimization. **European Journal of Operational Research**, v. 277, n. 3, p. 799–813, 2019. Disponível em: <https://linkinghub.elsevier.com/retrieve/pii/S0377221718307264>. .

ZAKERNEZHAD, H.; NAZAR, M. S.; SHAFIE-KHAH, M.; CATALÃO, J. P. S. Multi-level optimization framework for resilient distribution system expansion planning with distributed energy resources. **Energy**, v. 214, p. 118807, 2021. Disponível em: <https://linkinghub.elsevier.com/retrieve/pii/S0360544220319149>. .

ZARGAR, R. H. M.; YAGHMAEE, M. H. Energy exchange cooperative model in SDN-based interconnected multi-microgrids. **Sustainable Energy, Grids and Networks**, v. 27, p. 100491, 2021.

ZENG, B.; ZHAO, L. Solving two-stage robust optimization problems using a column-and-constraint generation method. **Operations Research Letters**, v. 41, n. 5, p. 457–461, 2013. Disponível em: <https://linkinghub.elsevier.com/retrieve/pii/S0167637713000618>. .

ZHANG, C.; LIU, L.; CHENG, H.; et al. Data-driven distributionally robust transmission expansion planning considering contingency-constrained generation reserve optimization. **International Journal of Electrical Power and Energy Systems**, v. 131, n. February, p. 106973, 2021. Elsevier Ltd. Disponível em: <https://doi.org/10.1016/j.ijepes.2021.106973>. .

ZHENG, Q.; LIU, J.; ZHANG, M.; et al. Robust Transmission Expansion Planning Incorporating Demand Response and N-1 Contingency. **DEStech Transactions on Environment, Energy and Earth Sciences**, v. 53, n. gmee, p. 1689–1699, 2019. Disponível em: <http://dpi-proceedings.com/index.php/dteees/article/view/27554>. .

ZOU, H.; MAO, S.; WANG, Y.; et al. A Survey of Energy Management in Interconnected Multi-Microgrids. **IEEE Access**, v. 7, p. 72158–72169, 2019.